MAPPING XYLAN BIOSYNTHESIS IN PLANT GOLGI
AND
TEACHING BIOLOGY USING EXAMPLE ANSWERS

by

Miranda J. Meents

B.Sc., The University of Lethbridge, 2009

A THESIS SUBMITTED IN PARTIAL FULFILLMENT OF
THE REQUIREMENTS FOR THE DEGREE OF

DOCTOR OF PHILOSOPHY
in
THE FACULTY OF GRADUATE AND POSTDOCTORAL STUDIES
(Botany)

THE UNIVERSITY OF BRITISH COLUMBIA
(Vancouver)

November 2018

The following individuals certify that they have read, and recommend to the Faculty of Graduate and Postdoctoral Studies for acceptance, the dissertation entitled:

Mapping Xylan Biosynthesis in Plant Golgi AND Teaching Biology Using Example Answers

submitted by Miranda J. Meents in partial fulfillment of the requirements for the degree of Doctor of Philosophy in Botany

Examining Committee:

Lacey Samuels, Botany
Supervisor

Shawn Mansfield, Wood Science
Supervisory Committee Member

Supervisory Committee Member

Ljerka Kunst, Botany
University Examiner

Wayne Vogl, Cell and Developmental Biology
University Examiner

Additional Supervisory Committee Members:

Harry Brumer, Michael Smith Laboratories and Department of Chemistry
Supervisory Committee Member

Geoff Wasteneys, Botany
Supervisory Committee Member

Abstract

Secondary cell walls (SCWs) containing the hemicellulose xylan are essential for normal plant growth and development. Great strides have been made to identify the many Golgi-localized biosynthetic enzymes that work in concert to make xylan, however, we still understand little about how these critical proteins and their product are organized in the Golgi to facilitate synthesis and trafficking. To address this question, I characterized the Arabidopsis Golgi in cells producing SCWs using a combination of confocal and transmission electron microscopy (TEM). This analysis indicates that the number of Golgi stacks increases significantly with the onset of SCW synthesis, and that during this process the randomly distributed Golgi stacks work together to produce and secrete xylan. Furthermore, nanoscale characterization of Golgi structure revealed significant increases in Golgi diameter, swelling of the cisternal margins, and secretory vesicle size. Loss of the xylan-biosynthetic enzyme IRREGULAR XYLEM 9 (IRX9) resulted in a dramatic increase in cisternal fenestration and a decrease in swollen margins, but did not affect the number or size of Golgi. Finally, immunogold labelling was used to map IRX9-GFP and xylan to different regions of Golgi cisternae, indicating that xylan is abundant in the outer margins of *trans*-cisternae, IRX9-GFP is abundant in an inner margin of medial-cisternae, and both are absent from cisternal centers. This new concentric circle model of Golgi organization has expanded our understanding of Golgi structure and function and has implications for Golgi function in other cell types and organisms.

The second part of this thesis explores problem-solving instruction in undergraduate cell biology classes, by testing how different teaching techniques affect student attitudes and performance. These results demonstrate that worked examples can be effective teaching techniques for cell biology problem-solving, with lower-performing students seeing greater benefits. Furthermore, providing worked examples did not ameliorate student desires for answer keys to practice problems. This work can be used to guide the appropriate level of instructional support for students of different expertise levels in future courses, and across curricula.

Lay Summary

In plant cells, structures called Golgi produce and deposit carbohydrates in the cell wall, which is essential for normal plant growth. In this thesis, high-powered microscopes are used to study how the Golgi is organized to efficiently make large amounts of these cell wall materials. Characterization of Golgi structure, and mapping the location of biosynthetic machinery and the cell wall products, led to the development of a new model of Golgi organization. These advances in our knowledge can now be applied to better understand Golgi function in other organisms.

The second part of this thesis explores problem-solving instruction in undergraduate biology classes, by testing how different teaching techniques affect student attitudes and performance. The best technique was to provide students with example answers, including an explanation of why the answer was correct. This work can be used to improve how problem-solving is taught in future.

Preface

Portions of Chapter 1 have been previously published as part of a review article, of which I am a co-author (Meents MJ, Watanabe Y, Samuels AL (2018) The cell biology of secondary cell wall biosynthesis. *Annals of Botany*). The text included in this thesis was written by Miranda J Meents with the assistance of Yoichiro Watanabe and Dr. Lacey Samuels. Figures 1.1 and 1.2 are reproduced with permission from Rennie EA and Sheller HV (2014) Xylan biosynthesis. *Current Opinion in Biotechnology*. Figure 1.2 was modified by Miranda J Meents to include the names of newly characterized proteins.

For Chapters 3 and 4, Dr. Lacey Samuels and Miranda Meents identified the research questions and designed the experiments. These experiments were conducted by Miranda Meents. Undergraduate laboratory assistants Sanya Motani and Sandeep Middar, under the supervision of Miranda Meents, assisted with screening transgenic lines, TEM imaging, analysis of Golgi ultrastructure, and cell size analysis of confocal microscopy images. The *irx10irx10L* line was provided by Dr. Simon Turner, and the VND7 induction system was provided by Dr. Taku Demura.

For Chapter 6, Dr. Robin Young, Dr. Sunita Chowrira, Dr. Lacey Samuels and Miranda Meents identified the research questions and designed the study. Ethics approval for this study was granted by the UBC Behavioural Research Ethics Board, Certificate Number (H16-01847). The BIOL362 case study assignments were designed by Dr. Robin Young, the step-by-step worksheet was written by Dr. Robin Young and Dr. Megan Barker, and the example answer worksheet was written by Miranda Meents and Dr. Robin Young. The BIOL200 practice problem sets were originally written by Dr. Robin Young and previous BIOL200 instructors, and they were edited and reformatted by Miranda Meents and Dr. Robin Young. The BIOL200 problem set answer keys were re-written as walkthroughs by Miranda Meents. Kevin Lyon, a BIOL200 graduate student teaching assistant, contributed to writing walkthroughs for practice questions used in tutorials. Miranda Meents collected and analyzed all the survey, interview and performance data. Undergraduate assistant Freddy Francis, under the supervision of Miranda Meents, assisted with analysis of BIOL200 survey and grade data. The codebook for qualitative analysis of BIOL200 survey responses was by developed by Miranda Meents with the assistance of Dr. Robin Young and Dr. Sunita Chowrira.

Appended to this thesis are an example of the BIOL362 case study assignment (Appendix A), and the step-by-step worksheet (Appendix B), and example answer worksheet (Appendix C). Also included is an excerpt from the BIOL200 problem set (Appendix D), examples of problem walkthroughs (Appendix E), the exam questions used to assess student performance (Appendix F), the list of survey questions administered (Appendix G), the codebook developed in the qualitative analysis (Appendix H), and the protocol used in interviewing BIOL200 peer tutors (Appendix I).

Table of Contents

Abstract ... **iii**
Lay Summary ... **iv**
Preface ... **v**
Table of Contents ... **vii**
List of Tables ... **xii**
List of Figures ... **xiii**
List of Symbols ... **xv**
List of Abbreviations ... **xvi**
Acknowledgements ... **xx**
Chapter 1: Introduction ... **1**
1.1 Plant cell walls ... 1
1.2 Xylan structure and biosynthesis ... 3
1.2.1 Xylan diversity in plants and algae ... 3
1.2.2 Xylan biosynthesis in the Golgi ... 4
1.3 The plant Golgi apparatus ... 7
1.3.1 Conservation of Golgi structure and function ... 8
1.3.2 Coordination of Golgi stacks in the Golgi apparatus ... 10
1.3.3 Relationship between Golgi ultrastructure and function ... 11
1.4 Protoxylem tracheary element differentiation as a model system ... 15
1.5 Research questions ... 16
Chapter 2: Materials and Methods ... **22**
2.1 Plant materials and growth conditions ... 22
2.2 Generation of constructs ... 22
2.3 Complementation testing ... 23
2.4 Confocal microscopy ... 24
2.4.1 Expression of *proIRX9:IRX9-GFP* and *proIRX10:IRX10:GFP* ... 24
2.4.2 Golgi stack abundance ... 25
2.4.3 Colocalization ... 26
2.5 TEM imaging ... 27

2.5.1 Sample preparation and imaging 27
2.5.2 Ultrastructure quantification 27
2.5.3 Organelle abundance 28
2.5.4 Organelle position 29
2.5.5 Immunogold labelling and mapping 29
2.6 Statistical analysis 31
Chapter 3: Characterizing the Golgi Apparatus During Secondary Cell Wall Synthesis 36
3.1 Introduction 36
3.2 Results 39
3.2.1 Development of functional fluorescently-tagged IRX9 and IRX10 39
3.2.2 Introduction of IRX9-GFP and IRX10-GFP into the VND7-induction system 39
3.2.3 Characterizing the stages of SCW production 41
3.2.4 IRX9-GFP colocalizes with MANI-mCherry 43
3.2.5 The number of Golgi stacks increases during SCW production 43
3.2.6 Golgi stacks are no closer to SCWs than random 46
3.3 Discussion 48
3.3.1 All Golgi stacks participate in xylan-biosynthesis 48
3.3.2 The onset of SCW production triggers an increase in the number of Golgi stacks 49
3.3.3 Cytoplasmic geometry constrains randomly-distributed Golgi near SCWs 50
3.3.4 Cytoplasm and mitochondria position during SCW deposition 52
3.3.5 Conclusions 53
Chapter 4: IRX9 and Xylan in Concentric Rings in Golgi Cisternae 65
4.1 Introduction 65
4.2 Results 67
4.2.1 Golgi ultrastructure during SCW biosynthesis 67
4.2.1.1 Cisternal diameter increases in SCW-producing cells 67
4.2.1.2 Cisternal margins and TGN vesicles increase in size during SCW production 68
4.2.1.3 Number of cisternal fenestrations increases in *irx9* 69
4.2.2 Mapping of xylan biosynthesis 70
4.2.2.1 Anti-xylan antibody selection 70

4.2.2.2 Anti-GFP antibody selection 71
4.2.2.3 Xylan and IRX9-GFP are found in different regions of the Golgi 72
4.3 Discussion 74
4.3.1 Mapping IRX9-GFP in the Golgi 74
4.3.1.1 The xylan backbone is synthesized in the medial Golgi 74
4.3.1.2 Xylan is synthesized near fenestrated cisternal domains 76
4.3.2 Mapping xylan in the Golgi 79
4.3.2.1 Xylan accumulates in the *trans*-Golgi margins 79
4.3.2.2 Xylan packaging in TGN vesicles contributes to vesicle size 80
4.3.3 Biosynthetic proteins and cargo are absent from the center of cisternae 81
4.3.4 During SCW synthesis, Golgi cisternae change in size but not number 82
4.3.4.1 Cisternal length increases during SCW synthesis 82
4.3.4.2 Number of cisternae is constant with the onset of SCW synthesis 83
4.3.5 Golgi tubules and fenestrations are apparent 84
4.3.6 Conclusions 85
Chapter 5: Using Example Answers to Teach Problem-Solving in Cell Biology 93
5.1 Introduction 93
5.1.1 Problem-solving in undergraduate biology 93
5.1.2 Research questions 94
5.2 Materials and Methods 96
5.2.1 BIOL362 96
5.2.1.1 Assignment design 96
5.2.1.2 Analysis of grades 97
5.2.1.3 Analysis of student feedback 98
5.2.2 BIOL200 98
5.2.2.1 Problem set and walkthrough design and implementation 98
5.2.2.2 Collection and analysis of exam grades 99
5.2.2.3 Collection and analysis of student feedback 100
5.3 Results 103
5.3.1 BIOL362 103

5.3.1.1 BIOL362 demographics were highly similar between years 103
5.3.1.2 Assignment grades worsened with step-by-step worksheet 103
5.3.1.3 Student feedback improved with the example answer approach 105
5.3.2 BIOL200 106
5.3.2.1 BIOL200 students were demographically similar in both years 107
5.3.2.2 Walkthroughs improve the performance of lower-performing students 107
5.3.2.3 Almost all students use practice problems and answers 109
5.3.2.4 Students use problem walkthroughs differently than answer keys 109
5.3.2.5 Walkthroughs improved student attitudes about problem sets 111
5.3.2.6 Student survey responses varied over time 112
5.3.2.7 Walkthroughs help students learn and employ transferrable skills 113
5.3.2.8 Walkthroughs do not resolve a desire for more answers 115
5.4 Discussion 118
5.4.1 Example answers improve performance of more novice students 118
5.4.2 Example answers improve student attitudes 121
5.4.3 Example answers do not ameliorate students' desire for answer keys 122
5.4.4 Conclusions 124
Chapter 6: Conclusions and Future Directions 137
6.1 Major findings of Chapters 3 and 4 137
6.2 Outstanding questions and future directions 140
6.2.1 Continuing dissection of xylan biosynthesis in the Golgi 140
6.2.2 Further exploration of the concentric circle model of the Golgi 141
6.2.3 Exploration of the *irx9* Golgi phenotype 142
6.3 Example answers help support biology problem-solving 143
References 146
Appendices 166
Appendix A BIOL362 - Example Case Study 166
Appendix B BIOL362 - Step-By-Step Worksheet 172
Appendix C BIOL362 - Example Answer Worksheet 173
Appendix D BIOL200 - Problem Sets Excerpt 175

Appendix E BIOL200 - Problem Walkthroughs Excerpt 182
Appendix F BIOL200 - Exam Questions 189
Appendix G BIOL200 - Survey Questions 194
Appendix H BIOL200 - Survey Codebook 197
Appendix I BIOL200 - Interview Protocol 203

List of Tables

Table 2.1 Constructs generated and primers employed. 34
Table 2.2 Summary of confocal Golgi density experiments..... 35
Table 2.3 Primary antibodies used in this study. 35
Table 5.1 Themes identified in student feedback about BIOL362 assignment. 126
Table 5.2 BIOL200 final exam questions analyzed in this study. 126
Table 5.3 Demographics of the BIOL362 classes. 127
Table 5.4 Demographics of the BIOL200 classes. 127

List of Figures

Figure 1.1 Generalized structures of xylan. 19
Figure 1.2 Proteins involved in xylan biosynthesis in the Golgi. 20
Figure 1.3 Membrane trafficking to and from the Golgi Apparatus and TGN. 21
Figure 2.1 Golgi ultrastructure features measured. 33
Figure 3.1 Mutant dwarf and irregular xylem phenotypes are complemented by IRX9-GFP and IRX10-GFP. 54
Figure 3.2 Native expression and subcellular localization in IRX9-GFP and IRX10 GFP in roots. 55
Figure 3.3 Stages of SCW deposition characterized using confocal microscopy. 56
Figure 3.4 The stage of SCW development varies within populations of transdifferentiating cells. 57
Figure 3.5 Stages of SCW deposition characterized using TEM. 58
Figure 3.6 IRX9-GFP and MANI-mCherry colocalize in the Golgi apparatus. 59
Figure 3.7 Golgi abundance increases with SCW deposition in *WT* and *irx9* cells. 60
Figure 3.8 IRX9-GFP-labelled Golgi increase in density as SCW deposition progresses. 61
Figure 3.9 Golgi density increases during SCW production regardless of promoter or Golgi marker. 62
Figure 3.10 Bias in size of SCW-producing cells does not bias confocal density measures. 63
Figure 3.11 Cytoplasmic geometry constrains Golgi stacks to regions near SCWs. 64
Figure 4.1 Changes in cisternal length and number during SCW deposition in *WT* and *irx9*. 86
Figure 4.2 Changes in cisternal margins and TGN during SCW deposition in *WT* and *irx9*. 87
Figure 4.3 Changes in number of putative fenestrations during SCW deposition in *WT* and *irx9*. 88
Figure 4.4 Anti-xylan antibody labels Golgi, TGN and SCW. 89
Figure 4.5 Immunogold anti-GFP signal is higher in IRX9-GFP plants than No-GFP plants. 90
Figure 4.6 Mapping of IRX9-GFP and Xylan in the Golgi. 91
Figure 4.7 Concentric circle model of IRX9 and xylan position in Golgi. 92
Figure 5.1 Altering they type of assignment support affects student performance. 128
Figure 5.2 Student feedback about BIOL362 case study assignments. 129

Figure 5.3 Comparison of student performance on BIOL200 final exam questions with answer keys or walkthroughs. 130
Figure 5.4 Percent of BIOL200 student respondents for non-Likert survey questions for classes with answer keys (K) and walkthroughs (W). 131
Figure 5.5 Frequency of student activities from online survey responses for BIOL200 classes with answer keys (K) and walkthroughs (W). 132
Figure 5.6 Comparison of student attitudes from online survey responses for BIOL200 classes with answer keys (K) and walkthroughs (W). 134
Figure 5.7 Comparison of in-class and online survey responses for the BIOL200 class provided with walkthroughs. 134
Figure 5.8 The effect of problem-solving instruction on novices and experts. 135
Figure 5.9 The challenge and support model of scaffolding. 136

List of Symbols

°C	Degrees Celsius
F1	Filial 1 Hybrid
F2	Filial 2 Hybrid
L	Litre
M	Molar
mL	Millilitre
n	Sample Size
nm	Nanometers
p	Probability
pH	Potential Hydrogen
s	Second
T2	Transformation Generation 2
T3	Transformation Generation 3
µg	Micrograms
µm	Micrometers

List of Abbreviations

1AB	Primary Antibody
ABRC	Arabidopsis Biological Resource Center
AGX	Arabinoglucuronoxylan
ANCOVA	Analysis of Co-Variance
ANOVA	Analysis of Variance
Ara*f*	Arabinofuranose
Ara*p*	Arabinopyranose
Arf1	ADP-Ribosylation Factor 1 Protein
attB	Attachment site on Bacteria
AX	Arabinoxylan
BasR	Basta Resistant
BF	Bright Field
BiFC	Bimolecular Fluorescence Complementation
BIOL	Biology
bp	Base Pair
BY2	Bright Yellow 2
CCD	Charged-Coupled Device
CCRC	Complex Carbohydrate Research Center
CESA	Cellulose Synthase Protein
CI	Confidence Interval
CoA	Coenzyme A
CoIP	Coimmunoprecipitation
Col-0	Columbia-0 Arabidopsis Ecotype
COPI	Coat Protein One Protein
COPII	Coat Protein Two Protein
DBER	Discipline-Based Education Research
DEX	Dexamethasone
DNA	Deoxyribonucleic Acid
e.g.	Exempli Gratia (Latin)

ER	Endoplasmic Reticulum
ESK1	Eskimo 1 Protein
et al.	Et Alia (Latin)
etc.	Et Cetera (Latin)
F8H	Fragile Fibre 8 Homolog Protein
FACS	Fluorescence-Activated Cell Sorting
FRA8	Fragile Fibre 8 Protein
GATL	Galacturonosyltransferase-Like Protein
GAUT	Galacturonosyltransferase Protein
GAX	Glucuronoarabinoxylan
GFP	Green Fluorescent Protein
Glc	Glucose
GlcA	Glucuronic Acid
GLZ	Gaolaozhuangren Protein
GM	Germination Media
gntyp	Genotyping
GR	Glucocorticoid Receptor
GT	Glycosyltransferase
gtwy	Gateway
GUS	β-glucuronidase
GUX	Glucuronic Acid Xylosyltransferase Protein
GX	Glucuronoxylan
GXMT	Glucuronoxylan Methyltransferase Protein
hrs	Hours
i.e.	Id Est (Latin)
IgG	Immunoglobulin G
IgM	Immunoglobulin M
IRX	Irregular Xylem
K	Answer Keys
KanR	Kanamycin Resistant

LM10	Leeds Monoclonal Antibody 10
LP	Left Primer
LR	London Resin
MANI	Mannosidase I Protein
mCherry	Monoclonal Cherry (Red) Protein
Me	Methyl
MES	2-(N-morpholino)ethanesulfonic acid
min	Minutes
Mito	Mitochondrion
MS	Murashige and Skoog
N/A	Not Applicable
NFDM	Non-Fat Dried Milk
ns	Not Significant
NSF	N-ethylmaleimide-Sensitive Factor Protein
PCR	Polymerase Chain Reaction
PCW	Primary Cell Wall
PI	Propidium Iodide
PM	Plasma Membrane
Pro	Promoter
Q#	Question Number
REO	Reducing End Oligosaccharide
RGP	Reversibly Glycosylated Protein
RP	Right Primer
RWA	Relative Wall Acetylation Protein
SCW	Secondary Cell Wall
SoTL	Scholarship of Teaching and Learning
ST	Sialytransferase
STEM	Science Technology Engineering Math
SV	Secretory Vesicle
TA	Teaching Assistant

TBL	Trichome Birefringence Like Protein
TBST	Tris-Buffered Saline Tween
TEM	Transmission Electron Microscopy
TGN	Trans-Golgi Network
UAfT	UDP-Arabinose Furanosyl Transporter Protein
UBQ	Ubiquitin Protein
UDP	Uridine Diphosphate
UGD	UDP-Glucose Dehydrogenase Protein
UGE	UDP-Glucose Epimerase
UMP	UDP Monophosphate
UUAT	UDP-Uronic Acid Transporter Protein
UXE	UDP-Xylose Epimerase
UXS	UDP-Xylose Synthase Protein
UXT	UDP-Xylose Transporter Protein
VND	Vascular-Related NAC-Domain
VP16	Viral Protein 16
W	Walkthroughs
WT	Wild-Type
X^2	Chi-squared
XAT	Xylan-Arabinosyl Transferase Protein
Xyl	Xylose
YFP	Yellow Fluorescent Protein

Acknowledgements

Firstly, I want to thank my supervisor, Dr. Lacey Samuels, for her extraordinary mentorship over the last six years. Your kindness, patience, and enthusiasm have been instrumental in shaping this work and my growth as a scientist and educator. I am especially grateful for your encouragement and support in my interest in teaching, including adding a chapter in my thesis on education research.

My thanks also go to my co-supervisor, Dr. Shawn Mansfield, for welcoming me into his lab group and for providing a reliable source of insightful feedback. Additionally, I wish to thank my excellent committee members, Dr. Harry Brumer and Dr. Geoff Wasteneys, for the gift of their careful and considerate expert advice throughout my program. To all members of my committee, I greatly appreciate your willingness to support the inclusion of the scholarship of teaching and learning in my thesis, and to take on evaluating this research outside your areas of expertise.

Thanks also to the members of the Samuels and Mansfield labs, past and present, as well as many of the members of the UBC Botany department, for providing a welcoming and supportive community of friends and colleagues. These many individuals have contributed enormously to my success and happiness here at UBC. I especially want to thank Dr. Mathias Schuetz and Dr. Yoichiro (Yoshi) Watanabe, for their mentorship and advice over the past six years. Furthermore, I am greatly appreciative of the support provided by Dr. Robin Young, Dr. Sunita Chowrira, and Melissa Guzman when conducting my biology education research. Dipping my toes into a whole new field of research would have been immensely more daunting and challenging without your kind assistance. This list would not be complete without mentioning the excellent work of my undergraduate assistants, Sanya Motani, Sandeep Middar, and Freddy Francis, who took on and mastered new challenges in support of this research.

Funding for this work was provided by NSERC Canada Graduate Scholarships (Master's and Doctoral), a Four-Year Doctoral Fellowship from UBC, and the UBC affiliated Li-Tze Fong award. Additional funding was provided by the UBC Public Scholars Initiative and the Working on Walls CREATE grant.

Finally, to my family, thank you for your love and support.

Chapter 1: Introduction

In plant cells the Golgi apparatus plays an essential role in glycoprotein processing, protein trafficking, and cell wall polysaccharide biosynthesis. These three functions are combined in the production of the patterned secondary cell walls (SCWs) which provide structural support to water-conducting xylem tracheary elements. This thesis uses xylan biosynthesis in the Arabidopsis Golgi as a model to investigate the structure, arrangement, and organization of the Golgi apparatus throughout SCW synthesis, to lend insight into how the Golgi produces and secretes large quantities of polysaccharide cargo.

1.1 Plant cell walls

The successful colonization of land by plants is due in part to the development of supportive and adaptable extracellular cell walls. The walls must be strong enough to resist the osmotic forces of turgor pressure, which pushes the plasma membrane against the wall, but malleable enough to allow expansion and growth of the cells. Spatial and temporal regulation of this balancing act allows plants to fine tune features such as cell shape and cell growth, thereby facilitating appropriate development of the plant and physiological responses. Cell walls are divided into primary cell walls (PCWs) or secondary cell walls (SCWs), based on differences in their composition and the timing of their deposition. PCWs are deposited as the cells continue to divide and expand, while the SCWs produced by some cell types are classically defined by their deposition after cell elongation has completed (Meents et al., 2018).

Both PCWs and SCWs contain cellulose, the load-bearing scaffolding of the cell wall, which is synthesized by complexes of cellulose synthase (CESA) proteins that move through the plasma membrane (McFarlane et al., 2014). The linear glucan chains extruded into the apoplast by these complexes are aligned in bundles called microfibrils, and their orientation in the wall is carefully controlled, as it contributes to the physical properties of the wall (Barnett and Bonham, 2004). Hemicelluloses are believed to cross-link the cellulose microfibrils, providing additional support. They consist of a more varied group of polysaccharides, generally grouped by the β-(1,4) linkages connecting the sugars in their backbones (Scheller and Ulvskov, 2010). The predominant hemicellulose of eudicot PCWs are the xyloglucans, with a glucose backbone and various patterns of oligosaccharide side chains (Pauly and Keegstra, 2016). The most abundant

hemicellulose of grass PCWs are arabinoxylans, which have a xylose backbone and simpler glucose or arabinose side chains (Rennie and Scheller, 2014). The walls of grasses also contain mixed linkage glucans, which differ in that the glucose molecules in their backbones are linked by a mixture of β-(1,3)- and β-(1,4) bonds (Burton and Fincher, 2009). The final polysaccharide component of PCWs are the pectins, which are thought to provide a matrix around the cellulose and hemicelluloses, where they affect the hydration of the wall, its firmness, and its structural integrity (Atmodjo et al., 2013; Anderson, 2016). Pectins have extremely diverse structures, varying from the almost linear homogalacturonan, to the highly branched rhamnogalacturonan II, though they have in common an abundance of galacturonic acid sugars. Unlike cellulose, hemicelluloses and pectins are synthesized intracellularly in the Golgi apparatus by various glycosyltransferases and other enzymes, prior to secretion to the apoplast where they are integrated into the wall (Atmodjo et al., 2013; Rennie and Scheller, 2014).

SCWs provide additional structural reinforcement to water conducting tracheary elements, to help these cells withstand the pressures of water transport, and fibres, which support the plant body. Disruption of normal SCW deposition in a wide array of mutants typically results in a dwarf growth phenotype and collapsed xylem tracheary elements (called irregular xylem; *irx*), illustrating the importance of proper SCW deposition for normal plant growth and development (Brown et al., 2005). To achieve the necessary strength and rigidity for SCWs, the extensibility and flexibility features of the PCW must be sacrificed (Cosgrove and Jarvis, 2012), and the composition of SCWs differs from that of PCWs to facilitate this change in function. One of the biggest differences is the deposition of a non-polysaccharide component called lignin. Lignin is a phenolic polymer, whose monolignol monomers derive from phenylalanine (Bonawitz and Chapple, 2010; Dixon et al., 2014). The monolignols are synthesized in the cytoplasm and exported to the apoplast where they polymerize at random with the assistance of secreted oxidative enzymes such as laccases and peroxidases (Meents et al., 2018).

The cellulose of SCWs is produced by a different set of CESA isoforms, and they produce cellulose with an increased degree of polymerization and with a different orientation and organization, thereby affecting the properties of the wall (Meents et al., 2018). While SCWs contain hemicelluloses, they are usually a different kind than is found in the PCW, usually xylans and mannans (Scheller and Ulvskov, 2010). Mannans are the most abundant

hemicellulose in conifer SCWs, and smaller amounts are also found in the walls of eudicots and grasses (Rodríguez-Gacio et al., 2012). These carbohydrates have a β-(1,4)-linked backbone of mannose and glucose, and in conifers, sidechains of galactose are observed. Xylans of the eudicot SCW are characterized by a β-(1,4)-linked xylose backbone, decorated with sidechains of glucuronic acid, while conifer xylans are also substituted with varying amounts of arabinose (Ebringerová, 2005). Xylans are essential for water transport and growth, as Arabidopsis mutants defective in xylan biosynthesis exhibit dwarf growth and collapsed xylem phenotypes (Rennie and Scheller, 2014). However, despite its importance, many aspects of xylan biosynthesis remain unresolved.

1.2 Xylan structure and biosynthesis

1.2.1 Xylan diversity in plants and algae

Xylans are a group of hemicelluloses having in common a xylose backbone. While the walls of some green algae contain (1,3)-β-xylans, and some red algae and Plantago seeds have (1,3),(1,4)-β-xylans in their walls, in land plants the xylan backbone is almost invariably composed of β-(1,4)-linked xylosyl residues (Ebringerová and Heinze, 2000; Popper et al., 2011; Domozych et al., 2012) (Figure 1.1). Xylans are then classified according to the type and degree of backbone substitution. Glucuronoxylans (GX) are substituted at the O-2 position by glucuronic acid, which may in turn be methylated. GX is the major hemicellulose component of eudicot SCWs (Scheller and Ulvskov, 2010), but may also be present in the SCWs of some monocots (Peña et al., 2016). Xylans can also be substituted with arabinose at the O-3 and/or O-2 position, producing arabinoglucuronoxylans (AGX), glucuronoarabinoxylans (GAX), and arabinoxylans (AX), depending on the degree of arabinose versus glucuronic acid substitution (Ebringerová, 2005). Arabinose-substituted xylans are generally absent from the SCW of eudicots, found in small amounts in the PCW of eudicots and conifers, and in greater quantities in the PCW and SCW of grasses and SCW of conifers (Scheller and Ulvskov, 2010; Peña et al., 2016). The arabinosyl residues of grasses can also be substituted at the O-5 position by phenolic acids like ferulic acid and *p*-coumaric acid, which can become cross-linked with lignin in SCWs (Scheller and Ulvskov, 2010). Like many cell wall polysaccharides, xylans are also often acetylated, in the case of xylan at the O-2 and/or O-3 position(s) (Gille and Pauly, 2012). GXs in

a variety of eudicots, gymnosperms and non-grass monocots also have a β-Xyl-(1,3)-α-Rha-(1,2)-α-Gal-(1,4)-β-Xyl sequence at their reducing end, sometimes referred to as a reducing end oligosaccharide (REO) (Scheller and Ulvskov, 2010; Peña et al., 2016). The REO has been hypothesized to be either a primer for synthesis of the xylan backbone, or a terminator sequence transferred to the reducing end upon completion of backbone synthesis (York and O'Neill, 2008).

In SCWs xylans interact with cellulose, by assuming a two-fold helical screw structure, allowing the unsubstituted face of the xylan to form hydrogen bonds with the hydrophilic surface of cellulose microfibrils (Busse-Wicher et al., 2014; Simmons et al., 2016). The even distribution of xylan backbone substitutions is therefore essential for proper xylan conformation in the wall, as has been demonstrated using mutants with altered acetyl and glucuronic acid substitution patterns (Grantham et al., 2017). An even pattern of substitutions has been found in both angiosperms and gymnosperms, and has therefore been proposed to be an important feature of xylans across the vascular plants (Busse-Wicher et al., 2016). This substitution pattern is set up during synthesis and processing of xylan by biosynthetic proteins in the Golgi, however, it is unclear how these biosynthetic proteins work together to assemble xylans of the appropriate structure.

1.2.2 Xylan biosynthesis in the Golgi

Synthesis of xylan requires the concerted action of several dozen proteins in the cytosol and Golgi, including substrate biosynthetic enzymes, substrate transporters, and glycosyltransferases (GTs) (Figure 1.2). Golgi-localized GTs assemble the polysaccharide using activated nucleotide sugars, while other enzymes are important for the addition of non-sugar side chains like methyl and acetyl groups. Current models predict that a complex of GTs in the Golgi use UDP-xylose to synthesize the xylan backbone. Two GTs from Glycosyltransferase Family 43 (GT43) called IRREGULAR XYLEM 9 (IRX9) and IRREGULAR XYLEM 14 (IRX14), and a member of GT47 called IRREGULAR XYLEM 10 (IRX10), were identified by their co-expression with SCW CESAs (Brown et al., 2005; Brown et al., 2007). Double mutant analysis revealed that these three proteins are partially redundant with their respective paralogs (IRX9L, IRX10L and IRX14L), and loss-of-function mutations result in dwarf growth phenotypes,

reduced xylan content, and lower xylosyltransferase activity (Brown et al., 2007; Peña et al., 2007; Brown et al., 2009; Wu et al., 2009; Keppler and Showalter, 2010; Lee et al., 2010; Wu et al., 2010). The interaction of these GTs was demonstrated using co-immunoprecipitation (CoIP) and bimolecular fluorescence complementation (BiFC) in the production of arabinoxylans in PCWs of wheat (*Triticum aestivum*) and asparagus (*Asparagus officianalis*), indicating that the xylan biosynthetic proteins orthologous to the Arabidopsis proteins have the potential to form a xylan biosynthetic complex (Zeng et al., 2010; Jiang et al., 2016; Zeng et al., 2016). Each protein was also proposed to homodimerize in planta. The formation of a core xylan biosynthetic complex containing IRX9, IRX10 and IRX14 may also be a prerequisite for their localization in the Golgi, as transiently expressed asparagus and wheat proteins were retained in the ER unless co-expressed with the other two proteins (Jiang et al., 2016; Zeng et al., 2016).

The different functions of IRX9, IRX10 and IRX14 in a xylan biosynthetic complex have been dissected using site-directed mutagenesis of the Arabidopsis (Ren et al., 2014) and asparagus proteins (Zeng et al., 2016). Mutation of the proposed glycosyltransferase catalytic site or the UDP-xylose substrate-binding domain of IRX9/IRX9L did not impede complementation of the mutant phenotype, or xylosyltransferase activity of the biosynthetic complex, indicating that their function may be structural, rather than enzymatic (Ren et al., 2014; Zeng et al., 2016). IRX14 has been proposed to be important for substrate binding (Zeng et al., 2016) or priming of xylan synthesis (Ren et al., 2014), as its function was impaired when the predicted substrate-binding site was mutated. Finally, catalytic function has been ascribed to IRX10/IRX10L, as heterologously expressed Arabidopsis IRX10L has been shown to have xylan xylosyltransferase activity *in vitro* (Urbanowicz et al., 2014). This function is likely to be conserved among IRX10 orthologues and paralogues, as xylosyltransferase activity has also been observed for IRX10 from psyllium (*Plantago ovata*) and *Physcomitrella patens* (Jensen et al., 2014). The above experiments suggest that SCW xylan backbone synthesis may be carried out by a xylan biosynthetic complex in the Golgi. However, it is unclear if this complex forms in the ER or the Golgi, and where precisely in the Golgi it might be active.

A xylan biosynthetic complex could also include a number of other proteins known to synthesize or transport substrate molecules, or to add various side-chains. Firstly, xylan biosynthesis requires the presence of the nucleotide sugar substrate, UDP-Xylose. UDP-Xylose

may be converted from xylose-1-phosphate by a pyrophosphorylase, or interconverted from UDP-arabionopyranose by UDP-Xylose Epimerases (UXEs), but the majority of UDP-Xylose is formed by the non-reversible decarboxylation of UDP-glucuronic acid by UDP-Xylose Synthases (UXSs) (Bar-Peled and O'Neill, 2011). Interestingly, three of the UXS isoforms in Arabidopsis have been localized to the Golgi and three to the cytosol, but it is the cytosolic UXS3, UXS5 and UXS6 that are important for xylan synthesis in Arabidopsis stem SCWs (Harper and Bar-Peled, 2002; Pattathil et al., 2005; Kuang et al., 2016; Zhong et al., 2016). The UDP-xylose is then transported into the Golgi by UDP-Xylose Transporters (UXTs), primarily UXT1, which has been hypothesized to associate with the xylan biosynthetic complex to ensure adequate substrate availability (Ebert et al., 2015).

Furthermore, as mentioned above, the interaction of xylan with other SCW components, such as cellulose microfibrils, is dependent on the side chains decorating the xylan, which are added by different sets of proteins. Members of the GT8 GUX family of proteins are xylan glucuronosyltransferases responsible for the majority of xylan glucuronic acid (GlcA) substitution, demonstrated by a lack of xylan glucuronyltransferase activity and loss of GlcA substitutions on the xylan backbone in GUX family mutants (Mortimer et al., 2010; Rennie et al., 2012). GUX1 and GUX2 add GlcA substitutions in different patterns, which contribute to the final shape of the xylan and therefore its function in the wall (Bromley et al., 2013). UDP-GlcA is synthesized from UDP-Glc in the cytosol by a UDP-Glc Dehydrogenase (UGD), or from a phosphorylated glucuronic acid by a UDP-sugar pyrophosphorylase (Bar-Peled and O'Neill, 2011). Recently the transporter UUAT was found to transport both UDP-GlcA and UDP-GalA, however the mutant had no reduction in GlcA substitution of xylan, perhaps due to functional redundancy with other nucleotide sugar transporters (Saez-Aguayo et al., 2017).

Methylation of the GlcA residues is catalyzed by glucuronoxylan methyltransferases (GXMTs) (Lee et al., 2012; Urbanowicz et al., 2012). The IRX15/IRX15L proteins have also been implicated in xylan methylation, but a catalytic function has not yet been demonstrated (Brown et al., 2011; Jensen et al., 2011). Instead these proteins may form a structural component of a methylation protein complex (Urbanowicz et al., 2012; Rennie and Scheller, 2014). Xylan is acetylated primarily by the protein ESK1^{TBL29}, (Xiong et al., 2013; Yuan et al., 2013; Urbanowicz et al., 2014) though other TBL proteins also acetylate xylan at different positions

and with different affinities (Yuan et al., 2016b; Yuan et al., 2016a; Zhong et al., 2017). A set of RELATIVE WALL ACETYLATION proteins are hypothesized to transport the substrate for xylan acetylation into the Golgi (Lee et al., 2011; Manabe et al., 2011; Gille and Pauly, 2012; Manabe et al., 2013).

Synthesis of the REO is not well understood, though three sets of GTs have been implicated in REO production based on the absence of the REOs in the cell walls of their mutants. These include the GT8 proteins IRX8^{GAUT12} (Peña et al., 2007; Persson et al., 2007) and PARVUS^{GATL,GLZ1} (Lao et al., 2003; Brown et al., 2007; Lee et al., 2007), and the GT47 proteins FRA8^{IRX7} and F8H^{IRX7L} (Zhong et al., 2005; Brown et al., 2007; Lee et al., 2009).

Each of the proteins described above contributes in some manner to xylan biosynthesis, however it is unclear how the cell coordinates their activity in the Golgi to ensure the proper production of xylan molecules for the SCW. The spatial distribution of these proteins within the Golgi is likely to contribute to this coordination, either by forming biosynthetic complexes to increase the efficiency of some processes, or segregating steps which occur successively or independently. This hypothesis can be tested by examining the distribution of xylan biosynthetic proteins in the Golgi stack.

1.3 The plant Golgi apparatus

It is clear that the numerous proteins and processes involved in xylan biosynthesis are coordinated in the Golgi apparatus, but arrangement of the xylan biosynthetic machinery in the Golgi is not known. The Golgi is an organelle at the center of the eukaryotic endomembrane system (Mowbrey and Dacks, 2009). Newly synthesized proteins from the endoplasmic reticulum (ER) must pass through the Golgi to be secreted from the cell, or to reach target destinations like the plasma membrane or the vacuole. Aside from this vital role in protein trafficking, the Golgi also specializes in the processing of glycoproteins and, in plants, the synthesis of several polysaccharide components of cell walls including xylan. Despite these essential cellular functions, many aspects of Golgi biology are still a mystery, including how complex biosynthetic processes like xylan production occur inside the Golgi. While the Golgi is typically depicted in cell wall reviews as a single large membrane sphere (see Figure 1.2), a much more complex picture of Golgi structure is observed using microscopy.

1.3.1 Conservation of Golgi structure and function

In many organisms, the Golgi consists of a stack of flattened membranous structures called cisternae (Figure 1.3). Within each cisterna is an internal space called the lumen, which contains the various proteins and substrates necessary for Golgi processing, as well as their products, including xylans. There is a distinct structural and functional polarity to the cisternae in the Golgi, starting with the ER-associated *cis*-Golgi cisterna, transitioning to the central medial-Golgi cisterna, followed by the *trans*-Golgi which associates with the Trans-Golgi Network (TGN) (Papanikou and Glick, 2014). The *cis*-cisterna exchanges membrane and proteins via vesicular traffic with the ER, including Coat Protein II (COPII)-mediated anterograde vesicle trafficking of materials for distribution throughout the cell, and COPI-mediated retrograde vesicle trafficking of escaped ER proteins and trafficking machinery (Brandizzi and Barlowe, 2013). The bulk of Golgi processing is believed to occur in the medial Golgi, where COPI plays additional roles in intra-Golgi trafficking (Day et al., 2013; Papanikou and Glick, 2014). At the other end of the Golgi, the TGN is a hub for the sorting and trafficking of materials headed to and from the Golgi, plasma membrane and vacuole (Rosquete et al., 2018). This is where cell wall polysaccharides are packaged into secretory vesicle clusters for export to the cell wall (Toyooka et al., 2009). A variety of coat proteins are observed at the TGN, including COPI and clathrin, but large secretory vesicles (SVs) are also prevalent (Kang et al., 2011). The change in function across the Golgi from *cis* to *trans* are accompanied by alteration in cisternal structure and composition. Moving from the *cis*-Golgi to the TGN, the cisternae become more elongated, the margins begin to swell, the protein and lipid composition changes, the lumen in the cisternal centers becomes more compressed, and the lumen becomes more acidic (Day et al., 2013; Shen et al., 2013; Papanikou and Glick, 2014).

Despite evolutionary conservation of many structural and functional features of the Golgi (Klute et al., 2011), there are also some species with interesting exceptions (Mowbrey and Dacks, 2009). In most species, including plants, the Golgi cisternae are stacked one on top of the other from *cis* to *trans*. However, in several fungal species, including the model yeast *Saccharomyces cerevisiae*, cisternae are not stacked, but are distributed individually within the cytoplasm (Preuss et al., 1992). There is also variation in the extent of connectedness between

stacks. In most eukaryotes, individual Golgi stacks are not physically connected and are dispersed throughout the cytoplasm. In vertebrates however, most cells have a highly complicated network of interconnected Golgi stacks, called the Golgi ribbon, which is largely immobile and found adjacent to the nucleus (Nakamura et al., 2012). Despite these differences in structure, the Golgi in these organisms carry out many of the same cellular functions as in plant cells, illustrating that Golgi structure can be highly plastic and still carry out conserved functions.

The process by which materials move through the Golgi has been a subject of debate for decades (Luini, 2011). Several models have been proposed to explain how the protein and polysaccharide products (*i.e.* Golgi cargo) traverse the Golgi stack from *cis* to *trans*, while the proteins carrying out cargo synthesis and modification (*i.e.* Golgi residents) are maintained in the Golgi. There is very strong support for a cisternal maturation model, which posits that cargo traverse the Golgi as the cisternae change over time from *cis*, to medial and then *trans*-cisternae (Glick and Luini, 2011). During this process, the population of resident proteins in the cisterna changes, as *cis*-type residents are replaced by more *trans*-type residents via retrograde trafficking from later to earlier cisternae. In the case of xylan production, this implies that xylan moves through the Golgi with the maturation of the cisternae, while the xylan biosynthetic enzymes are retained in the stack via active recycling to previous cisternae. The cisternal maturation model suggests that the *cis*-most Golgi compartment forms *de novo*, becoming the youngest in a maturing Golgi stack. At the opposite face of the Golgi, the *trans*-most cisternae are predicted to be shed from the Golgi, presumably maturing into TGN and secretory vesicles (Kang et al., 2011). While there is strong evidence supporting maturation of Golgi cisternae (Becker et al., 1995; Bonfanti et al., 1998; Losev et al., 2006; Matsuura-Tokita et al., 2006; Rizzo et al., 2013) the mechanisms of Golgi processing are not fully resolved, as other data cannot be explained via cisternal maturation alone (Glick and Luini, 2011). For example, artificial cisternal ‘staples’ remain trapped in *cis*-cisternae instead of progressing as predicted by the cisternal maturation model (Lavieu et al., 2013) and both cargo and residents have been observed to undergo intra-Golgi trafficking (Park et al., 2015).

1.3.2 Coordination of Golgi stacks in the Golgi apparatus

The number of Golgi stacks in a cell varies widely, from a single stack in the green algae *Chlamydomonas*, to thousands in large cotton fibres (Andreeva et al., 1998). The abundance of Golgi stacks also depends on developmental stage and cell type. For example, during development of the epidermis of Arabidopsis seeds, the number of Golgi stacks doubles, coinciding with the production of large quantities of pectin-rich cell wall mucilage in the Golgi (Young et al., 2008). Interestingly, the number of Golgi continues to double in the MUCILAGE MODIFIED 4 (MUM4) mutant deficient in pectin production, indicating that accumulation of polysaccharide cargo is not driving the increase in the number of Golgi stacks in these cells. Additionally, in tobacco BY2 cell cultures, the number of Golgi stacks present in cultures undergoing log growth was double that of non-dividing stationary cells (Toyooka et al., 2014). This increase is Golgi stacks is likely tied with the cell cycle, as the number of Golgi stacks also doubles prior to mitosis (Garcia-Herdugo et al., 1988; Seguí-Simarro and Staehelin, 2006). Despite this variation in Golgi abundance, the regulatory mechanisms controlling increases in Golgi number are not well understood.

Plant Golgi stacks are believed to proliferate by increasing Golgi diameter, followed by cisternal fission, cutting the stack in half (Ito et al., 2014). This model is supported by electron microscopy of plant Golgi with elongated and partially divided cisternae (Hirose and Komamine, 1989; Langhans et al., 2007; Staehelin and Kang, 2008). It is possible that the increase in cisternal membrane prior to division is tied to increased ER-Golgi traffic of protein cargo or Golgi residents. This may explain why Golgi proliferation appears to be tied to increased demand for Golgi processing. Identifying other circumstances in which Golgi proliferate may provide an insight into this process.

Another feature of the Golgi is its ability to carry out various kinds of glycoprotein processing and polysaccharide biosynthesis simultaneously. Immunolabelling of the PCW polysaccharides pectin and xyloglucan in the root cap and seed coat epidermis indicated that individual Golgi stacks produce both kinds of cargo at once (Zhang and Staehelin, 1992; Young et al., 2008). Similarly, Golgi in carrot suspension culture cells contained both secreted glycoproteins and polysaccharide cargo (Moore et al., 1991). Like xylan biosynthesis, all these processes require a host of proteins in the Golgi, such as GTs and transporters. It is unclear how

these disparate processes can be accommodated within the tight confines of the Golgi cisternae, though the formation of biosynthetic complexes (Oikawa et al., 2013), and spatial segregation of different processing steps (Schoberer and Strasser, 2011), have been proposed to facilitate efficient production. Similar Golgi multitasking has not yet been shown to occur during SCW synthesis, though it has been hypothesized that xylan and mannan biosynthesis, as well glycoprotein processing and protein trafficking, occur simultaneously in Golgi stacks during SCW production (Meents et al., 2018).

The plant Golgi apparatus is also interesting in that the individual stacks are highly mobile, characterized by rapid cytoplasmic streaming on the actin-myosin network, interrupted by occasional pausing (Boevink et al., 1998; Nebenführ et al., 1999). Secretion to targeted domains may be facilitated by directing Golgi stacks to desired sites of secretion. Indeed, a reported 85% of Golgi were found 'underneath' forming SCW bands when fluorescently-tagged Golgi were imaged using confocal microscopy (Schneider et al., 2017). Golgi may therefore be preferentially localized near the site of SCW deposition, where xylan and other Golgi cargo need to be released. However, this model does not agree with observations in other cell types, where Golgi appear to be evenly distributed despite ongoing targeted secretion. For example, Golgi were not concentrated near the seed surface in Arabidopsis epidermal seed coat cells, where large pectin-rich mucilage pockets form (Young et al., 2008). Similarly, Golgi are distributed throughout the cortical cytoplasm of Arabidopsis trichomes, and are not clustered near the forming branches (Lu et al., 2005). Furthermore, Golgi are found throughout the cytoplasm of tip-growing cells like pollen tubes and root hairs (Wei et al., 2005; Peremyslov et al., 2008; Cai et al., 2015). As the localization of Golgi to targeted domains during SCW deposition appears to differ from these other examples, additional investigation into Golgi distribution in this system is worthwhile.

1.3.3 Relationship between Golgi ultrastructure and function

Altering membrane fission and fusion dynamics can have a significant impact on the morphology of membranous organelles (Voeltz and Prinz, 2007). The Golgi is particularly sensitive to such perturbations, as it is a trafficking hub of the endomembrane system, regularly sending and receiving materials to and from the ER and TGN, as well as between individual

cisternae (Figure 1.3). Disruption of these processes can have strong effects on Golgi structure. For example, a forward-genetics approach in Arabidopsis identified a mutation in the N-ethylmaleimide-sensitive factor (NSF) protein which resets membrane docking machinery, and these mutant plants had alterations in the number and size of Golgi cisternae (Tanabashi et al., 2018). As such, characterization of Golgi ultrastructure, and how it changes with Golgi function, or in different mutant backgrounds, can provide an insight into how the Golgi works.

The number of cisternae in a Golgi stack varies with cell type, developmental stage, and species. In many plant species Golgi stacks contain 5 to 7 cisternae (Staehelin et al., 1990; Zhang and Staehelin, 1992; Samuels et al., 2002), while the alga *Scherffelia dubia* can have 20 cisternae in a stack (Becker et al., 1995; Donohoe et al., 2013) and the protist *Euglena* as many as 30 cisternae (Becker and Melkonian, 1996). Furthermore, a small increase in cisternal number is seen in root tip columella cells, compared to the root meristem (Staehelin et al., 1990). It is unclear what factors determine the number of cisternae in a stack, but it may be linked to the speed of cisternal maturation. In the yeast *Saccharomyces cerevisiae*, a disruption of Golgi processing, due to loss of the COPI and clathrin recruiting protein Arf1, results in a decrease in the speed of maturation of *cis*-cisternae, leading to an increase in the number of cisternae in the cell (Bhave et al., 2014). Interestingly, the Golgi cisternae in these cells also increased in diameter, suggesting the rate of maturation may also influence cisternal size. Plant Golgi stacks range from 0.5 to 2 μm in diameter, in a wide variety of cell types and plant species (Hirose and Komamine, 1989; Staehelin et al., 1990; Zhang and Staehelin, 1992). Within this range however, the diameter of Golgi can vary with cell type and developmental stage. For example, the Golgi in root cells almost double in diameter during differentiation from meristem into columella cells (Staehelin et al., 1990). As mentioned previously, an increase in the diameter of Golgi cisternae is thought to be a preliminary step in the fission of Golgi stacks to produce new stacks (Ito et al., 2014). As such, differences in Golgi diameter are also seen at different cell cycle stages, prior to an increase in the number of Golgi stacks (Hirose and Komamine, 1989; Seguí-Simarro and Staehelin, 2006).

Variation in cisternal number and diameter may also be accompanied by alterations in the shape of cisternae. The flattened cisternae slowly change shape from *cis* to *trans*; becoming longer, with more tightly compressed centers, and swollen margins (Staehelin et al., 1990; Zhang

and Staehelin, 1992; Samuels et al., 2002; Young et al., 2008; Wang et al., 2017). These differences in membrane structure reflect the contents of the membrane and lumen in each cisterna, as well as the membrane trafficking that is occurring. The impact of membrane trafficking can be seen in the *cis*-most cisterna, for example, which often has an irregular structure, as it acquires new membrane from ER-derived COPII-coated vesicles (Donohoe et al., 2013). Alternately, membrane proteins and lipids can facilitate the formation of highly curved membranes when introduced asymmetrically into the lipid bilayer (Voeltz and Prinz, 2007). Lastly, soluble cell wall polysaccharides accumulate in the margins of more *trans* cisternae, where they likely drive the swelling of these cisternal margins (Zhang and Staehelin, 1992; Samuels et al., 2002; Young et al., 2008; Wang et al., 2017). As a consequence of this close relationship between Golgi structure and function, the rapid production of large amounts of xylan for Arabidopsis SCWs is likely also having a drastic effect on Golgi structure. Investigating the nature of these changes in Golgi structure could therefore provide insight into Golgi function in general, and xylan biosynthesis in particular.

The polar structure of cisternae in a Golgi stack may also reflect the sequential processing of glycoproteins and polysaccharide cargo from *cis*-to-*trans*. Studies across eukaryotes provide examples of Golgi processing pathways where resident proteins and products are detected sequentially from *cis* to *trans* in the order they appear in the pathway. In plants, this is best characterized in the trimming and decoration of oligosaccharides for N-glycan processing (Schoberer and Strasser, 2011). In polysaccharide biosynthesis, xyloglucan biosynthetic enzymes were found preferentially in the *cis*, medial or *trans*-cisternae in the order they are believed to act during xyloglucan synthesis (Chevalier et al., 2010) However, these biosynthetic enzymes are typically in very low abundance, making experiments of this type difficult to conduct and interpret. For many polysaccharides, the order in which synthesis occurs is often entirely, or largely unknown. For example, while synthesis of the xylan backbone must occur before addition of sidechains, these side chains may be added nearly sequentially, or later in the Golgi. Furthermore, the REO has been proposed to be either a primer of xylan biosynthesis onto which the xylan backbone is synthesized, or a terminator transferred *en bloc* at the end of a finished xylan chain (York and O'Neill, 2008). A primer must be synthesized prior to backbone synthesis, while a terminator may be produced in parallel with xylan synthesis, and then added to

the xylan backbone later in the Golgi. The order in which xylan biosynthesis is conducted may be investigated by determining the order in which various biosynthetic enzymes and related proteins appear in the stack of Golgi cisternae.

The margins of Golgi cisternae are also often associated with vesicles, tubules, and fenestrations. In mammalian cells, COPI-coated vesicles are involved in intra-Golgi retrograde transport of Golgi resident proteins, while COPI tubules can mediate transport in both the anterograde and retrograde directions (Yang et al., 2011; Park et al., 2015). While COPI-coated tubules have not yet been reported in plant Golgi, intra-Golgi COPI vesicles have been identified (Donohoe et al., 2007). The cisternae of mammalian, yeast and plant Golgi can also be fenestrated to various extents (Mogelsvang et al., 2003; Mogelsvang et al., 2004; Koga and Ushiki, 2006; Kang and Staehelin, 2008; Kang et al., 2011; Donohoe et al., 2013). The function of fenestrations is not currently known, though they have been hypothesized to function as 'spot welds' to help prevent swelling of cisternae, to introduce membrane curvature to aid in vesicle formation, or as pathways facilitating the movement of materials through the cytoplasm (Ladinsky et al., 1999).

Less elaborated membrane regions are seen at the sheet-like center of the Golgi stack. This region has been proposed to contain arrays of GTs producing cell wall polysaccharides (Staehelin et al., 1990). More recently, cryo-focused ion beam milling and cryo-electron tomography of *Chlamydomonas* Golgi confirmed that the central regions of *trans*-cisternae contain protein arrays bridging the Golgi lumen, which may represent oligomerized GTs or structural proteins helping maintain cisternal shape and organization (Engel et al., 2015). Characterization of the distribution of GTs across the Golgi in finer resolution could clarify the function of these flattened cisternal centers.

Lastly, the TGN is a post-Golgi compartment composed of a network of tubules and vesicles, and acts as a hub of anterograde, retrograde and endocytic trafficking (Rosquete et al., 2018). In the cisternal maturation model, the TGN is postulated to form from the maturing trans-Golgi cisterna, as the cisternal structure collapses and Golgi-resident proteins are recycled back to the Golgi (Kang et al., 2011). When newly formed, the TGN will be closely associated with a Golgi stack, but is hypothesized to eventually dissociate into a free TGN (Kang et al., 2011). The structure of the TGN is interpreted to reflect the nature and abundance of the materials being

trafficked. COPI-coated vesicles are likely important for retrograde trafficking to the Golgi, clathrin coated vesicles for vacuolar sorting, and un-coated secretory vesicles for secretion of proteins and cell wall polysaccharides to the plasma membrane (Kang et al., 2011). Indeed, disruption of TGN function by loss-of-function of TGN-trafficking proteins such as *echidna* or *yips* can have dramatic effects on the structure of the plant TGN (Boutté et al., 2013). The many roles of the TGN have made it challenging to dissect the relationship between TGN structure and function. In SCW synthesis, these challenges are exacerbated by the dynamic traffic of SCW CESAs (Watanabe et al., 2015; Schneider et al., 2017) and the large volume of cell wall material being packaged at the TGN.

While there appear to be strong connections between various structural features of the Golgi apparatus and TGN, and the function of these organelles, many questions remain. Furthermore, our understanding of Golgi structure and function comes largely from studies of Golgi producing PCW polysaccharides, and it is unclear how applicable these studies are to other cell types, including cells producing SCWs. Examining the Golgi apparatus during SCW synthesis in Arabidopsis is a good candidate as a model system, as large amounts of xylan are produced, many highly-expressed xylan biosynthetic enzymes have been identified, and it is amenable to genetic manipulation and imaging.

1.4 Protoxylem tracheary element differentiation as a model system

While the protein machinery contributing glucuronoxylan biosynthesis is rapidly being elucidated (Figure 1.2), there remain many questions about where and how these proteins function in the complex and dynamic environment of the Golgi apparatus. Studying glucuronoxylan biosynthesis during SCW deposition has been challenging, as the cells producing SCWs are often less amenable to microscopy techniques, being relatively few in number, buried deep in plant organs, and often dead at maturity. These challenges can be addressed by taking advantage of an Arabidopsis model system that uses an inducible version of a ubiquitously expressed transcription factor called VASCULAR-RELATED NAC-DOMAIN 7 (VND7), which is a master regulator of protoxylem development (Kubo et al., 2005; Yamaguchi et al., 2008). In these plant lines, VND7 has been fused to an activating domain (VP16) and a glucocorticoid receptor (GR), and ubiquitously expressed. When treated with a glucocorticoid

hormone like dexamethasone (DEX), VND7 is activated, and cells throughout these plants begin to transdifferentiate into protoxylem tracheary elements with helical SCWs (Yamaguchi et al., 2010a). This system has been used successfully in studies examining the localization and movement of oxidative enzymes involved in lignification (Schuetz et al., 2014; Chou et al., 2018), vesicle fusion machinery (Vukašinović et al., 2017), and the sub-cellular dynamics of SCW CESAs (Watanabe et al., 2015; Li et al., 2016; Watanabe et al., 2018). Induction of VND7 activity is accompanied by increased glucuronoxylan production and elevated expression of xylan biosynthetic proteins such as IRX9 and IRX10 (Yamaguchi et al., 2011), making this an ideal system for studying xylan biosynthesis in the Golgi. A benefit of the VND7 induction system is that strong expression of xylan biosynthetic proteins can be triggered by their native promoters. Golgi localized proteins are frequently not abundant in the cell, making their localization challenging (Fukuda et al., 1996). However, over-expression of proteins using non-native promoters can lead to overexpression artefacts, including mislocalization of the protein (Brandizzi et al., 2004; Moore and Murphy, 2009). The protoxylem transdifferentiation model system allows introduction and localization of GFP-tagged versions of xylan biosynthetic proteins driven by their native promoters, providing greater confidence in the localization of these proteins within the cell.

1.5 Research questions

This study aims to localize xylan biosynthesis within the Golgi apparatus and individual Golgi stacks, to better understand how xylan biosynthesis occurs during SCW synthesis, and how the plant Golgi apparatus is organized more broadly. In doing this I will address the following questions:

1. **Does the number of Golgi stacks increase with the onset of SCW production?**
   The number of Golgi stacks in a cell appears to increase with increased demand for Golgi processing, including production of cell wall polysaccharides for the PCW (Garcia-Herdugo et al., 1988; Seguí-Simarro and Staehelin, 2006; Young et al., 2008; Toyooka et al., 2014). I therefore hypothesize that the number of Golgi stacks will increase similarly in order to accommodate the xylan production required for SCW deposition.

2. **Are all Golgi stacks in the Golgi apparatus participating in xylan biosynthesis?**
   During PCW production, individual Golgi stacks do not appear to have specialized functions (Moore et al., 1991; Zhang and Staehelin, 1992; Young et al., 2008). As such, I predict that all Golgi will similarly participate in xylan biosynthesis during SCW production.
3. **Do Golgi stacks preferentially associate with the plasma membrane lining SCW domains?**
   Live-cell imaging of fluorescently-labelled Golgi during protoxylem tracheary element development suggests that most Golgi stacks are found in very close proximity to SCW bands (Schneider et al., 2017). This distribution may be actively maintained by the cell to facilitate targeted secretion of Golgi cargo at SCW domains, in which case I would hypothesize that Golgi stacks will be closer to these sites of deposition than random.
4. **Does the structure of Golgi stacks change in response to the onset of SCW production and how is this altered in a xylan biosynthetic mutant?**
   Golgi structure can vary greatly in different cell types and developmental stages, especially when the Golgi begin producing greater quantities of polysaccharides (Staehelin et al., 1990; Zhang and Staehelin, 1992; Samuels et al., 2002; Young et al., 2008; Wang et al., 2017). Similar changes in Golgi structure are therefore predicted to occur during SCW synthesis in protoxylem tracheary elements, including an increase in the size of the swollen Golgi margins, the diameter of Golgi cisternae, and the size of secretory vesicles.
5. **How are xylan biosynthetic enzymes and their product distributed within a Golgi stack?**
   Golgi-resident glycosyltransferases have been predicted to be located in the cisternal centers of Golgi stacks, while Golgi cargo accumulates in the swollen margins (Staehelin et al., 1990). I therefore hypothesize that a similar distribution of xylan biosynthetic enzymes (in cisternal centers) and xylan (in the margins) will be observed during SCW deposition. Furthermore, xylans are predicted to be most abundant in *trans*-cisternae, as has been observed in other cell types for pectins and hemicelluloses (Zhang and Staehelin, 1992; Samuels et al., 2002; Young et al., 2008; Wang et al., 2017).

In Chapter 3, I address the first three questions concerning the function and distribution of the population of Golgi stacks which comprise the Golgi apparatus. I generated a fluorescently-tagged version of the xylan biosynthetic protein IRX9, driven by its native promoter, and introduced this into the VND7-induction system. I then used a combination of live-cell imaging and transmission electron microscopy (TEM) to examine the population of Golgi stacks prior to SCW deposition, and after triggering transdifferentiation into protoxylem tracheary elements by inducing VND7.

In Chapter 4, I address the final two questions, focusing more specifically on xylan production in individual Golgi stacks. Using the materials generated in Chapter 3, I conducted nanoscale mapping of wild-type Golgi ultrastructure prior to and during SCW deposition, and during SCW synthesis in the xylan biosynthetic mutant *irx9-2*. I then used immnoTEM to localize IRX9-GFP and xylan within specific regions of individual Golgi cisternae to reconcile the biochemistry of xylan backbone synthesis with a high-resolution understanding of Golgi structure during SCW synthesis.

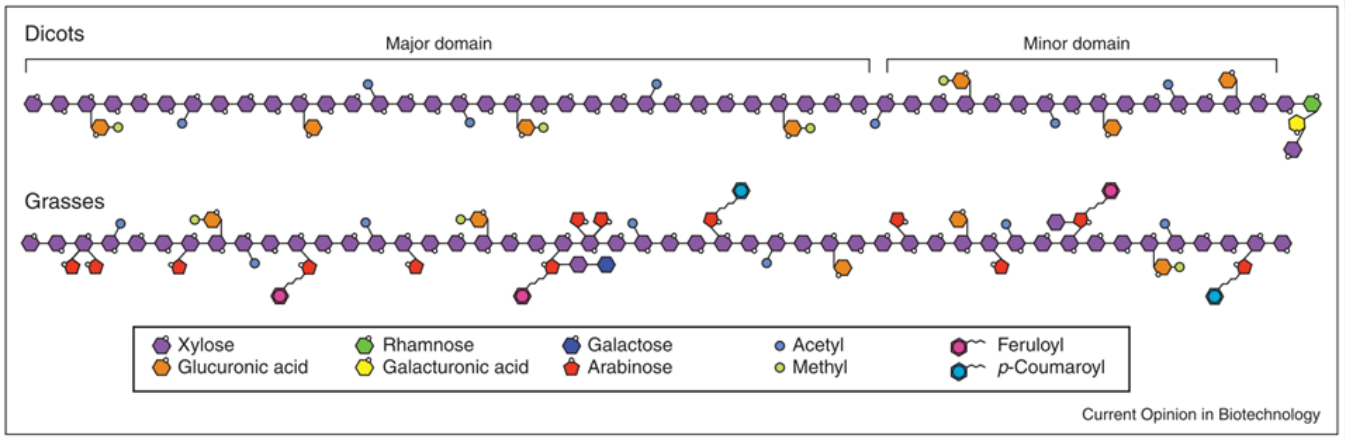

Figure 1.1 Generalized structures of xylan.

Eudicot xylan is substituted with GlcA, Me-GlcA, and acetate. Arabinose substitutions may be present but are frequently not found. The major domain has (Me-) GlcA on evenly spaced residues about eight xylose units apart, while the minor domain has (Me-) Glc more closely spaced. Rhamnose and galacturonic acid are found at the reducing end. In grasses, xylan may also be substituted with arabinose, xylose, galactose, and ferulic and coumaric acid. Reproduced with permission from Rennie and Scheller (2014) Copyright Elsevier © 2014 (**doi.org/10.1016/j.copbio.2013.11.013**).

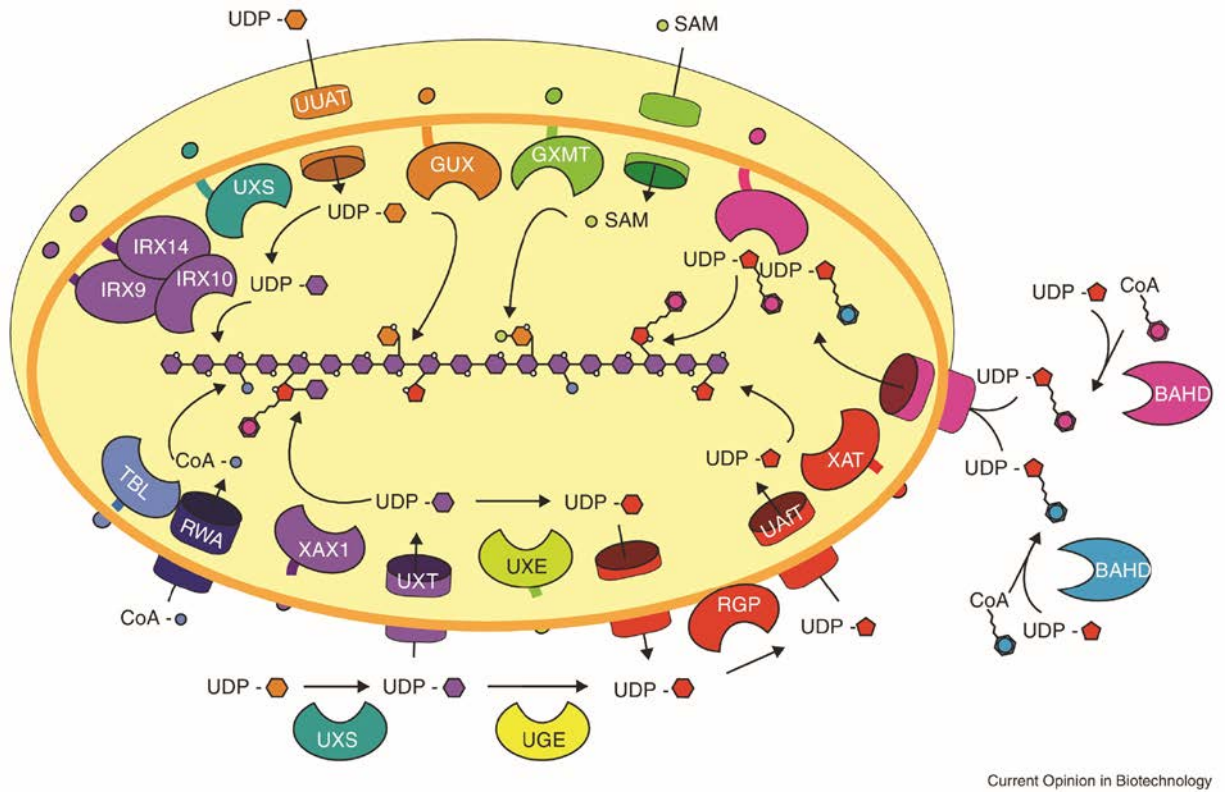

Figure 1.2 Proteins involved in xylan biosynthesis in the Golgi.

Xylan is synthesized in the Golgi apparatus by Type II membrane proteins anchored by a single N-terminal transmembrane domain and with their catalytic domains in the Golgi lumen. Some proteins, such as IRX10, are predicted to lack transmembrane domains. Substrates are synthesized in both the cytosol and in the lumen. UDP-GlcA is transported into the Golgi likely by a UDP-Uronic Acid Transporter (UUAT) (Saez-Aguayo et al., 2017) and converted into UDP-Xyl by UDP-Xyl Synthase (UXS). Another isoform of UXS is present in the cytosol, and UDP-Xyl synthesized there can be transported into the Golgi by a UDP-Xylose Transporter (UXT) (Ebert et al., 2015). The cytosolic UXS proteins are the major supplier of UDP-Xyl for xylan synthesis (Kuang et al., 2016; Zhong et al., 2016). UDP-Xyl is converted to UDP-Ara*p* inside the Golgi by UDP-Xyl Epimerase (UXE) and UDP-Ara*p* is converted to UDP-Ara*f* by the mutase Reversibly Glycosylated Protein (RGP), located on the outer Golgi membrane (Rautengarten et al., 2011). A transporter moves UDP-Ara*p* out of the Golgi, and UDP-Ara*f* is returned to the lumen by UDP-Arabinose furanosyl Transporters (UAfTs) (Rautengarten et al., 2017). Some isoforms of cytoplasmic UDP-Glc Epimerase (UGE) may also contribute to the conversion of UDP-Xyl to UDP-Ara*p*. UDP-Ara*f* is added to xylan by a Xylan-Arabinosyl Transferase (XAT) (Anders et al., 2012). BAHD acyltransferases in the cytosol are involved in xylan synthesis, and presumably transfer ferulic acid to an intermediate, such as UDP-Araf, which is then transported into the Golgi and transferred onto xylan by unknown proteins. Acetate is likely added to xylan by a family of Trichome Birefringence-like (TBL) proteins (Xiong et al., 2013; Yuan et al., 2013; Urbanowicz et al., 2014; Yuan et al., 2016b; Yuan et al., 2016a; Zhong et al., 2017). Reduced Wall Acetylation (RWA) proteins are also involved in acetylation and may serve as acetyl-CoA transporters (Lee et al., 2011; Manabe et al., 2011; Manabe et al., 2013). S-Adenosylmethionine, the substrate for xylan methylation, is synthesized in the cytosol and must also be transported into the lumen. Not shown are tranporters for coproducts such as CoA, and S0adneosyl homocysteine, which must be removed from the Golgi and recycled in the cytosol. UMP is removed from the Golgi by nucleotide sugar transporters, which function as antiporters. Modified from Rennie and Scheller (2014). Reproduced with permission; Copyright Elsevier © 2014 (**doi.org/10.1016/j.copbio.2013.11.013**).

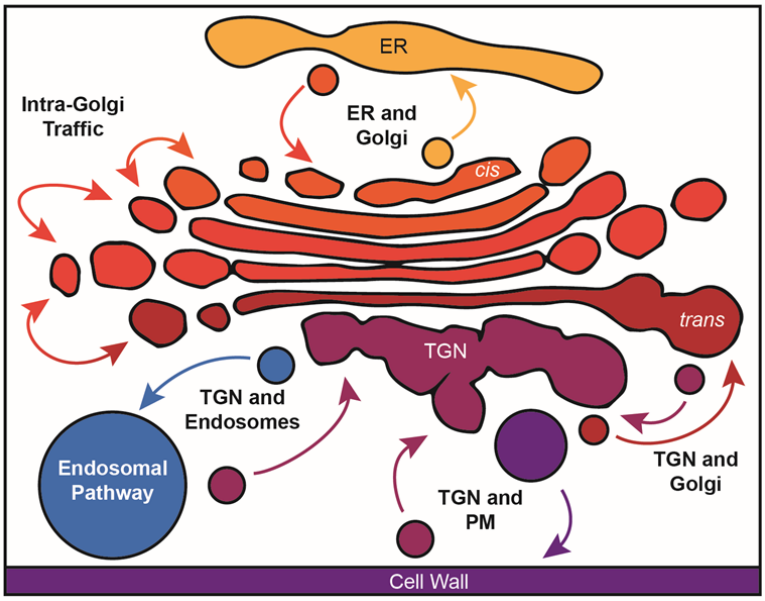

Figure 1.3 Membrane trafficking to and from the Golgi Apparatus and TGN.

The Golgi exchanges materials with the endoplasmic reticulum (ER), the Trans Golgi Network (TGN), the plasma membrane (PM), and organelles of the endosomal pathway like pre-vacuolar compartments. Individual Golgi cisternae also exchange membrane and cargo via intra-Golgi trafficking.

Chapter 2: Materials and Methods

This chapter provides detailed descriptions of the methods used to generate the results described in Chapters 3 and 4.

2.1 Plant materials and growth conditions

All Arabidopsis (*Arabidopsis thanliana*) seeds were sterilized using chlorine gas in a sealed container containing 100 mL of bleach and 3 mL of concentrated HCl for 3 - 6 hrs. Seeds were then plated on Germination Media (GM) [1x Murashige and Skoog (MS) 1% Sucrose, 1x Gamborg's Vitamin mix, 0.05% MES, 0.8% agar at pH 5.8] and then transferred to growth conditions. Plants were grown under long-day conditions (16 hrs light / 8 hrs dark) at 21 °C in a vertical position. The *irx9-2* (*irx9*) mutant line (SALK_057033) was obtained from the Arabidopsis Biological Resource Center (ABRC). The *irx10irx10L* (SALK055673 and GABI179G11) double mutant was obtained from Simon Turner (Brown et al., 2005; Brown et al., 2009). *35S:VND7-VP16-GR* seeds and plasmid were obtained from Taku Demura (Yamaguchi et al., 2010a). To induce VND7-VP16-GR activity, 4- to 7-day-old seedlings were treated with 10 ml of 10 µM dexamethasone (DEX) (Sigma) for 17 - 36 hrs, depending on the experiment. The Arabidopsis Columbia-0 ecotype was used to generate all transgenic lines using *Agrobacterium tumefaciens* (strain GV3101) and the floral dip method (Clough and Bent, 1998). Primary transformants were selected by plating on GM plates containing 50 µg/mL kanamycin, 25 µg/mL hygromycin, or 25 µg/mL Basta.

2.2 Generation of constructs

Constructs were primarily generated using Gateway cloning (Invitrogen), including PCR amplification with *att*B sequences (Table 2.1), Gateway Clonase-mediated insertion into a donor vector, and then transfer to the destination vector. PCR was conducted with Phusion High Fidelity DNA polymerase (New England Biolabs) followed by two-step adapter PCR to incorporate the full *att*B sequences for Gateway cloning.

The native promoters used for *IRX9* (AT2G37090) and *IRX10* (AT1G27440) consist of the 2045 bp and 828 bp intergenic sequences upstream of the start codon for each respective gene, as in published promoter-GUS experiments (Wu et al., 2009; Wu et al., 2010).

ProIRX9:IRX9 and *proIRX10:IRX10* were amplified from genomic DNA and cloned into pDONRzeo, and then into pMDC100 (Curtis and Grossniklaus, 2003) to incorporate an in-frame C-terminal GFP and stop codon, thereby generating *proIRX9:IRX9-GFP* and *proIRX10:IRX10-GFP*. *IRX9* and *IRX10* coding sequences were also amplified and cloned into pDONRzeo and then pMDC44, to add a *35S* promoter and an N-terminal GFP tag, resulting in *35S:GFP-IRX9* and *35S:GFP-IRX10*. The restriction sites SbfI and KpnI were then used to swap out the *35S* promoter for *proIRX9* or *proIRX10* to produce *proIRX9:GFP-IRX9* and *proIRX10:GFP-IRX10*, respectively. Note that *proIRX10* included the *IRX10* signal sequence upstream of the GFP, to ensure correct insertion of GFP-IRX10 into the ER.

Seeds and plasmids containing a *35S*-driven version of *Glycine max MANI-mCherry* were available (Nelson et al., 2007), but signal was largely absent due to silencing. To address this, *proUBQ10:MANI-mCherry* was generated by amplifying *MANI-mCherry* from the available *35S*-driven construct and cloned into pDONRzeo, and then pUB-DEST to add the *proUBQ10* promoter and an appropriate terminator (Grefen et al., 2010). To introduce an alternate promoter, *MANI-mCherry+terminator* was amplified and inserted into pDONRzeo and then pMDC100. The terminator sequence was included as this last plasmid does not contain a terminator downstream of the Gateway cloning site. The *proIRX9* and *proIRX10* sequences were then inserted using KpnI and AscI restriction sites to generate *proIRX9:MANI-mCherry* and *proIRX10:MANI-mCherry*, respectively.

Alternate versions of the published *35S:VND7-VP16-GR* (Kanamycin resistant; KanR) construct (Yamaguchi et al., 2010a) were generated to reduce ongoing silencing problems believed to be exacerbated by the *35S* promoter, and to provide an alternate plant selectable-marker for combining with the above *MANI*, *IRX9* and *IRX10* constructs. *VND7-VP16-GR* was amplified from the existing plasmid and cloned into pDONRzeo and then into pUB-DEST to generate *proUBQ10:VND7-VP16-GR* (Basta resistant; BasR), or pB2GW7 to generate *pro35S:VND7-VP16-GR* (BasR).

2.3 Complementation testing

Proper function of *proIRX9:IRX9-GFP* was tested by transforming the *irx9* mutant and looking for complementation of its dwarf and collapsed xylem phenotypes (Lee et al., 2010; Wu

et al., 2010). As *irx10* does not have an obvious phenotype, and *irx10irx10L* plants are sterile (Brown et al., 2009; Wu et al., 2009), function of *proIRX10:IRX10-GFP* was tested by transforming *irx10(±)irx10L* plants, and looking for complementation of the growth and xylem defects from *irx10irx10L,* in a subsequent generation. Restoration of wild-type height was measured in 40-day-old plants and averaged for 5 plants in each of the wild-type, mutant and complemented lines. Complementation of the irregular xylem (irx) phenotype was observed in hand sections from the bottom 1 cm of mature wild-type, mutant, and complemented inflorescence stems stained with 0.01% toluidine blue (Ted Pella) for 5 min and imaged on a Leica DMR microscope equipped with a QICAM digital camera (QIMAGING). Images were prepared in Image J.

2.4 Confocal microscopy

2.4.1 Expression of *proIRX9:IRX9-GFP* and *proIRX10:IRX10:GFP*

Live-cell imaging of *irx9/proIRX9:IRX9-GFP* and *irx10irx10L/proIRX10:IRX10-GFP* was conducted on a Perkin-Elmer UltraView VoX spinning disk confocal mounted on a Leica DMI6000 inverted microscope with a Hamamatsu 9100-02 CCD camera. Samples were mounted in water and expression in developing tracheary elements in the root was observed using a glycerol 20x objective (aperture 0.7), 488 nm excitation filter and 525 emission filter (GFP). All images were acquired using Volocity image analysis software (Improvision) and prepared in Image J.

The brightest *irx9/proIRX9:IRX9-GFP* and *irx10irx10L/proIRX10:IRX10-GFP* lines were transformed with *proUBQ10:VND7-VP16-GR* (BasR) or *35S:VND7-VP16-GR* (BasR). The T2 seedlings were treated with DEX and screened using brightfield imaging to identify lines with the greatest number of inducing cells as a measure of induction quality. Lines with sufficient inducing cells were then observed on the Perkin-Elmer spinning disk set-up, described above, using a 63X objective (aperture 1.2). Subsequent experiments revealed reliable induction for a single *irx9*/*proIRX9:IRX9-GFP*/*proUBQ10:VND7-VP16-GR* line, which was therefore selected for additional experiments. However, subsequent generations of this line suffered from decreases in successful SCW-production and IRX9-GFP expression, presumably due to silencing. To address this, *proIRX9:IRX9-GFP* was next transformed into a strongly-inducing *35S:VND7-*

VP16-GR (KanR) line from Taku Demura, and a number of suitable transformants were identified when T2 seeds were induced with DEX and screened for induction strength and intensity of IRX9-GFP expression. The brightest and best-inducing line was selected for further experiments, but later found to contain multiple copies of *proIRX9:IRX9-GFP* based on a X^2 analysis in Excel of T3 segregation ratios. This analysis also identified a secondary line with a single insertion of *proIRX9:IRX9-GFP*. The experiments utilizing each proIRX9:IRX9-GFP line (in the *irx9* background, or in the wild-type background with single or multiple insertions) are identified when used.

The developmental time-course of *proIRX9:IRX9-GFP* expression and IRX9-GFP subcellular localization was determined by imaging plants at two-hour increments from 17 - 30 hrs following induction with DEX in *proIRX9:IRX9-GFP* (2+ copies) */35S:VND7-VP16-GR* seedlings. Cells were categorized as 'Early' if a secondary cell wall was not visible in brightfield imaging, but IRX9-GFP was expressed. 'Mid'-development coincided with the appearance of faint SCWs in brightfield, and 'Late' development was defined by obvious SCWs. The differences in deposition of the SCW during these stages was validated by separate experiments where imaging of IRX9-GFP and SCWs in brightfield coincided with staining of the cell wall with 10 µg/ml propidium iodide (PI) for 5 min.

2.4.2 Golgi stack abundance

To quantify Golgi abundance throughout SCW deposition, plant cells expressing Golgi-localized proteins were imaged on a Perkin-Elmer UltraView VoX spinning disk confocal mounted on a Leica DMI DMi8 and a Hamamatsu VOXC9100-23B camera with a glycerol 63x objective (aperture 1.2) and the following excitation and emission filters: GFP (488, 525), RFP (561, 595). The plant lines examined, and number of experiments, seedlings and cells imaged, are given in Table 2.2. Pre-SCW-synthesis Golgi density was assessed using the *proUBQ10:MANI-mCherry* (*WT*.UMANI) line, and compared to Golgi density in SCW-producing cells using different Golgi-localized proteins (IRX9-GFP or MANI-mCherry) driven by different promoters (*proIRX9, proUBQ10*). All plants were treated with DEX for 17 - 30 hrs before imaging and at least three plants were imaged per time point for each experiment. For each cell analyzed, a single optical section through the cell cortex was selected and the number

of Golgi-like puncta was divided by the cell area in the section to calculate the Golgi density. All images were processed using Volocity image analysis software (Improvision) and Image J.

As stage of development varies from cell to cell in any one plant, the appearance of the SCW in brightfield imaging was used to assign the stage of SCW deposition, according to the definitions laid out in the previous time-course experiments. Approximately ten cells per plant were analyzed, unless VND7-induced SCW production was less successful, therefore limiting the number of cells available to be imaged (*WT*.VND7.UMANI, *WT*.VND7.9MANI, *WT*.VND7.IRX9+MANI). In these cases, all cells producing SCWs and/or expressing the protein of interest were analyzed. Replicate experiments were conducted for all plant lines with the exception of plants were very poor induction (Table 2.2) as these plants were deemed unsuitable for future experiments.

Over the various experiments it was noticed that smaller cells seemed more likely than larger cells to begin SCW synthesis upon DEX treatment. If Golgi density correlates with cell size, this would introduce a bias into the Golgi density measurements following SCW-synthesis. To investigate this possibility, in one of the experiments described above cell size was also calculated by measuring maximum cell width in brightfield for the Pre-SCW (90 cells), Early-SCW (80 cells), Mid-SCW (342 cells) and Late-SCW (113 cells) stages. The relationship between cell size and Golgi density was assessed in Excel (Microsoft) via regression analysis for all cells, and the cells in each stage.

2.4.3 Colocalization

Colocalization of IRX9-GFP and MANI-mCherry was conducted in F1 crosses of *proIRX9:IRX9-GFP*(2+ copies)*/pro35S:VND7-VP16-GR* with either *proUBQ10:MANI-mCherry* or *proIRX9:MANI-mCherry*. Plants were imaged on a Perkin-Elmer UltraView VoX spinning disk confocal mounted on a Leica DMI DMi8 and a Hamamatsu 9100-02 CCD camera and an immersion oil 100x objective (aperture 1.47). Extremely low numbers of cells expressing both *proIRX9:IRX9-GFP* and *proIRX9:MANI-mCherry* prevented quantification of colocalization in this cross. However, while suitable IRX9-GFP and MANI-RFP expression was also very low in the *proUBQ10:MANI-mCherry* cross, sufficient numbers of cells (26 cells) and seedlings (5 plants) were imaged to allow quantification of colocalization via Pearson's Correlation

Coefficient (PCC) and Mander's overlap coefficients (Manders et al., 1993) in Volocity (Improvision). All images were prepared in Image J.

2.5 TEM imaging

2.5.1 Sample preparation and imaging

For TEM analysis, hypocotyls and petioles of 4-day-old seedlings were high-pressure frozen, freeze-substituted, sectioned, and prepared for TEM as previously described (McFarlane et al., 2008). Briefly, dissected samples were loaded into copper hats (Ted Pella) with 1-hexadecene as a cryoprotectant, and high-pressure frozen using a Leica HPM-100 high-pressure freezer. Samples were transferred to freeze-substitution medium containing 2% (w/v) osmium tetroxide and 8% (v/v) dimethoxypropane in anhydrous acetone for morphological analysis, or 0.25% (v/v) glutaraldehyde, 0.1% (w/v) uranyl acetate, and 8% (v/v) dimethoxypropane in acetone for immunolabelling. Freeze substitution was performed for 5 days at -80 °C using an acetone/dry ice slush. Samples were transferred to -20 °C overnight, followed by 4 °C for 2 hrs, and transferred to room temperature. Samples were removed from the sample holders and rinsed in anhydrous acetone several times, before slowly infiltrating over the course of 4 days with increasing concentrations of Spurr's resin (Electron Microscopy Services) for analysis of morphology, or LR White for immunolabelling (London Resin Company Ltd.). Following polymerization at 60 °C, samples were sectioned using a Leica Ultracut UCT Ultramicrotome (Leica Microsystems). Thin sections (70 - 80 nm thick) were post-stained using 2% uranyl acetate in 70% methanol and Reynolds lead citrate and viewed on a Hitachi H7600 PC-TEM at an accelerating voltage of 80 kV. Photographs were taken using an ATM Advantage HR digital CCD camera and figures prepared in Image J.

2.5.2 Ultrastructure quantification

Golgi ultrastructure was quantified in TEM images of DEX-treated *WT* (*WT* Pre-SCW), *WT/35S:VND7-VP16-GR* (*WT* SCW), and *irx9/proUB10:VND7-VP16-GR* (*irx9* SCW) seedlings. For *WT/35S:VND7-VP16-GR*, Golgi were analyzed from both 16 - 18 hrs-induced (*WT* Early-SCW) and 22 - 30 hrs-induced (*WT* Late-SCW) plants. For each of *WT* Pre-SCW, *WT* Early-SCW, *WT* Late-SCW and *irx9* SCW, quantification data was collected from Golgi in cells with

visible SCWs from replicate seedlings (5, 5, 7, 3 respectively) and experiments (2, 2, 2, 1 respectively).

The '*cis*' cisternae were identified by lighter staining, visible lumen in the cisternal center, and smaller margins than cisternae on the opposite side of the stack (Staehelin et al., 1990; Samuels et al., 2002). The '*trans*' cisterna was defined as the last structure on the *trans*-face with a flattened, cisterna-like region. Cisternae adjacent to *cis* and *trans* were designated '*cis*+1' and '*trans*-1', respectively, and the remaining intervening cisterna(e) classified as 'mid' (Figure 2.1). The number of fenestrations in each cisterna was estimated by counting cisternal 'gaps' in 28 - 37 Golgi cross-sections for each developmental stage or genotype. These gaps, defined as breaks in a cisterna or regions of lighter staining corresponding with indentations in the cisternal membrane (Figure 2.1), were assumed to be fenestrations based on published Golgi tomography and transverse-sections of cisternae (Mollenhauer and Morré, 1998; Donohoe et al., 2013). Cisternal diameters were determined for 34 - 40 Golgi by measuring the length of each cisterna from one edge to the other (Figure 2.1). Golgi width was calculated by averaging cisternal diameter for *cis*+1, mid and *trans*-1 cisternae. *Cis* and *trans* cisternae were excluded as their structures were assumed to be changing rapidly as the cisterna forms or collapses, respectively. Cisternal margins are known to become swollen in more-*trans* cisternae (Staehelin et al., 1990; Samuels et al., 2002). Margin size across cisternae was therefore quantified in 34 - 38 Golgi by measuring the diameter of the margins of each cisterna (Figure 2.1). The diameter of 233 - 518 round profiles on TGN was also quantified to estimate the size of budding or secretory vesicles in 28 - 61 TGN (Figure 2.1). All measurements were conducted in ImageJ.

2.5.3 Organelle abundance

For each cell quantified, the number of Golgi or mitochondria (counts) were summed from non-overlapping images of the cell cortex in *WT* Pre-SCW, *WT* Late-SCW and *irx9* SCW cells. For the purposes of quantification of organelle abundance in TEM, Golgi counts included vesicle aggregations, as sections through cisternal margins could not be easily distinguished from the TGN. Counts/perimeter was then calculated by dividing the number of counts in each cell by the length of the cell perimeter in the images from which the counts were obtained. The area of cytoplasm in each image was then determined (excluding the vacuole, cell wall, plastids,

nucleus, and ER-bodies ~ 1 μm^2 or larger) and summed for all images in each cell. Counts/area was calculated by dividing the number of counts in each cell by this summed area. Increases in Golgi diameter would increase the probability of sectioning through individual Golgi in a cell, thereby artificially increasing Golgi counts using this method. To account for this, the percent increase in Golgi width between *WT* Pre-SCW and *WT* Late-SCW or *irx9* SCW was divided from the respective Golgi/perimeter and Golgi/area averages, thereby normalizing them to the width of *WT* Golgi. Average cytoplasm thickness was determined by dividing the measured perimeter length from the cytoplasmic area. For all parameters quantified, values were averaged for 31 cells taken from 4 - 5 seedlings prepared in 3 replicate experiments (*WT* Pre-SCW and *WT* Late-SCW) or 13 cells from 3 seedlings in 1 experiment (*irx9* SCW).

2.5.4 Organelle position

A subset of the images from the *WT* Late-SCW TEM organelle abundance quantifications were used to estimate the distance to the forming SCW from Golgi/TGN, mitochondria or random positions in the cytoplasm. A 500 nm grid was laid over each image, and Excel's random number generator used to select random points on the grid that a Golgi/mitochondrion could be found (ie. excluding the vacuole, cell wall, nucleus, plastids, and large ER bodies). The shortest distance between each Golgi, mitochondrion and random point and the nearest SCW was then measured. For each image, the same number of random points were selected as were Golgi/TGN in the image, giving 168 measures for Golgi and random points, and 114 measures for mitochondria, in 16 cells from 5 seedlings and 3 replicate experiments.

2.5.5 Immunogold labelling and mapping

Primary anti-xylan (Carbosource) and anti-GFP (Torrey Pine Biolabs and Invitrogen) antibodies used in this study are given in Table 2.3. Each antibody was tested at a variety of concentrations as outlined in the results, and CCRC M138 and Torrey Pines anti-GFP were selected for carrying out Golgi mapping. The strong non-specific binding of the Invitrogen anti-GFP was seen in SCWs and the Golgi, making it unsuitable for anti-GFP labelling in SCW-producing cells. Secondary antibodies included goat anti-rat (LM10), goat anti-mouse (CCRC antibodies) and goat anti-rabbit (anti-GFP) antibodies conjugated to 10 nm colloidal gold (Ted

Pella). For immunogold labelling, *WT* Late-SCW or *IRX9-GFP* Late-SCW (*proIRX9:IRX9-GFP* 2+copies/*35S:VND7-VP16-GR*) samples were induced for 22 – 24 hrs before high-pressure freezing, freeze-substitution, and embedding in LR-white, as described above. Formvar-coated nickel grids with 70 nm sections were blocked with 5% (w/v) non-fat dry milk (NFDM) in 1x Tris-buffered saline/ 0.1% (v/v) Tween 20 (TBST) for 20 min. After blotting to remove excess blocking solution, grids were transferred to the primary antibody which was undiluted (CCRC M-138) or diluted 1:50 with 1% (w/v) NFDM in 1x TBST (Torey Pines anti-GFP) for 60 min. After rinsing with 1x TBST, grids were transferred to appropriate secondary antibodies diluted 1:100 in 1% (w/v) NFDM in 1x TBST for 60 min, rinsed again with 1x TBST and then thoroughly washed with distilled water. Grids were post-stained for 5 min in uranyl acetate and 2 min in lead citrate before imaging as described above.

Ideal antibodies for Golgi mapping would have sufficient label in the Golgi of the cells making SCWs, but little or no label in negative controls. To assess this signal-to-noise ratio, anti-xylan labelling in *IRX9-GFP* Late-SCW cells with SCWs was compared to cells in the same seedling not making SCWs, and to cells with SCWs but not exposed to the primary antibody. Anti-GFP antibodies were tested by comparing labelling in *IRX9-GFP* Late-SCW to similar cells in the *WT* Late-SCW samples, as well as *IRX9-GFP* Late-SCW samples not exposed to the primary antibody. Quantification of gold label in anti-xylan negative controls, and anti-GFP no-primary-antibody controls, was unnecessary as they contained virtually no gold label. For comparison of anti-GFP label in *IRX9-GFP* Late-SCW and *WT* Late-SCW all Golgi in each cell examined were imaged and the number of gold particles in each Golgi was counted. For this purpose, 493 Golgi/TGN in 39 cells (*IRX9-GFP* Late-SCW) and 277 Golgi/TGN in 19 cells (*WT* Late-SCW) were imaged from 4 seedlings in 2 replicate experiments. The difference between anti-GFP label and non-specific binding was demonstrated by comparing the number of gold particles labelling Golgi in *IRX9-GFP* Late-SCW and *WT* Late-SCW.

Quantitative mapping in IRX9-GFP was completed using CCRC M-138 for xylan labelling, and Torrey Pines anti-GFP for IRX9-GFP labelling. Every gold particle in a cell labelling the Golgi or TGN was quantified, and the position of gold particles in the Golgi was assessed when plane-of-section and sample preservation permitted. The results shown consist of data from 24 cells (xylan mapping) and 39 cells (GFP mapping) from 4 seedlings and 2 replicate

experiments. This resulted in the high-resolution mapping of 136 gold particles in 17 cells (xylan mapping) and 182 gold particles in 33 cells (GFP mapping).

The cisterna with gold label was identified according to the parameters outlined in the ultrastructure characterization section above. The distance between the gold particle and the cisternal edge, as well was the diameter of the cisterna, was measured. The distance to the cisternal center was calculated by dividing the cisternal width in two and subtracting the distance to the cisternal edge. To compare the cisternal position of xylan and GFP label, the average distance to cisternal centers and cisternal edges was calculated, irrespective of which cisterna the gold particle was found in. To map the distribution of gold label across Golgi width, the distance to the cisternal edge was converted into a percent of Golgi width for each gold particle. Gold particles mapping to the same cisterna, and the same 10% block of cisternal width, were binned together for generation of the labelling heat maps. While mapping of gold label to the TGN was largely independent of plane of section and preservation quality, only ~50% Golgi label could be accurately mapped to a specific region of individual cisternae. As such, the amount of TGN label could not be directly compared to the Golgi-mapping frequencies. Instead, the proportion of TGN vs Golgi label prior to mapping was used to scale down the amount of TGN label to coincide with the amount of Golgi label that was actually mapped. Heat map colours were generated in Excel (Microsoft) based on these final distributions. For easier comparison of Golgi structure and the mapping distributions, the heat map colours were then manually transferred to a realistic Golgi outline based on Golgi ultrastructure imaging.

2.6 Statistical analysis

Statistical analysis was conducted using SPSS 25 (IBM). Before comparison of means, normality was assessed visually using histograms and Q-Q plots, supplemented with Kolgomov-Smirnov and Shapiro-Wilkes tests. If the data was approximately normally distributed a t-test for independent means was used to compare two means, or a one-way analysis of variance (ANOVA) used to compare more than two means. If the ANOVA showed a significant difference, Tukey HSD *post-hoc* analysis was conducted to identify significant differences. If the data was non-normal, data transformations were applied as indicated in the results, and normality re-tested as described above. If normality was achieved, the above parametric procedures were

followed. If the data continued to be non-normal, non-parametric tests were performed with either the Mann-Whitney test (U) for two means, or the Kruskal-Wallis test (H) for more than two means followed by *post-hoc* analysis using Dunn's procedure.

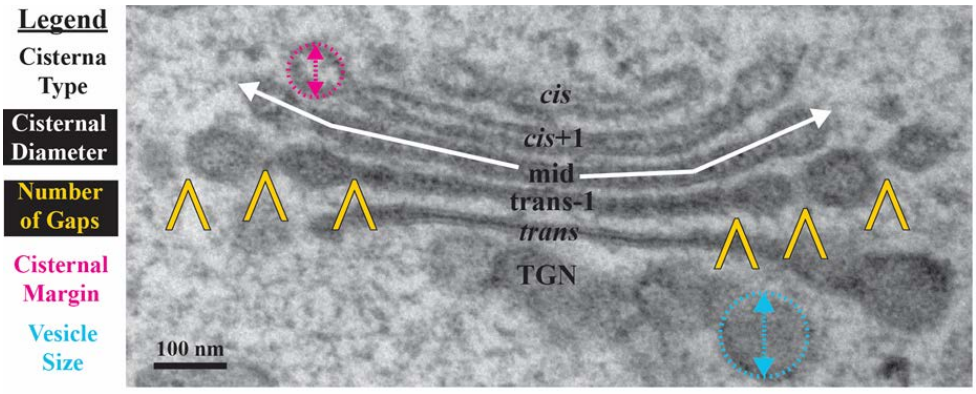

Figure 2.1 Golgi ultrastructure features measured.

Examples are shown on a xylan-producing Golgi, early in secondary cell wall production. The legend text colour is paired with the colour of the appropriate symbols or text on the example Golgi.

Table 2.1 Constructs generated and primers employed.

Text colour gives Gateway cloning sequences (orange), linker/spacer sequences (blue), and restriction sites (green).

	Construct or Mutant	Primer Name	Primer Sequence (5'→3')
GFP-tagged IRX9	*proIRX9:IRX9-GFP*	gtwy_pro+IRX9_LP	AAA AAG CAG GCT TC ATA GGT CTT CTT GAA CGA GAA CGG C
		gtwy_pro+IRX9_RP	AGA AAG CTG GGT C GGT GCT TAA ACG TGT TCT TGT GGG A
	35S:IRX9-GFP	gtwy_IRX9_LP	AAA AAG CAG GCT ATG GGA TCT CTA GAG AGA TCA AAG AAG
		ttpcr_IRX9_P10	AGA AAG CTG GGT TCA GGT GCT TAA ACG TGT TCT TGT G
	proIRX9:IRX9-GFP	proIRX9_SbfI_LP	GAA TTC CCT GCA GG ATA GGT CTT CTT GAA CGA GAA CGG C
		proIRX9_KpnI_RP	TGG CCA GGT ACC ACC CTC TCT TCA AGG AAG AAG GTT TC
GFP-tagged IRX10	*proIRX10:IRX10-GFP*	gtwy_pro+IRX10_LP	AAA AAG CAG GCT CG TGT CTT TGG ACT GAG AGA TCT
		gtwy_pro+IRX10_RP	AGA AAG CTG GGT C CCA AGG TTT CAG GTC AGC AAC
	35S:GFP-IRX10 (no signal sequence)	gtwy_GFP:IRX10_LP	AAA AAG CAG GCT TC AAT GTT CGG ACA GAG CGA AT
		gtwy_GFP:IRX10_RP	AGA AAG CTG GGT C TTA CCA AGG TTT CAG GTC AGC
	proIRX10:GFP-IRX10 (signal sequence before GFP)	proIRX10_SbfI_LP	GAA TTC CCT GCA GG TGT CTT TGG ACT GAG AGA TCT
		proIRX10_sig_KpnI_RP	TGG CCA GGT ACC CA TTG TTT AGC GGA AGA AGC AG
mCherry-tagged MANI	*proUBQ10:MANI-mCherry*	gtwy_MANI-mCherry_LP	AAA AAG CAG GC T ATG GCT AGC GGG AGC AGA TC
		gtwy_ManI-mCherry_RP	AGA AAG CTG GGT TTA CTT GTA CAG CTC GTC CAT GC
	proIRX9:MANI-mCherry & *proIRX10:MANI-mCherry*	gtwy_MANI-mCherry_LP	AAA AAG CAG GC T ATG GCT AGC GGG AGC AGA TC
		gtwy_ManI-mCherry-TERM_RP	AGA AAG CTG GGT CTC ATG TTT GAC AGC TTA TC
		proIRX9_KpnI_LP	GAA TTC GGT ACC ATA GGT CTT CTT GAA CGA GAA CG
		proIRX9_AscI_RP	TGG CCA GGC GCG CC ACC CTC TCT TCA AGG AA GAA GG
		proIRX10_KpnI_LP	GAA TTC GGT ACC TGTCTTTGGACTGAGAGATCT
		proIRX10_Asc1_RP	TGG CCA GGC GCG CC CTA CCG GAG ATG TGT TTG AAG
VND7 Induction	*35S:VND7-VP16-GR* (KanR) & *proUBQ10:VND7-VP16-GR* (BasR)	gtwy_VND7ind_LP	AAA AAG CAG GCT CG ATG GAT AAT ATA ATG CAA TCG TCA ATG
		gtwy_VND7ind_RP	AGA AAG CTG GGT C GCT AGC TTA CTC AGT TAG GTC G
	Gateway Adapter Sequences	gtwy_attB1_ADAPTER	GGG GAC AAG TTT GTA CAA AAA AGC AGG CT
		gtwy_attB2_ADAPTER	GGG GAC CAC TTT GTA CAA GAA AGC TGG GT
Genotyping	*irx9-2*	gntyp_SALK057033_irx9_LP	GCT GGT AAG GCC TCA TTT TTC
		gntyp_SALK057033_irx9_RP	AAC TTA CCA ACC CAC CCA TTC
	irx10	gntyp_SALK055673_irx10_LP	ACA AAA GCC GTG ATC AAT GAC
		gntyp_SALK055673_irx10_RP	AAA CAT CAC CAG CAC TTC CTG
	irx10L	gntyp_GABI179G11_ir10L_LP	TTG TTG TGC CTC ATG ACT TTG
		gntyp_GABI179G11_ir10L_RP	ACA CCA ATA TCT TCC CAA GGG

Table 2.2 Summary of confocal Golgi density experiments.

Plant lines used in conducting Golgi quantification using confocal microscopy, as well as their genetic background and the quality of induction, number of experiments (Exp), plants and cells from which data was collected for each line.

Plant Line	Genetic Background		VND7 Induction	Exp	Plants	Cells
WT.UMANI	*proUBQ10:MANI-mCherry*	T2 of MANI transformation	N/A	6	31	319
irx9.VND7.IRX9x1	*irx9* *proIRX9:IRX9-GFP* *proUBQ10:VND7-VP16-GR*	T2 of VND7 transformation	Fair	2	10	150
WT.VND7.IRX9x1	*proIRX9:IRX9-GFP* (1 copy) *pro35S:VND7-VP16-GR*	T2 of IRX9 transformation	Good	2	11	159
WT.VND7.IRX9x2	*proIRX9:IRX9-GFP* (2+ copies) *pro35S:VND7-VP16-GR*	T2 of IRX9 transformation	Good	4	78	795
WT.VND7.UMANI	*proUBQ10:MANI-mCherry* *pro35S:VND7-VP16-GR*	F1 cross	Poor	2	11	258
WT.VND7.9MANI	*proIRX9:MANI-mCherry* *pro35S:VND7-VP16-GR*	F1 cross	Very Poor	1	7	23
WT.VND7.IRX9+MANI	*proIRX9:IRX9-GFP* (2+ copies) *pro35S:VND7-VP16-GR* *proUBQ10:MANI-mCherry*	F1 cross with MANI	Very Poor	1	9	35

Table 2.3 Primary antibodies used in this study.

Primary antibodies used in this study as well as available information about their epitopes and examples of references justifying their selection.

Antibody	Epitope Info	Other Info	Other References
LM10	Unsubstituted xylan disaccharide (McCartney et al., 2005; Schmidt et al., 2015)	rat monoclonal IgG2c	Kim and Daniel, 2012
CCRC M138	Unsubstituted xylopentaose (Peralta et al., 2017)	mouse monoclonal IgM(κ)	Pattathil et al., 2010; Hao et al., 2014
CCRC M147	Unsubstituted xylan disaccharide (Schmidt et al., 2015)		Pattathil et al., 2010; Kulkarni et al., 2012
CCRC M149	Unsubstituted xylotriose (Peralta et al., 2017)		Pattathil et al., 2010; Tan et al., 2013; Hao et al., 2014
CCRC M153	Unsubstituted and arabinose substituted xylan (Schmidt et al., 2015; Peralta et al., 2017)		Pattathil et al., 2010
Torrey Pines anti-GFP (TP401)	wild-type GFP and variants	rabbit polyclonal IgG	Crowell et al., 2009; Stierhof and El Kasmi, 2010; Roppolo et al., 2011; Schiller et al., 2012; Sauer et al., 2013
Invitrogen anti-GFP (A6455)	wild-type GFP and variants	rabbit polyclonal IgG	McFarlane et al., 2010; Zhang et al., 2016

Chapter 3: Characterizing the Golgi Apparatus During Secondary Cell Wall Synthesis

3.1 Introduction

As a central site of endomembrane trafficking and synthesis in eukaryotic cells, the Golgi apparatus plays an essential role in a wide array of cellular processes. In plants, the Golgi apparatus is composed of a population of individual Golgi bodies, which tumble through the cytoplasm on an actin-myosin network (Boevink et al., 1998; Nebenführ et al., 1999). These Golgi bodies are composed of stacks of flattened membranous cisternae, through which secretory cargo passes from *cis* to *trans*. Across eukaryotes, the Golgi apparatus is important for processing and sorting proteins targeted to the *trans* Golgi network (TGN), plasma membrane, and vacuole/lysosome. In plant cells, the Golgi is also essential for synthesis and deposition of the plant cell wall, particularly the biosynthesis of non-cellulosic polysaccharides such as pectins (Atmodjo et al., 2013) in primary cell walls (PCWs) and hemicelluloses (Scheller and Ulvskov, 2010) in both PCWs (e.g. xyloglucan) and SCWs (e.g. xylan).

SCWs are deposited in specific cell types that require additional structural support, such as supportive fibres and water-conducting xylem tracheary elements. In addition to synthesis of SCW hemicellulose, in these cells the Golgi apparatus is also essential for proper deposition of cellulose and lignin. The formation of SCW cellulose synthase (CESA) complexes is believed to occur in the Golgi prior to transport to the plasma membrane (Haigler and Brown, 1986; Zhang et al., 2016). The Golgi also carries out glycoprotein processing (Schoberer and Strasser, 2011) of proteins like oxidative enzymes (Turlapati et al., 2011; Herrero et al., 2013) that facilitate polymerization of lignin monomers (Schuetz et al., 2014; Chou et al., 2018). Despite the importance of the Golgi in SCW synthesis, many aspects of Golgi biology have not been fully resolved in these cells. For example, it is not known whether the number of Golgi stacks increases with SCW synthesis. The number of Golgi stacks varies with cell type and developmental stage (Garcia-Herdugo et al., 1988; Seguí-Simarro and Staehelin, 2006; Young et al., 2008; Toyooka et al., 2014), thus the increased demand for Golgi products during SCW synthesis may require a similar proliferation of Golgi stacks. Individual Golgi stacks have also been found to carry multiple kinds of cargo, including different polysaccharides and

glycoproteins (Moore et al., 1991; Zhang and Staehelin, 1992; Young et al., 2008). Similar Golgi multitasking has not yet been shown to occur during SCW synthesis. However, the diverse roles of Golgi in SCW biosynthesis suggest similar multitasking is likely to occur in these cells. Some SCWs are deposited in specific patterns, which may be facilitated by preferential targeting of Golgi stacks to regions of SCW development where they can delivery their cargo. Ultimately, understanding the underlying composition and organization of the Golgi apparatus will help explain how it participates in the assembly of the complex, patterned SCWs.

It has been difficult to study the Golgi in SCW production, as it is challenging to image tracheary elements and fibres because they are buried deep in plant organs and often dead at maturity. Recently, a model system was developed in Arabidopsis, utilizing the transcription factor VASCULAR RELATED NAC-DOMAIN7 (VND7), which has been identified as a master regulator controlling the development of protoxylem tracheary elements (Kubo et al., 2005). In this system, a ubiquitously expressed VND7 is fused to a strong transcriptional activator (viral protein 16; VP16) and a glucocorticoid receptor (GR), causing cells throughout the plant to undergo transdifferentiation into protoxylem tracheary elements upon treatment with the glucocorticoid hormone dexamethasone (DEX) (Yamaguchi et al., 2010a). The increased number of SCW-producing cells facilitates quantitative analysis of microscopy images, and observation of transdifferentiated epidermal cells undergoing protoxylem development greatly increases the resolution of live-cell imaging (Schuetz et al., 2014; Watanabe et al., 2015). Furthermore, control over the timing of induction provides experimental consistency, allowing fine-tuned characterization of different stages of SCW deposition.

When Arabidopsis seedlings carrying the *35S:VND7-VP16-GR* construct are induced with DEX, cells undergo rapid SCW biosynthesis, including production of large amounts of the hemicellulose glucuronoxylan in the Golgi (Yamaguchi et al., 2010a). Indeed, microarray analysis showed upregulation of several xylan-backbone biosynthetic genes upon VND7-induction, including a 4.44-fold increase in IRREGULAR XYLEM 9 (IRX9) and a 2.61-fold increase in IRX10 (Yamaguchi et al., 2010b). IRX9 and IRX10 are therefore good candidates for GFP-tagging to use as markers of xylan-production in the plant Golgi apparatus during SCW synthesis. IRX9 is predicted to have a single transmembrane domain, while IRX10 is believed to reside in the Golgi lumen. This difference in topology is likely to alter the mechanism by which

each protein is retained in the Golgi (Atmodjo et al., 2011; Gao et al., 2014), which could affect their suitability as Golgi markers. As such, fluorescent tagging of both IRX9 and IRX10 was pursued.

In this chapter, I employed the VND7-induction system to study the Golgi apparatus during SCW deposition. I introduced GFP-tagged versions of the xylan biosynthetic proteins IRX9 and IRX10 into *irx9* and *irx10irx10L* mutant lines, respectively, then characterized the Golgi carrying these markers at different stages of SCW deposition. A combination of qualitative and quantitative confocal and TEM imaging was then employed to address the following questions: (1) Do specialized populations of Golgi stacks carry out separate tasks during SCW biosynthesis? (2) Does the number of Golgi stacks change with the onset of SCW production? (3) Do Golgi stacks preferentially associate with SCW domains?

3.2 Results

3.2.1 Development of functional fluorescently-tagged IRX9 and IRX10

C-terminal GFP fusions of IRX9 and IRX10, driven by their native promoters, were generated and tested for proper function by complementation of *irx9* and *irx10irx10L* mutant lines, respectively (Brown et al., 2009; Wu et al., 2009; Lee et al., 2010; Wu et al., 2010). The dwarf growth phenotypes of the mutants were restored to wild-type when *irx9* was transformed with *proIRX9:IRX9-GFP* or when *irx10irx10L* was transformed with *proIRX10:IRX10-GFP* (Figure 3.1 A). Wild-type vascular bundles have large, open tracheary elements in Toluidine blue-stained stem cross sections (Figure 3.1 B), which are frequently collapsed in *irx9* and *irx10irx10L* (Figure 3.1 C, D). Restoration of open vessel elements was apparent in the complemented lines (Figure 3.1 E-F). Complementation of the mutant phenotypes indicates that the GFP-tagged IRX9 and IRX10 are functional.

In live-cell imaging of seedling roots from plants containing *proIRX9:IRX9-GFP* and *proIRX10:IRX10-GFP*, GFP signal was detected in the paired cell files of the developing protoxylem tracheary elements (Figure 3.2 A, B). In these cells, IRX9-GFP and IRX10-GFP localized to ~1 μm punctae (Figure 3.2 C, D) that could be seen streaming through the cytoplasm, consistent with the predicted Golgi localization. Subsequent experiments were conducted with IRX9-GFP and IRX10-GFP because of their successful complementation and expression. N-terminal GFP fusions were also generated, but not tested.

While the native promoters drove expression in the appropriate cell types, imaging the tagged proteins in these cells demonstrated the typical low resolution associated with imaging native tracheary elements deep in an organ. Furthermore, the rapid programmed cell death of protoxylem tracheary elements meant that only a few cells per root could be imaged. To overcome these problems, the VND7-VP16-GR experimental system was adopted.

3.2.2 Introduction of IRX9-GFP and IRX10-GFP into the VND7-induction system

The *35S:VND7-VP16-GR* construct was often variable when crossed or re-transformed into different backgrounds (M. Schuetz, Y. Watanabe, personal comm.). In these cases, different lines/crosses would range widely in the number of transdifferentiating cells after VND7 induction (‘induction strength’), and as such, many lines would need to be screened to identify

those suitable for additional experiments. One potential source of this difficulty was that VND7-VP16-GR expression was driven by the *35S* promoter, which has been linked to trans-gene silencing (Daxinger et al., 2008; Mlotshwa et al., 2010). As such, a *proUBQ10*-driven version of VND7-VP16-GR was generated for testing.

Wild-type, *irx9/proIRX9:IRX9-GFP* and *irx10irx10L/proIRX10-GFP* plants were each transformed with *proUBQ10:VND7-VP16-GR* or *35S:VND7-VP16-GR*, and 4 – 5 T2 lines were treated with DEX and screened for SCW production using brightfield microscopy. Both *proUBQ10:VND7-VP16-GR* and *35S:VND7-VP16-GR* were able to trigger SCW synthesis in at least one transformed line, though in most cases only a few cells produced SCWs. This appears to be consistent with results obtained by others working with this system. Two lines, *irx9/proIRX9:IRX9-GFP/proUBQ10:VND7-VP16-GR* and *irx10irx10L/proIRX10-GFP/35S:VND7-VP16-GR*, had sufficient numbers of transdifferentiating cells to proceed with confocal microscopy. While GFP expression was found in transdifferentiating protoxylem tracheary elements for both lines, the IRX9-GFP line had a brighter GFP signal and stronger induction than the IRX10-GFP line. The IRX9-GFP line was selected for further experiments, including characterization of IRX9-GFP subcellular localization throughout SCW deposition.

Despite this early success, imaging of subsequent generations of the IRX9-GFP line revealed problematic decreases in induction strength and intensity of IRX9-GFP signal that created difficulties when using it in subsequent experiments. This was again presumed to be a result of trans-gene silencing, perhaps exacerbated by the transgenic load created by the T-DNA insertion in the *irx9-2* mutant background, the IRX9-GFP and VND7-induction constructs, and the various selectable resistance markers. The strategy taken to address this issue was to work in the *WT* background, rather than the *irx9-2* background, and to make use of a *35S:VND7-VP16-GR* line from our collaborator Taku Demura in which a very large number of cells undergo transdifferentiation. This line was transformed with *proIRX9:IRX9-GFP*, and 20 lines screened for SCW production in hypocotyls after DEX treatment, 9 of these lines were screened for IRX9-GFP intensity in native root protoxylem tracheary elements, and finally 3 lines were selected and screened for IRX9-GFP expression and localization in confocal imaging of VND7-induced hypocotyls. In these three newly generated lines, IRX9-GFP was observed in the same ring-shaped bodies streaming through the cytoplasm, which was consistent with IRX9-GFP in the

complemented mutant line and is typical of Golgi localized proteins (Boevink et al., 1998; Nebenführ et al., 1999). This indicated that the presence of wild-type IRX9 did not alter the localization of IRX9-GFP.

Of the 3 lines passing the screening, two were later found to have multiple insertions of IRX9-GFP based on chi-squared tests of T3 antibiotic resistance segregation ratios. The 'single insertion' line, *proIRX9:IRX9-GFP/35S:VND7-VP16-GR*, had an average segregation ratio of 3.41:1, which did not differ significantly from the 3:1 ratio expected from a single transformation (X^2, p = 0.408). The 'multiple insertion' line *proIRX9:IRX9-GFP* (2+ copies) */35S:VND7-VP16-GR* had a segregation ratio of 8.36:1, which was significantly different from the single transformation ratio (X^2, p = 0.0015). The multiple-insertion, 'high IRX9 copy number' line (*proIRX9:IRX9-GFP* (2+ copies) */35S:VND7-VP16-GR*), had the brightest IRX9-GFP signal and the greatest number of transdifferentiating cells, and proved to be the most useful experimentally. However, to control for the effect of IRX9 copy number, experiments were also performed on the single-insertion 'mid copy number' line (*proIRX9:IRX9-GFP/35S:VND7-VP16-GR*), and the *irx9*-complemented 'low copy number' line (*irx9/proIRX9:IRX9-GFP/proUBQ10:VND7-VP16-GR*).

Introduction of a functional IRX9-GFP into a system with reliable inducible transdifferentiation of cells into protoxylem tracheary elements, permitted investigation of Golgi function, number and position. It also represents a novel platform to localize cell wall glycosyltransferases within individual Golgi cisternae (Chapter 4).

3.2.3 Characterizing the stages of SCW production

Qualitatively, when the *proIRX9:IRX9-GFP/35S:VND7-VP16-GR* plants were induced and imaged, the timing of transdifferentiation varied substantially among different cells in the same seedling. To characterize this variability, hypocotyls from 4 – 7-day-old seedlings were examined with confocal microscopy 17 – 30 hrs following DEX treatment. The stage of SCW deposition in each cell was assigned according to the presence of IRX9-GFP signal and the appearance of the SCW, assessed using a combination of brightfield microscopy and propidium iodide staining. Cells in the early-SCW stage (Figure 3.3 A–E) had no visible SCW in brightfield (Figure 3.3 A), though SCW bands were sometimes detectable using propidium iodide staining

(Figure 3.3 B, C), and were expressing IRX9-GFP (Figure 3.3 D, E). The mid-SCW stage was characterized by the first faint appearance of SCW in brightfield (Figure 3.3 F–H), and continued IRX9-GFP signal (Figure 3.3 I, J). By the late-SCW stage the SCW was much more obvious in brightfield (Figure 3.3 K–O). The propidium iodide staining was imaged at different sensitivities (i.e. gain) to better detect and characterize weaker (e.g. early-SCW stage) and stronger (e.g. late-SCW stage) fluorescent signal. Cells expressing IRX9-GFP were assigned to a stage of SCW deposition using these definitions and the percentage of cells at each stage quantified. The early-SCW stage is abundant 17 – 20 hrs following VND7 induction, while the mid-SCW stage is more prevalent at 20 – 26 hrs, and the late-SCW stage at 26 – 30 hrs (Figure 3.4). It must be noted that not all cells undergo transdifferentiation, as some cells without SCWs and IRX9-GFP were present in the hypocotyl throughout the time course. This characterization of early-, mid- and late-SCW stages during transdifferentiation of protoxylem tracheary elements was then used to guide selection of DEX-treatment time points for subsequent experiments.

To map the features of tracheary elements during SCW deposition, the hypocotyls and petioles of 4 – 7-day-old seedlings were examined using transmission electron microscopy (TEM) (Figure 3.5). The length of DEX treatment was selected based on the abundance of cells at the different stages in confocal microscopy (Figure 3.4) to enrich for cells at the early-SCW (17 – 20 hrs) or late-SCW (22 – 30 hrs) stages. Seedlings were high-pressure-frozen/freeze-substituted and embedded in Spurr's resin for morphological characterization. Hypocotyl cells from plants lacking the VND7-induction construct (pre-SCW) were dominated by a large central vacuole, with a thin layer of cytoplasm visible between the more electron-lucent vacuole and the more electron-dense primary cell wall (PCW) (Figure 3.5 A). In early-SCW, small SCW intrusions (more electron-lucent than the PCW) were visible at repeating intervals along the cell periphery (Figure 3.5 B). In late-SCW, the SCWs began to protrude much more into the cell (Figure 3.5 C). In both early-SCW and late-SCW there was often very little cytoplasm between SCW thickenings and the tonoplast. Bundles of microtubules were often seen lining the plasma membrane at SCW-domains (Figure 3.5 C arrowheads). Integrating this characterization of SCW deposition in TEM with the stages of development outlined using confocal microscopy provides a multi-scale platform which can be used to examine the Golgi during SCW biosynthesis.

3.2.4 IRX9-GFP colocalizes with MANI-mCherry

To verify that the ring-shaped fluorescent bodies observed in confocal microscopy of IRX9-GFP represent Golgi bodies, the high-copy-number IRX9-GFP line was crossed with plants containing a well-characterized Golgi marker *proUBQ10:MANI-mCherry* (Nebenführ et al., 1999). As noted previously, increasing the transgene load led to a strong reduction in the number of transdifferentiating cells (induction strength) and the intensity of MANI-mCherry and IRX9-GFP fluorescence. However, in every cell expressing both IRX9-GFP and MANI-mCherry, all structures labelling IRX9-GFP also contained MANI-mCherry (Figure 3.6). 73.3% of IRX9-GFP signal overlapped with MANI-mCherry signal, when the Mander's colocalization coefficient (Manders et al., 1993) was averaged for 26 early-SCW cells from 5 seedlings, confirming the Golgi localization of IRX9-GFP.

Interestingly, within each Golgi stack, the IRX9-GFP signal displayed a ring-shaped localization, while the MANI-mCherry was distributed throughout the center of this ring (Figure 3.6). The lack of colocalization in the center of the Golgi stack resulted in a Pearson correlation coefficient of 0.322 and the Mander's colocalization coefficient indicated that 39.6% of MANI-mCherry signal overlapped with IRX9-GFP. Despite these differences in distribution of MANI-mCherry and IRX9-GFP within individual Golgi bodies, they were always found together, suggesting that all stacks in the Golgi apparatus in a cell participate in SCW production.

3.2.5 The number of Golgi stacks increases during SCW production

Given that every Golgi body in the cell was labeled with IRX9-GFP, I reasoned that the high production of xylan in the Golgi during SCW synthesis might have an impact on the abundance of Golgi stacks in the cell. To test this hypothesis, I quantified the number of Golgi stacks using TEM to survey the cortical cytoplasm surrounding the large central vacuole prior to SCW deposition (*WT* pre-SCW), and once SCW deposition had commenced (*WT* SCW) (Figure 3.7 A, B). As a control, mitochondrial abundance was also quantified for comparison purposes. For context, the approximate size of the TEM field of view is indicated using a white box on a confocal optical section through the center of the cell (Figure 3.7 C). In these cells cross sections of the propidium iodide-stained SCWs are found at regular intervals along the cell periphery, and the IRX9-GFP signal is absent from the center of the cell due to the presence of a large vacuole.

The TEM characterization showed that cells producing SCWs had a significantly thicker cortical cytoplasm (Figure 3.7 D), and therefore Golgi and mitochondrial abundance was adjusted by the cytoplasmic area (#/μm^2) and by the cell perimeter (#/μm), to isolate the change in organelle abundance from the change in cytoplasmic area. Golgi counts were also adjusted for differences in Golgi width (Chapter 4) to correct for potential inflation of Golgi abundance due to more frequent detection of larger Golgi in thin sections. The number of Golgi per cell perimeter increased significantly in *WT* SCW cells (Figure 3.7 E). After normalizing by Golgi size, the observed increase remained significant (Figure 3.7 F), indicating that SCW-production is accompanied by a significant increase in the number of Golgi stacks. Interestingly, the number of mitochondria per cell perimeter also increased significantly with SCW-production (Figure 3.7 G). Unlike Golgi number normalized by cell-perimeter, no significant increase in Golgi or mitochondrial abundance was apparent when normalized per cytoplasmic area in *WT* SCW versus *WT* pre-SCW cells (Figure 3.7 H–J). This suggests that the increase in Golgi and mitochondrial number is proportional to the increase in cytoplasm during SCW-production (Figure 3.7 D). These data indicate that the absolute number of Golgi did indeed increase during SCW production, and this was accompanied by an increase in cytoplasm thickness and mitochondrial abundance.

To test if xylan production contributes to increased Golgi abundance during SCW deposition, these analyses were repeated in the *irx9* mutant background. After normalizing to cell perimeter, Golgi abundance in *irx9* SCW cells was no different than WT SCW cells (Figure 3.7 F). Mitochondrial abundance was similarly unaffected in *irx9* SCW compared to *WT* SCW cells (Figure 3.7 G). Unlike *WT* SCW cells, Golgi abundance appeared higher in *irx9* SCW compared to *WT* pre-SCW cells when normalized to the cytoplasmic area (Figure 3.7 H). This can be attributed to an increase in the size of Golgi stacks in *irx9* (Chapter 4), as normalization by Golgi width caused this effect to disappear (Figure 3.7 I). The observed increase in Golgi numbers during SCW synthesis is therefore not dependent on IRX9 or xylan production in the Golgi.

Changes in Golgi abundance were also evaluated by quantifying the Golgi density in the cortical cytoplasm using confocal imaging of MANI-mCherry or IRX9-GFP (Figure 3.8 A, B). Golgi density was quantified for a low-copy number line (IRX9-GFP in the *irx9* background), a mid-copy number line (IRX9-GFP in the *WT* background), and a high-copy number line (IRX9-

GFP in the *WT* background with multiple insertions) to control for the number of copies of IRX9. There was a significant increase in Golgi abundance during SCW production compared with pre-SCW cells (Figure 3.8 C). Dividing cells into early-, mid- and late-SCW stages revealed a consistent, gradual increase in Golgi abundance over the course of SCW deposition for all three IRX9-GFP genotypes (Figure 3.8 D). A significant increase in Golgi abundance was also observed with increasing IRX9 copy number (Figure 3.8 C). While greater IRX9 copy number correlates with increasing Golgi density, all genotypes had larger numbers of IRX9-labelled Golgi during SCW biosynthesis.

Differences in Golgi density might be affected by the strength of Golgi-marker expression and the nature of the Golgi marker. To better understand what factors might contribute to differences in Golgi density, experiments were conducted to quantify Golgi density using different Golgi markers, driven by different promoters. The effect of the promoter was tested by comparing markers driven by *proUBQ10* versus *proIRX9*, while the effect of different marker proteins was tested by comparing the *cis*-localized MANI (Nebenführ et al., 1999), to the medial-localized IRX9-GFP (Chapter 4). Constructs driven by *proIRX9* but with different marker proteins had similar Golgi densities (Figure 3.9), indicating that differences in Golgi marker proteins had little effect on Golgi density. Conversely, the *proUBQ*-driven MANI-mCherry had a larger Golgi density than the *proIRX9*-driven version of the same marker (Figure 3.9), suggesting that overexpression of a Golgi marker can increase Golgi abundance. However, both of these results were confounded by silencing problems, as crossing the MANI-mCherry markers into the *35S:VND7-VP16-GR* line greatly reduced the number of transdifferentiating cells and often led to weaker MANI-mCherry signal, especially for the *proIRX9*-driven construct (Table 2.2). It is also important to note that the *proUBQ10* SCW density is likely inflated, compared to the other SCW lines. The early-SCW stage is identified by the appearance of a *proIRX9*-driven Golgi marker (either MANI-mCherry or IRX9-GFP) in cells lacking visible SCW thickenings (Figure 3.3). Furthermore, previous experiments demonstrated that this early-SCW stage had a lower Golgi density than later stages (Figure 3.8 D). As the *proUBQ10:MANI-mCherry* line does not contain a marker driven by *proIRX9*, cells in the Early-SCW stage could not be assessed, introducing a bias toward cells with higher Golgi densities in this line. There were clearly technical limitations to these comparisons, but two conclusions can be drawn: first, when driven

by a SCW-specific promoter both Golgi marker proteins had increased Golgi densities during SCW production, and second, despite the inflated value of the *proUBQ10:MANI-mCherry* line, the trend of increased Golgi density during SCW production was consistent.

When quantifying Golgi densities in confocal microscopy, it became apparent that smaller cells were more likely to undergo transdifferentiation than larger cells. Indeed, analysis of the data from one of the replicate Golgi density experiments confirmed that the SCW-producing cells quantified had a significantly smaller cell width than the Pre-SCW cells (Figure 3.10 A). If Golgi density changes with cell size, the bias toward smaller cells in the Post-SCW data would introduce a bias into the Golgi abundance measurements. To account for cell size, the mean Golgi density at each stage (Figure 3.10 B) was adjusted for covariation with cell width using Analysis of Covariance (ANCOVA) (Figure 3.10 C). After adjustment, the Golgi abundances were essentially unchanged, which is consistent with the lack of correlation between cell width and Golgi densities at all SCW stages (Figure 3.10 D-G). Together, these data show that while smaller cells are more likely to be induced to produce SCWs, the number of Golgi in a cell appears to increase proportionally with cell size, and cell size does not bias Golgi density measurements. Therefore, we can conclude that cell size does not need to be taken into consideration when measuring Golgi density using confocal microscopy.

3.2.6 Golgi stacks are no closer to SCWs than random

In live-cell imaging of Golgi labelled with YFP-tagged SCW CESAs, Golgi were observed to pause at SCW-domains (Watanabe et al., 2015) and 85% of Golgi were found ‘underneath’ SCW bands (Schneider et al., 2017). These results suggest that Golgi may preferentially associate with SCWs. Confocal microscopy however, cannot provide the cytoplasmic context necessary to test this hypothesis. Compare a top-down confocal image of the cell cortex, containing IRX9-GFP-labelled Golgi and propidium iodide-stained SCWs (Figure 3.11 A), with a cross-section through the cell cortex in TEM (Figure 3.11 B). In the TEM image, we can see that regions between SCW-thickenings may have very little cytoplasm due to the presence of other organelles such as chloroplasts (as seen here), large ER bodies, the nucleus, or the vacuole. This insight into the spatial organization of the cellular contents is lacking in fluorescence microscopy, as these other organelles are unlabelled.

To assess whether Golgi preferentially associate with SCWs, I therefore used TEM images of cortical cytoplasm of SCW-producing cells to measure the distance between Golgi stacks and the SCW (Figure 3.11 B). This was then compared to measurements of random points in the cytoplasm to provide predicted results if Golgi were randomly distributed. The majority of both Golgi and random points were found within 1 μm of a SCW (Figure 3.11 C). The distance between mitochondria and the SCW were also analysed as a control for comparison purposes. A similar percentage of Golgi (38.6%) and random points (41.7%) were found within 500 nm of a SCW (about half the width of a Golgi; Chapter 4), while a larger proportion of mitochondria (68.4%) were found within this distance (Figure 3.11 C). As distance from the SCW increased, the abundance of all three groups dropped exponentially (Figure 3.11 C). The average distance of Golgi stacks to the SCW was not significantly different from that of random points in the cytoplasm (Figure 3.11 D).

As both the random points and Golgi have the same close-proximity to SCWs, we can conclude that the cytoplasm and organelles in these cells are organized in such a way that proximity to the SCW is inevitable. The organization of cytoplasm is such that most of the free cytoplasmic space is near SCWs, therefore Golgi are naturally more abundant in these regions. We can contrast these results with the distribution of mitochondria, which are found nearer to SCWs than both random points and Golgi stacks (Figure 3.11 C). Together, these results show that mitochondria preferentially associate with SCWs, while Golgi do not. Comparing these results to the previously reported live-cell imaging data (Watanabe et al., 2015; Schneider et al., 2017) shows that confocal microscopy images must be carefully interpreted to avoid misinterpretation of the results, as proximity in confocal imaging does not necessarily indicate interaction.

3.3 Discussion

This chapter investigated how the Golgi stacks work together to carry out the functions of the Golgi apparatus during SCW biosynthesis. Live-cell imaging of a functional, fluorescently-tagged version of the xylan biosynthetic protein IRX9 (and the Golgi marker MANI) was used to assess xylan biosynthesis in the Golgi apparatus as a whole. This demonstrated that xylan biosynthesis was likely occurring in all Golgi stacks. A combination of live-cell and TEM imaging also showed that the number of Golgi increased during SCW production, reflecting an overall increase in cytoplasm. The geometry of the cytoplasm in these cells leads to the appearance of a close association between Golgi and SCW domains in confocal, but quantification of TEM data shows that Golgi are not preferentially associated with the growing SCW.

3.3.1 All Golgi stacks participate in xylan-biosynthesis

In cells co-expressing IRX9-GFP and MANI-mCherry, all Golgi contained both the xylan-biosynthetic protein IRX9, and the Golgi marker MANI (Figure 3.6), suggesting that all Golgi stacks carry out xylan biosynthesis. As MANI is involved in the early stages of glycoprotein processing in the Golgi (Schoberer and Strasser, 2011), we can also infer that each individual Golgi stack is carrying out glycoprotein processing and xylan biosynthesis simultaneously. This is consistent with previous work showing that Golgi stacks can produce both pectin and xyloglucan concurrently (Zhang and Staehelin, 1992; Young et al., 2008), and polysaccharide biosynthesis at the same time as glycoprotein processing (Moore et al., 1991). The conservation of Golgi stack multitasking across tissue types and species strongly suggests that this multitasking is a common feature of plant Golgi.

The colocalization of IRX9-GFP and MANI-mCherry also highlighted the difference in localization of each protein within individual Golgi stacks, with IRX9-GFP present in a ring with a MANI-mCherry center. This difference is likely due to localization in different Golgi cisternae. Cisternal centers become more compressed when moving from *cis* to *trans*, which may exclude proteins from the center of *trans* cisterna but not *cis* cisternae. Indeed, the evenly-distributed MANI is found in the *cis* Golgi (Nebenführ et al., 1999), while more *trans*-Golgi proteins like CESAs (Crowell et al., 2009) and sialyltransferase (Boevink et al., 1998) are found in a

characteristic ring pattern. The similar ring of IRX9-GFP in the Golgi suggests that IRX9 may also be present in cisternae downstream of MANI-mCherry.

3.3.2 The onset of SCW production triggers an increase in the number of Golgi stacks

TEM and confocal microscopy showed that the onset of SCW deposition is accompanied by a significant increase in the abundance of Golgi stacks (Figure 3.7, Figure 3.8). This suggests that a greater number of stacks are required to meet the increased demand for Golgi processing associated with SCW deposition. Increase in the abundance of Golgi stacks also occurs during the onset of mucilage production in Arabidopsis seed epidermal cells (Young et al., 2008), and during mitosis (Garcia-Herdugo et al., 1988; Seguí-Simarro and Staehelin, 2006; Toyooka et al., 2014). Two models have been proposed to explain how new Golgi stacks might form; either through the division of Golgi stacks or the *de novo* production of stacks at ER-exit sites (Ito et al., 2014). These models are not mutually exclusive, and there is evidence that different kinds of Golgi biogenesis are occurring in different eukaryotic species and cell types (Ito et al., 2014). The version occurring in plants has not yet been confirmed. While electron microscopy in various cell types have captured Golgi at what could be a 'mid-division' stage (Hirose and Komamine, 1989; Langhans et al., 2007; Staehelin and Kang, 2008), there is not yet definitive proof that Golgi proliferation in plants is a product of Golgi fission.

The regulatory mechanisms driving increases in Golgi number are also not well understood. Golgi number increase is unlikely to be a result of increased polysaccharide production, as Golgi proliferation during seed coat development was unaltered in a mutant producing significantly less pectin (Young et al., 2008). Alternatively, Golgi biogenesis might be stimulated by an increase in Golgi resident proteins. The confocal imaging of IRX9-GFP would seem to support this model, as plants with increasing copies of IRX9 had significant increases in Golgi density following VND7 induction (Fig 3.8 C). This would lead us to predict that decreasing IRX9 abundance would decrease Golgi proliferation. However, we do not see such a decrease in *irx9* when Golgi abundance was calculated in TEM images (Fig 3.7 F). This is especially telling, as loss of IRX9 may additionally disrupt Golgi-targeting of IRX10 and IRX14, which are also involved in xylan-backbone biosynthesis. Transiently-expressed Asparagus IRX9, IRX10 and IRX14 localized to the Golgi only when all three proteins were expressed (Zeng et

al., 2016). One reason why a decrease in Golgi abundance might not have been detected in *irx9*, is that the decrease in Golgi resident proteins may not be of sufficient magnitude. This explanation is slightly unsatisfying however, as it is unclear why addition of a single copy of IRX9-GFP should significantly increase Golgi abundance, but loss of a single copy of IRX9 (and potentially its partner proteins) would not cause a significant decrease in Golgi abundance.

Another possibility is that Golgi density may vary across transgenic lines due to confounding factors like differing VND7-induction strength, or expression levels of the Golgi marker due to the position and number of insertions. Supporting this hypothesis is the fact that the low-copy-number line with the smallest increase in Golgi density had the 'weakest' VND7 induction (fewest transdifferentiating cells). Meanwhile the high-copy-number line had the largest increase in Golgi density, and a very 'strong' VND7 induction (most transdifferentiating cells). While we cannot tease apart the factors contributing to differences in Golgi density between plant lines, the effect of promoter strength, the protein marker employed, the location of transgene insertion, and transgene copy number should all be taken into consideration. Ideally, comparisons should be made between different stages of development in a single transgenic line. In this study, we can have confidence that the number of Golgi increased significantly during SCW production, because this increase was observed in three individual *proIRX9:IRX9-GFP* lines, when comparing cells at the early-SCW vs late-SCW stages of biosynthesis (Figure 3.8 D).

3.3.3 Cytoplasmic geometry constrains randomly-distributed Golgi near SCWs

Confocal imaging of fluorescently-tagged Golgi following VND7 induction previously indicated that 85% of Golgi are found 'underneath' SCW bands (Schneider et al., 2017). However, my quantitative TEM analysis shows that Golgi are no closer to SCWs than randomly selected points in the cytoplasm (Figure 3.11). This discrepancy highlights some of the limitations of light microscopy in comparison to electron microscopy. The confocal imaging of Golgi in the cell cortex allows some characterization of the relationship between the Golgi and the SCW but gives little information about the organization of other cellular components. TEM imaging takes into account the volume and organization of the cytoplasm and other organelles allowing us to conclude that the close proximity of Golgi to SCWs is due to a concentration of free cytoplasmic space in this area. Indeed, the majority of both Golgi and random points are

found within 1 μm of a SCW. In other cell types with targeted secretion, Golgi have been found to be similarly randomly distributed. In Arabidopsis seed coat cells, Golgi were not concentrated near the outer surface of the seed where large amounts of pectin are secreted (Young et al., 2008). Similarly, in Arabidopsis trichomes, Golgi are distributed evenly throughout the cortical cytoplasm, not concentrated in the growing trichome branches (Lu et al., 2005). In tip growing cells like root hairs and pollen tubes, Golgi are found throughout the majority of the cell, and are actually excluded from the vesicle-rich growing tips (Sherrier and Vandenbosch, 1994; Chebli et al., 2013; Cai et al., 2015). These data suggest that plant Golgi do not need to preferentially associate with sites of cargo secretion.

In any plant cell, the organization of Golgi stacks at any given time is determined by the contribution of both moving and stationary Golgi. This 'stop-and-go' behaviour has been well characterized in several cell types, including BY2 cell cultures (Nebenführ et al., 1999), tobacco pavement cells (Boevink et al., 1998), and Arabidopsis trichomes (Lu et al., 2005). In native root tracheary elements, Golgi were similarly said to 'pause' in their rapid cytoplasmic streaming at SCW domains (Wightman and Turner, 2008). This was later demonstrated to also be the case in the VND7-induction system, where Golgi pausing near SCWs was found to last anywhere from 15 s to 3 min (Watanabe et al., 2015). The length of these pauses is again consistent with previously-described Golgi behaviours (Nebenführ et al., 1999; Lu et al., 2005). How can we explain both the pausing of Golgi at SCW domains, and their random distribution throughout the cytoplasm? One possible explanation is that Golgi paused at SCW domains may represent a small proportion of the population of Golgi stacks. The organization of the Golgi apparatus as a whole may then mask a relatively small number of stacks which are closely associated with SCWs. Indeed, it is unclear what proportion of Golgi at any given time are paused at SCW domains, paused at other domains, or streaming freely through the cytoplasm.

The proportion of Golgi in each of these phases may be important for different Golgi functions. Golgi pausing at cortical microtubules has been linked with delivery of cellulose synthase cargo in both primary (Crowell et al., 2009; Gutierrez et al., 2009) and SCWs (Watanabe et al., 2015). These results support the hypothesis that Golgi pausing is tied to cargo delivery (Nebenführ et al., 1999; Brandizzi and Wasteneys, 2013). However, it has not been shown that pausing is a requirement for delivery of Golgi cargo. Given that Golgi stacks can

receive materials from the ER while in motion (DaSilva et al., 2004), is seems unlikely that plasma membrane delivery could not also occur during Golgi movement. Golgi pausing may instead be due to physical barriers affecting free flow of cellular contents during cytoplasmic streaming. The SCW has been proposed to be a physical barrier which could disrupt the movement of Golgi travelling longitudinally through the cell cortex (Schneider et al., 2017). This hypothesis is supported by TEM imaging in these cells, as often very little cytoplasm is present between the intruding SCWs and the large central vacuole. In some fungi, cell wall architecture has been shown to help establish eddies in cytoplasmic streaming which are used to immobilize nuclei (Pieuchot et al., 2015). Similar eddies adjacent to SCWs could encourage Golgi pausing in these regions.

3.3.4 Cytoplasm and mitochondria position during SCW deposition

One surprising result of this study is the discovery that triggering tracheary element transdifferentiation leads to an increase in the number of mitochondria (Figure 3.7 G). Mapping the position of the mitochondria further revealed that they preferentially associate with SCW domains (Figure 3.11). The abundance of mitochondria is known to vary across cell types, and increases have been linked to higher energy demands in specific tissues or cells (Bereiter-Hahn, 1990). Mitochondria have also been shown to preferentially associate with energy-consuming organelles, presumably to supply this energy more efficiently (Bereiter-Hahn, 1990; Logan and Leaver, 2000). For example, in plants, it is well-documented that mitochondria closely associate with chloroplasts, where they may facilitate exchange of adenine nucleotides and/or set up oxygen concentration gradients (Logan and Leaver, 2000). Mitochondria are also relocated under various conditions. In dark-acclimated Arabidopsis palisade cells mitochondria are randomly distributed, but exposure to light leads to repositioning of mitochondria to periclinal regions where they colocalize with chloroplasts (Islam et al., 2009). These data demonstrate the dynamic nature of mitochondrial abundance and positioning in eukaryotic cells. The results in this chapter show that the onset of SCW synthesis similarly affects mitochondria, possibly due to a large demand for energy at SCW domains. While interesting on its own, characterization of mitochondria in these cells was also found to be a good positive control for the quantification of Golgi abundance and position that was the objective of this study.

Another surprising observation was the significant increase in cytoplasm seen during SCW-deposition (Figure 3.7 D). Similar increases in cytoplasmic volume have been shown to occur during cold acclimation in Arabidopsis leaves (Strand et al., 1999). In these cells, the authors attributed the larger cytoplasm to increased metabolic activity, due to an accompanying 2.5-fold increase in protein content. It is plausible that a similar increase in metabolic activity occurs as hypocotyl cells begin transdifferentiating into tracheary elements; shifting from the lower metabolic requirements of 'housekeeping' processes, to large amounts of transcription, translation, and production of SCW materials. This would then explain the concomitant increase in cytoplasmic volume, though the mechanism by which vacuole size decreases to accommodate this change is unclear.

3.3.5 Conclusions

In this chapter, I cloned and confirmed proper function of *proIRX9:IRX9-GFP* before introducing it into the VND7-induction system. I then characterized the function and organization of the Golgi apparatus during SCW deposition in transdifferentiating protoxylem tracheary elements. During this process, all Golgi stacks were found to contain IRX9-GFP, suggesting all Golgi in the Golgi apparatus are working in concert to carry out xylan biosynthesis. The onset of SCW deposition was also accompanied by a significant increase in the number of Golgi stacks. These data demonstrate that when the protoxylem tracheary element commits to the process of SCW biosynthesis, the entire Golgi apparatus is dedicated to the production of xylan. Finally, while Golgi stacks were found very near SCWs in TEM, this proximity appeared to be a by-product of the organization of the cytoplasm rather than specific targeting of Golgi to these domains. This suggests that while secretion to SCW domains may be facilitated by the close proximity of Golgi to these regions, this association does not require active targeting of Golgi stacks.

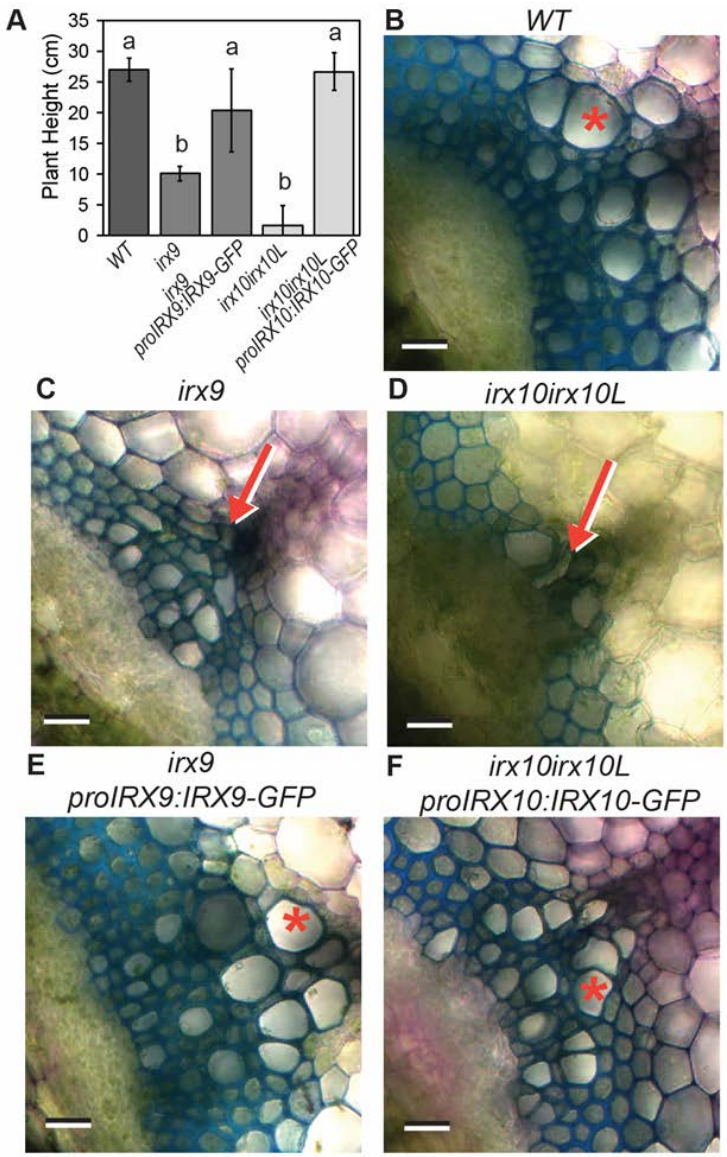

Figure 3.1 Mutant dwarf and irregular xylem phenotypes are complemented by IRX9-GFP and IRX10-GFP. **(A)** Plant height of Arabidopsis inflorescence stems showing *irx9* and *irx10irx10L* dwarf phenotypes in 40-day-old plants, and recovery of the wild-type growth with the introduction of *proIRX9:IRX9-GFP* and *proIRX10:IRX10-GFP*, respectively. Statistics = one-way ANOVA and Tukey HSD *post-hoc* analysis ($p<0.05$) for n = 5. **(B-F)** Cross-sections of xylem vascular bundles in basal inflorescence stems of Arabidopsis stained with Toluidine blue from **(B)** wild-type *(WT)*, **(C)** *irx9*, **(D)** *irx10irx10L*, **(E)** *irx9/proIRX9:IRX9-GFP* and **(F)** *irx10irx10L/proIRX10:IRX10-GFP* plants. Open xylem tracheary elements (asterisks) are collapsed (arrows) in *irx9* and *irx10* and restored in the complemented lines. Scale = 20 μm.

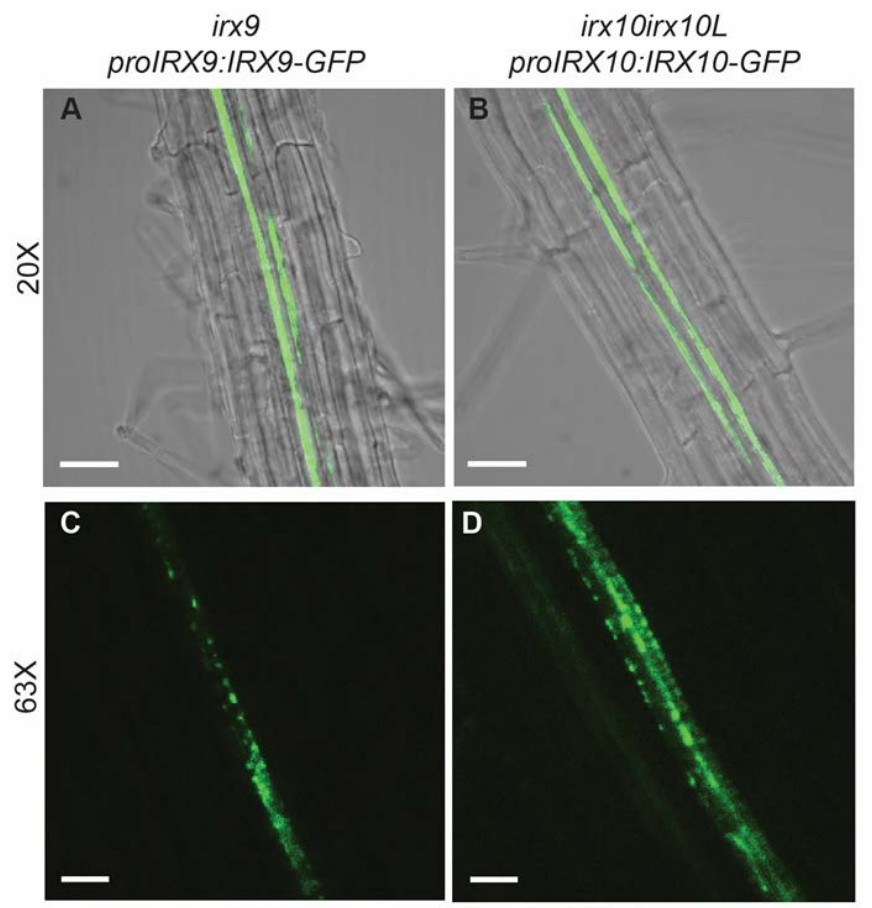

Figure 3.2 Native expression and subcellular localization in IRX9-GFP and IRX10 GFP in roots.

(A-B) Developing root protoxylem vessel cell files expressing **(A)** *proIRX9:IRX9-GFP* and **(B)** *proIRX10:IRX10-GFP*. **(C-D)** Subcellular localization of **(C)** IRX9-GFP and **(D)** IRX10-GFP in Golgi-like puncta in developing root protoxylem. Scale = 150 μm (A,B) and 10 μm (C,D).

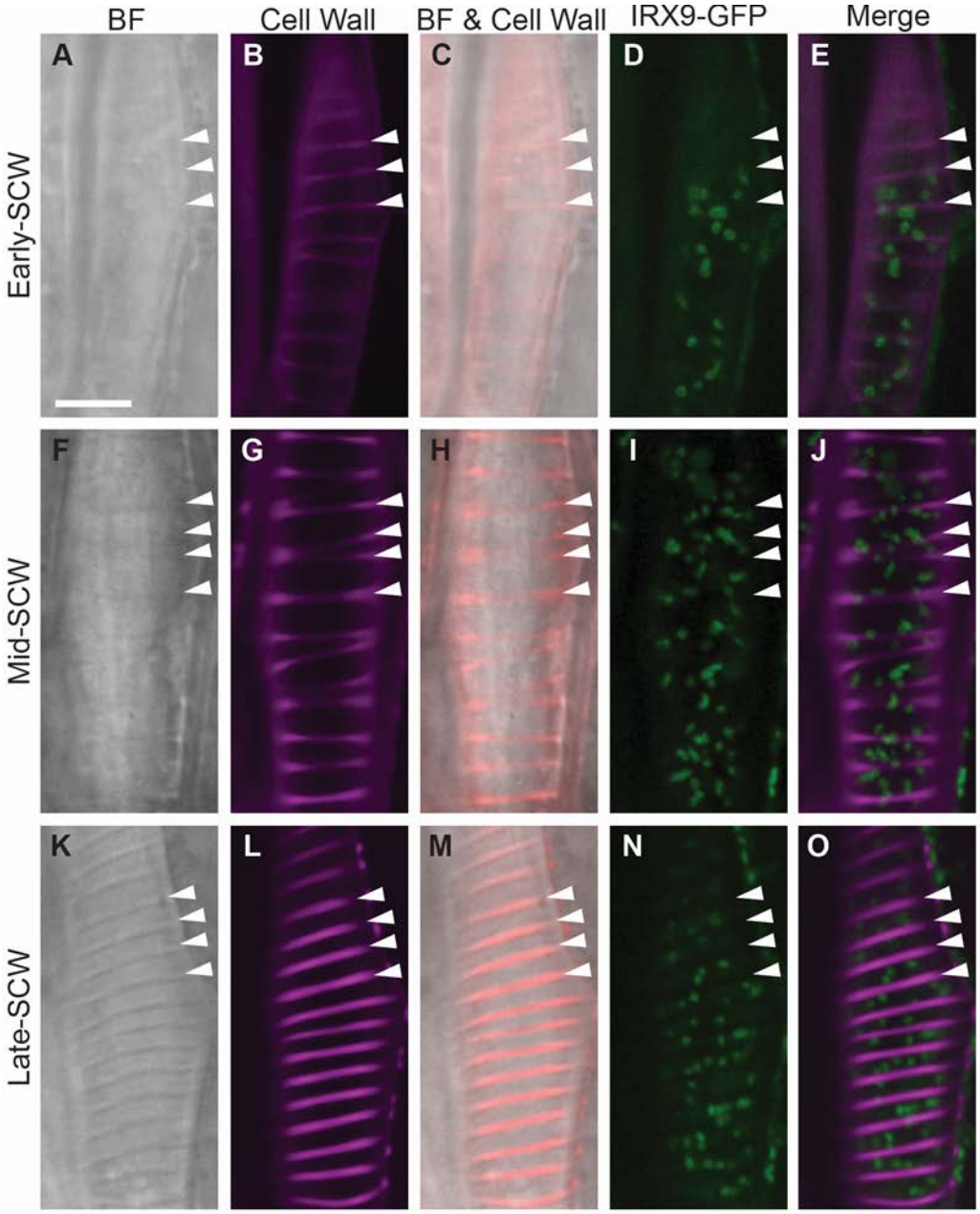

Figure 3.3 Stages of SCW deposition characterized using confocal microscopy.

Representative images of single optical sections through the cell cortex in cells at the **(A-E)** early-SCW **(F-J)** mid-SCW and **(K-O)** late-SCW stages. **(A, F, K)** Brightfield (BF) and **(B, G, L)** propidium iodide stained cell walls are merged in **(C, H, M)**. **(D, I, N)** IRX9-GFP in Golgi-like puncta are **(E, J, O)** merged with cell wall images. Arrowheads = SCW bands from (B, G, L). Cell wall images were acquired using different sensitivities (Early = 104, Mid = 54, Late = 21). Scale = 10 µm.

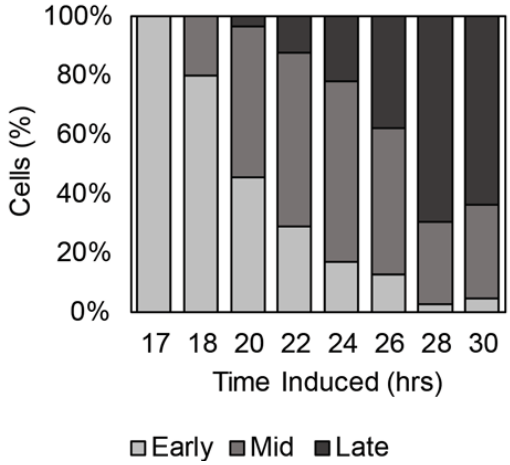

Figure 3.4 The stage of SCW development varies within populations of transdifferentiating cells.

The percent of IRX9-GFP expressing cells assigned to the early, mid or late stage of SCW-deposition at each time point following treatment with DEX. Early-SCW cells express IRX9-GFP but SCWs are not visible in brightfield, mid-SCW cells have SCWs that are just visible in brightfield, and late-SCW cells have obvious SCW bands. 60 - 204 cells were included per time point, across 4 replicate experiments.

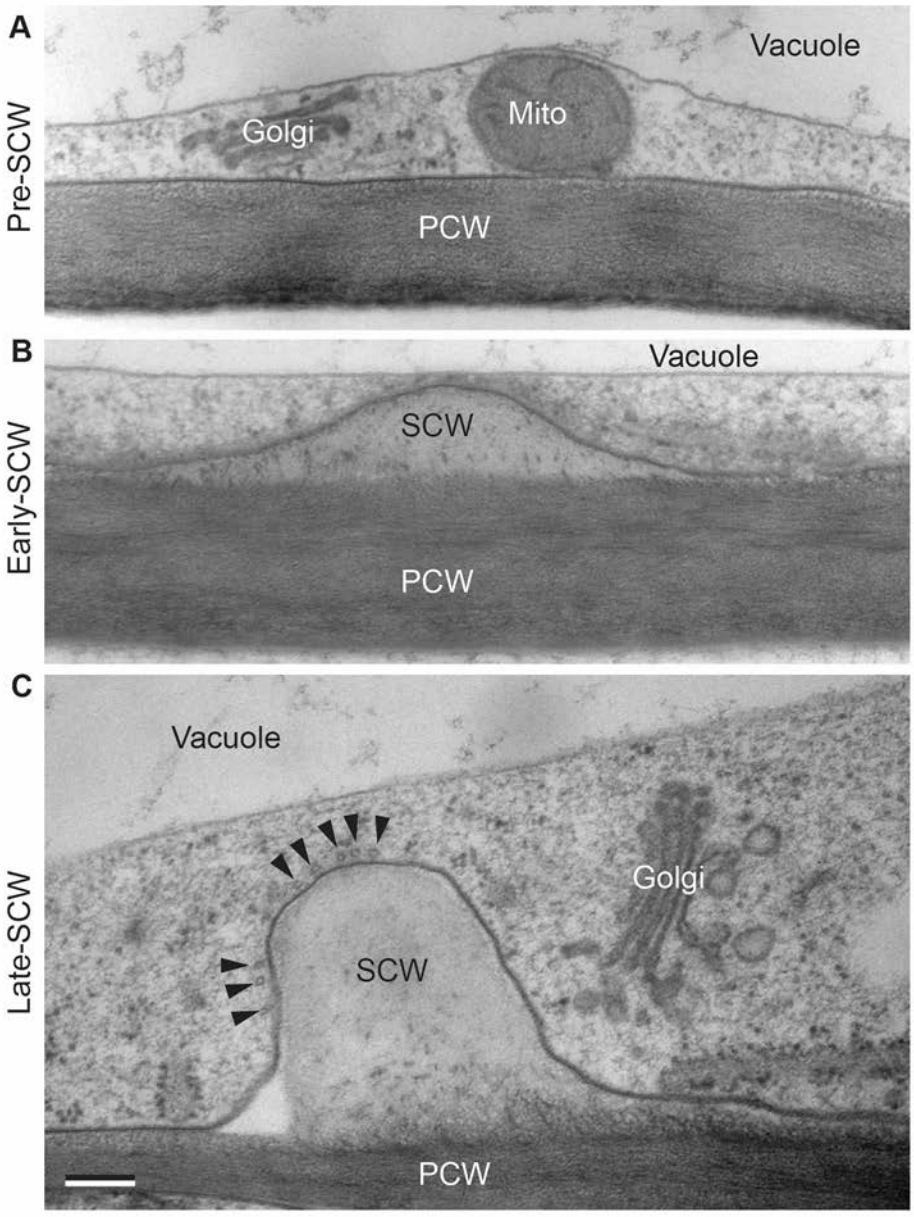

Figure 3.5 Stages of SCW deposition characterized using TEM.

TEM images of cells **(A)** prior to SCW deposition, **(B)** early in SCW deposition, and **(C)** late in SCW deposition. Mito = mitochondrion, PCW = primary cell wall, arrowheads = microtubules lining SCW domain. Representative images from 2+ replicate experiments. Scale = 200 nm.

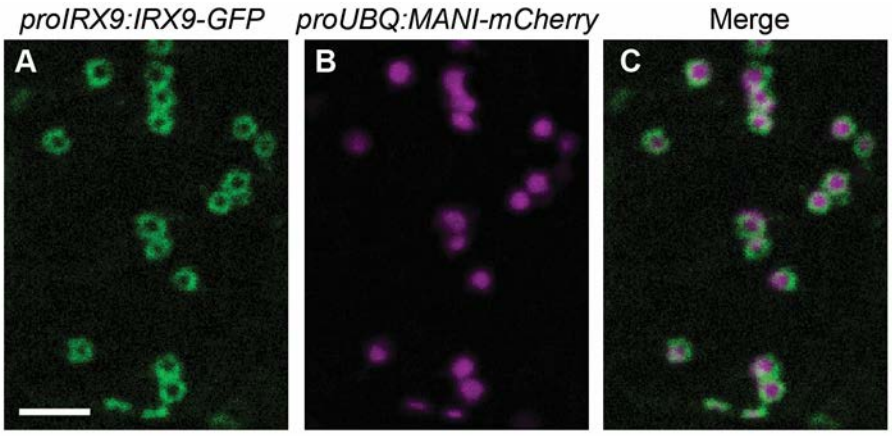

Figure 3.6 IRX9-GFP and MANI-mCherry colocalize in the Golgi apparatus.

Spinning disk confocal colocalization of **(A)** the xylan biosynthetic IRX9-GFP and **(B)** the Golgi-marker MANI-mCherry. The co-occurrence of the proteins in every Golgi stack is apparent in the **(C)** merged image. Distinct distributions within the Golgi are visible as ring-shaped IRX9-GFP and more central MANI-mCherry signals. Scale = 5 µm.

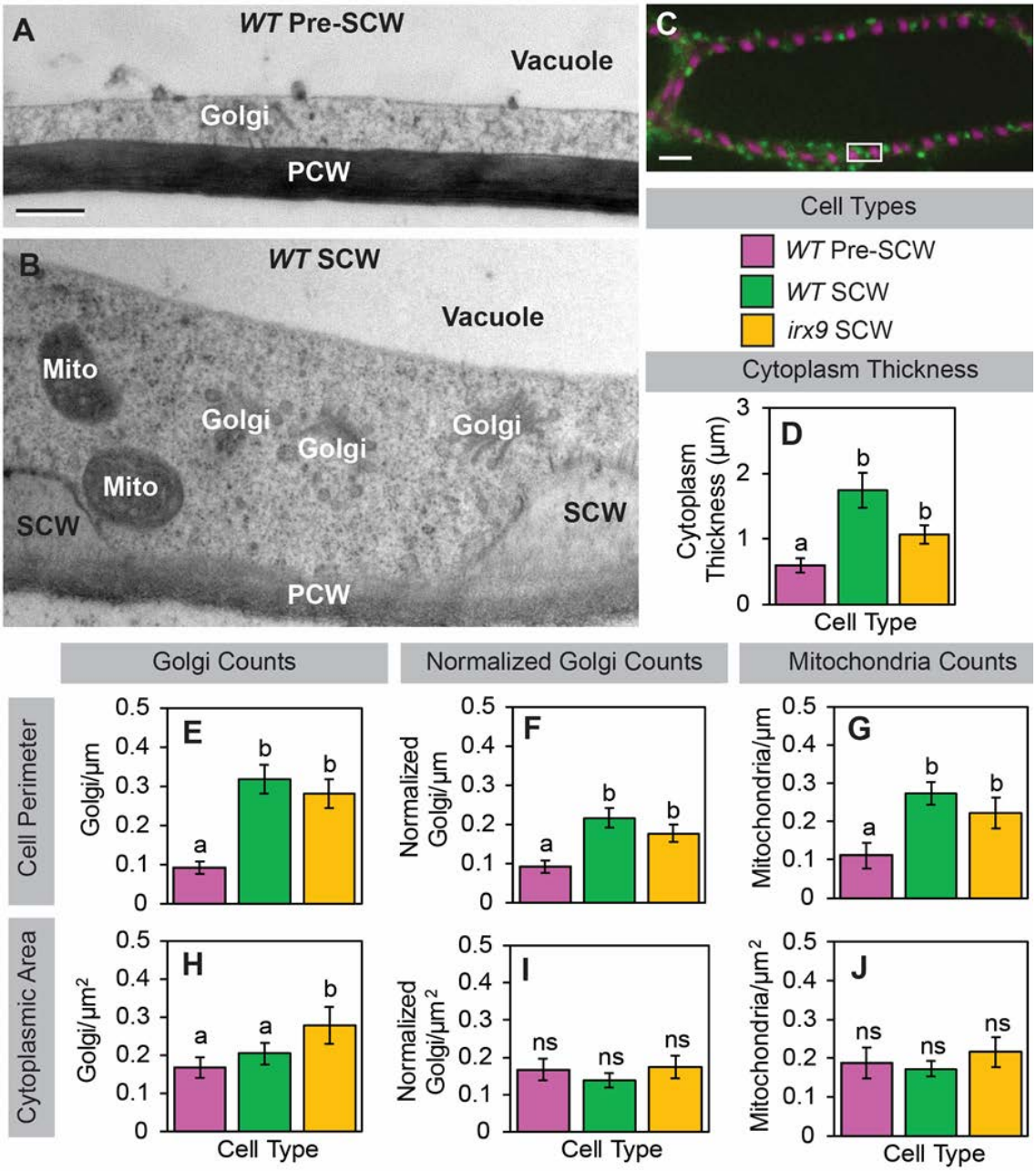

Figure 3.7 Golgi abundance increases with SCW deposition in *WT* and *irx9* cells.

(A-B) Representative TEM images of **(A)** wild-type cells prior to SCW deposition (*WT* pre-SCW) and **(B)** during SCW deposition (*WT* SCW) used to estimate organelle abundance and cellular features. Mitochondria (Mito), primary cell wall (PCW), secondary cell wall (SCW). Scale = 500 nm. **(C)** Optical cross-section through the center of a *WT*-SCW cell with IRX9-GFP in green and propidium iodide-stained SCWs in magenta. White box shows approximate field of view in (B). Scale = 5 µm. **(D-J)** Quantification of cellular features in *WT* pre-SCW, *WT* SCW and *irx9* SCW cells. **(D)** Thickness of cortical cytoplasm. Golgi and mitochondrial abundance was calculated **(E, F, G)** per cell perimeter or **(H, I, J)** per cytoplasmic area. Quantification included **(E, H)** Golgi counts, **(F, I)** Golgi counts normalized by Golgi width, and **(G, J)** Mitochondrial counts. Means ± 95% CI. Statistics = one-way ANOVAs with Tukey HSD *post hoc* tests ($p<0.05$), ns = not significant. *WT* Pre-SCW and *WT* SCW (n = 31 cells, 4-5 seedlings, 3 replicate experiments), *irx9* SCW (n = 13 cells, 3 seedlings, 1 experiment).

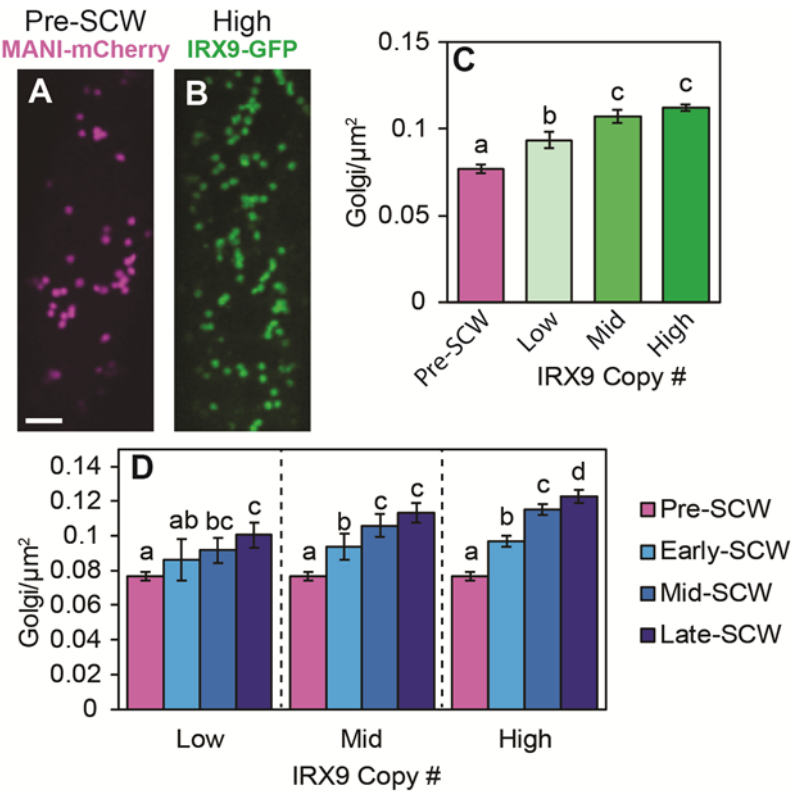

Figure 3.8 IRX9-GFP-labelled Golgi increase in density as SCW deposition progresses.

(A-B) Representative images used to quantify Golgi Density, showing a cell with a Golgi density near the average for **(A)** a pre-SCW cell expressing *proUBQ10:MANI-mCherry*, or **(B)** a post-SCW expressing multiple copies of IRX9-GFP in the wild-type background (i.e. high copy number). Scale = 5 µm. **(C)** Golgi densities averaged across all SCW stages show increases in Golgi density with increased copy number (i.e. Low < Mid < High) compared to pre-SCW stage. **(D)** Golgi density increases as SCW-development progresses for all three IRX9-GFP lines. Pre-SCW data is repeated for each copy number group. Statistics = one-way ANOVAs and Tukey HSD *post hoc* test ($p<0.05$). Means ± 95% CI. For (D) each genotype was analysed using independent one-way ANOVAs. For each genotype in (C) n = 150 - 795 cells, 10 - 78 plants, 2 - 6 replicate experiments.

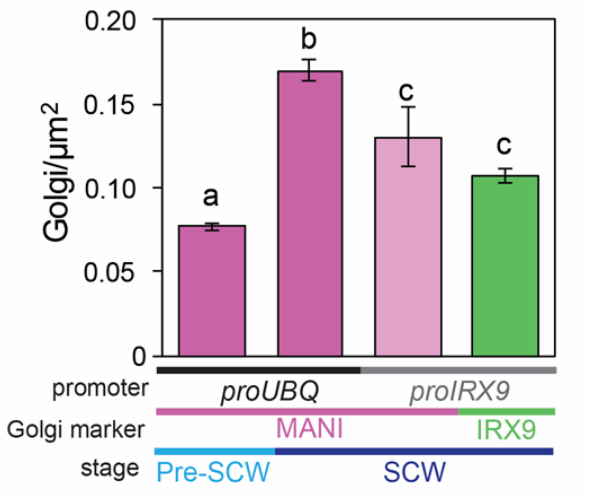

Figure 3.9 Golgi density increases during SCW production regardless of promoter or Golgi marker.

Plant lines driven by different promoters (*proUBQ* vs *proIRX9*) and driving different Golgi-localized proteins (MANI vs IRX9) had different Golgi densities following SCW-deposition. For comparison with the other *proIRX9*-driven protein, the IRX9-GFP genotype shown is the 'mid-copy number' line, with a single insertion of IRX9-GFP into the *WT* background. Statistics = Kruskal-Wallis and *post hoc* tests ($p<0.05$). Means ± 95% CI. For Pre-SCW and *proIRX9:IRX9-GFP* (n = 159-795 cells, 11-78 plants, 2-6 replicate experiments), *proIRX9:MANI-mCherry* (n = 23 cells, 7 seedlings, 1 experiment), *proUBQ:MANI-mCherry* (n = 258 cells, 11 seedlings, 2 experiments).

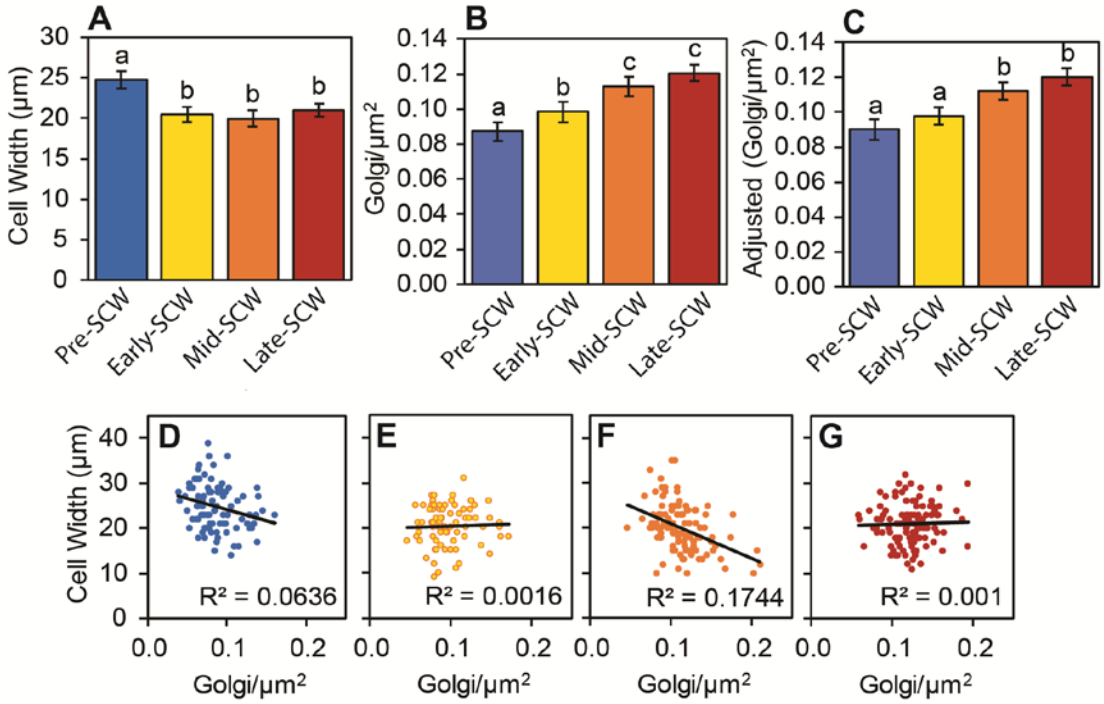

Figure 3.10 Bias in size of SCW-producing cells does not bias confocal density measures.

(A) Cells selected for Golgi abundance measurement are significantly smaller in pre-SCW than other SCW stages. **(B-C)** Golgi abundance in different developmental stages for **(B)** un-adjusted means and errors **(C)** means and errors adjusted for covariation with cell width (ANCOVA with Bonferroni adjustment). **(D-G)** Plots of cell width and Golgi abundance at the **(D)** pre-SCW, **(E)** early-SCW, **(F)** mid-SCW, and **(G)** late-SCW stages showing linear best-fit lines and R^2 values. Statistics = (A,B) one-way ANOVA with (A, B) Tukey HSD *post-hoc* or (C) Bonferroni adjustment ($p<0.05$). pre-SCW (n= 90), early-SCW (n = 80), mid-SCW (n = 342) and late-SCW (n = 113) from a single experiment. Means ± 95% CI.

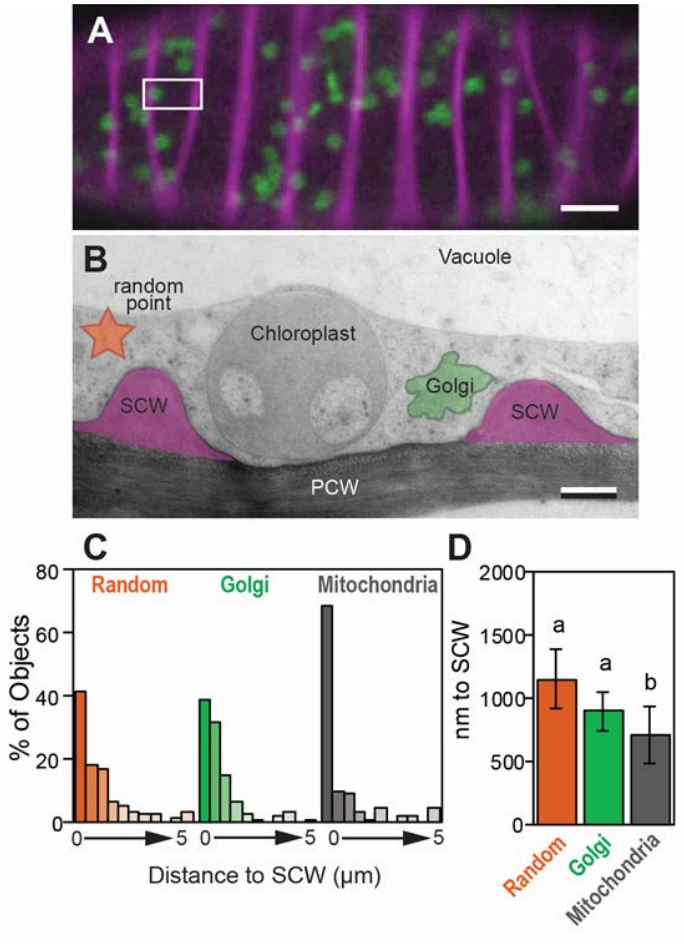

Figure 3.11 Cytoplasmic geometry constrains Golgi stacks to regions near SCWs.

(A) Top-down view of the cortical cytoplasm in a cell expressing IRX9-GFP (green) in the Golgi and stained with propidium iodide (magenta). Box shows approximate field of view in (B) for reference. Scale = 5 µm. **(B)** TEM cross-section of cortical cytoplasm showing the position of a Golgi stack (green) and a random point (orange) relative to the SCW (magenta). Scale = 500 nm. **(C)** Histogram showing the distance to the SCW in TEM images of random points, Golgi and mitochondria using 500 nm bins. **(D)** Average distance to SCW from random points, Golgi or mitochondria. Statistics = one-way ANOVA with Tukey HSD *post-hoc* ($p<0.05$) for square-root transformed distances. Means ± 95% CI. n = 168 (Random, Golgi) and 114 (Mitochondria) from 16 cells, 5 seedlings and 3 replicate experiments.

Chapter 4: IRX9 and Xylan in Concentric Rings in Golgi Cisternae

4.1 Introduction

In the previous chapter, it was shown that the onset of SCW synthesis is accompanied by a significant increase in the number of Golgi stacks, which then work in concert to produce xylan for the developing SCW. During this transition, the Golgi apparatus is remobilized from PCW production to begin assembly of xylans and mannans, and modification and trafficking of the large numbers of proteins required for proper cellulose and lignin deposition (Meents et al., 2018; Watanabe et al., 2018). This process requires loading the flattened, membrane-bound cisternae of the Golgi stacks with the many proteins necessary to meet this increased demand for Golgi processing. These changes in Golgi resident proteins and cargo are almost certainly accompanied by changes in Golgi ultrastructure. Golgi width, the number of cisternae, and the size of secretory vesicles, often change during different developmental stages and in different cell types (Staehelin et al., 1990; Samuels et al., 2002; Young et al., 2008). The shape and organization of organelles is usually considered to be optimized for organelle function (Voeltz and Prinz, 2007). Characterization of changes in Golgi ultrastructure during SCW deposition, can therefore help us better understand how xylan biosynthesis occurs in the Golgi.

Part of this characterization involves considering how cisternal structure changes across the Golgi stack. These cisternae are divided into *cis*-, medial-, and *trans*-types based on their position in the stack and their ultrastructure in TEM imaging (Staehelin et al., 1990; Zhang and Staehelin, 1992). These different cisternae are also considered to specialize in sequential stages of Golgi processing, thus creating a gradient in Golgi structure and function across the stack (Day et al., 2013). Though many aspects of cisternal structure are well characterised, it is still unclear how this structure facilitates Golgi function. Part of the difficulty in filling in this gap in our understanding, is that few Golgi resident proteins or products have been localized to specific regions of the Golgi stack. The few exceptions include some N-glycan processing (Schoberer and Strasser, 2011) and xyloglucan biosynthetic enzymes (Chevalier et al., 2010), which are found preferentially in a subset of cisternae, and polysaccharide cargo, which are found in cisternal margins (Zhang and Staehelin, 1992; Samuels et al., 2002; Young et al., 2008; Wang et al., 2017). These distributions however, are often not characterized on a small enough scale for structure/function correlation, as cisternal structure changes between adjacent cisternae, and from

margins to centers of cisternae (Kang and Staehelin, 2008; Kang et al., 2011; Donohoe et al., 2013). To better elucidate the relationship between cisternal structure and function, it is therefore necessary to map the distribution of different Golgi processes in each of these dimensions. Theoretically, this could be accomplished by quantifying the distribution of Golgi-resident biosynthetic enzymes and their products across the Golgi stack using immunoTEM. In practice this is challenging because the abundance of resident proteins like glycosyltransferases is often too low to detect (Fukuda et al., 1996).

Xylan biosynthesis in the VND7-induction system (Yamaguchi et al., 2010a) provides an excellent model system for this purpose. The previous chapter describes how VND7-induction rapidly activates expression of a functional IRX9-GFP fusion protein and triggers SCW synthesis. I hypothesized that the abundant IRX9-GFP and xylan biosynthesis would permit immunogold localization of xylan biosynthesis (using anti-GFP), and xylan accumulation (using anti-xylan), to specific cisternae, and regions of cisternae. This map of Golgi function can then be correlated with characterization of Golgi ultrastructure at the nanometer scale, to provide insight into how Golgi structure accommodates xylan biosynthesis. In addition, in this system Golgi function can be perturbed and then tested for changes in Golgi structure. For example, I hypothesized that the *irx9-2* knock-out mutant, which lacks functional IRX9 and produces little SCW xylan (Lee et al., 2010; Wu et al., 2010; Petersen et al., 2012), would have altered Golgi structure during SCW production.

In this chapter, I use qualitative and quantitative TEM and immunoTEM to conduct a nm-scale characterization of Golgi structure and organization during SCW-production to answer the following questions: (1) How does the structure of the Golgi stack change in response to SCW synthesis? (2) How is this altered in the *irx9-2* mutant? (3) How are Golgi residents and their products distributed within the Golgi stack?

4.2 Results

4.2.1 Golgi ultrastructure during SCW biosynthesis

VND7-induction triggers cell transdifferentiation into protoxylem tracheary elements, a process which results in a shift in Golgi function, from PCW production to SCW production (Watanabe et al., 2018; Chapter 3). As Golgi structure is known to change with Golgi function, I hypothesized that the onset of abundant SCW production would lead to increases in the size of cisternae and secretory vesicle buds. Conversely, disruption of xylan biosynthesis in the Golgi of *irx9* mutants was predicted to counteract these changes to Golgi structure. To test these hypotheses, Golgi ultrastructure was examined using TEM imaging of cryo-fixed *WT* (*WT* pre-SCW), *WT/35S:VND7-VP16-GR* (*WT* early-SCW and *WT* late-SCW) and *irx9/proUBQ10:VND7-VP16-GR* (*irx9* SCW) cells. Variation in VND7-induction across plant lines (Chapter 3) made it challenging to align the stage of SCW deposition in *irx9* vs *WT* cells, especially as SCWs are thinner in *irx9* (Lee et al., 2010; Wu et al., 2010). This was addressed by comparing *irx9* SCW Golgi to Golgi in both *WT* early-SCW and *WT* late-SCW cells. Plants were treated with DEX for 22 – 28 hr, except for the *WT* early-SCW plants, which were exposed for 17 – 20 hr (Chapter 3). Clear qualitative differences were observed in the structure of Golgi stacks (Figure 4.1 A–D), and quantification of various Golgi features was used to develop a more nuanced picture of how cisternal structure changes within individual Golgi stacks, and across the different sample types.

4.2.1.1 Cisternal diameter increases in SCW-producing cells

Cisternae were categorized as *cis*, *cis*+1, mid, *trans*-1 and *trans*, based on their position in the stack and their physical features as described in the methods. The length of each cisterna from edge to edge was then measured in Golgi cross-sections (Figure 4.1 A–D). The largest cisternae in both pre-SCW and SCW-producing Golgi were the mid- and *trans*-1 cisternae, and there was a significant decrease (10 – 20%) from the *trans*-1 to *trans* cisterna (Figure 4.1 E). There was a significant (2-fold) change in cisternal diameter from the smallest to largest cisternae for all sample types (Figure 4.1 E). Averaging the diameter of *cis*+1 to *trans*-1 cisternae provides an estimate of Golgi size that can be used to compare Golgi width in the different samples. After SCW production initiated, Golgi width increased ~ 50% and remained at this size

throughout this process (Figure 4.1 F). These data demonstrate that while within each stack there was a consistent cis-to-trans pattern of cisternal diameters, in wild-type developing protoxylem tracheary elements, SCW production increases the overall Golgi cisternal width.

To examine the consequences of loss of IRX9 function on Golgi structure, *irx9* SCW cells were compared with *WT* early-SCW and *WT* late-SCW stages. This revealed that Golgi in the *irx9* mutant increase in width to the same extent as the wild-type SCW-producing Golgi (Figure 4.1 F). Most Golgi contained 5 or 6 cisternae, though there was a small but significant increase in the number of cisternae in *irx9* SCW compared to the *WT* pre-SCW control (Figure 4.1 G). These data suggest that during SCW production, loss of IRX9 and xylan synthesis does not affect the size of Golgi cisternae, but slightly increases the number of cisternae.

4.2.1.2 Cisternal margins and TGN vesicles increase in size during SCW production

Each Golgi cisterna has a flattened central region with margins (i.e. the rounded profiles at the edge of each cisterna) that increase in size from *cis* to *trans*. This increase is attributed to larger quantities of polysaccharide cargo, culminating in the production of secretory vesicles at the TGN (Zhang and Staehelin, 1992; Young et al., 2008; Wang et al., 2017). This same trend was apparent in all Golgi sampled with a greater increase in margin size and TGN vesicle bud diameters (Figure 4.2 A–H). Quantification of margin size revealed that there is a significant increase in margin size in *trans* vs *cis* cisternae, 13% for *WT* pre-SCW, 51-64% for *WT* early-SCW, 51% for *WT* late-SCW, and 44% for *irx9* post-SCW (Figure 4.2 I). In *WT* SCW-producing cells, the cisternal margins were significantly larger than in *WT* pre-SCW Golgi, with a ~18% increase in the margins of *cis*-cisternae, and a dramatic increase of ~65% for *trans*-cisternae (Figure 4.2 I). Interestingly, the *irx9* post-SCW Golgi margins were not statistically different from the control *WT* pre-SCW (Figure 4.2 J). These data indicate that the observed increase in Golgi margins during SCW production is tied to the production of xylan by IRX9.

The TGN is composed of interconnected clusters of tubules, secretory vesicle clusters and clathrin-coated vesicle buds (Young et al., 2008; Toyooka et al., 2009; Kang et al., 2011; Boutté et al., 2013). As the size of these buds can vary depending on the type of vesicle and its contents, TGN function before and during SCW production was assessed by quantifying the size of these swollen membrane regions, termed ‘TGN vesicles’. For all sample types the size of

TGN vesicles was not significantly different than the size of the *trans*-cisternal margins, supporting a model where the *trans*-most cisterna matures into the TGN. A large increase in the size of TGN vesicles accompanied the onset of SCW production (Figure 4.2 E-H). This can be seen in the distribution of vesicle sizes (Figure 4.2 K) and the significant increase in mean vesicle size from ~ 60 nm prior to SCW, up to ~105 nm during SCW synthesis (Figure 4.2 J). Loss of xylan biosynthesis in *irx9* SCW cells also resulted in an intermediate TGN vesicles size with a mean of ~ 75 nm (Figure 4.2 J). The *irx9* SCW TGN also had a more hybrid structure, with tubular regions like *WT* pre-SCW TGN, and regions with large vesicle buds more like the *WT* cells producing SCWs. These different structures are represented in a bimodal distribution of *irx9* TGN vesicle sizes (Figure 4.2 K). This shows that while the packaging of xylan in secretory vesicles contributes to increased TGN vesicle size during SCW production, other cargo are likely contributing as well.

4.2.1.3 Number of cisternal fenestrations increases in *irx9*

Another key feature of many Golgi cisternae are fenestrations, which often appear as gaps in cisternal edges in Golgi cross-sections (Kang and Staehelin, 2008; Kang et al., 2011; Donohoe et al., 2013). Despite this ubiquity, the function of Golgi fenestrations has not been resolved. To better understand what factors might be contributing to fenestration formation, the number of fenestrations in each cisterna was estimated by counting the number of gaps in cisterna cross-sections. Gaps were observed in cisternae of all Golgi sampled, and fenestrae were visible in both Golgi cross-sections (Figure 4.3 A–D) and in sections through tilted Golgi (Figure 4.3 E–H). The number of gaps in each cisterna was largest in the medial-cisternae (Figure 4.3 I). The *irx9* SCW Golgi had a significant (3-fold) increase in the number of cisternal gaps compared to all other samples (Figure 4.3 J). This difference is very clear in the 'Top View' image of an *irx9* Golgi (Figure 4.3 H), showing a highly tubulated, web-like cisterna with large and numerous fenestrations. Like the *WT* Golgi, the *irx9* Golgi also have the greatest number of gaps in the mid-cisterna, dropping significantly in the more *cis* and *trans* cisternae (Figure 4.3 J).

Fine-scale quantification of cisternal architecture provided a precise account of the changes in cisternal length, margin size, and number of fenestrations across the Golgi stack in all samples. It also confirmed that altering Golgi function by triggering SCW synthesis changes

Golgi structure. The onset of SCW synthesis caused increases in Golgi width and the size of cisternal margins and TGN-vesicles, however there were no significant differences between *WT* early-SCW and *WT* late-SCW Golgi. Conversely, decreased xylan production in the *irx9* mutant background led to a reduction in the size of the cisternal margins and TGN vesicles. Interestingly, the *irx9* Golgi cisternae were also highly tubulated, with a significant increase in the number of fenestrations. These data indicate that during wild-type SCW biosynthesis, the Golgi expands to accommodate the production of xylan by increasing cisternal length, margin width, and TGN vesicle size. Furthermore, the presence of IRX9 promotes the formation of smooth cisternal sheets, at the expense of fenestrations and tubules.

4.2.2 Mapping of xylan biosynthesis

4.2.2.1 Anti-xylan antibody selection

In live-cell imaging, IRX9-GFP is found in a ring around the center of the Golgi stack (Figure 3.6), but current models based on freeze-fracture data propose that Golgi biosynthetic proteins like IRX9 reside in these cisternal centers (Staehelin et al., 1990). To reconcile this difference, and test the existing model, I quantified the distribution of the Golgi-resident protein IRX9 and its product xylan, across different domains of Golgi cisternae. I used immunoTEM of high-pressure frozen/freeze-substituted *proIRX9:IRX9-GFP/35S:VND7-VP16-GR* samples that were treated with DEX for 22 - 26 hrs to localize and quantify IRX9-GFP and xylan in SCW-producing cells.

The anti-xylan antibodies LM10 and LM11 are popular choices for immunolabelling of xylans. LM10 binds to xylans with little or no substitutions, while LM11 binds low-substituted xylans and arabinoxylans (McCartney et al., 2005). Both LM10 and LM11 bind to SCWs with equal success in immunofluorescence and immunoTEM of Arabidopsis stems (Kim and Daniel, 2012), and LM10 labelling was used previously in immunofluorescence characterization of xylan mutants, including *irx9* and *irx10irx10L* (Peña et al., 2007; Wu et al., 2009; Wu et al., 2010). The LM10 antibody was therefore selected for testing for immunoTEM labelling of the Golgi in SCW-producing cells. Seedlings were cryofixed in glutaraldehyde and acetone before embedding in LR white for immunogold labelling at concentrations from 1:5 to 1:20. SCWs

consistently labelled with at least a few gold particles, however labelling of Golgi was rare, making it challenging to acquire sufficient data for quantification of xylan distribution.

The Complex Carbohydrate Research Centre (CCRC) has developed a suite of carbohydrate antibodies used to profile cell wall composition, including a number of anti-xylan antibodies which have been used to label Arabidopsis SCWs in immunofluorescence experiments (Pattathil et al., 2010). Four of these anti-xylan antibodies, CCRC-M138, -M147, -M149 and -M153, were selected for testing because they recognized small unsubstituted xylose chains, an epitope expected to be common in glucuronoxylan (Bromley et al., 2013). CCRC-M138 recognizes unsubstituted xylopentaose (Peralta et al., 2017), CCRC-M147 unsubstituted xylan disaccharides (Schmidt et al., 2015), CCRC-M149 unsubstituted xylotriose (Peralta et al., 2017) and CCRC-M153 unsubstituted and arabinose substituted xylan (Schmidt et al., 2015; Peralta et al., 2017). Immunogold labelling with all four of the anti-xylan antibodies produced successful labelling of SCWs and Golgi/TGN in cells producing SCWs, and little or no labelling of cells not producing SCWs. Though any of the four antibodies could likely have been used successfully for xylan mapping in the Golgi, qualitatively CCRC-M138 labelling appeared to be slightly better so it was used for all subsequent experiments.

CCRC-M138 labelled Golgi, TGN and SCWs in all cells with visible SCWs (Figure 4.4 A–C). In total, 57% of Golgi and 57% of TGN were labelled with one or more gold particles, averaging 1.17 gold particles per Golgi and 1.36 gold particles per TGN. The secondary antibody was specific to CCRC-M138, as no gold labelling was seen in the Golgi, TGN or SCW in the absence of the primary antibody (Figure 4.4 D–F). The heterogeneity of VND7-induction between cells in the same seedling allowed comparison of cells producing SCWs with those that were not. Gold labelling was never seen in cells not producing SCWs (Figure 4.4 G), suggesting CCRC-M138 is specific to an epitope present in the Golgi, TGN and SCW of cells producing SCWs, which is consistent with xylan specificity. Together, this indicates that CCRC-M138 is a suitable antibody for xylan mapping in the Golgi and TGN during SCW synthesis.

4.2.2.2 Anti-GFP antibody selection

The LifeTech antiGFP antibody (A6455) has been used extensively for immunoTEM localization of GFP-tagged proteins (McFarlane et al., 2010; Zhang et al., 2016). Testing this

antibody in concentrations ranging from 1:200 to 1:5 however, showed non-specific binding in swollen cisternal margins, TGN vesicles and the SCWs of plants not containing GFP. This pattern of non-specific binding indicates that the LifeTech antiGFP is not suitable for labelling cells producing SCWs. The Torrey Pines' antiGFP (TP401) has also been used successfully in immunogold labelling (Crowell et al., 2009; Stierhof and El Kasmi, 2010; Roppolo et al., 2011; Sauer et al., 2013), and was therefore tested at 1:10, 1:50 and 1:100 concentrations. At 1:50, this antibody showed consistent label in Golgi in plants containing IRX9-GFP (Figure 4.5 A), and little non-specific label in Golgi (Figure 4.5 B), TGN and SCWs. There was also very good signal in the Golgi of IRX9-GFP containing plants, compared to background label in wild-type plants lacking IRX9-GFP. When anti-GFP binding was quantified in IRX9-GFP lines, 46% of Golgi or TGN contained one or more gold particles, while only 7% of Golgi were labelled in the plants not containing GFP (Figure 4.5 C). The average number of gold particles per Golgi/TGN increased 92%, from 0.07 gold particle per Golgi in wild-type cells lacking IRX9-GFP, to 0.83 in IRX9-GFP cells. The gold label in IRX9-GFP Golgi was significantly different than that of background label, according to a chi squared test ($p<0.001$). The Torrey Pines antiGFP was therefore deemed suitable for anti-GFP mapping of IRX9-GFP.

4.2.2.3 Xylan and IRX9-GFP are found in different regions of the Golgi

To map xylan and IRX9 distribution in Golgi and TGN, seedlings containing *proIRX9:IRX9-GFP* were prepared for immunoTEM using the CCRC-M138 (xylan) and the Torrey Pines anti-GFP (IRX9-GFP) antibodies. In anti-xylan labelling of Golgi in 24 cells, 43% of gold particles across 17 cells were found in Golgi of sufficient preservation quality and cross-sectional orientation to allow mapping to individual regions of each cisterna (Figure 4.6 A). Of Golgi/TGN label, 60% of the gold particles labelled the TGN and 40% labelled the Golgi. Mapping to individual cisternae shows that label first appears in small quantities in the mid-cisternae (2.3% of label), becoming much more significant in *trans*-cisternae (21.9% of label) (Figure 4.6 B). In anti-GFP mapping of 39 cells, 44% of gold particles across 33 cells could be mapped to distinct regions of the Golgi. Gold particles were found in all cisternae, but peak label (33.9%) was in the mid-cisternae, tapering to 8.6% in *cis*-cisternae, and 12.4% in *trans*-cisternae (Figure 4.6 B). A very small proportion of label was found in the TGN (2.2%). Within each

cisterna, lateral mapping of IRX9-GFP and xylan was conducted by measuring the distance from each gold particle to the edge and center of the cisterna. Both GFP and xylan label was found significantly closer to the margin than the center of cisternae (Fig 4.6 C). Xylan label was significantly closer to the margin than GFP (104 nm and 157 nm respectively) (Fig 4.6 C).

To better visualize the distribution of label across Golgi cisternae, every Golgi cisterna was divided into ten equal parts (giving 5 blocks for each half cisterna from the cisternal center to the margin, and 25 blocks total including all cisternae) (Figure 4.6 A, D, E). The number of gold particles falling into each block was then tallied and the distribution visualized using a heat map (Figure 4.6 D–E). As suggested by the previous analysis, IRX9-GFP and xylan label only overlapped slightly. IRX9-GFP label is most abundant in *cis*+1, mid and *trans*-1 cisternae in more central regions of the cisternae (Figure 4.6 D) while xylan label was found predominantly in the outermost edges of *trans*-1 and *trans* cisternae (Figure 4.6 E). To better understand the distribution of label within the quantified architecture of Golgi stacks, the size of the heat maps was then scaled to account for the changing diameter of Golgi cisternae using the calculated cisternal length of cisternae in *WT* SCW-producing cells (Figure 4.1 E). Both IRX9-GFP and xylan label are low in the center of cisternae, and each is found in spatially distinct regions of the Golgi (Figure 4.6 F, G). As xylan label appeared to overlap with the swollen cisternal margins (Figure 4.6 G, and refer to Figure 4.2 I), the correlation between xylan label and margin size was calculated (Figure 4.6 H). As predicted, xylan label highly correlated with the size of the cisternal margins, while IRX9-GFP label did not. However, the IRX9-GFP label appeared to be abundant in regions of the Golgi which are highly fenestrated (Figure 4.3 I). Indeed, the amount of IRX9-GFP label in each cisterna was highly correlated with the average number of fenestrations, which was not the case for xylan label (Figure 4.6 I).

These results show that IRX9-GFP and its xylan product localize to distinct sub-domains of the Golgi, from both *cis*-to-*trans*, and centers-to-margins. These distributions also correlate with different structural features of the Golgi, with xylan abundance correlating with the size of the cisternal margins, and IRX9-GFP labelling with the number of putative fenestrations.

4.3 Discussion

In this chapter, an in-depth characterization of Golgi ultrastructure was conducted in cells prior to SCW production, at the Early-SCW and Late-SCW stages, and in *irx9* cells producing SCWs. This analysis was then used to guide immunoTEM mapping of IRX9-GFP and xylan within different regions of the Golgi stack. Together, the data in this chapter informs a concentric circle model of cell wall polysaccharide processing in the Golgi, using xylan biosynthesis as an example (Figure 4.7). In this model, the xylan biosynthetic complex makes xylan in an inner-margin of the medial cisternae, where the fenestrated margin and the flattened central zone of the cisternae come together. In more *trans*-cisternae, a decrease in the presence of the xylan biosynthetic complex coincides with increasing amounts of xylan. The xylan produced accumulates in the swollen cisternal edges, which continue to widen in *trans* cisternae as more cargo is produced. By the time the xylan is packaged into secretory vesicles at the TGN, it has been successfully segregated from the biosynthetic machinery that remains in the inner-margin of medial cisternae.

4.3.1 Mapping IRX9-GFP in the Golgi

4.3.1.1 The xylan backbone is synthesized in the medial Golgi

GFP-tagging of IRX9 allowed localisation of this xylan biosynthetic protein to specific cisternae using an anti-GFP antibody and immunogold labelling. IRX9-GFP was most abundant in the medial cisternae, and almost entirely absent from the *cis*-Golgi and the TGN (Figure 4.6). The appearance of substantial IRX9-GFP in the Golgi also coincides with a rapid increase in the size of xylan-filled cisternal margins. The *cis*-to-*trans* distribution of enzymes in the Golgi is proposed to correlate with the progressive production of Golgi cargo. It is well established that Golgi resident proteins can localize to different cisternae, such as the *cis*-localized MANI-mCherry used in this study (Nebenführ et al., 1999), or another common Golgi marker, sialyltransferase (ST), which is found in the *trans*-Golgi (Boevink et al., 1998). This difference in distribution is believed to reflect the presence of sequential processing steps in different Golgi cisternae. In plants, N-glycan processing involves successive trimming and decoration of oligosaccharides on glycoproteins by a set of enzymes in the Golgi, which are spatially separated into different cisternae according to the order in which they act (Schoberer and Strasser, 2011).

A similar ‘assembly-line model’ has been proposed for synthesis of pectin (Atmodjo et al., 2013) and xyloglucan (Brummell et al., 1990). In these models, carbohydrate backbone synthesis is often proposed to occur earlier in the Golgi, followed by addition of side chains, methylation and acetylation. For xyloglucan, this is supported by a study which found that GFP-tagged enzymes catalyzing subsequent steps in xyloglucan biosynthesis were most abundant in *cis*, medial and *trans* cisternae in turn (Chevalier et al., 2010).

Some degree of successive synthesis is likely also occurring during xylan biosynthesis. Production of the xylan backbone for Arabidopsis SCWs is thought to require three sets of proteins: IRX9/IRX9L (Lee et al., 2010; Wu et al., 2010), IRX10/IRX10L (Brown et al., 2009; Wu et al., 2009), and IRX14/IRX14L (Keppler and Showalter, 2010). Mapping of IRX9 to the inner margin of medial Golgi therefore suggests that synthesis of the xylan backbone is occurring in these domains. The other proteins involved in backbone synthesis may be similarly localized, as a number of experiments suggest that xylan is synthesized by a biosynthetic complex. Co-immunoprecipitation and bimolecular fluorescence complementation (BiFC) studies during PCW production of arabinoxylans in wheat (*Triticum aestivum*) and asparagus (*Asparagus officianalis*), have demonstrated *in planta* heterodimerization of xylan biosynthetic proteins orthologous to the Arabidopsis proteins (Zeng et al., 2010; Jiang et al., 2016; Zeng et al., 2016). Each protein was also shown to homodimerize *in planta*, further increasing the size of the proposed xylan biosynthetic complex to at least six members (Zeng et al., 2016). Proteins involved in decorating the xylan backbone may also be incorporated into the protein complex, as a PCW xylan biosynthetic complex isolated from wheat also showed arabinosyltransferase and glucuronosyltransferase activity necessary for side chain addition (Zeng et al., 2010). Furthermore, because the UDP-xylose substrate for xylan backbone synthesis is now believed to be synthesized by cytosolic UDP-Xylose Synthases (UXSs) (Kuang et al., 2016; Zhong et al., 2016), the Golgi-localized UDP-xylose transporters, especially UXT1, are hypothesized to be similarly associated with the xylan biosynthetic complex to ensure adequate substrate availability (Ebert et al., 2015).

Other aspects of xylan synthesis are likely occurring in different regions of the Golgi, however. Analysis of xylans in various xylan biosynthetic mutants suggests that the methylation rate of glucuronic acid residues is independent of the rate of xylan synthesis, which is consistent

with a model where methylation occurs following backbone synthesis (Zhong et al., 2005; Peña et al., 2007; Kuang et al., 2016). Xylans are also acetylated in the Golgi (Urbanowicz et al., 2014) and then deacetylated prior to deposition in the wall (Zhang et al., 2017). The resulting pattern of acetylation was found to be essential for xylan interaction with cellulose (Grantham et al., 2017). Xylan acetylation and deacetylation almost certainly happen in different regions of the Golgi. Another example of progressive xylan synthesis involves the conserved reducing-end oligosaccharide (REO) found in many SCW xylans (Peña et al., 2016), which has been hypothesized to be either a primer for consecutive xylan synthesis, or a terminator of synthesis transferred *en bloc* to the completed xylan backbone (York and O'Neill, 2008). In either case, different steps in xylan synthesis are proposed to occur sequentially. Xylans also have alternating 'major' and 'minor' domains with differing patterns of glucuronic acid substitution (Bromley et al., 2013). These different domains may reflect variation in the rate of substitution on a consecutively synthesized xylan backbone, but they could also be synthesized independently and then assembled into a single strand later in the Golgi.

With the localization of xylan backbone synthesis to the medial Golgi, we can now formulate hypotheses about the relative location of other steps in xylan biosynthesis. For example, if the REO is a primer of xylan biosynthesis, then we would expect the enzymes producing REOs to appear in *cis*-cisterna. However, if the REO is a xylan terminator the biosynthetic enzymes may appear in more *trans*-cisternae. The mapping of IRX9 therefore allows the medial Golgi to be used as a benchmark to guide mapping of a variety of different steps of xylan biosynthesis.

4.3.1.2 Xylan is synthesized near fenestrated cisternal domains

In the concentric circle model, xylan biosynthetic proteins are found in an inner margin of medial cisternae, where they are separated from the bulk of their biosynthetic product, but also largely absent from the cisternal centers. This localization is consistent with my confocal data consistently showing a ring-shaped distribution of IRX9-GFP in the Golgi (Figure 3.6). A few other Golgi-resident proteins have been found to have similar localization pattern, including IRX9L (Zhang et al., 2016), CESAs (Crowell et al., 2009), and several COPI-related proteins (Ritzenthaler et al., 2002). Interestingly, the regions in which IRX9-GFP labelling was abundant

coincide with cisternae in which fenestrations are frequently found. Indeed, the *cis*-to-*trans* distribution of IRX9-GFP is highly correlated with the number of fenestrations in each cisterna (Figure 4.6 I), with the greatest IRX9-GFP label and number of fenestrations in mid-cisternae (Figure 4.3 I).

The presence of cisternal fenestrations has been documented in TEM tomography of Golgi in root meristem cells (Kang and Staehelin, 2008; Kang et al., 2011; Donohoe et al., 2013). In these studies, fenestrations appear most abundant in *trans*-cisternae, in contrast to their prevalence in medial cisternae in this study. This difference may be related to differences in Golgi function in these cell types, as tomography of heavily secreting Golgi from Arabidopsis seed coat cells appear to show large numbers of fenestrations in a medial cisterna (Young et al., 2008), and cross sections of Golgi in root caps show large numbers of cisternal gaps in medial cisternae (Staehelin et al., 1990). Fenestrations are also highly abundant in mammalian (Mogelsvang et al., 2004; Koga and Ushiki, 2006) and yeast Golgi (Mogelsvang et al., 2003). Interestingly, the mammalian clathrin-coated *trans* cisterna shows a similar decrease in fenestrations resembling those seen during SCW production. Despite the conservation of Golgi fenestrations across eukaryotes, their function is not known. The analysis in this chapter may provide a clue, as it suggests that fenestration abundance is linked with abundance of a Golgi resident protein, but not with its biosynthetic product. If the greater IRX9 content is linked to larger fenestration abundance in wild-type Golgi, why does the *irx9* mutant have increased rather than decreased number of fenestrations?

In *irx9*, the Golgi stacks are lacking the large quantities of xylan which normally accumulate in the margins, but they are also lacking a Golgi resident protein, IRX9. Furthermore, in transient expression of an IRX9 homolog in tobacco, IRX9 did not localize to the Golgi unless also expressed with IRX10 and IRX14 (Zeng et al., 2016). The absence of *irx9* in this study may therefore similarly prevent Golgi localization of other xylan biosynthetic proteins. To what extent then can we attribute the changes in Golgi structure in *irx9* to loss of Golgi polysaccharide cargo, vs. Golgi residents? Examination of fenestration distribution in *irx9* cisternae (Figure 4.3 D, H) suggests that the additional fenestrations in *irx9* are closer to the center of the cisternae where IRX9-GFP is usually found, and xylan absent (Figure 4.3 B, C, F, G). The increased abundance of fenestrations in more central regions of cisternae may therefore be attributed

largely to the lack of IRX9, rather than xylan, which is not abundant in these areas. Further experiments will be required to elucidate the mechanism by which IRX9 inhibits Golgi fenestration. One possibility is that a large xylan biosynthetic complex in the Golgi lumen physically prevents spontaneous fusion of the membrane on either side.

As cisternae mature, the lumen becomes increasingly compressed in the cisternal centers. Though the membranes on either side of the lumen get very close, they must not fuse, or a fenestration would form. A large xylan biosynthetic complex on the luminal face of the cisternal membrane could provide a barrier preventing the opposing membrane from getting close enough to fuse. If IRX9 was a central component of this complex, its absence could therefore permit the additional fenestration formation seen in the *irx9* mutant. How then do fenestrations form in regions known to contain IRX9-GFP in wild-type SCW-producing Golgi? One possibility is that IRX9 might only inhibit fenestrations when in a xylan biosynthetic complex. Dissociation of the complex to allow retrograde recycling may then allow cisternal membranes to become close enough for fusion, and fenestration formation. Therefore, regions of cisterna containing fenestrations may have fewer IRX9 proteins in xylan biosynthetic complexes than more central domains. This suggests that in addition to a *cis*-to-*trans* gradient in Golgi function, there may also be a center-to-margin gradient.

Experiments in a variety of organisms are beginning to suggest that shifts between the cisternal margin and center are linked to oligomerization of both Golgi cargo and residents. In plants, the ring-shaped distribution of the primary cell wall CESA3 was lost in the *stello* mutant background, when the CESAs shifted toward the center of Golgi cisternae (Zhang et al., 2016). This shift was found to coincide with a decrease in the formation of CESA complexes, implying a link between oligomerization of cargo and localization to the Golgi margins. Similar shifts between Golgi margins and centers have been found in mammalian cells using engineered proteins that aggregate and disaggregate in the absence or presence of a drug. One group found that aggregated membrane-associated cargo accumulates in more central regions of the cisternae, while soluble aggregations are present in the edges (Lavieu et al., 2013). Conversely, aggregation of Golgi resident proteins shifts them to cisternal centers, and disaggregation returns them to the rims (Rizzo et al., 2013). Furthermore, localization closer to the margins was required to maintain position of the protein in its specified cisternae. This suggests that the large

protein aggregates were excluded from retrograde trafficking and thus carried downstream with cisternal maturation. Together, these data could reflect size-dependant sorting with different outcomes for residents vs. cargo (i.e. large Golgi cargo shifting toward cisternal margins (Lavieu et al., 2013; Zhang et al., 2016), and complexes of resident proteins localizing closer to cisternal centers (Rizzo et al., 2013)).

The studies looking at oligomerization of proteins in the Golgi support the model that the formation of a large xylan biosynthetic complex may shift the localization of these proteins toward the center of cisternae, while allowing the soluble cargo to accumulate in the margins. If large complex formation impedes trafficking of the constituents, as seen in other systems (Rizzo et al., 2013), the complexes will move towards the *trans*-Golgi as the cisternae mature. To allow return of the proteins to their proper position in an earlier cisterna, the complex may dissociate, allowing individual proteins to move to fenestrated regions of the Golgi where they can be transported back toward the *cis*-Golgi, and then reform a complex to begin xylan biosynthesis anew. The IRX9-GFP mapped in this study encompasses proteins at all stages of this cycle, not just those currently producing xylan in a biosynthetic complex.

4.3.2 Mapping xylan in the Golgi

4.3.2.1 Xylan accumulates in the *trans*-Golgi margins

In the concentric circle model, the outer cisternal margins become swollen with polysaccharide cargo in more *trans*-cisternae. While the size of cisternal margins increased from *cis* to *trans* for all cell types imaged in this study, wild-type Golgi in SCW-producing cells had significantly larger margins than in pre-SCW cells (Figure 4.2 J). This difference is largely due to increased abundance of polysaccharide cargo in the cisternal periphery, as supported by the reduction in margin size in *irx9* Golgi to pre-SCW margin widths. Furthermore, immunoTEM labelling indicates that xylan is found primarily in theses margins in later cisternae (Figure 4.6 G), and the size of the margins strongly correlates with the amount of xylan label in each cisterna (Figure 4.6 H). This decrease in margin size in *irx9* is analogous to a similar decrease observed during Arabidopsis seed coat development in a mutant with substantially reduced pectin biosynthesis (Young et al., 2008). Furthermore, the presence of cell wall polysaccharides in cisternal margins agrees with immunogold labelling of mannan in pine xylem (Samuels et al.,

2002), and pectin and xyloglucan in Arabidopsis seed coat (Young et al., 2008), sycamore maple suspension culture (Zhang and Staehelin, 1992), and alfalfa root tips (Wang et al., 2017). While a pectin antibody recognizing a more 'mature' pectin side chain was similarly abundant in TGN and *trans*-cisternae, a different antibody binding methylesterified pectin was most abundant in the mid-cisternae (Zhang and Staehelin, 1992).

It is important to note that the localization of polysaccharide products in specific cisternae does not necessarily mean they are synthesized only in these cisternae. In the case of xylan synthesis, the xylan biosynthetic enzyme IRX9, is detected in medial Golgi, while xylan is abundant in *trans*-cisternae. Similarly, while xyloglucan epitopes are detected in *trans*-cisternae (Zhang and Staehelin, 1992), several xyloglucan biosynthetic enzymes are detected in earlier cisternae (Chevalier et al., 2010). This spatial separation likely reflects the difference between the site of polysaccharide synthesis, versus the site of polysaccharide accumulation. Detection of cargo in specific cisternae can only tell you that the biosynthetic enzymes must be present at some point upstream.

4.3.2.2 Xylan packaging in TGN vesicles contributes to vesicle size

At the *trans*-face of the Golgi, the xylan is packaged into TGN vesicle buds. The size of TGN vesicles buds quantified in this study ranged from 30 nm up to over 150 nm (Figure 4.2 K). Comparably-sized vesicles (65 – 100 nm) have been documented in the Arabidopsis root meristem (Donohoe et al., 2007; Kang et al., 2011). Cells secreting large amounts of pectin often have much larger TGN vesicles (Staehelin et al., 1990; Young et al., 2008), ranging between 150 nm and 300 nm in alfalfa root tips (Wang et al., 2017). The size of TGN vesicles also increases with SCW production. Some of this increase is similarly attributable to increased polysaccharide production, as loss of xylan in *irx9* results in significantly smaller TGN vesicles. One population of vesicle buds decreases dramatically in size, becoming more similar to regions of tubular TGN in pre-SCW cells (Figure 4.2 K). However, this data also suggests that during SCW synthesis, not all the large vesicles on the TGN are filled with xylan. In *irx9*, there is also a population of larger TGN vesicle buds that are not quite as big as those seen in wild-type SCW-producing TGN. These intermediate-sized TGN vesicle buds are likely important for trafficking other kinds of cargo, perhaps cellulose synthases (CESAs) (Meents et al., 2018). The *ixr9* plants still produce

patterned SCWs containing cellulose (Petersen et al., 2012), so the CESAs must still be trafficked to and from the SCW domains. If xylans are packed in different vesicles than CESAs at the TGN, then we can conclude that xylans are packaged into the larger TGN vesicles absent in *irx9*, and CESAs into the smaller ones remaining in *irx9*. Alternatively, xylans could be packaged into the same vesicles as CESAs, and the absence of xylan simply decreases the size of these vesicles, resulting in the intermediate vesicle size of *irx9* compared to *WT* pre-SCW and post-SCW TGN.

Plant TGN are also known to be a hub of anterograde, retrograde and endocytic trafficking (Rosquete et al., 2018). As such, the TGN vesicle buds characterized in this study may contain cargo heading for the plasma membrane, Golgi residents recycling back to the Golgi, or materials destined somewhere along the pathway to the vacuole. The results of this study also represent vesicle buds from both Golgi-associated and free TGN. Different kinds of vesicle buds likely form on different kinds of TGN, as a greater amount of endocytic trafficking is believed to occur at free vs Golgi-associated TGN (Kang et al., 2011). Additional experiments will be required to fully tease apart the trafficking occurring at TGN in SCW-producing cells.

4.3.3 Biosynthetic proteins and cargo are absent from the center of cisternae

At the very center of the Golgi cisternae is a flattened region with a very compressed Golgi lumen that contains neither IRX9 nor xylan. This region in *cis*-cisternae likely contains other biosynthetic proteins, as the N-glycan processing enzyme MANI appears to be evenly distributed across the *cis*-cisterna (Figure 3.6). It is not yet clear what is occurring in the central region of more *trans*-cisternae however. Cryo-focused ion beam milling and cryo-electron tomography of *Chlamydomonas* Golgi revealed that these regions contained protein arrays that appeared to bridge the lumen between two cisternal membranes (Engel et al., 2015). These protein arrays may represent oligomerized glycosyltranferases but could also be structural proteins contributing to the shape and organization of the cisternae. Arabidopsis Golgi appear to have a similar morphology of *trans*-cisternae, so it is possible that similar protein arrays, with a similar function, are also present in cisternal centers of xylan-producing Golgi.

4.3.4 During SCW synthesis, Golgi cisternae change in size but not number

All Golgi examined in this study had common features in TEM, including *cis* cisternae with a more open lumen and lighter staining. More *trans* cisternae had compressed lumens in the center of the cisternae, larger cisternal margins, more electron dense membranes, and longer cisternae. This characteristic appearance of plant Golgi is consistent with previous descriptions of Golgi in many cell types and species, including Arabidopsis seed coat (Young et al., 2008), developing secondary xylem in pine (Samuels et al., 2002), sycamore maple suspension culture (Zhang and Staehelin, 1992), and the developing root cap of alfalfa (Wang et al., 2017), Arabidopsis and *Nicotiana* (Staehelin et al., 1990). Golgi structure in this chapter is also consistent with TEM tomography characterizing the three-dimensional structure of plant Golgi (Kang and Staehelin, 2008; Kang et al., 2011; Donohoe et al., 2013; Wang et al., 2017). Many of these studies relied on a qualitative assessment of Golgi structure, though a few supplemented these analyses with quantification, with which we can compare.

4.3.4.1 Cisternal length increases during SCW synthesis

In this study, Golgi stacks ranged in size from 400 nm to 1500 nm (Figure 4.1 E), which is consistent with Golgi sizes reported in sycamore cell culture (Zhang and Staehelin, 1992), *Catharanthus roseus* suspension culture (Hirose and Komamine, 1989), and Arabidopsis and tobacco root caps (Staehelin et al., 1990). There was also a significant increase in Golgi size from around 550 nm to 800 nm with the onset of SCW synthesis (Figure 4.1 F). Similar changes in Golgi size have been observed in the transition from root meristem cells with 600 nm Golgi, to columella cells with Golgi around 1000 nm in diameter (Staehelin et al., 1990). It is unclear what is driving these changes in Golgi size, though it has been suggested that increases in size may be a preliminary step in Golgi proliferation, prior to cisternal fission (Ito et al., 2014). Indeed, during cytokinesis of *Catharanthus roseus* cell culture, some Golgi stacks double in length, and several stacks appear to have been caught ‘mid-fission’ (Hirose and Komamine, 1989). However, it has not been shown conclusively that plant Golgi are produced by division of existing stacks (Ito et al., 2014), and other studies have seen no difference in the size of Golgi stacks at different cell cycle stages (Garcia-Herdugo et al., 1988).

Instead, variation in cisternal size may be a by-product of altered membrane flow (Voeltz and Prinz, 2007). Membrane trafficking at the Golgi is complex, with vesicles arriving from the ER at the *cis* face, from the TGN at the *trans* face, and between individual cisternae throughout the stack. Furthermore, this membrane flow is happening as the cisternae gradually mature, eventually becoming TGN themselves (Kang et al., 2011). The volume and direction of membrane flow, and the rate of cisternal maturation, will therefore contribute to changes in the amount of membrane present in any one cisterna. This is supported by data from Arabidopsis, showing that cisternal size changes in a mutant where resetting of the membrane docking machinery is impaired (Tanabashi et al., 2018). Increases in cisternal size have also been linked to slowing the rate of cisternal maturation in yeast (Bhave et al., 2014). However, it is unclear exactly how membrane flow might be changing with the onset of SCW synthesis to bring about the observed increase in Golgi diameter. One factor that is almost certainly contributing to this is increased ER-Golgi traffic, as there is likely to be a surge in Golgi cargo (e.g. SCW cellulose synthases) and new Golgi residents (e.g. proteins required for xylan biosynthesis). We can conclude that the presence of xylan in the Golgi does not drive the increased Golgi diameter, as loss of xylan-production in *irx9* did not significantly reduce the cisternal size.

4.3.4.2 Number of cisternae is constant with the onset of SCW synthesis

Most of the Golgi imaged in this study had 5 or 6 cisternae, with a few containing 4 or 7. This is consistent with the number of cisternae seen in pine secondary xylem (Samuels et al., 2002), sycamore maple cell culture (Zhang and Staehelin, 1992) and Arabidopsis and *Nicotiana* root tips (Staehelin et al., 1990). Small differences in cisternal number are sometimes seen in different cell types, as most Golgi in the root meristem have 6 cisternae, while those in columella cells usually contain 7 cisternae (Staehelin et al., 1990). Some species also have very large numbers of cisternae, such as the scale-forming algae *Scherfillia dubia*, whose Golgi can contain 15 – 20 cisternae (Donohoe et al., 2007). The precise mechanisms governing the number of cisternae in a Golgi stack are not known, though slowing the rate of cisternal maturation has been linked to increased numbers of cisternae in yeast (Bhave et al., 2014). Golgi products requiring longer processing times may need a decreased maturation rate, yielding stacks with larger numbers of cisternae. The significant increase in number of cisternae in *irx9* (Figure 4.1

G) may be similarly due to decreased maturation, perhaps because of the disruption of Golgi architecture in these cells. Alternatively, the decrease in large vesicle buds on the *trans*-face of *irx9* Golgi (Figure 4.2) may increase the size of flattened cisternal regions in these structures, making them more likely to be counted as cisternae in *irx9* than in *WT* Golgi. If true, the apparent increase in cisternal number in *irx9* is likely simply an artifact of the quantification method chosen.

4.3.5 Golgi tubules and fenestrations are apparent

In addition to an increase in the number of fenestrations, *irx9* Golgi also appeared highly tubulated. Golgi tubules have been previously documented in mammalian Golgi (Marsh et al., 2004), but membrane tubulation is also commonly seen for ER membranes (Hu et al., 2011), during cell plate formation (Samuels et al., 1995), and at endosomes (Frost et al., 2009). Tubulation is similar to vesicle and fenestration formation in that it requires introduction of highly curved membrane regions. Indeed, there is no clear distinction between a highly fenestrated cisterna and a network of cisternal tubules. The highly curved membranes of fenestrations, tubules and vesicles can be maintained by introducing a lipid or protein asymmetry into the leaflets of the bilayer, or with the help of coat proteins which act as scaffolding (Voeltz and Prinz, 2007). Indeed in mammalian cells, the formation of Golgi tubules is facilitated by the coat protein COPI (Yang et al., 2011). These tubules were later shown to be involved in intra-Golgi anterograde movement of small cargo, and retrograde movement of residents (Park et al., 2015). Though similar inter-cisternal tubules have not yet been reported in plant Golgi, tubules protruding from the cisternal edges were apparent in Golgi both prior to, and during SCW deposition. Furthermore, these tubules appeared enhanced in the *irx9* mutant. The previously reported COPI Golgi tubules bear a strong resemblance to those observed in this study (Yang et al., 2011; Park et al., 2015). Much of the machinery governing Golgi structure and function, including vesicle formation and fusion proteins, are highly conserved among eukaryotes (Klute et al., 2011). The tubules seen in plant Golgi may therefore have similar functions in intra-Golgi trafficking of anterograde moving small cargo, and retrograde trafficking of Golgi-resident proteins, as has been demonstrated to occur in mammals, which is a topic worthy of further investigation.

4.3.6 Conclusions

In this chapter, I have developed a model of Golgi processing where nanoscale changes in Golgi structure from *cis*-to-*trans*, and centers-to-margins, reflect changes in the contents of the Golgi in these regions (Figure 4.7). In the proposed concentric circle model (1) xylan accumulates in the cisternal margins of more *trans*-cisternae, where the rounded membranes provide a large luminal volume, (2) xylan biosynthetic proteins not in complexes are found in fenestrated regions of the medial cisternae, where there is a greater membrane area, (3) these proteins come together to form biosynthetic complexes in a flat inner margin of the medial cisternae, where they make xylan and inhibit fenestration formation, (4) cisternal centers of *trans*-cisternae lack both xylan biosynthetic proteins and their product, and (5) changes in membrane flow to and from the Golgi leads to an increase in cisternal diameter during SCW synthesis.

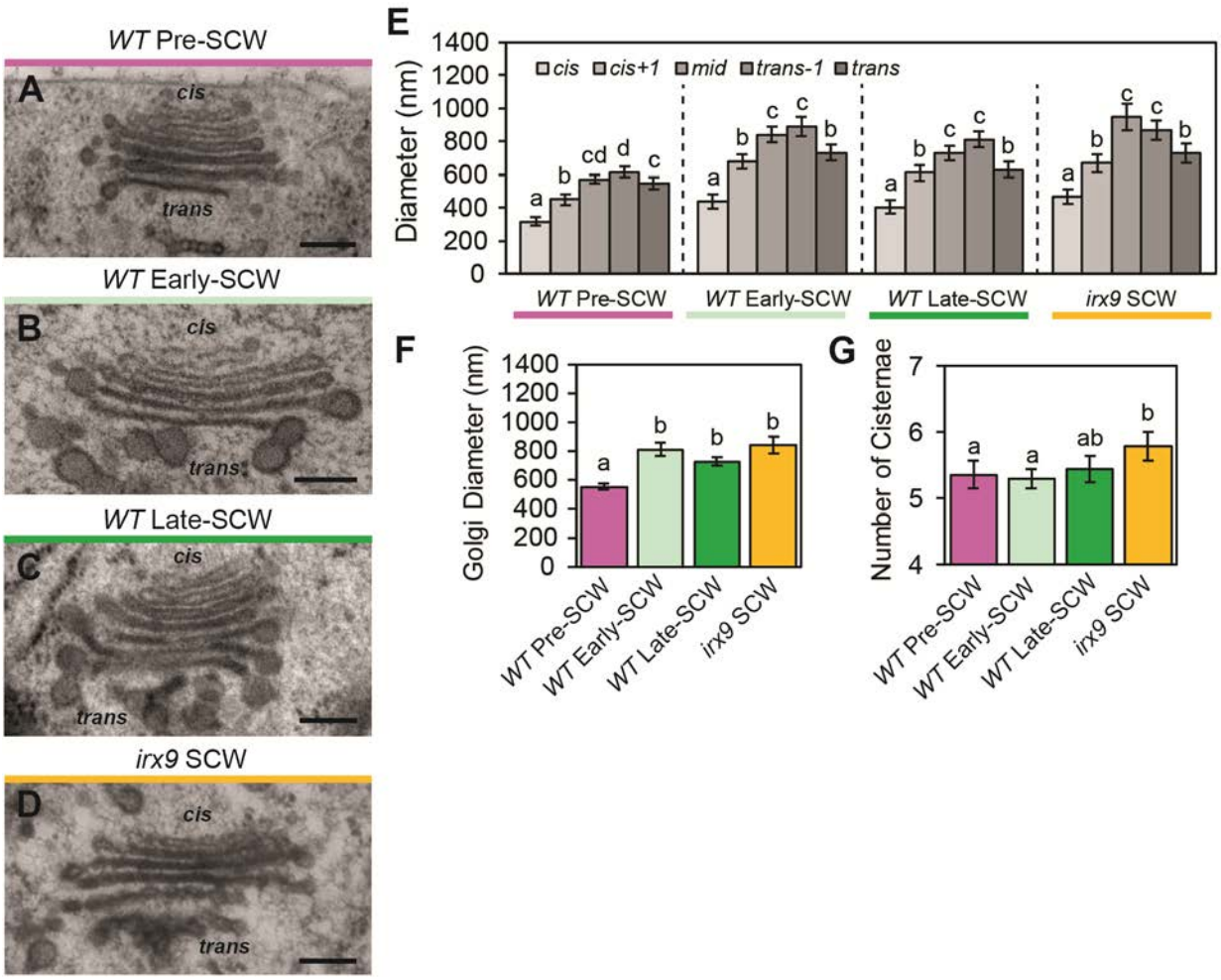

Figure 4.1 Changes in cisternal length and number during SCW deposition in *WT* and *irx9*.

(A-D) Representative TEM images of Golgi cross-sections showing cisternal length and numbers in **(A)** *WT* pre-SCW, **(B)** *WT* early-SCW, **(C)** *WT* late-SCW, or **(D)** *irx9* SCW cells. Scale = 200 nm. **(E)** Length of cisternae in each kind of cell grouped by sample type. **(F)** Golgi diameter. Averaged from *cis+1* to *trans-1* cisternae. **(G)** Number of cisternae in Golgi. Means ± 95% CI. Statistics = Separate one-way ANOVAs and Tukey HSD *post-hoc* analysis, (F-G) Kruskal-Wallis and *post-hoc* analysis ($p<0.05$). n = 34 – 40 Golgi in 3 - 5 seedlings from one (*irx9* SCW) or two replicate experiments (all others).

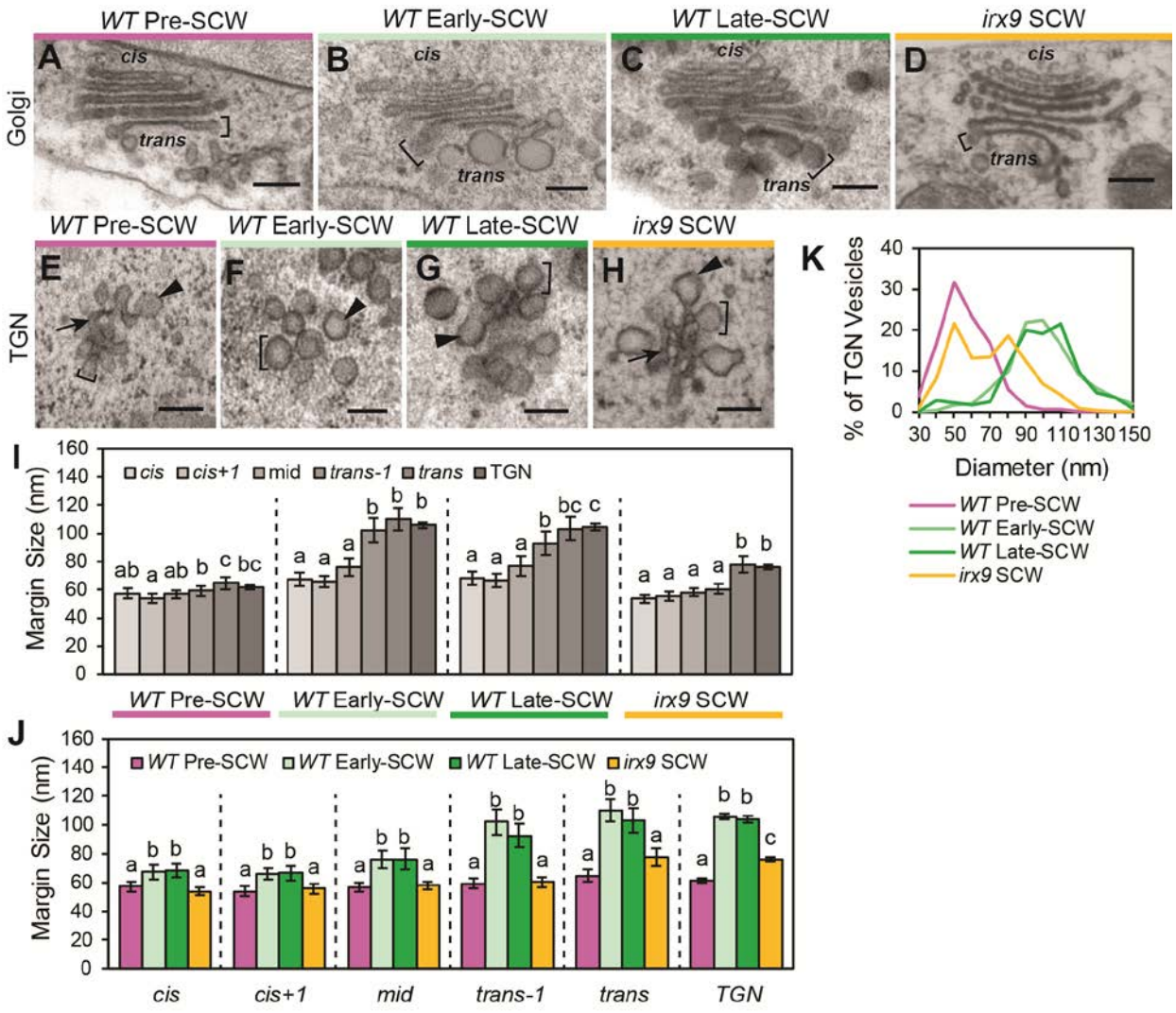

Figure 4.2 Changes in cisternal margins and TGN during SCW deposition in *WT* and *irx9*.

(A-D) Representative TEM images of Golgi cross-sections showing variation in the size of cisternal margins in **(A)** *WT* pre-SCW, **(B)** *WT* early-SCW, **(C)** *WT* late-SCW, or **(D)** *irx9* SCW cells. Brackets give an example of margin size measurement in *trans*-cisterna. **(E-H)** Representative TEM images of TGN showing the size of vesicle buds in **(E)** *WT* pre-SCW, **(F)** *WT* early-SCW, **(G)** *WT* late-SCW, or **(H)** *irx9* SCW cells. arrowheads = formation of large vesicles, arrows = small tubules. Brackets given an example of vesicle bud size measurement. **(I-J)** Thickness of cisternal margins in each kind of cell, grouped by **(I)** sample type or **(J)** cisterna. **(K)** Distribution of TGN vesicle sizes. Means ± 95% CI. Statistics = separate Kruskal-Wallis and *post-hoc* analysis ($p<0.05$). n = 20 – 35 Golgi and 233 – 518 TGN vesicles in 3 - 5 seedlings from one (*irx9* SCW) or two replicate experiments (all others). Scale = 200 nm.

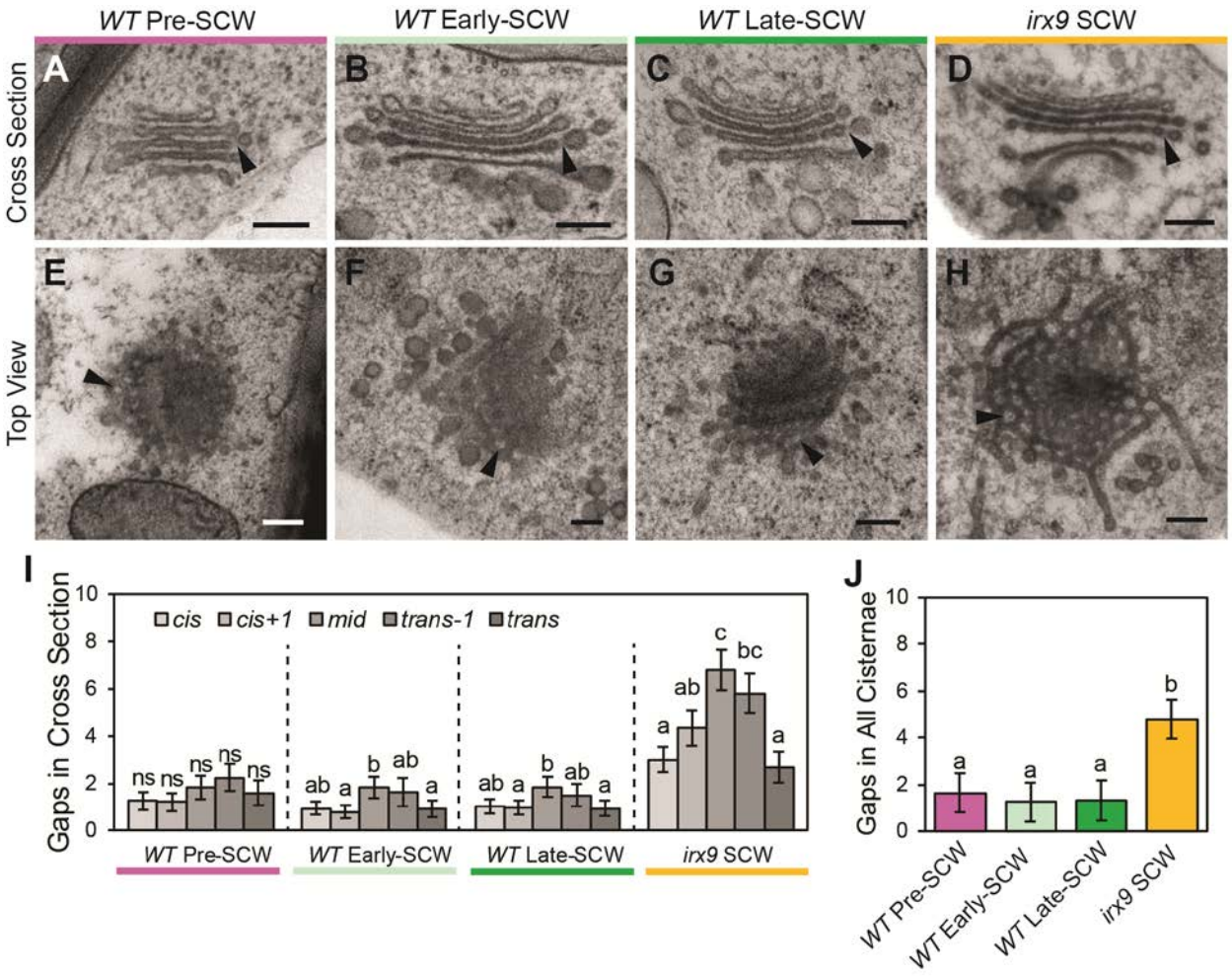

Figure 4.3 Changes in number of putative fenestrations during SCW deposition in *WT* and *irx9*.

(A-D) Representative TEM images of Golgi cross-sections showing putative fenestrations as 'gaps' (arrowheads) in the cisternae from **(A)** *WT* pre-SCW, **(B)** *WT* early-SCW, **(C)** *WT* late-SCW, or **(D)** *irx9* SCW cells. **(E-H)** Representative sections through tilted 'Top View' Golgi showing fenestrations (arrowheads) in the cisternae from **(E)** *WT* pre-SCW, **(F)** *WT* early-SCW, **(G)** *WT* late-SCW, or **(H)** *irx9* SCW cells. **(I-J)** Number of cisternal gaps **(I)** separated by cisterna type or **(I)** when all cisternae are pooled. Means ± 95% CI. Statistics = separate Kruskal-Wallis and *post-hoc* analyses ($p<0.05$). n = 28 – 37 Golgi in 3 - 5 seedlings from one (*irx9* SCW) or two replicate experiments (all others). Scale = 200 nm.

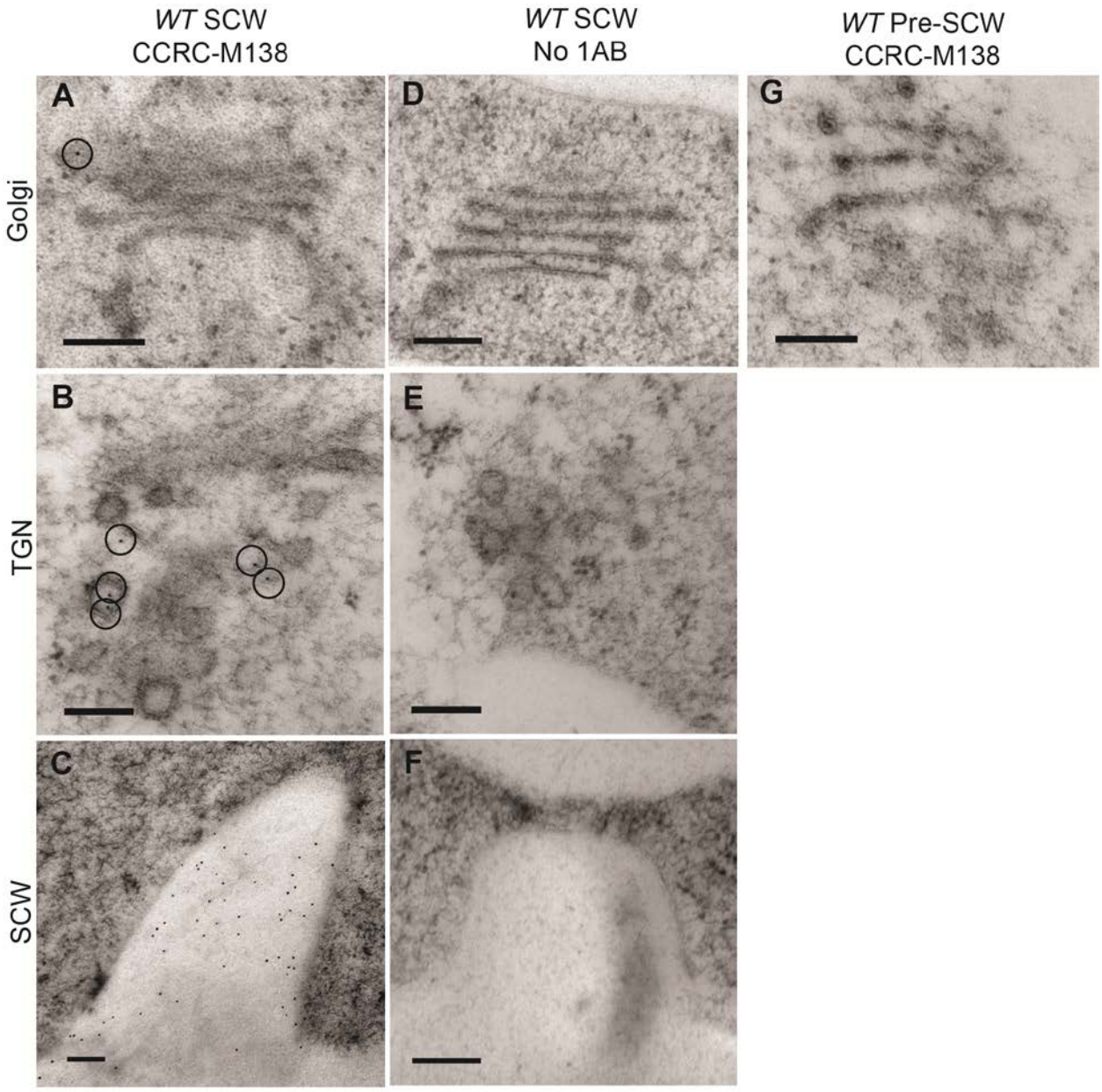

Figure 4.4 Anti-xylan antibody labels Golgi, TGN and SCW.

(A-C) Anti-xylan antibody binding and 10nm gold label is seen in **(A)** Golgi, **(B)** TGN and **(C)** SCWs during SCW production. **(D-F)** Cells producing SCWs but not exposed to the primary antibody (1AB) have no gold label in the **(D)** Golgi, **(E)** TGN, or **(F)** SCW. **(G)** Cells not producing SCWs do not have anti-xylan label. All gold particles are outlined with black rings except for those in **(C)**. Representative images from 4 seedlings across 2 replicate experiments. Scale = 200 nm.

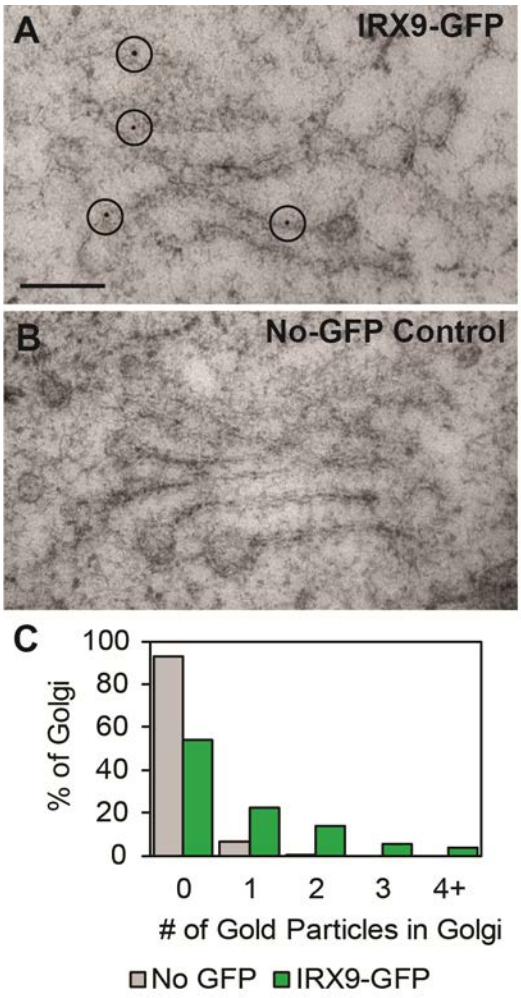

Figure 4.5 Immunogold anti-GFP signal is higher in IRX9-GFP plants than No-GFP plants.

(A-B) Representative images of Golgi in a plant **(A)** containing IRX9-GFP or **(B)** lacking IRX9-GFP. Black rings outline gold particles. Scale = 200 nm. **(C)** Distribution of gold label among Golgi in SCW-producing controls which lack IRX9-GFP (No GFP) and similar cells in plants containing IRX9-GFP. No GFP (n = 20 gold particles in 277 Golgi from 19 cells), IRX9-GFP (n = 410 gold particles in 493 Golgi from 39 cells). Representative images from 4 seedlings across 2 replicate experiments. Scale = 200 nm.

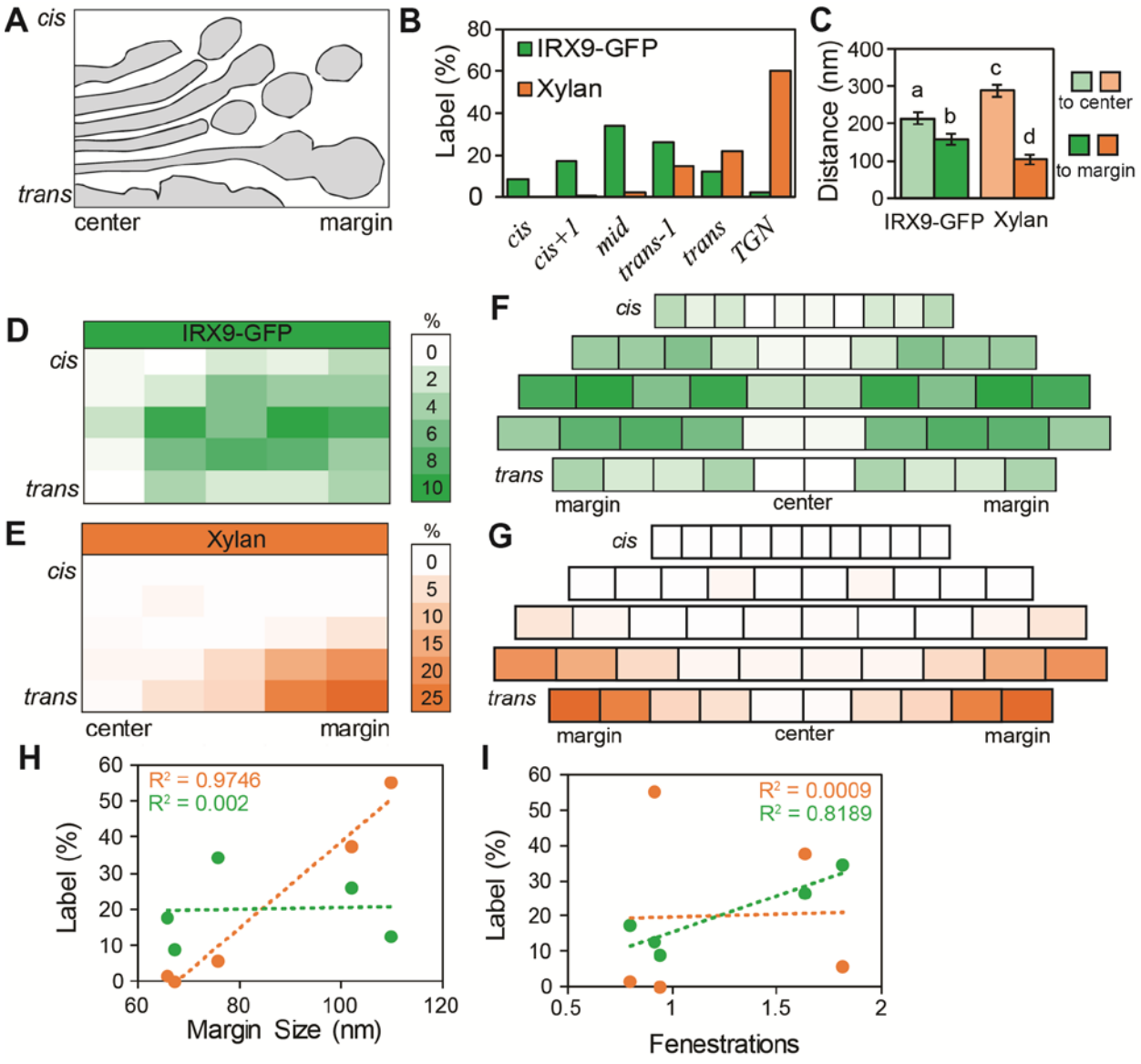

Figure 4.6 Mapping of IRX9-GFP and Xylan in the Golgi.

(A) Schematic of half a Golgi in cross-section illustrating '*cis* to *trans*' and 'center to margin' mapping. **(B)** Percent of gold particles in Golgi cisternae from *cis* cisternae through to the TGN for anti-GFP (IRX9-GFP) or CCRC-M138 anti-xylan (Xylan). **(C)** Average distance from gold label to the cisterna center and margin. All gold particles were pooled, regardless of cisterna labelled. Statistics = one-way ANOVA with Tukey HSD *post-hoc* ($p<0.05$). Means ± 95% CI. **(D-E)** Heat map of gold distribution across the Golgi from *cis* to *trans* and in 10% blocks of cisternal diameter from the center to the edge of each cisterna. Distribution of **(D)** IRX9-GFP and **(E)** xylan. **(F-G)** Distributions of **(F)** IRX9-GFP and **(G)** xylan adjusted for changes in cisternal width from *cis* to *trans* using the average cisternal diameters of early-SCW Golgi. Blocks represent 10% of the cisternal diameter. **(H-I)** Correlation of cisternal **(H)** margin size or **(I)** number of fenestrations with amount of GFP or xylan label in each cisterna. Xylan (n = 136 gold particles, 17 cells), GFP (n = 182 gold particles, 33 cells). Data from 4 seedlings and 2 replicate experiments.

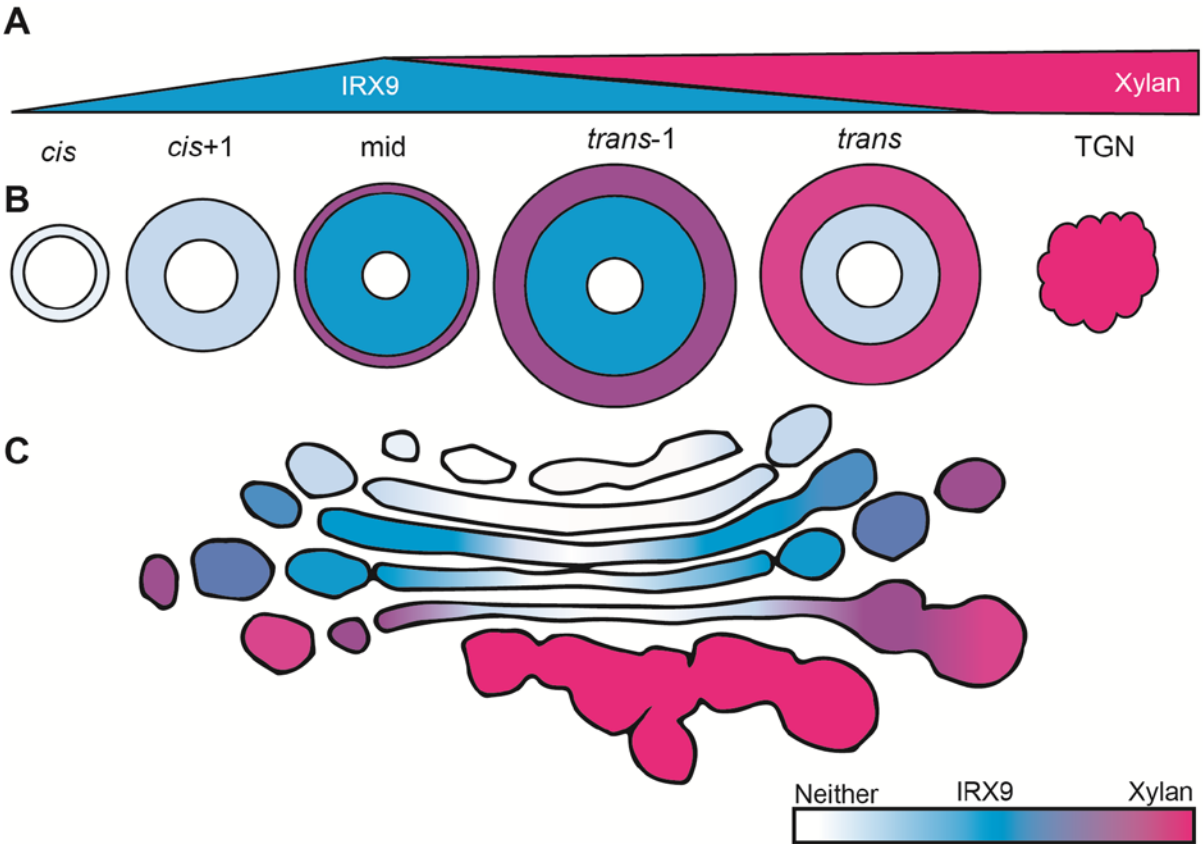

Figure 4.7 Concentric circle model of IRX9 and xylan position in Golgi.

(A) Schematic of relative abundance of IRX9 and xylan moving from *cis* to *trans*. **(B)** Top-down view of simplified cisternae showing the organization of IRX9 and xylan in concentric circles within each cisterna. The size of each cisternae is adjusted to represent actual cisternal size in a *WT* Early-SCW Golgi. **(C)** Approximation of IRX9 and xylan distribution superimposed on the outline of a *WT* Early-SCW Golgi cross section.

Chapter 5: Using Example Answers to Teach Problem-Solving in Cell Biology

5.1 Introduction

Development of problem-solving skills is an essential component of undergraduate biology education. Instructors often support student problem-solving with a variety of instructional practices, which may vary greatly between disciplines. However, it is not always clear that a practice that works well in one field will be similarly effective in a different context. In this chapter, teaching practices concerning problem-solving in two undergraduate cell biology courses are examined. This analysis offers insight into how providing example-solutions can improve student performance and attitudes in problem-solving.

5.1.1 Problem-solving in undergraduate biology

The acquisition of problem-solving skills is frequently identified as a key goal of education in general, and the sciences in particular (Gagne, 1980; Council of Canadian Academies, 2015; Henderson et al., 2017). Problem-solving is the process undertaken when the steps required to solve a task are uncertain and the task cannot simply be achieved by following previously memorized procedures (Martinez, 1998). The ubiquity with which we encounter these kinds of problems in our personal and professional lives make mastering the problem-solving process important for all members of society. In biology, problem-solving often centers on the formulation of a scientific argument; where data is interpreted and used as evidence in the construction of a logical argument that supports a hypothesis (Wisehart and Mandell, 2008; Hoskinson et al., 2013). This process requires that students master and integrate divergent and complex skills ranging from data analysis to academic writing, that can make biology problem-solving extremely challenging for students. Facilitating student learning of problem-solving is therefore often an important, and often difficult, task for biology instructors.

The role of the instructor in the student's learning process depends on one's philosophical perspective about how learning occurs. In modern science education, the popular constructivist theory of learning posits that learning occurs when new information is integrated with a student's existing knowledge (Crowther, 1997; Baviskar et al., 2009; Hartle et al., 2012). This process requires students to actively construct their knowledge by removing, adding or shifting existing knowledge structures to accommodate new ideas. Instructors strive to provide students with the

tools they need to do go through this process most effectively. Optimal learning occurs then, when instructors provide a challenge significant enough to allow learning to occur, but with sufficient resources to avoid student frustration and anxiety while fostering independence and engagement (Vygotsky, 1978; Mezirow, 1991; Wilson and Devereux, 2014).

In the sciences, a scientific treatment of problem-solving has been recommended as a constructivist teaching method (Gil-Pérez et al., 2002). Indeed, educators often encourage learning of problem-solving by challenging students to solve problems on their own. Several studies have investigated the effect of various teaching practices on the development of biology-related problem-solving skills like data analysis and interpretation (Glazer, 2011), hypothesis building (Lawson et al., 2000), and evidence-based argumentation (Hamilton, 2016; Litman et al., 2017), as well as the problem-solving process as a whole (Doering and Veletsianos, 2007; Wisehart and Mandell, 2008; Hoskinson et al., 2013). However, these studies are often conducted in controlled environments, are entirely theoretical, or examine disciplines other than biology. As such, it is not always clear that the conclusions from this literature can be effectively extrapolated and applied to a biology classroom. This latter issue is particularly important, as differences in the culture and practices of disciplines can mean that instructional approaches suitable for one discipline, may need to be modified, or abandoned in another (Talanquer, 2014; Henderson et al., 2017). Instead, biology researchers can utilize their disciplinary expertise to investigate teaching practices particularly important or relevant to biology education. This kind of Discipline-Based Education Research (DBER) falls within the Scholarship of Teaching and Learning (SoTL), which is concerned with a systematic investigation of teaching and learning in order to maximize learning at undergraduate institutions (Potter and Kustra, 2011; Singer et al., 2012; Felten, 2013). The principles of SoTL and DBER research can therefore be applied to investigate and improve problem-solving education in undergraduate biology.

5.1.2 Research questions

The aim of this study is to examine how changes in instructional practices affect student problem-solving in undergraduate cell biology classes. In doing this I will address the following questions:

1. **What forms of problem-solving support are available to cell biology students and how do they use them?**
2. **Do some kinds of support result in greater increases in problem-solving performance in cell biology courses?**
3. **How do changes in instructional support affect student perspectives about problem-solving in cell biology classes?**

To answer these questions, two lecture-based undergraduate cell biology classes were studied, each teaching similar types of problem-solving in different ways. Biology 362 (BIOL362) is a mid-sized, upper-level class where students work in groups to complete a set of in-class problem-solving assignments across the term. In contrast, Biology 200 (BIOL200) is a multi-section, lower-level class where students can use optional practice problems in studying for their exams. Over several years, instructor support of these problem-solving activities was altered in order to improve student problem-solving skills and student attitudes about problem-solving. The effectiveness of these approaches was evaluated by examining student performance on problem-solving questions, and students' attitudes in surveys and interviews.

5.2 Materials and Methods

5.2.1 BIOL362

BIOL362 is a third-year, lecture-based elective focused on cell physiology, particularly the cytoskeleton, cell dynamics and regulation of cellular activities. The course typically has a single instructor, and one or two teaching assistants (TAs). A major component of the course is a set of problem-solving assignments.

5.2.1.1 Assignment design

Students worked in groups of two to five members to complete four assignments worth a cumulative total of 15% of their course grade. For each assignment they were given three to five pieces of experimental data and asked to make a connection between the data and a 'big-picture' problem (see example in Appendix A). They would hand in a one to two sentence hypothesis (i.e. a hypothetical model) that answers the question asked, and a one to two paragraph rationale justifying their hypothesis using the data and background information from class. Each assignment was made available and completed within a single class period (85 min). The third and fourth assignments were altered so students would complete their hypothesis and rationale part way through the class and then receive new data in the second part. They would evaluate whether the new data supported or contradicted their hypothesis and write a new hypothesis if necessary, and then justify their decision based on the new data.

While the content of the assignments changed very little from 2014 to 2016, the support offered to the students varied in each year. In the first year a 'Traditional' approach was utilized where students completed each assignment, and received both general advice and specific feedback on their work, before the next assignment. In the second year a 'Step-by-Step' approach was adopted where, for the first case study, the students were provided with a worksheet created by Drs. Robin Young and Megan Barker, that walked the students through the steps that an expert would take when approaching the task (Appendix B). This included identifying the central question being asked, making conclusions about the data provided, bringing these conclusions together to generate a reasonable hypothesis, and then supporting the hypothesis using a rationale built on the conclusions from the data. Each section of the worksheet was graded separately, but only grades for the hypothesis and rationale were included for

comparison with the other approaches tested in this study. In subsequent case studies students could refer to the original worksheet, but they were required to submit their hypothesis and rationale in the same manner as in the Traditional approach. In the final year the first case study was instead adapted to provide students with 'Example Answers'. The students would begin by analyzing the data and writing a hypothesis as in the Traditional approach, but they would not submit their work for marking. Instead, halfway through the class they were given a worksheet that I designed with the instructor, which provided two hypotheses and rationales of varying quality, as well as instructions and a rubric for grading them (Appendix C). The students would use the rubrics to assign marks, and then comment on the pros and cons of each example. These worksheets were then handed in for participation marks. All subsequent case studies were completed as in the Traditional approach.

The course instructor was the same for all three years, but the teaching assistants differed. In the fall of 2016 all students were contacted via email and given the opportunity to opt-out of the study. If one member of a group opted-out, the data for the whole group was excluded. The final data set includes 16 groups for the traditional approach, 17 for the step-by-step approach, and 18 for the example answers approach.

5.2.1.2 Analysis of grades

The quality of student answers in each year was determined using assignment grades. All assignments were graded by the TA(s) with supervision of the course instructor. While the rubrics used depended on the content of the case study in question, in general, marks were awarded for correct data interpretation, construction of an evidence-based logical argument, and writing quality. The grades were also broken down into the marks received for the hypothesis and the rationale, and for assignments two and three the marks for part two were compared. Because the number of marks assigned to each component of the assignment was not always consistent between assignments/years, the grades were converted into percentages for comparison purposes. Statistical analysis was conducted in SPSS 25 (IBM). Before comparison of means, normality was assessed visually using histograms and Q-Q plots, supplemented with Kolgomov-Smirnov and Shapiro-Wilkes tests. If the data was approximately normally distributed a Student's *t*-test for independent means was used to compare two means, or a one-

way analysis of variance (ANOVA) used to compare more than two means. If the ANOVA showed a significant difference, Tukey HSD *post-hoc* analyses were conducted to identify significant differences.

5.2.1.3 Analysis of student feedback

Every year, students had the opportunity to provide written feedback about the assignments with the submission of the last assignment. In addition, students occasionally commented on the assignments in term-end feedback to the instructor, or in e-mails to the instructor. These comments were collected for each year of the course and were analyzed manually to identify abundant and recurring themes (Table 5.1). Each comment contributing to a theme was counted and expressed as a percentage of the total number of comments.

5.2.2 BIOL200

BIOL200 is a second-year lecture-based course which is a core requirement for a number of programs. Content focuses on the structure and function of plant and animal cells, including membrane biology, organelles and the cytoskeleton. The ~1200 students attend a ~250-person lecture with one of the five instructors, and a weekly 25-student tutorial with one of approximately 20 TAs, where they focus on problem-solving practice. Problem-solving is a key component of the midterm and final exams, which are typically worth 20% and 50% of the course grade, respectively. Student problem-solving is supported by a set of practice problem set questions which can be completed for optional homework.

5.2.2.1 Problem set and walkthrough design and implementation

The BIOL200 problem sets are a collection of practice problems largely consisting of exam-style questions where students must analyze and interpret novel data (see Appendix D). Questions are included for every topic in the seven units in the course. Ten of these problems are addressed in mandatory weekly tutorials, and most instructors select some other questions to cover in lectures. Instructors strongly encourage students to work through these questions, but this is optional. Students looking for help with the questions could meet with a TA or instructor, work with their classmates, or make use of an online discussion board.

While full answer keys were not provided to the students, answers were available for a small selection of questions, though with different designs and implementations in 2015 and 2016. In the first year, ten questions across the problem sets were provided with simple answer keys, where the answers were as brief as possible and focused on the main concepts or ideas that were important for a correct mark. In the second year, I wrote problem walkthroughs to replace these answer keys. The problem walkthroughs provided a full example answer, as well as explanatory commentary explaining how the correct answer was reached, and tips and tricks for answering questions of this type (see Appendix E). This format of the walkthroughs was designed to make the example answers more effective; including breaking the solution down into sub goals, fully articulating explanations of problem-solving steps, integrating images with text, and highlighting instances where students could generalize an approach to other kinds of questions (Atkinson et al., 2000; Margulieux and Catrambone, 2016). In addition to the ten questions for which answer keys were available previously, I also wrote problem walkthroughs for the questions addressed in tutorial, but which had not had answer keys, bringing the number of questions with answers up to twenty-three.

Additionally, in the second year the format and organization of the problem sets was altered in an attempt to increase the use and utility of the problem sets for students. As the small number of walkthroughs were intended to help students work through related questions, we wanted to help students identify similar questions in different units by adding a table of contents and index. This was further aided by the addition to each question of hashtags for key techniques and topics (see Appendix D). There was also some concern that it was unrealistic to expect students to answer the large number of questions in the original problems sets, so the number of questions was lowered from 207 to 137, with an average of 25 questions per unit dropping to 19 questions per unit. The problem sets were also made available as a collection of documents for each unit, or in a consolidated document, to allow students to choose the version that works best for them.

5.2.2.2 Collection and analysis of exam grades

To assess the impact of providing problem walkthroughs versus answer keys, I examined student performance on five final exam questions that had little to no changes from one year to

the next (see Appendix F). While some questions did not have related practice problems in the problem sets, others had highly similar practice questions, including some with keys/walkthroughs (Table 5.2). The questions tested students on a variety of topics, with different difficulties as assessed using Bloom's taxonomy and the Blooming Biology Tool (Crowe et al., 2008) (Table 5.2). The average grade on each question, as well as the exam total, was then compared between years. To determine if students at different performance levels were impacted by walkthroughs in different ways, the students were also assigned to low-, mid-, and high-performing groups if they fell below the first quartile, between the first and third quartile, or above the third quartile, respectively, on midterm exam grades. The performance of students in these groups was then compared between each year of the course using the difference in final exam grades.

The students from the 2015 course were contacted around 10 months after their course ended so those who did not wish to participate could opt-out, resulting in the participation of 1241 students, representing 94% of the class, including 100% of the high- and mid-performing students, and 88% of the low-performing students. In the 2016 course, students who wanted to participate opted-in during an in-class survey, resulting in the participation of 817 students, representing 66% of the class, with 63% of the high-performing students, 70% of the mid-performing students, and 60% of the low performing students. Statistically significant difference in exam grades was analysed in Excel (Microsoft) using Student's *t*-test for independent means.

5.2.2.3 Collection and analysis of student feedback

To assess student attitudes about the changes made to the problem sets, online surveys were conducted following the conclusion of the course (10 months after for 2015, and 4 months after for 2016). The survey consisted of 55 closed-response questions (see Appendix G) and included categories on frequency of use of problem sets and answers, as well as attitudes about their utility and format. Likert-type responses were converted into numerical values from 1 to 5, which were then averaged to summarize the response for each question, and each year. To investigate the relationship between student performance and their responses to the survey, the respondents were also grouped based on low-, mid- and high-performance as described above,

and the analyses repeated. Statistically significant differences in student responses were analyzed in Excel (Microsoft) using Student's *t*-test for independent means.

A small selection of questions from the online survey were selected to be asked in two, five-question, in-class surveys in 2016, when problem walkthroughs were employed. The survey was administered using the classroom response system iClicker, which is mandatory for students in this class. The first in-class survey was administered just after the midterm exam, before students received their grades, and on the last day of class, prior to their final exam. Questions repeated in the in-class and online surveys were compared in order to test if student responses changed throughout or following the course.

A more qualitative assessment of student attitudes about the problem sets was achieved by combining analysis of survey responses and semi-quantitative interviews. In the survey above, students were given opportunities to provide long-form comments about what they liked or would change about the problem sets and the answers provided. These answers were compiled, then a team consisting of myself and two BIOL200 instructors analyzed a subset of comments to identify common and recurring themes guided by published qualitative analysis approaches (MacQueen et al., 1998; Fonteyn et al., 2008; Saldana, 2009). Initial coding focused on identification of patterns using a grounded theory approach, and then refined and supplemented these codes with the guidance of coding approaches focusing on descriptive coding to identify what students liked or disliked, and emotion coding to help capture student affect (Saldana, 2009). Themes identified in the first round of analysis were collected, defined and provided with usage examples in a draft codebook. The team then used the draft codebook to independently analyze a second subset of survey comments, and any discrepancies or ambiguities identified were clarified in a new codebook, which was then approved by the whole team (see Appendix H). This codebook was then used to provide a qualitative description of student attitudes about the problem sets and example answers. Coding development and coding was conducted using the qualitative data analysis software package, NVivo (QSR International).

Additional qualitative data was gathered by conducting interviews with four undergraduate students who were students in the class in 2015, and were employed as undergraduate assistants (*i.e.* peer mentors or peer tutors) in the 2016 class. In this role, the peer tutors attend lecture, hold office hours, run study sessions, and moderate questions on the online

discussion board. As many of these activities involve helping students with the practice problems in the problem set, the peer tutors were in the unique position of having worked with both versions of the problem sets and could provide important insight and context to my analysis. A semi-structured interview protocol was chosen, where consistency in the questions asked is provided by a pre-prepared list of questions, but flexibility in follow-up questions and further discussion is allowed. The interview protocol (see Appendix I) was written using published guidelines (Whiting, 2008; Rabionet, 2011; Jacob and Furgerson, 2012) and with a focus on student attitudes about the class, how the problem sets were used, and what the students felt about the changes that were made to the problem sets and answers. These interviews were recorded and transcribed, and then analyzed for themes using the codebook described above as a guide.

5.3 Results

5.3.1 BIOL362

One of the key transferrable skills learned in an undergraduate biology program is being able to construct a logical argument using scientific data to support a claim. In a third-year cell biology class at the University of British Columbia, students were encouraged to develop these skills in a series of four in-class group assignments, where students investigated a scientific question by analysing data, and then wrote a hypothesis answering the question and a short rationale explaining how the evidence supported their claims (see Appendix A). Students initially appeared to find these assignments extremely difficult and frustrating, as they didn't understand the instructor's expectations for completing the assignments. As such, the instructor experimented with variations in the assignment format to better support the students. The success of these different formats was assessed by comparing student performance and attitudes about the assignments in each year of the course.

5.3.1.1 BIOL362 demographics were highly similar between years

As this study requires comparing different cohorts of students, several demographic parameters were compared to determine if the cohorts were of a similar composition (Table 5.3). While the number of students enrolled in the class decreased substantially each year, the student population was highly similar in terms of stage of degree, percentage of biology majors, and gender distribution. These similarities provide greater confidence that differences found between each year of the course are due to the changes made in assignment implementation, rather than a changing cohort.

5.3.1.2 Assignment grades worsened with step-by-step worksheet

The effect of different assignment formats on student performance was assessed using assignment grades. In the traditional approach (see Appendix A) the overall grade increased steadily from an initial average of 54% up to 74% for the final assignment (Figure 5.1 A). These increases reflect very large improvements in hypothesis quality (Figure 5.1 B) and smaller gains in rationale quality (Figure 5.1 C). Despite these increases in assignment performance over time, students expressed strong concerns about the low scores in the first assignments, leading to

adjustment of the assignments in subsequent years to better support student learning early in the course.

The next year, the first assignment was modified to include a step-by-step worksheet guiding students through the problem-solving process (see Appendix B). Interestingly, this approach did not result in the gradual improvement with each assignment seen in the traditional approach, as these students performed worse than in the traditional approach, then better, and then worse again, on subsequent assignments (Figure 5.1 A). The decreased performance in the first assignment is due to a significant decrease in rationale quality (Figure 5.1 C), as the hypothesis quality was similar to that of the traditional approach (Figure 5.1 B). Improved overall grades in assignment two reflect an improvement in rationale quality (Figure 5.1C), as well as significantly stronger hypotheses in the step-by-step approach, which were maintained in subsequent assignments (Figure 5.1 B). These gains were not maintained in assignment three, which dropped in quality due to poorer rationales (Figure 5.1 C) and the second half of the assignment (Figure 5.1 D). Students did slightly better on these two components for assignment four. Together, these results indicate that the step-by-step approach decreases student performance, primarily by negatively affecting rationale quality. Furthermore, these students appear to be more negatively affected by the alteration in assignment structure in assignment three.

The next year the first assignment was adapted again to instead include a worksheet where students used a rubric to grade example hypotheses and rationales (see Appendix C). As such, in this approach, students did not submit hypotheses or rationales for the first assignment. Despite this, these students performed equally well to the traditional approach in all subsequent assignments (Figure 5.1 A). The quality of the hypotheses (Figure 5.1 B), rationales (Figure 5.1 C), and the second parts of assignments three and four (Figure 5.1 D) closely match or slightly improve on the traditional approach for all assignments. The largest improvement is seen in hypothesis quality for assignment two, representing a 16% increase in hypothesis grade with the example answer approach compared to the traditional approach (Figure 5.1 B). The example answer approach may therefore allow students to learn to write high quality hypotheses earlier in the course than the traditional approach. Together these data suggest that students perform as

well or better on these assignments with the example answer approach, compared to the traditional approach.

5.3.1.3 Student feedback improved with the example answer approach

To assess student attitudes about the assignments in each year of the course, student feedback was collected with the final assignment and from term end feedback to the instructor. Analysis of the feedback revealed recurring themes. A substantial proportion of commenters from all three years expressed their enjoyment of the assignments, with the largest numbers for the example answer approach (80%) and the lowest for the traditional approach (40%) (Figure 5.2 A). Each year approximately 40% of comments indicated that students appreciated the usefulness of the assignments, including comments like:

> *"Although I didn't like the case studies at first, they turned out to have a positive effect on learning."*
> *(Traditional Approach)*

> *"I felt they were good for exam practice because I improved my ability to interpret data under pressure."*
> *(Step-by-Step Approach)*

Alternatively, negative comments primarily brought up issues with assignment difficulty, though these comments dropped markedly with the step-by-step approach, and even more with the example answer approach (Figure 5.2 B). Assignment difficulty was often linked to the tight time constraints, as the assignments had to be completed during a single class. Interestingly, with the step-by-step approach, while students commented on the assignment difficulty, no student mentioned not having enough time (Figure 5.2 B). This contrasts with the example answer approach, where many students felt rushed or unable to complete the assignment satisfactorily in the time allotted.

> *"We felt the marking was very strict and we didn't have enough time, [especially] when there was part 2."*
> *(Traditional Approach)*

"I found that time was really tight for the case studies, especially the ones with potentially rewriting the hypothesis, so I was a bit stressed. At least two times my group had to finish writing the hypothesis and rational outside."
(Example Answer Approach)

Lastly, several comments centered on uncertainty or ambiguity about how to complete the assignment to the instructor's expectations. These comments were most numerous with the step-by-step approach, and least prevalent with example answers (Figure 5.2 B).

"The case studies were interesting but the criteria for what was expected was way too vague."
(Traditional Approach)

"The case studies were awful and unfair. It felt like getting a good mark was based more on luck [than] anything else and when you got a 6/10 you didn't feel like you made mistakes, you felt cheated."
(Step-by-Step Approach)

Interestingly, one commenter spontaneously brought up the example answer worksheet used in the first assignment, saying:

"I liked [assignment one], because it taught me how to construct the hypothesis and rationale [by] comparing my answers to a previous student. You become more critical."
(Example Answer Approach)

Overall, with example answers student comments were most positive and least negative compared to the traditional and step-by-step approaches.

5.3.2 BIOL200

As example answers were successful in helping the BIOL362 students' problem-solving, this could represent an effective technique for teaching these skills in other biology courses. One such course was a large second-year cell biology class (BIOL200), which surveys broad content areas but also emphasizes teaching students to use that content in the analysis and interpretation of novel data. This aspect of the course has been supported by a set of practice exam problems, some of which are covered during class time, but most of which are not (see Appendix D). In the

past, very concise answer keys were released for a small proportion of these questions. However, instructors often heard from students that they did not understand the expectations for answering these kinds of questions, and that they would appreciate a larger number of answers. The instructors were reluctant to provide full answer keys however, as studies have shown that these may, in fact, impede student performance (Kim et al., 2012). Alternatively, example answers were very successful in addressing similar concerns in BIOL362. Therefore, the answer keys in BIOL200 were converted into problem "walkthroughs" containing example answers (see Appendix E). These walkthroughs were written following many of the best practices found to make example answers more effective, including extensive explanatory commentary (Atkinson et al., 2000). To evaluate the effectiveness of walkthroughs, student performance and attitudes were then compared in the year prior to, and following, walkthrough implementation.

5.3.2.1 BIOL200 students were demographically similar in both years

As this study depends on comparing students in different years of the course, available demographic information was used to assess how comparable the populations were in each year. The two populations were found to be similar in terms of the number of students, their program year, and in the proportion of biology majors (Table 5.4). As many students were in their first year and had not chosen a major, the percent of students in the faculty of science was also compared and found to be similar in each year of the course (Table 5.4). This analysis suggests that the student populations were of similar composition in each year of the course and comparisons between them are more likely to reflect changes in teaching practices rather than a change in the cohort.

5.3.2.2 Walkthroughs improve the performance of lower-performing students

The impact of problem walkthroughs on student problem-solving was evaluated by comparing performance on highly similar or identical final exam questions, and overall exam grades (see Appendix F). Grades increased significantly for the overall exam, and specifically for questions two, three and five (Figure 5.3 A). These three questions increased by similar amounts (Figure 5.3 B). Conversely, when walkthroughs were provided, student performance did not change for question one, and decreased significantly for question four (Figure 5.3).

To further investigate the cause of the change in performance for each question, students were grouped by low-, mid-, and high-performance using their midterm exam grades. Using midterm grades provides an approximation of learning gains over the course of the class. This revealed that in the second year, performance on questions two, three and five increased the most for low-performing students, followed by mid- then high-performing students (Figure 5.3 B). Indeed, high-performing students did not perform significantly better with walkthroughs on any question, and performed significantly worse on questions one, three and four (Figure 5.3 B). Interestingly, the questions that the overall class did not improve on with walkthroughs (questions one and four), did not show the same trend with low-performing students benefiting more than mid- and high-performing students (Figure 5.3 B).

Questions showing improvement with walkthroughs tested the higher Bloom's Taxonomy category of "Synthesis: Create" (questions two, three and five) (Table 5.2). Furthermore, related problem walkthroughs were available for both questions two and five, which likely contributed to student improvement for these questions. While there was not a similar walkthrough for question three (Table 5.2), where students also improved, the skills required for addressing each component of question three were highlighted individually in a number of walkthroughs. In contrast, question one tested a lower Bloom's Taxonomy level, requiring students to make predictions based on recollection and application of facts (Table 5.2). Furthermore, question four was one of only two questions without a similar problem with a key or walkthrough (Table 5.2) and required student interpretation of a specific kind of data (fluorescence-activated cell sorting, FACS) which was not necessarily covered extensively elsewhere in the course.

Together, these results indicate that the benefits of walkthroughs are question-specific, as they benefit students the most on more complex question. When similar walkthroughs were available for questions requiring higher-order skills, lower-performing students benefited disproportionately compared to higher-performing students. However, when questions tested lower-order skills, or did not have related walkthroughs, similar improvements were absent in all students, regardless of performance level. This suggests that walkthroughs can be an effective tool in helping students learn higher-order skills.

5.3.2.3 Almost all students use practice problems and answers

In addition to improving student performance, alteration to the problem sets and provision of problem walkthroughs was intended to improve student use and attitudes about the problem sets. This was primarily assessed via surveys about how students use the problem sets and what they think about them, as well as interviews with undergraduate peer tutors. These peer tutors were students in the course in the first year, and part of the instructional team in the second year.

As far as the general use and format of the problem sets, the survey results indicate that in both years of the course, over 90% of students used the problem set questions (Q# 1), and over 80% used the answer keys or walkthroughs (Q# 34 and 35; Figure 5.4). Furthermore, most students felt that the number of practice problems was good (Q#2), and that they were appropriately challenging (Q#3). Conversely, over 75% of students wanted more questions to have answers available (Q#36, Figure 5.4). For most questions, the responses to these questions did not differ between each year of the course, even when respondents were divided into low-, mid- and high-performing students, as described above (Figure 5.4).

The exception appears to be the question of how many practice problems students wanted, with over twice as many low-performing students saying there were too many questions in the year with answer keys, compared to the year with walkthroughs (compare low-performing in K and W for Q#2; Figure 5.4). This shift likely reflects the reduction in the number of practice problems by 34% from 207 to 137 in the second year of the course. The survey results suggest that lower-performing students are the ones most affected by problem sets that might be too large. We can therefore conclude that while practice problems and their answers were heavily used by students in the class, it is important to make sure the number of practice questions does not become too large.

5.3.2.4 Students use problem walkthroughs differently than answer keys

To take a closer look at how students use the problem sets over the course of the class, we looked at the frequency of various activities the students might engage in using the problem sets. The survey results indicated that regardless of the format of problem set answers, most students worked on the problem set questions on their own a few times a month (Q# 4 and 5),

and that they were most frequently supported in these efforts by reading posts on the course discussion board (Q# 11; Figure 5.5), and by consulting the problem set answer keys or problem walkthroughs (Q 37–40; Figure 5.5). Students less frequently sought out classmates for help (Q# 6–10), and only rarely approached members of the instructional team (Q# 12–14; Figure 5.5). Interestingly, students more frequently made use of the keys/walkthroughs than the practice problems themselves (compare Q# 4 and 5 to question 38 in Figure 5.5). Together, these results suggest that the problem set answers and the discussion board may be better ways to support students working on the problem set questions.

In general, students used the problem sets and various forms of support similarly in each year of the course, with a few exceptions. With walkthroughs, students more frequently went over problem set answers with their classmates in person (Q#8; Figure 5.5), though it is unclear how changes in the problem sets might have facilitated this. Dividing students by performance level revealed that with problem walkthroughs, lower-performing students less frequently made use of the discussion board to support problem-solving practice (Q# 10–11) and made use of the walkthroughs less frequently than the answer keys (Q# 38–40; Figure 5.5). This latter result may reflect the more comprehensive nature of walkthroughs versus keys, which may make walkthroughs more amenable to infrequent but in-depth reading for lower-performing students, rather than frequent but casual perusal which they may find easier in the more-simple answer keys.

In the second year of the course, answer walkthroughs were available for problem set questions covered in mandatory tutorials, in addition to other problem set questions that previously had answer keys. Interestingly, low-performing students less frequently made use of walkthroughs for questions not covered in tutorial, while high-performing students more frequently used these walkthroughs (compare Q# 37 and 38, Figure 5.5). This may reflect different study habits in low- and high-performing students, as low-performing students may only frequently use walkthroughs for the weekly tutorials but look at walkthroughs for other questions only in preparation for exams. The impact of problem walkthroughs may therefore be increased for lower-performing students if they are integrated more routinely into lecture or tutorial.

Together these results suggest that students are frequently using the answers to practice problems to aid their studying, making improvements to these answers is therefore a plausible mechanism by which instructors can help students to solve these kinds of problems. Furthermore, they show that students use problem walkthroughs differently than answer keys, especially lower-performing students, who appear to use walkthroughs less frequently, and may be less likely to take advantage of this resource when it is presented as an optional activity.

5.3.2.5 Walkthroughs improved student attitudes about problem sets

I next examined student attitudes about using the problem sets and the answer keys/walkthroughs. In both years of the course, students tended to agree that the problem sets and answers were important and relevant for the midterm exam (Q# 15–16 and 42), final exam (19–20 and 43), and the course in general (Q# 30 and 47) (Figure 5.6). While they knew how to use the practice problems to study (Q# 23), students found it too hard to tell if they were answering the practice questions correctly (Q# 24) (Figure 5.6). This issue was not improved by providing walkthroughs rather than answer keys, as in both years over 75% of students expressed a strong desire for a greater number of answers to the practice problems (Q#36; Figure 5.4).

Though walkthroughs did not appear to fully address student desires for more expansive answer keys, the walkthroughs did change student attitudes about the answers compared to the answer key. Indeed, the biggest shift in survey responses was in questions about the problem set answers (Q# 42–48), reflecting the fact that these were the biggest changes made to the problem sets. In the class as a whole, problem walkthroughs appear to make it easier to understand why the answers given are correct (Q# 44), they make it easier to use the answers to attempt other questions in the problem sets (Q# 45), they are better at helping students feel like their problem-solving skills have improved (Q# 46), and they do a better job of helping students judge the instructors' expectations in answering problems (Q# 47) (see All in Figure 5.6). This shift in student responses demonstrates that more students appreciate the utility of the problem walkthroughs compared to answer keys, representing a significant improvement in student attitudes about the problem sets and the answers provided.

When comparing the responses of students at different performance levels, it becomes clear that while for most of the survey questions above the attitudes of students improved for all

performance levels, the higher-performing students saw greater increases (compare K and W for low, mid and high in Q# 42–48; Figure 5.6). Indeed, significantly greater agreement with the above statements in walkthrough years was only seen for the mid- and high-performing students. This may suggest that a minimum level of knowledge or skills are required to fully appreciate the increased benefits of walkthroughs versus answer keys. This is supported by that fact that regardless of year, the lower performing students were less likely to see the benefits of having answers to the problem sets compared to the more highly-performing students (compare low, mid and high in Q 42–48; Figure 5.6).

Together, these survey responses suggest that walkthroughs better support students than answer keys. While students continued to ask for additional answers to problem set questions when walkthroughs were provided, rather than answer keys, the students appreciated the problem sets more and student attitudes about the answers and their utility improved, especially for higher-performing students.

5.3.2.6 Student survey responses varied over time

As the online surveys were conducted several months after each course ended, several questions from these surveys were selected for inclusion in two in-class surveys, to investigate how student responses might have changed over time. The responses to the survey administered after the midterm exam were similar to those from the online survey, though more students agreed that it was easy to understand why the answers were correct in the in-class survey (Q#44; Figure 5.7). Conversely, in the survey before the final exam there was a significant difference in the response for every question compared to the online survey (Figure 5.7). Firstly, students responded more negatively to the questions about the utility of the practice problems and walkthroughs when surveyed at the end of term (Q# 24, 44, 45), and secondly, students claimed to use the practice problems and walkthroughs more frequently when questioned during the term than after term ended (Q# 5 and 38; Figure 5.7). As responses differed across the surveys, it is unclear which survey provides a better estimate of student attitudes and activities, highlighting the importance of administering surveys at similar times, as was the case with the two online surveys. However, these data also indicate that surveys conducted during a course will likely

provide a better picture of how students feel at the time, rather than after the course when their feelings have mellowed.

5.3.2.7 Walkthroughs help students learn and employ transferrable skills

To more fully explore student perspectives about the problem sets and the answer keys/walkthroughs, a qualitative analysis of student long-form survey responses, and undergraduate peer tutor interviews, was conducted. The long-form responses were used to develop a codebook which identifies and defines common and recurring themes in the students' comments about what they liked and didn't like about the problem sets (see Appendix H). Many of these themes were then explored more fully in interviews with the peer tutors (see Appendix I). This analysis confirmed the importance of including questions in the survey about the number of practice problems and answer keys/walkthroughs, the difficulty level of the practice problems, and the usefulness of the problem sets for exam preparation, as these topics also came up repeatedly in the long-form comments. These data also more fully explore the reasons for the responses the students gave in the closed-response questions of the survey.

Interestingly, in the year with answer keys, many students suggested that providing sample answers and explanations of why the answers were correct and how to approach a problem would have been beneficial; precisely the changes that were implemented in problem walkthroughs the following year.

> *"Perhaps providing more of a guided answer to the practice problems [would be good], as I remember occasionally getting a practice problem wrong and not understanding the correct answer."*
> *(2015 – Answer Keys)*

> *"…I would also have liked to see extra examples of correct answers/wording – It would have also been good to give specific key words that were being looked for."*
> *(2015 – Answer Keys)*

Comments from the following year illustrate why the students found these more explanatory answers beneficial. While students from both years mentioned the importance of practice problem answers for exam studying and assessing their ability to answer the practice questions, walkthroughs were frequently credited with aiding learning on their own. This

difference is supported by the increased number of students who felt the walkthroughs helped develop their problem-solving skills and their ability to use the answers to attempt other problems (Q#46; Figure 5.6). This shift appears to reflect the major differences between answer keys and walkthroughs, as the walkthroughs were intended to aid skill building and transferability between different questions by highlighting the common skills that a student is practicing by answering the questions.

> *"[The walkthroughs] broke the questions down in a way to lead us to the answer; it didn't just straight up give us the answer to the problem. In a way, they taught us how to solve the problem instead, which I found very beneficial!"*
> *(2016 – Walkthroughs)*

> *"The fact that some questions that were completely foreign to me had answers to them made it possible for me to then do other questions."*
> *(2016 – Walkthroughs)*

> *"[I liked] the question tags for sure. Just type Cntrl-F and whatever [question you] were looking for pops up."*
> *(2016 – Walkthroughs)*

> *"I liked how all of the example answers were clear and outlined what was expected. For some there was "example student answers" and "instructor feedback" in different coloured fonts that helped give us tips and further outlined expectations…"*
> *(2016 – Walkthroughs)*

> *"I liked the fact that [the walkthroughs] were very detailed, as if someone was explaining it to you in person from scratch."*
> *(2016 – Walkthroughs)*

The interviews with the peer tutors provided further context, explaining how the switch from answer keys to walkthroughs may help introduce students to more complex forms of problem-solving they may not have seen in previous classes.

> *"I mean BIOL200 is the first time that a lot of the students have been asked not just to give the correct content in the answer, but also to deliver it well. You're also building scientific writing skills. So, if you have just a straight answer key, and you've written your answer, I think you might compare it content wise to the answers. Like, I hit this point, I hit this point, I hit this point. But when you have the walkthrough, which I think includes a more in-depth reasoning as to why the logic of the argument is correct, why they were ordered this way, why it's important that you*

present your argument in this level of detail and this kind of order. I think is really useful."
(Peer Tutor Interview)

"I think the walkthrough was very helpful. When I read through them it's something that I wished I had when I was taking the course, because it shows you how to approach the courses. Even though in tutorials we do questions as well, and the TA will tell you how to answer the questions, I just feel like it's not enough as a student. If there's more walkthrough problems I can read it over, and over. And then just think about repeatedly. And in tutorial when the TA says something, sometimes you don't have time to take it down, and it's just gone. And you won't have a way to review from that. But if it's written in a document and can refer back to it constantly, that's very helpful."
(Peer Tutor Interview)

"… Students that are really struggling maybe just don't know where to start, and they just don't have any idea whether the answer they're providing is what the instructor is looking for. So having that walkthrough, the in-depth, not just "this is the answer to this question", but the in-depth, "this is the style of the answer we're looking for". "This is how you should be analyzing the question". "This is the level of detail we're looking for in an answer". Definitely would jumpstart those kind of students that aren't quite getting it, to get started with the rest of the problem set."
(Peer Tutor Interview)

These comments exemplify themes found repeatedly in the qualitative analysis, suggesting that these perspectives are representative of a larger population of students in each class. In comparing the discussion about answer keys and walkthroughs, it becomes apparent that the increased detail in the walkthroughs changed how students think about the purpose of answers to practice problems, which in turn is helping them feel better supported in learning and employing the skill involved like problem-solving, critical thinking, logical reasoning, and data analysis.

5.3.2.8 Walkthroughs do not resolve a desire for more answers

While students appear to find the walkthrough more valuable than answer keys, the survey responses indicate that in both years a large majority of students would have preferred more questions with answers (Q# 36; Figure 5.4). This sentiment was reflected in the long-form responses from the survey, where students often spoke passionately about their desire for a full, or expanded, answer key for a variety of reasons. One recurring theme was how students were

unable to check their answers using other methods, which is supported by the survey data showing that students only infrequently seek help from their classmates or the instructional team (Q# 12-14; Figure 5.5).

> *"Having problems without answers is of no use to me. It does not make me think more about the question, or if it does, who knows if I may be thinking about it correctly. Many students do not form the study groups that these questions are designed for, for a variety of reasons. For me, social anxiety is a large problem preventing me from doing so. For someone else it might be time, or location if they take a long commute. Thus I feel that not giving the answers can be an unfair advantage. Additionally, I personally always [learn] better by working through answers and then applying them to other questions. So I feel that a large part of what I need to study was lacking from this aspect of the course."*
> *(2015 – Answer Keys)*

> *"[I want] more [answers]! Not just for one or two questions. I frankly did not have time to go personally and ask about the questions and sometimes the peer tutor took ages to reply and/or is frustrated with my excessive questions."*
> *(2015 – Answer Keys)*

> *"… I remember for the first midterm, I diligently studied off of the problem sets believing that my answers were correct, which [resulted in] a terrible mark in my midterm and that indicates that clearly I had the wrong understanding of doing the problem sets. How would I know to do them correctly?"*
> *(2016 – Walkthroughs)*

Many of these concerns were expanded upon in the interviews with the peer tutors, who talked about the conflict between enjoying learning new things and getting a good grade, as well as the importance of formative feedback prior to the midterm exam, and how having answers can affect student motivation to work on the problems.

> *"I think [the students] do know, they know that it's better for their learning, for their development as scientists over all, [to not have a full answer key]. But in three and a half months of trying to cram as much cell biology into your head as possible, to achieve a good grade, it <u>feels</u> detrimental to not have answer keys, even though it's not."*
> *(Peer Tutor Interview)*

> *"I did the problem sets but I was probably writing down incorrect answers. I wasn't hitting the points that they were looking for. But then because there was no feedback*

from the answer key or anything, so I didn't realize that it was wrong. So I used the same wrong approach on the midterm, and that's when I finally realized, getting feedback that it was wrong. So after that I realized I need to change it, how can I change it? And then went to more peer tutor office hours, prof office hours, to ask them about my answers. And later I realized, at the end I was able to formulate a way to answer these questions and then hitting the points that the markers would want and then get the marks."
(Peer Tutor Interview)

"…I think like, one downside of not giving out answer keys is some students just stop trying in the course. They think "Even if I do it I'm not going to know if I'm getting it right or wrong so whatever." And then when it gets busy they kind of just leave it behind."
(Peer Tutor Interview)

While this qualitative analysis supports the quantitative survey data, it also highlights many of the reasons students may request expanded answer keys, even when told answer keys may impede performance. The variety of ways in which students feel answer keys impact their success in the course also highlights why it is important for instructors to consider how their instructional decisions may disproportionately impact students with less access to other kinds of feedback. As walkthroughs don't appear to address the needs of these kinds of students, alternative solutions should be investigated. In the surveys, students suggested releasing answers after a delay, having review sessions to go over answers, providing a grade breakdown for the practice problems, or assigning a few problems a week for homework.

5.4 Discussion

This chapter examined several approaches instructors can use to support students in learning complex problem-solving in undergraduate cell biology classes. In a class with more experienced students, the best outcomes were achieved when students analyzed and graded example answers, compared to a traditional approach of iterative assignments and feedback, or an activity deconstructing the problem-solving process into its various steps. In a class with more-novice problem solvers, improvements were observed when several practice questions were provided with example answers and explanations, rather than simple answer keys. Furthermore, lower- and higher-performing students benefited from example answers in different ways.

5.4.1 Example answers improve performance of more novice students

In the BIOL200 exam, students provided with walkthrough example answers performed better on several exam questions than with answer keys alone (Figure 5.3). Similar improvements in student problem-solving have been previously attributed to the worked example effect, where students that first examine a completed problem prior to working on practice problems learn the same amount in a shorter time, or learn a greater amount more quickly, than students doing practice problems alone (Booth et al., 2015). This effect can be explained by cognitive load theory, which posits that individuals have a limited cognitive capacity available to them, and learning new information or skills is impaired when the cognitive load of a task exceeds the cognitive capacity of the student (Sweller et al., 2011). When students analyze completed answers to a problem, the cognitive load is decreased, allowing them to focus more attention on understanding the concepts supporting correct problem-solving. Improvements associated with the worked example effect are most well-studied in math, physics and the computer sciences (Hoskinson et al., 2013; Booth et al., 2015), though their benefits have also been demonstrated in chemistry (McLaren et al., 2006; Cardellini, 2014) and evolutionary biology classes (Yu, 2015). The example answers and walkthroughs utilized in BIOL362 and BIOL200 share many features with classic worked examples, including example answers and an explanatory component (Atkinson et al., 2000; Lee et al., 2016; Margulieux and Catrambone, 2016). The results of this chapter therefore suggest that the benefits of worked examples can be

expanded beyond the more calculation-based problems of math and physics, into the less well-structured problems encountered in cell biology classes. Interestingly, the biology problems used in this study also focus on practicing students' academic writing skills, including evidence-based argumentation. Previous studies have supported the conclusion that student analysis of example writing benefits the acquisition of academic language literacy (Wilson and Devereux, 2014; Hamilton, 2016). Improvement in BIOL200 problem-solving suggests that activities examining example writing could be similarly applied to improve student acquisition of academic writing skills in the discipline of biology. However, this would need to be tested by analyzing examples of student writing in the presence or absence of example writing.

Despite the results described above, this study also suggests that improvements in problem-solving with example answers only occur for questions testing higher Bloom's levels (Table 5.2; Appendix F). Bloom's Taxonomy of cognitive domains is commonly used to categorize educational objectives according to the kinds of cognitive skill required (Bloom et al., 1956; Anderson et al., 2001). This taxonomy has also been adapted for the analysis of biology questions, allowing for the discrimination of biology questions requiring more straightforward or complex skills and thinking (Crowe et al., 2008). In this study, the BIOL200 exam questions with the highest Bloom's levels (questions 2, 3, and 5) required students to create a model or argument which synthesizes information from disparate sources (see Appendix F). Alternatively, questions testing lower-order skills like analysis and interpretation of data (question 4), or the application of information to make experimental predictions (question 1), did not show improvement with example answers. One possible explanation for this result is that the complex questions impose a greater cognitive load on students. As such, a reduction in cognitive load via worked examples may be more effective for more challenging exam questions, as was seen for the exam questions in BIOL200 (Figure 5.3).

In BIOL200, lower-performing students benefited more than higher-performing students when walkthroughs were provided (Figure 5.3). This inconsistency may reflect differences in the utility of worked examples for problem solvers of different experience levels. Similar effects were seen when the more experienced BIOL362 students also did not improve their performance when example answers were provided compared to the traditional approach (Figure 5.1). While one might assume that instructional techniques that benefit novices would also benefit, or at least

not harm, experts, this is not necessarily the case. Experts have more well-developed knowledge structures, i.e. a mental map of facts and knowledge about a topic and the connections between them (Figure 5.8 A). These complex knowledge structures increase performance on tasks specific to an area of expertise, as larger chunks of relevant knowledge structure can be rapidly recalled and applied to the task (Kalyuga et al., 2012). When studying example answers, novices are assisted in building on their less well-developed knowledge structures with the help of detailed explanations, which reinforce background knowledge and step-by-step procedures, allowing novices to become more expert-like (Figure 5.8 B). However, these same approaches can impede the learning of experts, as a greater proportion of their cognition becomes preoccupied with processing redundant information rather than assimilating new knowledge or practicing speed and accuracy (Figure 5.8 C-D, Atkinson et al., 2003; Renkl and Atkinson, 2003; Sweller et al., 2011). This phenomenon, where the improvement of experts is negatively affected by techniques effective for novices, is called the expertise reversal effect (Kalyuga et al., 2001). The expertise reversal effect may explain why lower-performing novice-like BIOL200 students benefited from example answers, but higher-performing expert-like students were unaffected or negatively effected (Figure 5.3). Similarly, the more-senior students in BIOL362 may not have seen improved assignment performance with the example answer approach (Figure 5.1) because they already possessed expert-like knowledge in this domain.

The expertise reversal effect may also explain the decrease in performance of BIOL362 students when the assignments were scaffolded with a step-by-step worksheet (Figure 5.1). The step-by-step worksheet deconstructed the problem-solving process to a much greater degree than the example answer worksheet (see Appendices B and C). Indeed, the step-by-step worksheet focused primarily on more procedural aspects of the problem that students may already have some expertise in, at the expense of more advanced skills like composing a well-written, logically-reasoned rationale. Furthermore, this latter component of the assignments is one of the most time-consuming tasks, meaning students exposed to the step-by-step approach were under less time pressure than in other years, as evidenced by the dramatic absence of negative student comments regarding time constraints (Figure 5.2). Interestingly, experts improve more quickly when tasks are made more challenging, including introduction of a speed component (Kalyuga et al., 2012). With the step-by-step approach, the reduced time pressure then compounded the

effects of the expertise reversal effect due to a focus on novice-type skills, resulting in less productive problem-solving practice than with the traditional or example answer approaches, leading to significant decreases in assignment grades (Figure 5.1).

5.4.2 Example answers improve student attitudes

An important result in this study was that while providing example answers did not necessarily improve the performance of more-expert students, it did have a significant positive effect on student attitudes about problem-solving. In BIOL362, students generally made fewer negative comments and more positive comments about the assignments when provided with example answers, compared to the previous two years (Figure 5.2). Especially impressive is a doubling in the number of students finding the assignments enjoyable, while comments about the assignments being too difficult dropped by three-quarters. Similar improvements in student attitudes about problem-solving were seen among higher-performing students in BIOL200 when walkthroughs were provided (Figure 5.6). This included increases in student perception of the importance of the practice problems for exam studying and the utility of the answers for understanding why an answer is correct, attempting other problems, clarifying instructor expectations, and improving problem-solving skills.

These kinds of shifts in attitude can have important effects on student motivation and persistence that may have long-term consequences. For example, high drop-out rates are a problem in STEM fields (Simon et al., 2015), and programs that improve student attitudes about STEM have been proposed as a means of increasing retention (Sithole et al., 2017). Low student retention in STEM fields has also been linked to declines in student motivation, which may have longer-lasting impacts on student success (Young et al., 2018). Motivation of students in general (Mayer, 1998), and STEM students in particular (Simon et al., 2015), increase when learners feel they can achieve something on their own (self-efficacy), and if they can gain skills and demonstrate their learning (mastery and performance achievement goals). In BIOL200 and BIOL362, students responded more positively to questions related to both self-efficacy (e.g. being able to attempt other problems in BIOL200, and a being happier with the assignment difficulty level in BIOL362) and mastery (e.g. improved problem-solving in BIOL200 and increased enjoyment of assignments in BIOL362). Improvement in student attitudes in these

classes may then be translated into increased persistence and motivation to continue in biology, though this requires further investigation.

It is also important to consider the potential for improved student attitudes to positively impact student well-being more generally. Indeed, recently greater attention has been placed by institutions and education researchers on programs promoting student physical and mental health (Stanton et al., 2016; Slemp, 2017). The learning environment, and the experiences students have there, are an important component of student well-being (Stanton et al., 2016). Changes in classroom practices can therefore promote well-being, which can improve student engagement and satisfaction with learning (Stanton et al., 2016). The improvement in student attitudes with example answers and walkthroughs in BIOL362 and BIOL200, respectively, can therefore be considered advantageous, even though performance many not have improved for all students.

5.4.3 Example answers do not ameliorate students' desire for answer keys

One of the key objectives of providing problem walkthroughs in BIOL200 was to improve the utility of the answers provided, so students could better judge when they were answering a problem successfully without having a full answer key. Though more students could use problem walkthroughs to attempt other questions compared to answer keys (Figure 5.6), the walkthroughs did not ameliorate student desires for answer keys.

Practice problems are frequently assigned as homework, or for optional practice, in undergraduate courses to aid student learning (Kim et al., 2012). In these cases, answer keys may be provided to allow students to check if they have achieved the correct answer. For questions involving calculations, answer keys can provide feedback on student success or failure without exposing each problem-solving step. This forces students to first attempt a problem and then check their answer, as reading the answer alone would not be very informative. However, an answer key for many cell biology practice problems must include the logical thought process, as these questions typically require an explanation of the logical reasoning behind the analysis and interpretation of data, or hypothesis formulation, for example (see Appendices E and F). Students can therefore realize some benefit from these kinds of answer keys without attempting the problem, which could then decrease how much students practice the more time-consuming, authentic problem-solving. The absence of answer keys in BIOL200 therefore created a tension

between students, who could benefit from reading an answer key even if they might not attempt questions authentically, and instructors, who feel that reading an answer key without attempting the problems is not as effective for student learning. This latter argument is supported by a study showing that students in an economics class performed more poorly when provided with an answer key for their practice problem set (Kim et al., 2012). The compromise attempted in BIOL200 was originally to include a small selection of answer keys, which were then re-written into the walkthroughs, however the walkthroughs did not reduce students' desire for answer keys.

Though the literature suggests that withholding answer keys may benefit student learning, qualitative analysis of student comments in this study indicate that this practice likely disproportionately disadvantages students already facing challenges. While students can check their answers with members of the instructional team or their peers, these options are less available for students who work, have families to support, have mental health issues like social anxiety, or who commute long distances. Students with greater demands on their time may also not be able to attempt every practice problem, but could benefit to some extent by reading an answer key, which would be less time-consuming. BIOL200 students also felt that it was unfair to penalize those who would use problem sets correctly by attempting practice problems before reading answer keys, simply because a subset of students might use them inappropriately. Furthermore, the large number of practice problems and students in BIOL200, relative to the size of the instructional team, means that students cannot reasonably expect to get personalized feedback on every question that they attempt. Worse, because many students do not receive feedback on their practice problems prior to the midterm exam, they may not know that they are making mistakes, and are therefore unaware that they should seek help. Comments about this issue are validated by the well-documented importance of instructor feedback that diagnoses and corrects student difficulties (i.e. formative assessment), in addition to more summative assessments of student learning like exams (Dixson and Worrell, 2016).

Together, this analysis of student comments illustrates many real and important problems with the no-answer key policy in BIOL200, which should be investigated and addressed. While it is unclear if student performance would decrease if a full answer key was provided, the literature suggests this may be the case (Kim et al., 2012), making simply providing an answer key a less

than ideal option. Many alternative approaches were suggested by the students in their comments in the survey, including delayed release of answers, an increase in the number of answers compared to questions, and increased answers in the first half of the course prior to the midterm. This last suggestion has merit, as many studies of the worked example effect suggest that fading problem-solving support over time can be an effective way to transition learners from more novice-like to expert-like learning (Atkinson et al., 2003; Renkl and Atkinson, 2003). Several students also commented on how class discussion boards can be used to good effect to support answering the practice problems, though this depends on having a very active instructional team to moderate the discussions and provide feedback, which students indicated was not the case for every instructor or class section. Furthermore, more students read the discussion board than comment themselves, meaning students can interact with the answers posted just as they would an answer key. Whichever approach is attempted however, students would likely benefit from an increase in formative feedback on their problem-solving attempts, especially early in the term.

5.4.4 Conclusions

Analysis of exam grades and student feedback indicate that walkthroughs and example answers can be effective tools in supporting student problem-solving in cell biology classes. This demonstrates that the worked example effect can be successfully employed to improve student learning in real-world biology classrooms, with interesting implications for instructional best practices in these settings. For example, these results illustrate the importance of tailoring scaffolding according to the expertise level of the students, and fading this scaffolding as students acquire expertise (Atkinson et al., 2003; Renkl and Atkinson, 2003). The importance of correctly gauging the level of scaffolding fits well with a model of instructional support whereby students learn the most when the instructor strikes a balance between challenging students and supporting them (Figure 5.9). In this model, a question provided to novice students will be more challenging, requiring greater support to ensure student success, than if the same problem was given to more expert students. Importantly, this model also highlights the role of student attitudes and emotions in learning. Problems that are too easy foster boredom, while those that are too difficult result in frustration and anxiety, and both result in decreased learning. By improving

student attitudes, walkthroughs and example answers helped move students along this continuum toward greater learning and well-being. Finally, a qualitative analysis of student interviews and survey commentary provided important context which can facilitate discussions about the future of problem sets and answer keys in biology courses.

Table 5.1 Themes identified in student feedback about BIOL362 assignments.

Abundant and recurring positive and negative themes are listed with descriptions of when these themes apply.

	Theme	Description
Positive	Enjoyable	Comment describes assignments as “interesting”, “fun”, “rewarding”, etc.
	Useful	Comment describes assignments as “useful”, “realistic”, “good practice”, “important” etc.
	Gained Skills	Commenting on how they got better over time. May mention a specific skill (e.g. problem-solving, critical thinking, group work)
Negative	Too Difficult	Comments describing assignments as “unfair”, “strict”, “too hard” or “harsh”, especially regarding marking.
	Expectations Unclear	Comments that students were unsure about how assignments were marked, asking for a rubric, or that the marking seemed “arbitrary”.
	Not Enough Time	Comments asking for additional time, that they were rushed or that they were not able to complete the assignment in the time allotted.
	Not Enjoyable	Comment describes the assignments as “frustrating”, “awful”, “not enjoyable”, etc.
	Not Useful	Comments that students preferred classes with lectures to assignment classes, disliking the focus on writing, or claiming that the assignments are not “useful” or “helpful”.
	Hard to Improve	Comments that students didn’t get better over time, or that the feedback was not sufficient to allow for improvement.

Table 5.2 BIOL200 final exam questions analyzed in this study.

Final exam questions analyzed in this study, including general topic, whether a related practice question was present in the problem sets, if one or more of those questions were provided with an answer key or walkthrough, and the type of question according to Bloom’s taxonomy as determined using the Blooming Biology Tool (Crowe et al., 2008). The questions can be seen in Appendix F.

Q#	Topic	Related Practice Problem(s)	Key/ Walkthrough	Bloom’s Taxonomy (Level) Category: Verb
1	Protein Targeting	yes	yes	(3) Application: Predict
2	Cytoskeleton Dynamics	yes	yes	(5) Synthesis: Create
3	Cell Signalling	no	no	(5) Synthesis: Create
4	Cell Cycle	yes	no	(4) Analysis: Infer
5	Essay Outline	yes	yes	(5) Synthesis: Create

Table 5.3 Demographics of the BIOL362 classes.

The number of students, average program year, percent of biology majors, and ration of female to male students in each year of the BIOL362 course.

	Traditional (2014)	Step-by-Step (2015)	Example Answers (2016)
# Students	111	73	51
Program Year	3.1	3.2	3.1
% Biology Majors	79.3	79.5	78.4
Ratio Female:Male	1.3	1.2	1.3

Table 5.4 Demographics of the BIOL200 classes.

The number of students, average program year, percent of biology majors, and percent of students in the faculty of science in each year of the BIOL200 course.

	Answer Keys (2015)	Walkthroughs (2016)
# Students	1301	1261
Program Year	2.0	1.6
% Biology Majors	26.0	21.0
% Faculty of Science	76.8	76.3

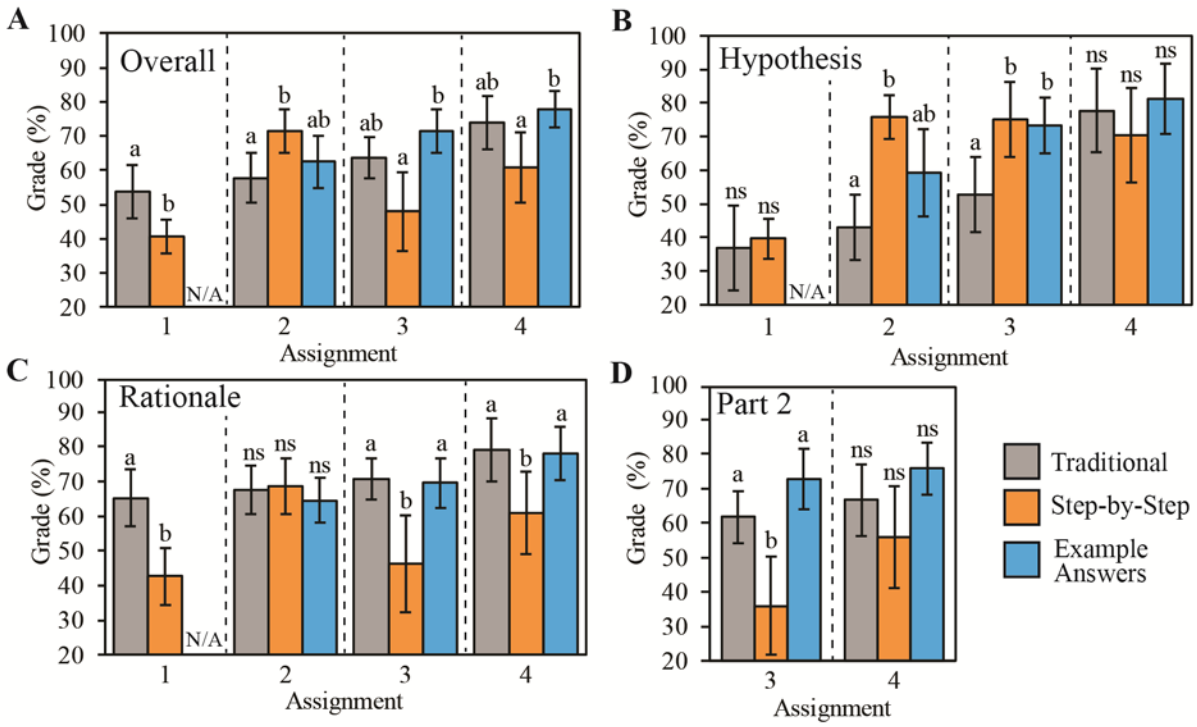

Figure 5.1 Altering they type of assignment support affects student performance.

Student performance on BIOL362 assignments when employing the traditional, step-by-step or example answers approaches. The **(A)** overall grade is broken down into grades for the **(B)** hypothesis and **(C)** rationale, and for assignments 3 and 4 the marks for the **(D)** second part of the assignment are shown. The N/A reflects that students did not hand in hypotheses and rationales for assignment 1 in the example answer approach. 'Part 2' refers to the second part of assignments 3 and 4 where students were given new data and a chance to modify their hypothesis. Statistics = Student's *t*-test (assignment 1) or one-way ANOVA followed by Tukey *post-hoc* test (all other assignments) ($p<0.05$), n = 16 - 18, means ± 95% CI.

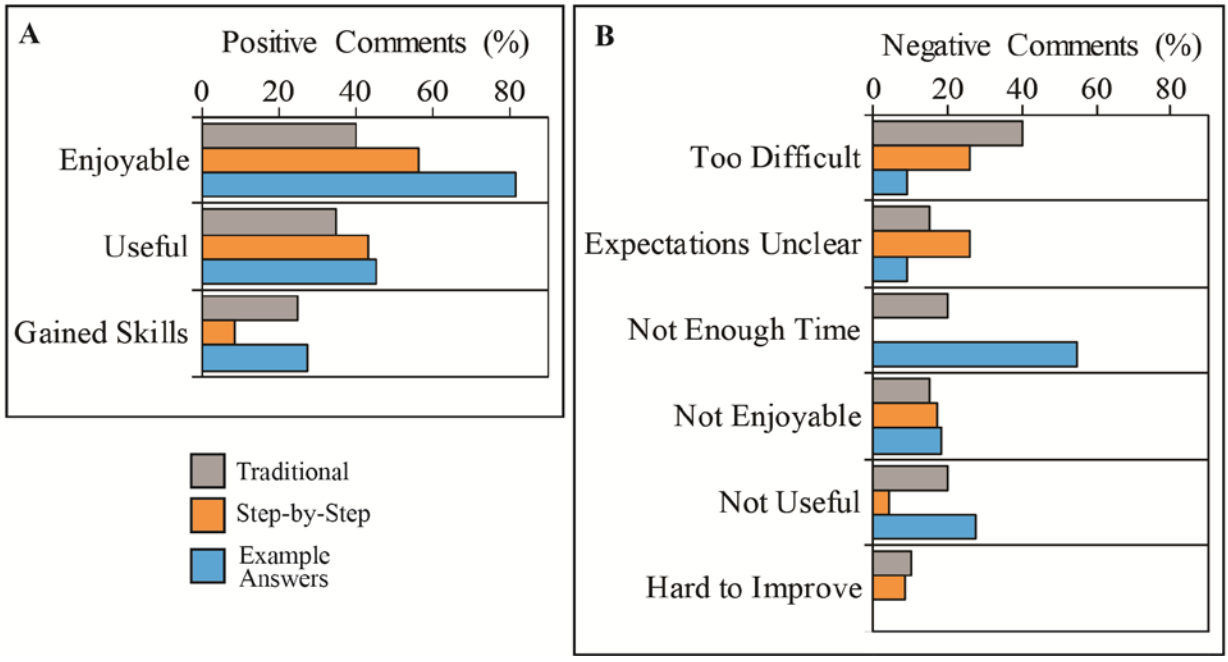

Figure 5.2 Student feedback about BIOL362 case study assignments.

Percent of **(A)** positive or **(B)** negative comments about the BIOL362 assignments with the traditional, step-by-step or example answer approach. Comments are grouped into categories based on an analysis of recurring themes.

A

Lower Grade — Higher Grade

Grade (%)	All		Low		Mid		High	
Question	K	W	K	W	K	W	K	W
Q1 Protein Targetting	70.8	70.2	55.6	53.7	71.7	70.4	**83.1**	**79.7** •
Q2 Cytoskeleton Dynamics	**68.7**	**72.5** •	**54.1**	**61.1** •	**70.0**	**73.1** •	79.3	80.6
Q3 Cell Signalling	**80.4**	**83.6** •	**68.6**	**77.5** •	**80.9**	**87.1** •	**90.0**	**88.0** •
Q4 Cell Cycle	**75.0**	**72.9** •	**61.0**	**55.4** •	75.1	73.4	**88.0**	**83.1** •
Q5 Essay Outline	**63.0**	**66.5** •	**50.6**	**57.3** •	**63.7**	**67.7** •	72.4	73.9
Total	**71.2**	**72.7** •	58.1	59.4	**72.0**	**73.9** •	81.7	81.5

B

Worsened — Improved

% Difference with Walkthroughs	All	Low	Mid	High
Question				
Q1 Protein Targetting	-0.6	-1.9	-1.3	**-3.4** •
Q2 Cytoskeleton Dynamics	**3.8** •	**7.0** •	**3.1** •	1.2
Q3 Cell Signalling	**3.2** •	**8.9** •	**6.2** •	**-2.0** •
Q4 Cell Cycle	**-2.2** •	**-5.5** •	-1.7	**-4.9** •
Q5 Essay Outline	**3.5** •	**6.6** •	**4.0** •	1.6
Total	**1.5** •	1.3	**1.9** •	-0.1

Figure 5.3 Comparison of student performance on BIOL200 final exam questions with answer keys or walkthroughs.

(A) Mean student grade on highly similar or identical final exam questions showing higher (blue) and lower (red) marks for classes provided with answer keys (K) or answer walkthroughs (W). **(B)** The percent difference in student grades with walkthroughs, showing improvement when walkthroughs were provided (blue) and worsened performance when answer keys were provided (red). For both (A) and (B), the grades of all students (All) were then grouped by low-, mid- and high-performance on the midterm exam. Significant differences between the answer key and answer walkthrough classes are shown by bolded numbers and bullets (•). Statistics = Student's *t*-test ($p<0.05$), All (n = 1023-1241), Low (n = 187-278), Mid (n = 432-630), High (n = 195-315).

Q#	Survey Question	Response	Respondents (%) All K	All W	Low K	Low W	Mid K	Mid W	High K	High W
1	While enrolled in Biology 200, did you use the problem set practice questions outside of tutorial/lecture?	yes	91.2	94.7	92.6	90.2	90.5	94.2	91.9	100.0
34	While enrolled in Biology 200, did you use the 'example answers' for questions not covered in tutorial?	yes	91.8	88.8	88.0	77.5	92.5	88.8	93.2	98.3
35	While enrolled in Biology 200, did you use the 'example answers' for questions that were covered in tutorial?	yes	N/A	84.3	N/A	80.0	N/A	81.6	N/A	94.9
2	Regarding the number of practice questions in the problem sets, there were:	not enough	11.8	6.8	11.1	7.3	12.7	1.9	10.8	16.4
		enough	66.2	76.2	40.7	73.2	70.6	75.0	67.6	75.4
		too many	21.9	17.0	48.1	19.5	16.7	23.1	21.6	8.2
36	Regarding the number of example answers for the problem sets, there were:	not enough	75.9	75.5	76.0	72.5	77.5	79.6	74.3	69.5
		enough	24.1	23.7	24.0	25.0	22.5	20.4	25.7	28.8
		too many	0.0	0.8	0.0	2.5	0.0	0.0	0.0	1.7
3	Regarding the difficulty of the practice questions in the problem sets, the problems were:	not callenging enough	5.3	2.6	3.7	0.0	6.3	1.9	4.1	3.3
		challenging enough	85.5	86.4	85.2	85.4	83.3	87.5	89.2	90.2
		too challenging	9.2	10.9	11.1	14.6	10.3	10.6	6.8	6.6
49	What format do you prefer when accessing the problem sets and example answers?	separate	N/A	52.4	N/A	53.8	N/A	54.1	N/A	47.4
		combined	N/A	6.9	N/A	10.3	N/A	5.1	N/A	10.5
		both	N/A	40.7	N/A	35.9	N/A	40.8	N/A	42.1

Figure 5.4 Percent of BIOL200 student respondents for non-Likert survey questions for classes with answer keys (K) and walkthroughs (W).

Proportion of respondents for non-Likert style survey questions with fewer respondents in red and more respondents in blue. All responses (All) were broken down by in to low-, mid- and high-performing students using midterm exam. No significant differences were found between the answer key (K) and answer walkthrough (W) classes using chi-squared tests ($p<0.05$). All (n = 200-268), Low (n = 23-42), Mid (n = 96-126), High (n = 53-74).

Survey Question		All		Low		Mid		High	
Q#	Please indicated how frequently you did the following:	K	W	K	W	K	W	K	W
4	Read through the problems	3.08	3.05	2.96	2.93	3.11	3.02	3.08	3.15
5	Attempted problems on my own	3.11	3.08	3.04	2.90	3.09	3.02	3.18	3.23
6	Attempted problems with classmates in person	2.31	2.47	2.37	2.59	2.30	2.44	2.31	2.38
7	Attempted problems with classmates online	2.00	2.06	2.33	2.10	1.93	2.07	2.00	1.98
8	Went over answers with classmates in person	**2.32**	**2.53** •	2.44	2.61	2.31	2.39	2.31	2.52
9	Went over answers with classmates online	2.15	2.15	2.30	1.93	2.08	2.16	2.24	2.11
10	Posted about the problems on the class discussion board	1.80	1.78	**2.00**	**1.56** •	1.70	1.85	1.88	2.00
11	Read things other people had posted about the problems on the discussion board	2.95	3.00	**3.30**	**2.56** •	**2.86**	**3.11** •	2.99	3.16
12	Contacted or met with an instructor about the problems	1.56	1.53	1.52	1.44	1.51	1.51	1.65	1.57
13	Contacted or met with a TA about the problems outside of tutorial	1.65	1.59	1.59	1.73	1.64	1.58	1.68	1.62
14	Contacted or met with a peer tutor about the problems	1.38	1.44	1.26	1.54	1.41	1.42	1.37	1.54
37	Read through the example answers for questions covered in tutorial	N/A	3.05	N/A	2.90	N/A	3.00	N/A	3.12
38	Read through the example answers for questions NOT covered in tutorial	3.25	3.08	**3.40**	**2.68** •	**3.22**	**3.06** •	3.26	3.25
39	Attempted problems with example answers before looking at the answer	3.32	3.16	3.12	2.93	**3.27**	**3.10** •	3.50	3.47
40	Used an example answer to help me answer a different problem set question	3.03	2.97	3.24	2.80	**3.09**	**2.89** •	2.86	3.09
50	Used the table of contents	N/A	2.14	N/A	1.95	N/A	2.31	N/A	1.88
51	Used the question tags	N/A	1.96	N/A	2.18	N/A	1.97	N/A	1.86
52	Used the index	N/A	1.81	N/A	1.95	N/A	1.82	N/A	1.67

1 = Never
2 = Rarely (a few times a term)
3 = Occasionally (a few times a month)
4 = Frequently (once a week)
5 = Very Frequently (more than once a week)

Less Frequent — More Frequent

Figure 5.5 Frequency of student activities from online survey responses for BIOL200 classes with answer keys (K) and walkthroughs (W).

Survey response as an average using a scale from 1 to 5 (bottom) for Less Frequent (red) to More Frequent (blue) as appropriate. The responses of all students (All) were then grouped by low-, mid- and high-performance on the midterm exam. Significant differences between the answer key (K) and answer walkthrough (W) classes are shown by bolded numbers and bullets (•). Questions are grouped by type, those not included in a survey are given as N/A. Statistics = Student's *t*-test ($p<0.05$), All (n = (00-268), Low (n = 23-42), Mid (n = 96-126), High (n = 53-74).

Q#	Survey Question: To what extent to you agree or disagree with each of the following statements?	All K	All W		Low K	Low W		Mid K	Mid W		High K	High W	
15	Using the problem sets was an important part of my studying for the midterm	**3.82**	**4.00**	•	3.52	3.54		**3.66**	**3.91**	•	**3.95**	**4.39**	•
16	The questions in the problem sets were similar to those on the midterm exam	**3.47**	**3.87**	•	3.19	3.61		**3.39**	**3.74**	•	**3.43**	**4.21**	•
17	I wish I had spent more time on the problem sets when studying for the midterm exam	3.57	3.68		3.74	4.07		3.71	3.60		3.15	3.15	
18	I wanted to work more on the problem sets when studying for the midterm, but I didn't have the time	3.75	3.68		4.30	3.76		3.66	3.73		3.54	3.28	
19	Using the problem sets was an important part of my studying for the final exam	4.15	4.11		3.81	3.54		4.03	3.96		4.24	4.33	
20	The questions in the problem sets were similar to those on the final exam	3.79	3.86		3.48	3.51		3.78	3.66		**3.71**	**4.05**	•
21	I wish I had spent more time on the problem sets when studying for the final exam	**3.36**	**3.65**	•	3.89	3.71		**3.38**	**3.57**	•	3.00	3.32	
22	I wanted to work more on the problem sets when studying for the final, but I didn't have the time	**3.43**	**3.62**	•	3.56	3.54		3.42	3.59		3.23	3.26	
23	I was not sure how to use the practice problems to study	2.45	2.42		2.59	2.68		2.45	2.46		2.36	2.07	
24	It was too hard to tell if I was successfully answering the questions	3.93	4.02		4.22	4.34		3.93	3.96		3.79	3.82	
25	I am happy with how much help I received from instructors, TAs, and peer tutors on problem set questions	3.13	3.18		2.63	2.59		2.67	2.76		3.26	3.32	
26	If I wanted more practice for a specific type of question, it was easy to find an example in the problem sets	2.94	3.05		3.03	2.93		2.85	2.96		3.03	3.10	
27	The problem sets helped me understand the connections between different topics and units	3.39	3.49		3.11	3.34		3.35	3.47		3.40	3.54	
28	The wording of questions in the problem sets made it easy to understand what was being asked	2.99	3.01		2.81	2.63		2.87	2.95		3.13	3.25	
29	Using the problem sets helped me improve my problem solving skills	3.64	3.67		3.59	3.41		3.58	3.61		3.66	3.89	
30	The problem sets are an important part of the course	3.92	4.03		3.85	3.83		3.83	3.88		4.03	4.26	
31	Working on the practice problems was frustrating	3.62	3.66		3.85	3.88		3.58	3.53		3.52	3.55	
32	Working on the practice problems was rewarding	3.36	3.43		3.07	3.41		3.39	3.30		3.36	3.57	
33	Working with the practice problems helped me interpret real experimental results	3.46	3.60		3.07	3.29		3.40	3.52		3.61	3.87	
41	It was easy to find the example answers on the course website	3.40	3.25		3.39	2.92		3.25	3.35		3.53	3.39	
42	Using the example answers was an important part of my studying for the MIDTERM	3.91	3.99		3.52	3.18		3.74	3.85		**3.96**	**4.31**	•
43	Using the example answers was an important part of my studying for the FINAL EXAM	3.97	4.08		**3.68**	**3.13**	•	3.84	3.93		**3.94**	**4.32**	•
44	It was easy to understand why the example answers were correct	**3.47**	**3.68**	•	3.08	3.20		**3.28**	**3.51**	•	**3.63**	**3.97**	•
45	I could use the example answers to help me attempt other questions in the problem sets	**3.53**	**3.72**	•	2.92	2.98		**3.44**	**3.62**	•	**3.63**	**3.97**	•
46	Using the example answers helped improve my problem solving skills	**3.49**	**3.81**	•	3.04	3.25		**3.43**	**3.67**	•	**3.56**	**4.02**	•
47	The example answers were an important part of the course	**3.87**	**4.09**	•	3.44	3.40		**3.76**	**4.04**	•	3.99	4.25	
48	The example answers helped me figure out what the instructor expected of me	**3.82**	**4.05**	•	3.36	3.30		**3.66**	**3.90**	•	**3.93**	**4.36**	•
53	The table of contents is a valuable resource	N/A	3.43		N/A	2.77		N/A	3.17		N/A	3.26	
54	The question tags are a valuable resource	N/A	3.23		N/A	2.62		N/A	2.90		N/A	3.32	
55	The index is a valuable resource	N/A	3.21		N/A	2.62		N/A	2.83		N/A	3.13	

1 = Strongly Disagree
2 = Disagree
3 = Neither Agree nor Disagree
4 = Agree
5 = Strongly Agree

Disagree — Agree

(Previous Page)

Figure 5.6 Comparison of student attitudes from online survey responses for BIOL200 classes with answer keys (K) and walkthroughs (W).

Survey response as an average using a scale from 1 to 5 (bottom) for Disagree (red) to Agree (blue) as appropriate. The responses of all students (All) were then grouped by low-, mid- and high-performance on the midterm exam. Significant differences between the answer key (K) and answer walkthrough (W) classes are shown by bolded numbers and bullets (•). Questions are grouped by type, those not included in a survey are given as N/A. Statistics = Student's *t*-test ($p<0.05$), All (n = 200-268), Low (n = 23-42), Mid (n = 96-126), High (n = 53-74).

	Survey Question	Online	In Class	
Q#	To what extent to you agree or disagree with each of the following statements?	W	#1	#2
15	Using the practice problems was an important part of my studying for the midterm	4.00	3.97	N/A
16	Using the problem walkghroughs was an important part of my studying for the midterm	3.87	4.03	N/A
24	It was too hard to tell if I was successfully answering the practice problems	4.02	4.07	**3.73** •
44	It was easy to understand why the example answers in the walkthrough are correct	3.68	**3.85** •	**2.59** •
45	I can use the information in the walkthroughs to help me attempt other questions in the problem sets	3.72	3.59	**2.54** •
Q#	Please indicated how frequently you did the following:	W	#1	#2
5	Attempted the practice problems on my own	3.08	N/A	**3.57** •
38	Read through the problem walkthroughs for questions NOT covered in tutorial	3.08	N/A	**4.11** •

1 = Strongly Disagree
2 = Disagree
3 = Neither Agree nor Disagree
4 = Agree
5 = Strongly Agree

Disagree — Agree
Less Frequent — More Frequent

1 = Never
2 = Rarely (a few times a term)
3 = Occasionally (a few times a month)
4 = Frequently (once a week)
5 = Very Frequently (more than once a week)

Figure 5.7 Comparison of in-class and online survey responses for the BIOL200 class provided with walkthroughs.

Survey response as an average using a scale from 1 to 5 for Disagree to Agree, or Less Frequent to More Frequent (right) as appropriate. For the class with problem set walkthroughs (W), five question in-class (In-Class) surveys were collected after the midterm exam before marks were released (#1), and on the last day of class before the final exam (#2), in addition to the full online survey administered after the course was completed (Online). Significant differences between the In-Class and Online responses are shown by bolded numbers and bullets (•). Questions not asked in the survey are given as N/A. Statistics = Student's *t*-test ($p<0.05$), In-Class (n = 166-194), Online (n = 240-265).

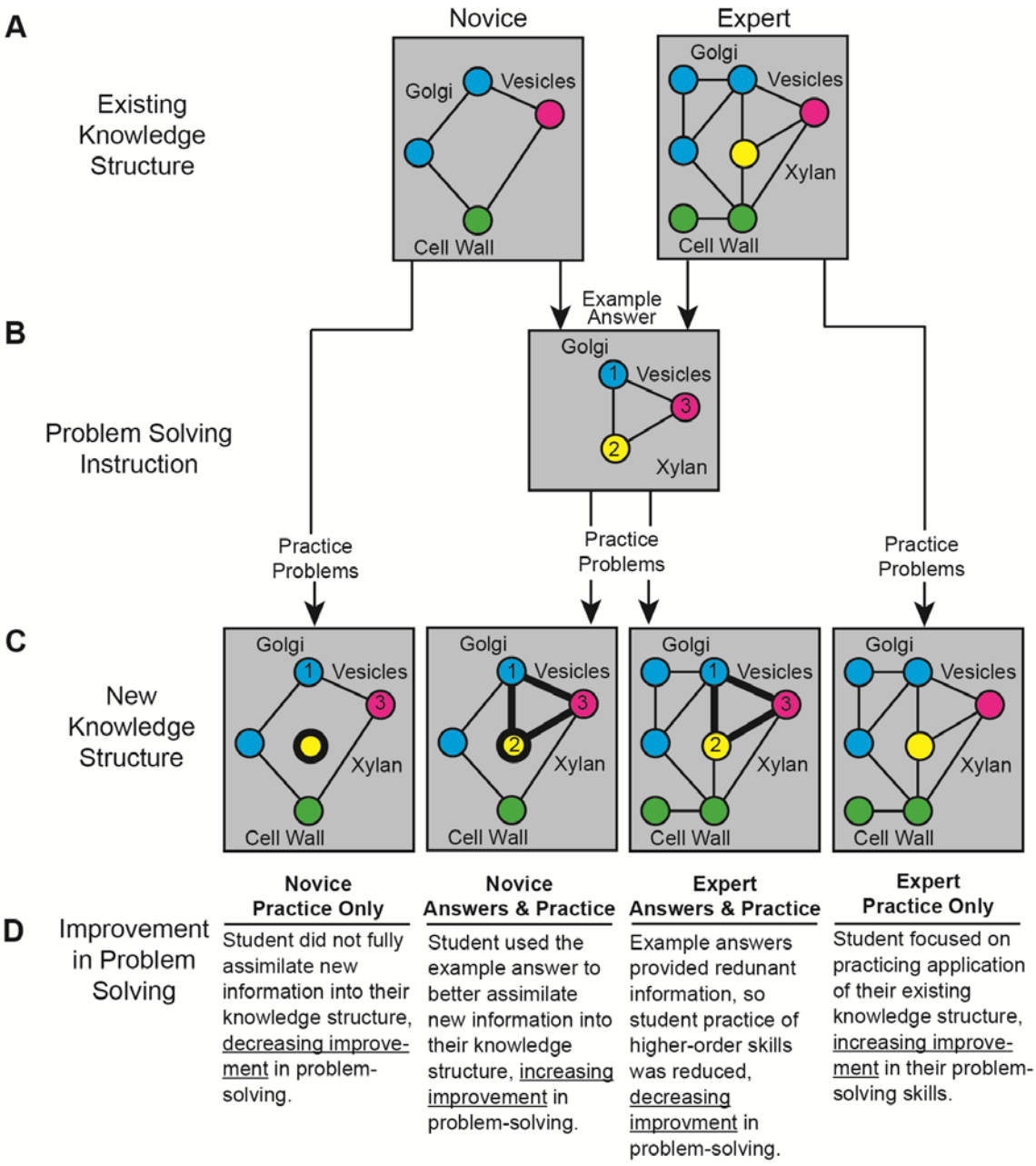

Figure 5.8 The effect of problem-solving instruction on novices and experts.

(A) Novices have less well-developed knowledge structures compared to experts, using the biology concepts Golgi, vesicles, xylan and cell walls as examples. Nodes represent knowledge and edges give relationships between nodes. **(B)** Practice problems and example answers may be used to help students improve their problem-solving skills. The diagram shows an example answer reinforcing knowledge about Golgi, vesicles and xylan, and providing a problem-solving procedure (numbers). **(C)** The knowledge structures of novices and experts change in different ways in response to different problem-solving instruction. Bolded nodes and edges show components of the knowledge structure that have been introduced or reinforced by the problem-solving instruction. **(D)** Improvement in problem-solving skills depends on the kind problem-solving instruction novices and experts receive.

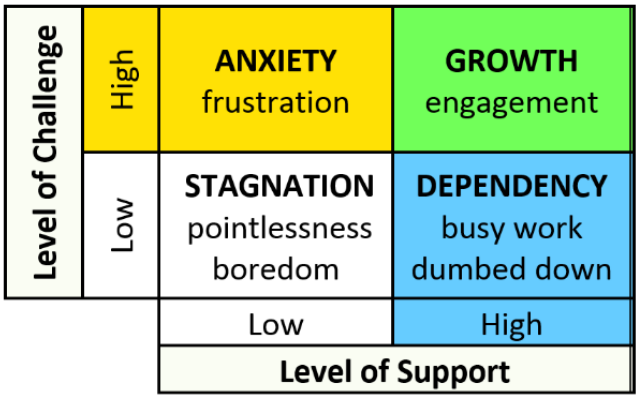

Figure 5.9 The challenge and support model of scaffolding.

Optimal learning is believed to occur when students are both challenged and supported, as this fosters student growth and engagement. In this dichotomy, low challenge results in decreased learning due to stagnation or dependence, while low support for highly challenging tasks results in student anxiety and frustration. Adapted from Mezirow (1991) and Wilson and Devereux (2014).

Chapter 6: Conclusions and Future Directions

This dissertation had two general focuses, firstly to better understand how xylan biosynthesis occurs in the Golgi during secondary cell wall (SCW) deposition, and secondly to explore how instructors can better support student problem-solving in undergraduate cell biology courses. These two components of the thesis may appear entirely unrelated, however there are synergistic benefits to combining disciplinary and education research. As a cell biologist, I can draw from my expertise in this field to design instructional materials that help students deal with authentic cell biology problems. I am intimately familiar with the priorities and pitfalls inherent in this kind of problem-solving and am therefore in a prime position to help guide students through this process. On the other hand, in my education research I focused on how to help students clearly and concisely communicate complex biological models and the evidence that supports them, the very skills that I utilize in my disciplinary research. This had the effect of concentrating my attention on the key principles of scientific argumentation and reasoning, which I believe helped me grow my skills in this area. I then used these skills to define and defend a new model for xylan biosynthesis in the plant Golgi. Both the disciplinary and the education components of this thesis were therefore made better by the effort I put into the other. As a result, I was able to make significant advances in two *prima facie* disparate fields and identify interesting opportunities for future investigation.

6.1 Major findings of Chapters 3 and 4

In Chapter 3, I investigated how the population of Golgi stacks in plant cells are marshalled to facilitate the deposition of SCWs. Previous studies had indicated that an increase in demand for Golgi-produced pectin in the seed coat resulted in a doubling of the number of Golgi stacks in a cell (Young et al., 2008), leading to the hypothesis that a similar increase in Golgi number may facilitate production of SCWs. Indeed, confocal microscopy and TEM quantification of Golgi stacks revealed a significant increase in the number of Golgi coinciding with the onset of SCW production. Interestingly, this proliferation appears to be independent of the presence of IRX9 and xylan production, as Golgi proliferation was unaffected in the *irx9* mutant background. Furthermore, the entire Golgi apparatus appears to be working in concert to produce xylan and process glycoproteins, based on co-localization in every Golgi stack of the

xylan biosynthetic enzyme IRX9-GFP, and the glycoprotein processing protein MANI-mCherry. Finally, previous characterization of Golgi distribution during SCW deposition suggested that Golgi may preferentially associate with the forming SCWs (Schneider et al., 2017), however when I analyzed Golgi position using TEM, I revealed that the close association of Golgi with SCWs simply reflects cytoplasmic organization and was no different than random.

In summary, the results of this chapter support a model where the number of Golgi stacks is responsive to changing demands for Golgi processing, and where each Golgi stack may be treated as a representative of the Golgi apparatus as a whole. Furthermore, targeted delivery of SCW cargo does not appear to require preferential targeting of streaming Golgi to SCW domains. This latter point illustrates the importance of supplementing live-cell imaging of fluorescently-tagged proteins with other imaging techniques which provide a better picture of the cellular context in which these proteins and organelles are found.

In Chapter 4 I conducted a nanoscale characterization of Golgi stacks at different time points in SCW deposition. Previous studies of Golgi ultrastructure suggested that there is a tight relationship between Golgi structure and function, as changing the contents of the Golgi, and the volume and direction of membrane trafficking, is frequently accompanied by changes in the size, shape and number of Golgi cisternae (Staehelin et al., 1990; Samuels et al., 2002; Young et al., 2008). A review of this literature led me to hypothesize that the onset of SCW deposition would result in an increase in the size of cisternal margins, to accommodate storage of large amounts of xylan. Furthermore, I predicted an increase in cisternal diameter, as this is believed to be a prerequisite for Golgi proliferation, which I had already demonstrated was occurring in these cells. Both these hypotheses were supported by TEM quantification of Golgi structure prior to and following SCW deposition.

More surprising were the changes in Golgi structure in the *irx9* mutant background. I hypothesized that the size of the Golgi margins would decrease due to the absence of xylan, which was observed as predicted. More striking however was the dramatic increase in Golgi fenestration and tubulation, which suggests that the resident and cargo composition of the Golgi plays a significant role in maintaining cisternal structure. Furthermore, while fenestrations are found in Golgi throughout eukaryotes (Mogelsvang et al., 2003; Mogelsvang et al., 2004; Koga and Ushiki, 2006; Kang and Staehelin, 2008; Kang et al., 2011; Donohoe et al., 2013), to my

knowledge no mutant has been characterized with increased fenestration. The increased fenestration in *irx9* Golgi may provide a valuable model in which to investigate fenestration formation and function, which has so far been largely theoretical. Additionally, while recent years have seen characterization of the structure and function of Golgi tubules in mammalian cells (Yang et al., 2011; Park et al., 2015), tubulation did not previously appear to be a major feature of plant Golgi. However, the presence of Golgi tubules throughout all stages of my analysis, and their increase in the *irx9* mutant, suggest that Golgi tubules may play a more prominent role in plant Golgi processing than previously thought.

In Chapter 4 I also complemented the analysis of Golgi ultrastructure with high-resolution mapping of the distribution of IRX9-GFP and xylan in the Golgi using immunoTEM. In a previous model based on freeze-fracture analysis of pectin-producing Golgi in the root cap, glycosyltransferases (GTs) were predicted to be arranged in protein arrays in cisternal centers, while polysaccharide products accumulate in the margins (Staehelin et al., 1990). However, there was little direct evidence to support this model, and live-cell imaging of fluorescently-tagged Golgi-resident proteins in a ring-shaped pattern (Chapter 3), suggested that GTs may actually be excluded from the center of cisternae. In order to reconcile this apparent discrepancy, I used immunoTEM to localize IRX9-GFP and xylan to specific regions of Golgi cisternae during SCW deposition. The results supported the live-cell imaging data, indicating that IRX9-GFP is depleted from the center of cisternae. However, comparing the distribution of IRX9-GFP and xylan supports the original model, in that the biosynthetic enzyme is spatially segregated from the polysaccharide products which accumulate in the swollen margins.

Indeed, the presence of IRX9-GFP in the inner-margin of cisternae led to the development of the concentric circle model (Figure 4.7), which emphasizes the importance of both the *cis*-to-*trans* and center-to-margins distribution of Golgi residents and cargo in Golgi cisternae. This model has important implications for research in both xylan biosynthesis and Golgi function. For example, the formation of a transient xylan biosynthetic complex may facilitate both xylan synthesis in the inner margin, and maintenance of the position of these proteins in the Golgi via retrograde transport from more peripheral areas of the cisternae.

6.2 Outstanding questions and future directions

The results described above open up a number of promising opportunities for future research to further improve our understanding of both xylan biosynthesis and the mechanisms facilitating Golgi processing.

6.2.1 Continuing dissection of xylan biosynthesis in the Golgi

IRX9 is just one of dozens of proteins known to contribute to xylan biosynthesis (Figure 1.2). The procedure I used to map IRX9-GFP can be readily adapted to map other proteins contributing to xylan biosynthesis, and the distribution of IRX9-GFP characterized in this work can provide an important reference point for comparison. High on a list of candidates are IRX10 and IRX14, which have been hypothesized to form a xylan biosynthetic complex with IRX9 (Rennie and Scheller, 2014). As such we would predict that these proteins will have an identical distribution in the Golgi to IRX9. The UDP-Xylose Transporters (UXTs) that provide the substrate for backbone synthesis, may also associate with a xylan biosynthetic complex to improve efficiency (Zhao et al., 2018), making localization of these proteins another priority. Also of interest are the proteins implicated in the synthesis of the reducing end oligosaccharide (REO), as mapping their distribution in the Golgi could help clarify if the REO is a primer of xylan biosynthesis, in which case it should appear in the Golgi prior to IRX9, or a terminator, in which case it may appear in more-*trans* cisternae (York and O'Neill, 2008). A wide variety of anti-xylan antibodies are also available from the Complex Carbohydrate Research Center (Pattathil et al., 2010), any of which could be tested for immunoTEM mapping of the distribution of a variety of xylan epitopes. Indeed, by combining additional immunoTEM mapping of both resident proteins and cargo, we could fully resolve the location in the Golgi of each step of xylan biosynthesis, with the presence of overlapping distributions indicating the potential for interaction between the proteins and epitopes involved in each step.

Many of the recent advances in our understanding of the cell biology of xylan synthesis have focused on primary cell wall synthesis of xylans in species like asparagus and wheat (Zeng et al., 2010; Song et al., 2015; Jiang et al., 2016; Zeng et al., 2016). While these studies have led to interesting hypotheses about the formation and function of xylan biosynthetic complexes, it is unclear to what extent these results can be extrapolated to SCW synthesis. However, this thesis,

and other work (Schuetz et al., 2014; Watanabe et al., 2015; Li et al., 2016; Vukašinović et al., 2017; Chou et al., 2018; Watanabe et al., 2018), have demonstrated how the VND7 induction system can be leveraged to study SCW synthesis *in planta* in ways that were not previously feasible. For example, GFP-tagged versions of Arabidopsis IRX9, IRX10 and IRX14 could be introduced combinatorially into the *irx9*, *irx10irx10L* and *irx14irx14L* mutant backgrounds (Brown et al., 2009; Wu et al., 2009; Keppler and Showalter, 2010; Lee et al., 2010; Wu et al., 2010), to test if the fluorescently-tagged proteins become trapped in the ER in the absence of their putative partners, as was suggested when the asparagus and wheat homologs were transiently expressed in tobacco (Jiang et al., 2016; Zeng et al., 2016). Furthermore, experiments isolating partially purified arabinoxylan biosynthetic complexes in wheat (Zeng et al., 2010; Jiang et al., 2016) and asparagus (Zeng et al., 2016), could be replicated in the VND7 system to isolate and characterize a SCW xylan biosynthetic complex. If the results concerning PCW xylan synthesis can be replicated for SCW synthesis, it would suggest that there are basic principles governing xylan synthesis regardless of species or cell type.

6.2.2 Further exploration of the concentric circle model of the Golgi

The additional Golgi mapping described above would also serve to expand upon the concentric circle model of Golgi organization outlined in Chapter 4. Specifically, to test if other xylan biosynthetic proteins and xylan epitopes are similarly arranged in concentric circles in the Golgi. The distribution of other Golgi-synthesized polysaccharides and their biosynthetic enzymes should also be investigated, to help determine if the concentric circle model is a ubiquitous feature of plant Golgi organization. One model system that is likely amenable to this investigation is pectin production in the Arabidopsis seed coat, as the enzymes involved in pectin production are fairly well characterized, and these cells produce very large amounts of pectin-rich mucilage during their development (Arsovski et al., 2010; Anderson, 2016).

Furthermore, having ascertained the spatial distribution of IRX9-GFP and xylan in this work, the mechanisms establishing and maintaining this spatial organization should be investigated. One experiment that could shed light on this is mapping the distribution of the COPI coat protein, which is important for intra-Golgi transport (Donohoe et al., 2007). If IRX9-GFP is able to recycle from the inner-margin of cisternae, we can hypothesize that COPI will

also localize to this region. Teasing apart the role of COPI in establishing this gradient may also be facilitated by disrupting COPI function using the drug Brefeldin A and observing how the distribution of biosynthetic proteins and polysaccharides changes (Driouich et al., 1993; Nebenführ et al., 2002).

Another unresolved question is why IRX9-GFP is excluded from cisternal centers in *trans*-cisternae. One possibility is that the close apposition of the membrane on either side of the Golgi lumen physically squeezes Golgi resident proteins closer to the periphery of the cisternae. While the cause of the compression of cisternal centers has not been fully elucidated, it is likely facilitated by establishing a proton gradient across the Golgi membrane via proton pumps (Staehelin et al., 1990; Dettmer et al., 2006). Indeed, drugs that disrupt this gradient by making the membranes leaky (e.g. monensin), or interfering with the proton pumps (e.g. concanamycin A) result in severe disruptions in Golgi structure, including cisternal swelling (Zhang et al., 1993; Robinson et al., 2004; Dettmer et al., 2006). If IRX9-GFP is excluded from the cisternal centers by the physical limitations of cisternal structure, we can hypothesize that treatment with these drugs should allow IRX9-GFP to localize in more central cisternal regions.

6.2.3 Exploration of the *irx9* Golgi phenotype

One of the most exciting results coming out of this work, was the unusual increase in fenestration and tubules in *irx9* Golgi. Future experiments will be required to clarify if this phenotype is the result of the loss of xylan, IRX9 or both. This can be achieved by examining Golgi structure when the substrate of xylan biosynthesis is not available, as in mutants of the cytosolic UDP-Xylose Synthases (UXSs; Kuang et al., 2016; Zhong et al., 2017). In these mutants, xylan abundance should be drastically reduced without removing any Golgi resident proteins, allowing dissection of the effect of removing residents vs cargo on Golgi morphology.

It is also unclear if the *irx9* mutant phenotype is unique, or if the Golgi in other xylan biosynthetic mutants, like *irx10irx10L* or *irx14irx14L*, are similarly disrupted (Brown et al., 2009; Wu et al., 2009; Keppler and Showalter, 2010; Lee et al., 2010; Wu et al., 2010). This could be tested by characterizing Golgi structure in these other xylan biosynthetic mutants. The *irx9* Golgi phenotype may also not be unique to xylan biosynthesis, as Golgi structure has not been a focus of studies of the GT mutants affecting pectin or xyloglucan biosynthesis. Again,

pectin biosynthesis in the Arabidopsis seed epidermis would be a good model system to investigate this further.

The prevalence of fenestration and tubulation in *irx9* is also important because the function of cisternal fenestrations has been largely speculative, and Golgi tubulation has not been a focus in plant biology research. The *irx9* Golgi could be an important model system to investigate the composition and function of these structures, for example, by testing for COPI localization at Golgi tubules using anti-COPI antibodies. COPI has been found to be involved in formation of Golgi tubules in mammalian cells (Yang et al., 2011; Park et al., 2015), so they may serve a similar function in plants. Additionally, TEM tomography could be employed to examine where *irx9* Golgi tubules might connect to. This is especially interesting because the Golgi tubules in mammalian cells form inter-cisternal or inter-Golgi connections transporting residents and/or cargo (Marsh et al., 2004; Mogelsvang et al., 2004; Polishchuk and Mironov, 2004), but these have never been reported in plants. Further characterization of *irx9* Golgi is also of interest, to see how other aspects of Golgi functions continue despite disruption in Golgi structure, including CESA trafficking and glycoprotein processing of monolignol oxidative enzymes. One experiment of interest would be to examine how the distribution of glycoprotein processing enzymes like MANI, and protein cargo like CESAs, change in the *irx9* mutant. These distributions may provide clues about the mechanisms of Golgi organization, and could lead to elaboration of the concentric circle model.

6.3 Example answers help support biology problem-solving

Development of problem-solving skills is a central component of an undergraduate education in biology. However, the most effective means of teaching these skills to students is often unclear. The education literature can provide a great deal of theoretical advice, based on controlled experiments and classroom studies in other disciplines, but their efficacy in a real biology class is often uncertain. In Chapter 5, a variety of instructional practices designed to support student problem-solving were employed in two different undergraduate cell biology courses. This resulted in significant differences in both student problem-solving performance and attitudes. In particular, the provision of example answers with explanatory commentary was found to be an effective teaching method. This result supports a body of literature about the

worked example effect, a consequence of cognitive load theory whereby students learn more when given a completed problem to examine prior to attempting problems on their own (Atkinson et al., 2000; Booth et al., 2015). The students in this study also felt better about problem-solving in these classes, which could have broader implications for student retention in biology and student well-being.

Furthermore, the data in Chapter 5 indicate that the impact of the worked example effect depends on the expertise of the student. More novice students realize greater performance benefits when provided with example answers, while the learning of experts can actually be impeded by too much instructional guidance. Again, this result is predicted by decades of research into the expertise reversal effect, which has been documented in other disciplines (Kalyuga et al., 2012). Together, these data provide important validation that principles of learning which have been identified in vastly different disciplines can provide important insights into best practices for biology education. However, the data also illustrate why these techniques should be adapted and tested for efficacy before they are employed more broadly, as their implementation may have unforeseen challenges or consequences due to the idiosyncrasies of biology courses.

The final conclusion from Chapter 5 was that despite their efficacy in supporting student problem-solving, example answers did not provide adequate feedback to students attempting to solve other practice problems. A lack of answers to the practice problem sets was found to disproportionately disadvantage students already facing challenges in the course. Furthermore, without a way for all students to check their answers, students are less motivated to attempt the practice problems, and less likely to realize they have made a mistake and should seek help when they do attempt a problem. As the practice problems are viewed by both instructors and students as an important component of the course, this in an area in which problem-solving instruction can be improved.

The results of Chapter 5 also highlight many areas worthy of future investigation. In the case of problem sets, it may be worthwhile to provide full answer keys, to finally resolve the question of whether keys harm or help student performance in this class. If performance is negatively affected, alternative mechanisms of providing feedback to students should be explored. It would also be interesting to investigate the effect of student enjoyment and attitudes

in biology courses on student retention in the program and their well-being. While some activities and assignments may not improve performance, they may still be worth implementing if they improve student enjoyment. Additional opportunities for research include investigating when in their degree biology students shift from more novice- to expert-like problem-solving, and how courses on either side of this transition can be adapted to maximize student learning. This could then be extrapolated to identify general best-practices in biology problem-solving education across a curriculum.

References

Anders N, Wilkinson MD, Lovegrove A, Freeman J, Tryfona T, Pellny TK, Weimar T, Mortimer JC, Stott K, Baker JM, et al (2012) Glycosyl transferases in family 61 mediate arabinofuranosyl transfer onto xylan in grasses. Proc Natl Acad Sci USA **109**: 989–993

Anderson CT (2016) We be jammin': an update on pectin biosynthesis, trafficking and dynamics. J Exp Bot **67**: 495–502

Anderson LW, Krathwohl DR, Bloom BS (2001) A taxonomy for learning, teaching, and assessing: A revision of Bloom's taxonomy of educational objectives. Longman, New York, NY

Andreeva A V, Kutuzov MA, Evans DE, Hawes C (1998) The structure and function of the Golgi aparatus: A hundred years of questions. J Exp Bot **49**: 1281–1291

Arsovski AA, Haughn GW, Western TL (2010) Seed coat mucilage cells of *Arabidopsis thaliana* as a model for plant cell wall research. Plant Signal Behav **5**: 796–801

Atkinson RK, Derry SJ, Renkl A, Wortham D (2000) Learning from examples: Instructional principles from the worked examples research. Rev Educ Res **70**: 181–214

Atkinson RK, Renkl A, Merrill MM (2003) Transitioning from studying examples to solving problems: Effects of self-explanation prompts and fading worked-out steps. J Educ Psychol **95**: 774–783

Atmodjo MA, Hao Z, Mohnen D (2013) Evolving views of pectin biosynthesis. Annu Rev Plant Biol **64**: 747–779

Atmodjo MA, Sakuragi Y, Zhu X, Burrell AJ, Mohanty SS, Atwood JA, Orlando R, Scheller H V, Mohnen D (2011) Galacturonosyltransferase (GAUT)1 and GAUT7 are the core of a plant cell wall pectin biosynthetic homogalacturonan:galacturonosyltransferase complex. Proc Natl Acad Sci USA **108**: 20225–20230

Bar-Peled M, O'Neill MA (2011) Plant nucleotide sugar formation, interconversion, and salvage by sugar recycling. Annu Rev Plant Biol **62**: 127–155

Barnett JR, Bonham VA (2004) Cellulose microfibril angle in the cell wall of wood fibres. Biol Rev Camb Philos Soc **79**: 461–472

Baviskar SN, Todd Hartle R, Whitney T, Hartle RT, Whitney T (2009) Essential criteria to characterize constructivist teaching: Derived from a review of the literature and applied to five constructivist-teaching method articles. Int J Sci Educ **31**: 541–550

Becker B, Bolinger B, Melkonian M (1995) Anterograde transport of algal scales through the Golgi complex is not mediated by vesicles. Trends Cell Biol **5**: 305–307

Becker B, Melkonian M (1996) The secretory pathway of protists: spatial and functional organization and evolution. Microbiol Rev **60**: 697–721

Bereiter-Hahn J (1990) Behavior of mitochondria in the living cell. Int. Rev. Cytol. pp 1–63

Bhave M, Papanikou E, Iyer P, Pandya K, Jain BK, Ganguly A, Sharma C, Pawar K, Austin J, Day KJ, et al (2014) Golgi enlargement in Arf-depleted yeast cells is due to altered dynamics of cisternal maturation. J Cell Sci **127**: 250–257

Bloom BS, Krathwohl DR, Masia BB (1956) Taxonomy of educational objectives, the classification of educational goals. D. McKay, New York, NY

Boevink P, Oparka K, Cruz SS, Martin B, Betteridge A, Hawes C, Santa Cruz S, Martin B, Betteridge A, Hawes C (1998) Stacks on tracks: the plant Golgi apparatus traffics on an actin/ER network. Plant J **15**: 441–447

Bonawitz ND, Chapple C (2010) The genetics of lignin biosynthesis: Connecting genotype to phenotype. Annu Rev Genet **44**: 337–363

Bonfanti L, Mironov AA, Martínez-Menárguez JA, Martella O, Fusella A, Baldassarre M, Buccione R, Geuze HJ, Luini A, Farmacologiche R, et al (1998) Procollagen traverses the Golgi stack without leaving the lumen of cisternae: evidence for cisternal maturation. Cell **95**: 993–1003

Booth JL, McGinn KM, Young LK, Barbieri C (2015) Simple practice doesn't always make perfect: Evidence from the worked example effect. Policy Insights from Behav Brain Sci **2**: 24–32

Boutté Y, Jonsson K, McFarlane HE, Johnson E, Gendre D, Swarup R, Friml J, Samuels L, Robert S, Bhalerao RP, et al (2013) ECHIDNA-mediated post-Golgi trafficking of auxin carriers for differential cell elongation. Proc Natl Acad Sci USA **110**: 16259–16264

Brandizzi F, Barlowe C (2013) Organization of the ER–Golgi interface for membrane traffic control. Nat Rev Mol Cell Biol **14**: 382–392

Brandizzi F, Irons SL, Johansen J, Kotzer A, Neumann U (2004) GFP is the way to glow: bioimaging of the plant endomembrane system. J Microsc **214**: 138–158

Brandizzi F, Wasteneys GO (2013) Cytoskeleton-dependent endomembrane organization in plant cells: an emerging role for microtubules. Plant J **75**: 339–349

Bromley JR, Busse-Wicher M, Tryfona T, Mortimer JC, Zhang Z, Brown DM, Dupree P (2013) GUX1 and GUX2 glucuronyltransferases decorate distinct domains of glucuronoxylan with different substitution patterns. Plant J **74**: 423–434

Brown DM, Goubet F, Wong VW, Goodacre R, Stephens E, Dupree P, Turner SR (2007) Comparison of five xylan synthesis mutants reveals new insight into the mechanisms of

xylan synthesis. Plant J **52**: 1154–1168

Brown DM, Wightman R, Zhang Z, Gomez LD, Atanassov I, Bukowski J-P, Tryfona T, McQueen-Mason SJ, Dupree P, Turner SR (2011) *Arabidopsis* genes *IRREGULAR XYLEM* (*IRX15*) and *IRX15L* encode DUF579-containing proteins that are essential for normal xylan deposition in the secondary cell wall. Plant J **66**: 401–413

Brown DM, Zeef LAH, Ellis J, Goodacre R, Turner SR (2005) Identification of novel genes in *Arabidopsis* involved in secondary cell wall formation using expression profiling and reverse genetics. Plant Cell **17**: 2281–2295

Brown DM, Zhang Z, Stephens E, Dupree P, Turner SR (2009) Characterization of IRX10 and IRX10-like reveals an essential role in glucuronoxylan biosynthesis in *Arabidopsis*. Plant J **57**: 732–746

Brummell DA, Camirand A, Maclachlan GA (1990) Differential distribution of xyloglucan glycosyl transferases in pea Golgi dictyosomes and secretory vesicles. J Cell Sci **96**: 705–710

Burton RA, Fincher GB (2009) (1,3;1,4)-beta-D-glucans in cell walls of the poaceae, lower plants, and fungi: a tale of two linkages. Mol Plant **2**: 873–882

Busse-Wicher M, Gomes TCF, Tryfona T, Nikolovski N, Stott K, Grantham NJ, Bolam DN, Skaf MS, Dupree P (2014) The pattern of xylan acetylation suggests xylan may interact with cellulose microfibrils as a two-fold helical screw in the secondary plant cell wall of *Arabidopsis thaliana*. Plant J **79**: 492–506

Busse-Wicher M, Li A, Silveira RL, Pereira CS, Tryfona T, Gomes TCF, Skaf MS, Dupree P (2016) Evolution of xylan substitution patterns in gymnosperms and angiosperms: implications for xylan interaction with cellulose. Plant Physiol **171**: 2418–2431

Cai G, Parrotta L, Cresti M (2015) Organelle trafficking, the cytoskeleton, and pollen tube growth. J Integr Plant Biol **57**: 63–78

Cardellini L (2014) Problem solving: How can we help students overcome cognitive difficulties. J Technol Sci Educ **4**: 237–249

Chebli Y, Kroeger J, Geitmann A (2013) Transport logistics in pollen tubes. Mol Plant **6**: 1037–1052

Chevalier L, Bernard S, Ramdani Y, Lamour R, Bardor M, Lerouge P, Follet-Gueye M-L, Driouich A (2010) Subcompartment localization of the side chain xyloglucan-synthesizing enzymes within Golgi stacks of tobacco suspension-cultured cells. Plant J **64**: 977–989

Chou EY, Schuetz M, Hoffmann N, Watanabe Y, Sibout R, Samuels AL (2018) Distribution, mobility, and anchoring of lignin-related oxidative enzymes in *Arabidopsis* secondary cell walls. J Exp Bot **69**: 1849–1859

Clough SJ, Bent AF (1998) Floral dip: a simplified method for Agrobacterium-mediated transformation of *Arabidopsis thaliana*. **16**: 735–743

Cosgrove DJ, Jarvis MC (2012) Comparative structure and biomechanics of plant primary and secondary cell walls. Front Plant Sci **3**: 1–6

Council of Canadian Academies (2015) Some assembly required: STEM skills and Canada's economic productivity. Council of Canadian Academies, Ottawa, ON

Crowe A, Dirks C, Wenderoth MP (2008) Biology in bloom: Implementing Bloom's taxonomy to enhance student learning in biology. CBE Life Sci Educ **7**: 268–381

Crowell EF, Bischoff V, Desprez T, Rolland A, Stierhof Y-D, Schumacher K, Gonneau M, Höfte H, Vernhettes S (2009) Pausing of Golgi bodies on microtubules regulates secretion of cellulose synthase complexes in *Arabidopsis*. Plant Cell **21**: 1141–1154

Crowther DT (1997) The constructivist zone. Electron J Sci Educ **2**: 1–10

Curtis MD, Grossniklaus U (2003) A Gateway cloning vector set for high-throughput functional analysis of genes in planta. Plant Physiol **133**: 462–469

DaSilva LLP, Snapp EL, Denecke J, Lippincott-Schwartz J, Hawes C, Brandizzi F (2004) Endoplasmic reticulum export sites and Golgi bodies behave as single mobile secretory units in plant cells. Plant Cell **16**: 1753–1771

Daxinger L, Hunter B, Sheikh M, Jauvion V, Gasciolli V, Vaucheret H, Matzke M, Furner I (2008) Unexpected silencing effects from T-DNA tags in *Arabidopsis*. Trends Plant Sci **13**: 4–6

Day KJ, Staehelin LA, Glick BS (2013) A three-stage model of Golgi structure and function. Histochem Cell Biol **140**: 239–249

Dettmer J, Hong-Hermesdorf A, Stierhof Y-D, Schumacher K (2006) Vacuolar H+-ATPase activity is required for endocytic and secretory trafficking in *Arabidopsis*. Plant Cell **18**: 715–730

Dixon RA, Srinivasa Reddy MS, Gallego-Giraldo L (2014) Monolignol biosynthesis and its genetic manipulation: The good, the bad, and the ugly. Recent Adv. Polyphen. Res. John Wiley & Sons, Ltd, Chichester, UK, pp 1–38

Dixson DD, Worrell FC (2016) Formative and summative assessment in the classroom. Theory Pract **55**: 153–159

Doering A, Veletsianos G (2007) Multi-scaffolding environment: An analysis of scaffolding and its problem-solving ability. J Educ Comput Res **37**: 107–129

Domozych DS, Ciancia M, Fangel JU, Mikkelsen MD, Ulvskov P, Willats WGT (2012) The

cell walls of green algae: A journey through evolution and diversity. Front Plant Sci **3**: 1–7

Donohoe BS, Kang B-H, Gerl MJ, Gergely ZR, McMichael CM, Bednarek SY, Staehelin LA (2013) Cis-Golgi cisternal assembly and biosynthetic activation occur sequentially in plants and algae. Traffic **5**: 551–567

Donohoe BS, Kang B-H, Staehelin LA (2007) Identification and characterization of COPIa- and COPIb-type vesicle classes associated with plant and algal Golgi. Proc Natl Acad Sci USA **104**: 163–168

Driouich A, Zhang GF, Staehelin LA (1993) Effect of brefeldin A on the structure of the Golgi apparatus and on the synthesis and secretion of proteins and polysaccharides in sycamore maple (*Acer pseudoplatanus*) suspension-cultured cells. Plant Physiol **101**: 1363–1373

Ebert B, Rautengarten C, Guo X, Xiong G, Stonebloom S, Smith-Moritz AM, Herter T, Chan LJG, Adams PD, Petzold CJ, et al (2015) Identification and characterization of a Golgi-localized UDP-xylose transporter family from *Arabidopsis*. Plant Cell **27**: 1218–1227

Ebringerová A (2005) Structural diversity and application potential of hemicelluloses. Macromol Symp **232**: 1–12

Ebringerová A, Heinze T (2000) Xylan and xylan derivatives - biopolymers with valuable properties. Macromol Rapid Commun **21**: 542–556

Engel BD, Schaffer M, Albert S, Asano S, Plitzko JM, Baumeister W (2015) In situ structural analysis of Golgi intracisternal protein arrays. Proc Natl Acad Sci USA **112**: 11264–11269

Felten P (2013) Principles of Good Practice in SoTL. Teach Learn Inq **1**: 121–125

Fonteyn ME, Vettese M, Lancaster DR, Bauer-Wu S (2008) Developing a codebook to guide content analysis of expressive writing transcripts. Appl Nurs Res **21**: 165–168

Frost A, Unger VM, De Camilli P (2009) The BAR domain superfamily: membrane-molding macromolecules. Cell **137**: 191–196

Fukuda M, Bierhuizen MF, Nakayama J (1996) Expression cloning of glycosyltransferases. Glycobiology **6**: 683–689

Gagne R (1980) The conditions of learning, 3rd ed. Hold, Rinehart & Winston, New York, NY

Gao C, Cai Y, Wang Y, Kang B-H, Aniento F, Robinson DG, Jiang L (2014) Retention mechanisms for ER and Golgi membrane proteins. Trends Plant Sci **19**: 508–515

Garcia-Herdugo G, González-Reyes JA, Gracia-Navarro F, Navas P (1988) Growth kinetics of the Golgi apparatus during the cell cycle in onion root meristems. Planta **175**: 305–312

Gil-Pérez D, Guisasola J, Moreno A, Cachapuz A, de Carvalho AMP, Torregrosa JM,

Salinas J, Valdés P, González E, Duch AG, et al (2002) Defending constructivism in science education. Sci Educ **11**: 557–571

Gille S, Pauly M (2012) O-acetylation of plant cell wall polysaccharides. Front Plant Sci **3**: 1–7

Glazer N (2011) Challenges with graph interpretation: A review of the literature. Stud Sci Educ **47**: 183–210

Glick BS, Luini A (2011) Models for Golgi traffic: A critical assessment. Cold Spring Harb Perspect Biol **3**: 1–15

Grantham NJ, Wurman-Rodrich J, Terrett OM, Lyczakowski JJ, Stott K, Iuga D, Simmons TJ, Durand-Tardif M, Brown SP, Dupree R, et al (2017) An even pattern of xylan substitution is critical for interaction with cellulose in plant cell walls. Nat Plants **3**: 859–865

Grefen C, Donald N, Hashimoto K, Kudla J, Schumacher K, Blatt MR (2010) A ubiquitin-10 promoter-based vector set for fluorescent protein tagging facilitates temporal stability and native protein distribution in transient and stable expression studies. Plant J **64**: 355–365

Gutierrez R, Lindeboom JJ, Paredez AR, Emons AMC, Ehrhardt DW (2009) *Arabidopsis* cortical microtubules position cellulose synthase delivery to the plasma membrane and interact with cellulose synthase trafficking compartments. Nat Cell Biol **11**: 797–806

Haigler CH, Brown RM (1986) Transport of rosettes from the Golgi apparatus to the plasma membrane in isolated mesophyll cells of *Zinnia elegans* during differentiation to tracheary elements in suspension culture. Protoplasma **134**: 111–120

Hamilton J (2016) The “training wheels” of academic essay writing: Considered, coordinated and collaborative use of writing models for commencing HE students. J Acad Lang Learn **10**: A48–A56

Hao Z, Avci U, Tan L, Zhu X, Glushka J, Pattathil S, Eberhard S, Sholes T, Rothstein GE, Lukowitz W, et al (2014) Loss of *Arabidopsis* GAUT12/IRX8 causes anther indehiscence and leads to reduced G lignin associated with altered matrix polysaccharide deposition. Front Plant Sci **5**: 1–21

Harper AD, Bar-Peled M (2002) Biosynthesis of UDP-xylose. Cloning and characterization of a novel *Arabidopsis* gene family, *UXS*, encoding soluble and putative membrane-bound UDP-glucuronic acid decarboxylase isoforms. Plant Physiol **130**: 2188–2198

Hartle RT, Baviskar S, Smith R (2012) A field guide to constructivism in the college science classroom: Four essential criteria and a guide to their usage. Bioscene **38**: 31–35

Henderson C, Connolly M, Dolan EL, Finkelstein N, Franklin S, Malcom S, Rasmussen C, Redd K, John KS (2017) Towards the STEM DBER alliance: Why we need a discipline-

based STEM education research community. J Eng Educ **106**: 349–355

Herrero J, Esteban-Carrasco A, Zapata JM, Miguel J (2013) Looking for *Arabidopsis thaliana* peroxidases involved in lignin biosynthesis. Plant Physiol Biochem **67**: 77–86

Hirose S, Komamine A (1989) Changes in ultrastructure of Golgi apparatus during the cell cycle in a synchronous culture of *Catharanthus roseus*. New Phytol **111**: 599–605

Hoskinson AM, Caballero MD, Knight JK (2013) How can we improve problem solving in undergraduate biology? Applying lessons from 30 years of physics education research. CBE Life Sci Educ **12**: 153–161

Hu J, Prinz WA, Rapoport TA (2011) Weaving the web of ER tubules. Cell **147**: 1226–1231

Islam MS, Niwa Y, Takagi S (2009) Light-dependent intracellular positioning of mitochondria in *Arabidopsis thaliana* mesophyll cells. Plant Cell Physiol **50**: 1032–1040

Ito Y, Uemura T, Nakano A (2014) Formation and maintenance of the Golgi apparatus in plant cells. Int Rev Cell Mol Biol **310**: 221–287

Jacob SA, Furgerson SP (2012) Writing interview protocols and conducting interviews : Tips for students new to the field of qualitative research. Qual Rep **17**: 1–10

Jensen JK, Johnson NR, Wilkerson CG (2014) *Arabidopsis thaliana* IRX10 and two related proteins from psyllium and *Physcomitrella patens* are xylan xylosyltransferases. Plant J **80**: 207–215

Jensen KJ, Kim H, Cocuron J-C, Orler R, Ralph J, Wilkerson CG (2011) The DUF579 domain containing proteins IRX15 and IRX15-L affect xylan synthesis in *Arabidopsis*. Plant J **66**: 387–400

Jiang N, Wiemels RE, Soya A, Whitley R, Held M, Faik A (2016) Composition, assembly, and trafficking of a wheat xylan synthase complex. Plant Physiol **170**: 1999–2023

Kalyuga S, Chandler P, Tuovinen J, Sweller J (2001) When problem solving is superior to studying worked examples. J Educ Psychol **93**: 579–588

Kalyuga S, Rikers R, Paas F (2012) Educational implications of expertise reversal effects in learning and performance of complex cognitive and sensorimotor skills. Educ Psychol Rev **24**: 313–337

Kang B-H, Nielsen E, Lai M, Mastronarde D, Andrew L, Preuss ML, Staehelin LA, Mastronarde D, Staehelin LA (2011) Electron tomography of RabA4b- and PI-4Kβ1-labeled trans Golgi network compartments in *Arabidopsis*. Traffic **12**: 313–329

Kang B-H, Staehelin LA (2008) ER-to-Golgi transport by COPII vesicles in *Arabidopsis* involves a ribosome-excluding scaffold that is transferred with the vesicles to the Golgi

matrix. Protoplasma **234**: 51–64

Keppler BD, Showalter AM (2010) IRX14 and IRX14-LIKE, two glycosyl transferases involved in glucuronoxylan biosynthesis and drought tolerance in *Arabidopsis*. Mol Plant **3**: 834–841

Kim JS, Daniel G (2012) Immunolocalization of hemicelluloses in *Arabidopsis thaliana* stem. Part I: temporal and spatial distribution of xylans. Planta **4**: 1275–1288

Kim MH, Cho M-H, Leonard KM (2012) The impact of problem sets on student learning. J Educ Bus **87**: 185–192

Klute MJ, Melançon P, Dacks JB (2011) Evolution and diversity of the Golgi. Cold Spring Harb Perspect Biol **3**: 1–17

Koga D, Ushiki T (2006) Three-dimensional ultrastructure of the Golgi apparatus in different cells: high-resolution scanning electron microscopy of osmium-macerated tissues. Arch Histol Cytol **69**: 357–374

Kuang B, Zhao X, Zhou C, Zeng W, Ren J, Ebert B, Beahan CT, Deng X, Zeng Q, Zhou G, et al (2016) The role of UDP-glucuronic acid decarboxylase (UXS) in xylan biosynthesis in *Arabidopsis*. Mol Plant **9**: 1119–1131

Kubo M, Udagawa M, Nishikubo N, Horiguchi G, Yamaguchi M, Ito J, Mimura T, Fukuda H, Demura T (2005) Transcription switches for protoxylem and metaxylem vessel formation. Genes Dev **19**: 1855–1860

Kulkarni AR, Peña MJ, Avci U, Mazumder K, Urbanowicz BR, Pattathil S, Yin Y, O'Neill MA, Roberts AW, Hahn MG, et al (2012) The ability of land plants to synthesize glucuronoxylans predates the evolution of tracheophytes. Glycobiology **22**: 439–451

Ladinsky MS, Mastronarde DN, McIntosh JR, Howell KE, Staehelin LA (1999) Golgi structure in three dimensions: Functional insights from the normal rat kidney cell. J Cell Biol **144**: 1135–1149

Langhans M, Hawes C, Hillmer S, Hummel E, Robinson DG (2007) Golgi regeneration after brefeldin A treatment in BY-2 cells entails stack enlargement and cisternal growth followed by division. Plant Physiol **145**: 527–538

Lao NT, Long D, Kiang S, Coupland G, Shoue DA, Carpita NC, Kavanagh TA (2003) Mutation of a family 8 glycosyltransferase gene alters cell wall carbohydrate composition and causes a humidity-sensitive semi-sterile dwarf phenotype in *Arabidopsis*. Plant Mol Biol **53**: 647–661

Lavieu GG, Zheng H, Rothman JE (2013) Stapled Golgi cisternae remain in place as cargo passes through the stack. Elife **2**: 1–19

Lawson AE, Clark B, Cramer-Meldrum E, Falconer KA, Sequist JM, Kwon Y-J (2000) Development of scientific reasoning in college biology: Do two levels of general hypothesis-testing skills exist? J Res Sci Teach **37**: 81–101

Lee C, Teng Q, Huang W, Zhong R, Ye Z-H (2010) The *Arabidopsis* family GT43 glycosyltransferases form two functionally nonredundant groups essential for the elongation of glucuronoxylan backbone. Plant Physiol **153**: 526–541

Lee C, Teng Q, Huang W, Zhong R, Ye Z-H (2009) The F8H glycosyltransferase is a functional paralog of FRA8 involved in glucuronoxylan biosynthesis in *Arabidopsis*. Plant Cell Physiol **50**: 812–827

Lee C, Teng Q, Zhong R, Ye Z-H (2011) The four *Arabidopsis* reduced wall acetylation genes are expressed in secondary wall-containing cells and required for the acetylation of xylan. Plant Cell Physiol **52**: 1289–1301

Lee C, Teng Q, Zhong R, Yuan Y, Haghighat M, Ye Z-H (2012) Three *Arabidopsis* DUF579 domain-containing GXM proteins are methyltransferases catalyzing 4-O-methylation of glucuronic acid on xylan. Plant Cell Physiol **53**: 1934–1949

Lee C, Zhong R, Richardson E a, Himmelsbach DS, McPhail BT, Ye Z-H (2007) The *PARVUS* gene is expressed in cells undergoing secondary wall thickening and is essential for glucuronoxylan biosynthesis. Plant Cell Physiol **48**: 1659–1672

Lee HS, Betts S, Anderson JR (2016) Embellishing problem-solving examples with deep structure information facilitates transfer. J Exp Educ **0973**: 1–25

Li S, Bashline L, Zheng Y, Xin X, Huang S, Kong Z, Kim SH, Cosgrove DJ, Gu Y (2016) Cellulose synthase complexes act in a concerted fashion to synthesize highly aggregated cellulose in secondary cell walls of plants. Proc Natl Acad Sci USA **113**: 11348–11353

Litman C, Marple S, Greenleaf C, Charney-Sirott I, Bolz MJ, Richardson LK, Hall AH, George MA, Goldman SR (2017) Text-based argumentation with multiple sources: A descriptive study of opportunity to learn in secondary English language arts, history, and science. J Learn Sci **26**: 79–130

Logan DC, Leaver CJ (2000) Mitochondria-targeted GFP highlights the heterogeneity of mitochondrial shape, size and movement within living plant cells. J Exp Bot **51**: 865–871

Losev E, Reinke CA, Jellen J, Strongin DE, Bevis BJ, Glick BS (2006) Golgi maturation visualized in living yeast. Nature **441**: 1002–1006

Lu L, Lee Y-RJ, Pan R, Maloof JN, Liu B (2005) An internal motor kinesin is associated with the Golgi apparatus and plays a role in trichome morphogenesis in *Arabidopsis*. Mol Biol Cell **16**: 811–823

Luini A (2011) A brief history of the cisternal progression-maturation model. Cell Logist **1**: 6–

MacQueen KM, McLellan E, Kay K, Milstein B (1998) Codebook development for team-based qualitative analysis. Cult Anthropol Methods **10**: 31–36

Manabe Y, Nafisi M, Verhertbruggen Y, Orfila C, Gille S, Rautengarten C, Cherk C, Marcus SE, Somerville S, Pauly M, et al (2011) Loss-of-function mutation of *REDUCED WALL ACETYLATION2* in *Arabidopsis* leads to reduced cell wall acetylation and increased resistance to *Botrytis cinerea*. Plant Physiol **155**: 1068–1078

Manabe Y, Verhertbruggen Y, Gille S, Harholt J, Chong S-L, Pawar PM-A, Mellerowicz EJ, Tenkanen M, Cheng K, Pauly M, et al (2013) REDUCDE WALL ACETYLATION proteins play vital and distinct roles in cell wall O-acetylation in *Arabidopsis*. Plant Physiol **163**: 1107–1117

Manders EMM, Verbeek FJ, Aten JA (1993) Measurement of co-localization of objects in dual-colour confocal images. J Microsc **169**: 375–382

Margulieux LE, Catrambone R (2016) Improving problem solving with subgoal labels in expository text and worked examples. Learn Instr **42**: 58–71

Marsh BJ, Volkmann N, McIntosh JR, Howell KE (2004) Direct continuities between cisternae at different levels of the Golgi complex in glucose-stimulated mouse islet beta cells. Proc Natl Acad Sci USA **101**: 5565–5570

Martinez ME (1998) What is poblem solving? Phi Delta Kappan **79**: 605–609

Matsuura-Tokita K, Takeuchi M, Ichihara A, Mikuriya K, Nakano A (2006) Live imaging of yeast Golgi cisternal maturation. Nature **441**: 1007–1010

Mayer RE (1998) Cognitive, metacognitive, and motivational aspects of problem solving. Instr Sci **26**: 49–63

McCartney L, Marcus SE, Knox JP (2005) Monoclonal antibodies to plant cell wall xylans and arabinoxylans. J Histochem Cytochem **53**: 543–546

McFarlane HE, Döring A, Persson S (2014) The cell biology of cellulose synthesis. Annu Rev Plant Biol **65**: 69–94

McFarlane HE, Shin JJH, Bird DA, Samuels AL (2010) *Arabidopsis* ABCG transporters, which are required for export of diverse cuticular lipids, dimerize in different combinations. Plant Cell **22**: 3066–3075

McFarlane HE, Young RE, Wasteneys GO, Samuels AL (2008) Cortical microtubules mark the mucilage secretion domain of the plasma membrane in *Arabidopsis* seed coat cells. Planta **227**: 1363–1375

McLaren BM, Lim SJ, Gagnon F, Yaron D, Koedinger KR (2006) Studying the effects of personalized language and worked examples in the context of a web-based intelligent tutor. *In* M Ikeda, K Ashley, T-W Chans, eds, Lect. Notes Comput. Sci. Springer-Verlag, Berlin, Heidelberg, pp 318–328

Meents MJ, Watanabe Y, Samuels AL (2018) The cell biology of secondary cell wall biosynthesis. Ann Bot **121**: 1107–1125

Mezirow J (1991) Transformative dimensions of adult learning. Jossey-Bass, San Francisco, CA

Mlotshwa S, Pruss GJ, Gao Z, Mgutshini NL, Li J, Chen X, Bowman LH, Vance V (2010) Transcriptional silencing induced by *Arabidopsis* T-DNA mutants is associated with 35S promoter siRNAs and requires genes involved in siRNA-mediated chromatin silencing. Plant J **64**: 699–704

Mogelsvang S, Gomez-Ospina N, Soderholm J, Glick BS, Staehelin LA (2003) Tomographic evidence for continuous turnover of Golgi cisternae in *Pichia pastoris*. Mol Biol Cell **14**: 2277–2291

Mogelsvang S, Marsh BJ, Mark S, Howell KE (2004) Predicting function from structure : 3D structure studies of the mammalian Golgi complex. Traffic **5**: 338–345

Mollenhauer HH, Morré DJ (1998) The tubular network of the Golgi apparatus. Histochem Cell Biol **109**: 533–543

Moore I, Murphy AS (2009) Validating the location of fluorescent protein fusions in the endomembrane system. Plant Cell **21**: 1632–1636

Moore PJ, Swords KMM, Lynch MA, Staehelin LA (1991) Spatial organization of the assembly pathways of glycoproteins and complex polysaccharides in the Golgi apparatus of plants. J Cell Biol **112**: 589–602

Mortimer JC, Miles GP, Brown DM, Zhang Z, Segura MP, Weimar T, Yu X, Seffen KA, Stephens E, Turner SR, et al (2010) Absence of branches from xylan in *Arabidopsis gux* mutants reveals potential for simplification of lignocellulosic biomass. Proc Natl Acad Sci USA **107**: 17409–17414

Mowbrey K, Dacks JB (2009) Evolution and diversity of the Golgi body. FEBS Lett **583**: 3738–3745

Nakamura N, Wei J-H, Seemann J (2012) Modular organization of the mammalian Golgi apparatus. Curr Opin Cell Biol **24**: 467–474

Nebenführ A, Gallagher LA, Dunahay TG, Frohlick JA, Mazurkiewicz AM, Meehl JB, Staehelin LA (1999) Stop-and-go movements of plant Golgi stacks are mediated by the acto-myosin system. Plant Physiol **121**: 1127–1142

Nebenführ A, Ritzenthaler C, Robinson DG (2002) Brefeldin A: deciphering an enigmatic inhibitor of secretion. Plant Physiol **130**: 1102–1108

Nelson BK, Cai X, Nebenführ A (2007) A multicolored set of in vivo organelle markers for co-localization studies in *Arabidopsis* and other plants. Plant J **51**: 1126–1136

Oikawa A, Lund CH, Sakuragi Y, Scheller HV (2013) Golgi-localized enzyme complexes for plant cell wall biosynthesis. Trends Plant Sci **1**: 49–58

Papanikou E, Glick BS (2014) Golgi compartmentation and identity. Curr Opin Cell Biol **29C**: 74–81

Park S-Y, Yang J-S, Schmider AB, Soberman RJ, Hsu VW (2015) Coordinated regulation of bidirectional COPI transport at the Golgi by CDC42. Nature **521**: 529–532

Pattathil S, Avci U, Baldwin D, Swennes AG, McGill JA, Popper Z, Bootten T, Albert A, Davis RH, Chennareddy C, et al (2010) A comprehensive toolkit of plant cell wall glycan-directed monoclonal antibodies. Plant Physiol **153**: 514–525

Pattathil S, Harper AD, Bar-Peled M (2005) Biosynthesis of UDP-xylose: characterization of membrane-bound AtUxs2. Planta **221**: 538–548

Pauly M, Keegstra K (2016) Biosynthesis of the plant cell wall matrix polysaccharide xyloglucan. Annu Rev Plant Biol **67**: 235–259

Peña MJ, Kulkarni AR, Backe J, Boyd M, O'Neill MA, York WS (2016) Structural diversity of xylans in the cell walls of monocots. Planta **244**: 589–606

Peña MJ, Zhong R, Zhou G-K, Richardson EA, O'Neill MA, Darvill AG, York WS, Ye Z-H (2007) *Arabidopsis irregular xylem 8* and *irregular xylem 9*: Implications for the complexity of glucuronoxylan biosynthesis. Plant Cell **19**: 549–563

Peralta AG, Venkatachalam S, Stone SC, Pattathil S (2017) Xylan epitope profiling: An enhanced approach to study organ development-dependent changes in xylan structure, biosynthesis, and deposition in plant cell walls. Biotechnol Biofuels **10**: 1–13

Peremyslov V V, Prokhnevsky AI, Avisar D, Dolja V V (2008) Two class XI myosins function in organelle trafficking and root hair development in *Arabidopsis*. Plant Physiol **146**: 1109–1116

Persson S, Caffall KH, Freshour G, Hilley MT, Bauer S, Poindexter P, Hahn MG, Mohnen D, Somerville CR (2007) The *Arabidopsis irregular xylem 8* mutant is deficient in glucuronoxylan and homogalacturonan, which are essential for secondary cell wall integrity. Plant Cell **19**: 237–255

Petersen PD, Lau J, Ebert B, Yang F, Verhertbruggen Y, Kim JS, Varanasi P, Suttangkakul A, Auer M, Loqué D, et al (2012) Engineering of plants with improved

properties as biofuels feedstocks by vessel-specific complementation of xylan biosynthesis mutants. Biotechnol Biofuels **5**: 84–102

Pieuchot L, Lai J, Loh RA, Leong FY, Chiam KH, Stajich J, Jedd G (2015) Cellular subcompartments through cytoplasmic streaming. Dev Cell **34**: 410–420

Polishchuk RS, Mironov AA (2004) Structural aspects of Golgi function. Cell Mol Life Sci **61**: 146–158

Popper ZA, Michel G, Hervé C, Domozych DS, Willats WGT, Tuohy MG, Kloareg B, Stengel DB (2011) Evolution and diversity of plant cell walls: from algae to flowering plants. Annu Rev Plant Biol **62**: 567–590

Potter MK, Kustra E (2011) The relationship between scholarly teaching and SoTL: Models, distinctions, and clarifications. Int J Scholarsh Teach Learn **5**: 1–18

Preuss D, Mulholland J, Franzusoff A, Segev N, Botsteint D (1992) Characterization of the *Saccharomyces* Golgi complex through the cell cycle by immunoelectron microscopy. Mol Biol Cell **3**: 789–803

Rabionet SE (2011) How I learned to design and conduct semi-structured Interviews : An ongoing and continuous journey. Qual Rep **16**: 563–567

Rautengarten C, Birdseye D, Pattathil S, McFarlane HE, Saez-Aguayo S, Orellana A, Persson S, Hahn MG, Scheller HV, Heazlewood JL, et al (2017) The elaborate route for UDP-arabinose delivery into the Golgi of plants. Proc Natl Acad Sci USA **114**: 4261–4266

Rautengarten C, Ebert B, Herter T, Petzold CJ, Ishii T, Mukhopadhyay A, Usadel B, Scheller H V (2011) The interconversion of UDP-arabinopyranose and UDP-arabinofuranose is indispensable for plant development in *Arabidopsis*. Plant Cell **23**: 1373–1390

Ren Y, Hansen SF, Ebert B, Lau J, Scheller HV (2014) Site-directed mutagenesis of IRX9, IRX9L and IRX14 proteins involved in xylan biosynthesis: Glycosyltransferase activity is not required for IRX9 function in *Arabidopsis*. PLoS One **9**: 1–9

Renkl A, Atkinson RK (2003) Structuring the transition from example study to problem solving in cognitive skill acquisition: A cognitive load perspective. Educ Psychol **38**: 15–22

Rennie EA, Hansen SF, Baidoo EEK, Hadi MZ, Keasling JD, Scheller H V (2012) Three members of the *Arabidopsis* glycosyltransferase family 8 are xylan glucuronosyltransferases. Plant Physiol **159**: 1408–1417

Rennie EA, Scheller HV (2014) Xylan biosynthesis. Curr Opin Biotechnol **26**: 100–107

Ritzenthaler C, Nebenführ A, Movafeghi A, Stussi-Garaud C, Behnia L, Pimpl P, Staehelin LA, Robinson DG (2002) Re-evaluation of the effects of brefeldin A on plant cells using

tobacco Bright Yellow 2 cells expressing Golgi-targeted green fluorescent protein and COPI antisera. Plant Cell **14**: 237–261

Rizzo R, Parashuraman S, Mirabelli P, Puri C, Lucocq J, Luini A (2013) The dynamics of engineered resident proteins in the mammalian Golgi complex relies on cisternal maturation. J Cell Biol **201**: 1027–1036

Robinson DG, Albrecht S, Moriysu Y (2004) The V-ATPase inhibitors concanamycin A and bafilomycin A lead to Golgi swelling in tobacco BY-2 cells. Protoplasma **224**: 255–260

Rodríguez-Gacio MDC, Iglesias-Fernández R, Carbonero P, Matilla AJ (2012) Softening-up mannan-rich cell walls. J Exp Bot **63**: 3976–3988

Roppolo D, De Rybel B, Tendon VD, Pfister A, Alassimone J, Vermeer JEM, Yamazaki M, Stierhof Y-D, Beeckman T, Geldner N (2011) A novel protein family mediates Casparian strip formation in the endodermis. Nature **473**: 380–383

Rosquete MR, Davis DJ, Drakakaki G (2018) The plant trans-Golgi network: Not just a matter of distinction. Plant Physiol **176**: 187–198

Saez-Aguayo S, Rautengarten C, Temple H, Sanhueza D, Ejsmentewicz T, Sandoval-Ibañez O, Doñas D, Parra-Rojas JP, Ebert B, Lehner A, et al (2017) UUAT1 is a Golgi-localized UDP-uronic acid transporter that modulates the polysaccharide composition of *Arabidopsis* seed mucilage. Plant Cell **29**: 129–143

Saldana J (2009) The coding manual for qualitative researchers. SAGE Publications, Inc., Thousand Oaks, CA

Samuels AL, Giddings TH, Staehelin LA (1995) Cytokinesis in tobacco BY-2 and root tip cells: A new model of cell plate formation in higher plants. J Cell Biol **130**: 1345–1357

Samuels AL, Rensing KH, Douglas CJ, Mansfield SD, Dharmawardhana DP, Ellis BE (2002) Cellular machinery of wood production: differentiation of secondary xylem in *Pinus contorta* var. latifolia. Planta **216**: 72–82

Sauer M, Delgadillo MO, Zouhar J, Reynolds GD, Pennington JG, Jiang L, Liljegren SJ, Stierhof Y-D, De Jaeger G, Otegui MS, et al (2013) MTV1 and MTV4 encode plant-specific ENTH and ARF GAP proteins that mediate clathrin-dependent trafficking of vacuolar cargo from the trans-Golgi network. Plant Cell **25**: 2217–2235

Scheller HV, Ulvskov P (2010) Hemicelluloses. Annu Rev Plant Biol **61**: 263–289

Schiller M, Massalski C, Kurth T, Steinebrunner I (2012) The *Arabidopsis* apyrase AtAPY1 is localized in the Golgi instead of the extracellular space. BMC Plant Biol **12**: 1–16

Schmidt D, Schuhmacher F, Geissner A, Seeberger PH, Pfrengle F (2015) Automated synthesis of arabinoxylan-oligosaccharides enables characterization of antibodies that

recognize plant cell wall glycans. Chem Eur J **21**: 5709–5713

Schneider R, Tang L, Lampugnani ER, Barkwill S, Lathe R, Zhang Y, McFarlane HE, Pesquet E, Niittyla T, Mansfield SD, et al (2017) Two complementary mechanisms underpin cell wall patterning during xylem vessel development. Plant Cell **29**: 2433–2449

Schoberer J, Strasser R (2011) Sub-compartmental organization of Golgi-resident N-glycan processing enzymes in plants. Mol Plant **4**: 220–228

Schuetz M, Benske A, Smith RA, Watanabe Y, Tobimatsu Y, Ralph J, Demura T, Ellis B, Samuels AL (2014) Laccases direct lignification in the discrete secondary cell wall domains of protoxylem. Plant Physiol **166**: 798–807

Seguí-Simarro JM, Staehelin LA (2006) Cell cycle-dependent changes in Golgi stacks, vacuoles, clathrin-coated vesicles and multivesicular bodies in meristematic cells of *Arabidopsis thaliana*: A quantitative and spatial analysis. Planta **223**: 223–236

Shen J, Zeng Y, Zhuang X, Sun L, Yao X, Pimpl P, Jiang L (2013) Organelle pH in the *Arabidopsis* endomembrane system. Mol Plant **6**: 1419–1437

Sherrier DJ, Vandenbosch KA (1994) Secretion of cell-wall polysaccharides in *Vicia* root hairs. Plant J **5**: 185–195

Simmons TJ, Mortimer JC, Bernardinelli OD, Pöppler A-CC, Brown SP, DeAzevedo ER, Dupree R, Dupree P, Scheller H V., Ulvskov P, et al (2016) Folding of xylan onto cellulose fibrils in plant cell walls revealed by solid-state NMR. Nat Commun **7**: 1–9

Simon RA, Aulls MW, Dedic H, Hubbard K, Hall NC (2015) Exploring student persistence in STEM programs: A motivational model. Can J Educ **1**: 1–27

Singer SR, Nielsen NR, Schweingruber HA (2012) Discipline-based education research. National Academies Press, Washington, DC

Sithole A, Chiyaka ET, McCarthy P, Mupinga DM, Bucklein BK, Kibirige J (2017) Student attraction, persistence and retention in STEM programs: Successes and continuing challenges. High Educ Stud **7**: 46–59

Slemp GR (2017) University settings: A new frontier for positive education. Futur. Dir. Well-Being

Song L, Zeng W, Wu A, Picard K, Lampugnani ER, Cheetamun R, Beahan C, Cassin A, Lonsdale A, Doblin MS, et al (2015) *Asparagus* spears as a model to study heteroxylan biosynthesis during secondary wall development. PLoS One **10**: 1–22

Staehelin LA, Giddings TH, Kiss JZ, Sack FD (1990) Macromolecular differentiation of Golgi stacks in root tips of *Arabidopsis* and *Nicotiana* seedlings as visualized in high pressure frozen and freeze-substituted samples. Protoplasma **157**: 75–91

Staehelin LA, Kang B-H (2008) Nanoscale architecture of endoplasmic reticulum export sites and of Golgi membranes as determined by electron tomography. Plant Physiol **147**: 1454–1468

Stanton A, Zandvliet D, Dhaliwal R, Black T (2016) Understanding students' experiences of well-being in learning environments. High Educ Stud **6**: 90–99

Stierhof Y-D, El Kasmi F (2010) Strategies to improve the antigenicity, ultrastructure preservation and visibility of trafficking compartments in *Arabidopsis* tissue. Eur J Cell Biol **89**: 285–297

Strand A, Hurry V, Henkes S, Huner N, Gustafsson P, Gardeström P, Stitt M (1999) Acclimation of *Arabidopsis* leaves developing at low temperatures. Increasing cytoplasmic volume accompanies increased activities of enzymes in the Calvin cycle and in the sucrose-biosynthesis pathway. Plant Physiol **119**: 1387–1397

Sweller J, Ayres P, Kalyuga S (2011) Cognitive load theory. Springer New York, New York, NY

Talanquer V (2014) DBER and STEM education reform: Are we up to the challenge? J Res Sci Teach **51**: 809–819

Tan L, Eberhard S, Pattathil S, Warder C, Glushka J, Yuan C, Hao Z, Zhu X, Avci U, Miller JS, et al (2013) An *Arabidopsis* cell wall proteoglycan consists of pectin and arabinoxylan covalently linked to an arabinogalactan protein. Plant Cell **25**: 270–287

Tanabashi S, Shoda K, Saito C, Sakamoto T, Kurata T, Uemura T, Nakano A (2018) A missense mutation in the NSF gene causes abnormal Golgi morphology in *Arabidopsis thaliana*. Cell Struct Funct **43**: 41–51

Toyooka K, Goto Y, Asatsuma S, Koizumi M, Mitsui T, Matsuoka K (2009) A mobile secretory vesicle cluster involved in mass transport from the Golgi to the plant cell exterior. Plant Cell **21**: 1212–1229

Toyooka K, Sato M, Kutsuna N, Higaki T, Sawaki F, Wakazaki M, Goto Y, Hasezawa S, Nagata N, Matsuoka K (2014) Wide-range high-resolution transmission electron microscopy reveals morphological and distributional changes of endomembrane compartments during log to stationary transition of growth phase in tobacco BY-2 cells. Plant Cell Physiol **55**: 1544–1555

Turlapati P V, Kim KW, Davin LB, Lewis NG (2011) The laccase multigene family in *Arabidopsis thaliana*: Towards addressing the mystery of their gene function(s). Planta **233**: 439–470

Urbanowicz BR, Peña MJ, Moniz HA, Moremen KW, York WS (2014) Two *Arabidopsis* proteins synthesize acetylated xylan in vitro. Plant J **80**: 197–206

Urbanowicz BR, Peña MJ, Ratnaparkhe S, Avci U, Backe J, Steet HF, Foston M, Li H, O'Neill MA, Ragauskas AJ, et al (2012) 4-O-methylation of glucuronic acid in *Arabidopsis* glucuronoxylan is catalyzed by a domain of unknown function family 579 protein. Proc Natl Acad Sci USA **109**: 14253–14258

Voeltz GK, Prinz WA (2007) Sheets, ribbons and tubules - how organelles get their shape. Nat Rev Mol Cell Biol **8**: 258–264

Vukašinović N, Oda Y, Pejchar P, Synek L, Pečenková T, Rawat A, Sekereš J, Potocký M, Žárský V (2017) Microtubule-dependent targeting of the exocyst complex is necessary for xylem development in *Arabidopsis*. New Phytol **213**: 1052–1067

Vygotsky LS (1978) Mind in society: The development of higher psychological processes. Harvard University Press, Cambridge, MA

Wang P, Chen X, Goldbeck C, Chung E, Kang B-H (2017) A distinct class of vesicles derived from the trans-Golgi mediates secretion of xylogalacturonan in the root border cell. Plant J **38**: 42–49

Watanabe Y, Meents MJ, McDonnell LM, Barkwill S, Sampathkumar A, Cartwright HN, Demura T, Ehrhardt DW, Samuels AL, Mansfield SD (2015) Visualization of cellulose synthases in *Arabidopsis* secondary cell walls. Science (80-) **350**: 198–203

Watanabe Y, Schneider R, Barkwill S, Gonzales-Vigil E, Hill JL, Samuels AL, Persson S, Mansfield SD (2018) Cellulose synthase complexes display distinct dynamic behaviors during xylem transdifferentiation. Proc Natl Acad Sci USA **115**: 1–9

Wei L, Liu B, Li Y (2005) Distribution of a kinesin-related protein on Golgi apparatus of tobacco pollen tubes. Chinese Sci Bull **50**: 2175–2181

Whiting LS (2008) Semi-structured interviews: guidance for novice researchers. Nurs Stand **22**: 35–40

Wightman R, Turner SR (2008) The roles of the cytoskeleton during cellulose deposition at the secondary cell wall. Plant J **54**: 794–805

Wilson K, Devereux L (2014) Scaffolding theory: High challenge, high support in Academic Language and Learning (ALL) contexts. J Acad Lang Learn **8**: 91–100

Wisehart G, Mandell M (2008) Problem solving in biology: A methodology. J Coll Sci Teach **37**: 24–29

Wu A-M, Hörnblad E, Voxeur A, Gerber L, Rihouey C, Lerouge P, Marchant A (2010) Analysis of the *Arabidopsis IRX9/IRX9-L* and *IRX14/IRX14-L* pairs of glycosyltransferase genes reveals critical contributions to biosynthesis of the hemicellulose glucuronoxylan. Plant Physiol **153**: 542–554

Wu A-M, Rihouey C, Seveno M, Hörnblad E, Singh SK, Matsunaga T, Ishii T, Lerouge P, Marchant A (2009) The *Arabidopsis* IRX10 and IRX10-LIKE glycosyltransferases are critical for glucuronoxylan biosynthesis during secondary cell wall formation. Plant J **57**: 718–731

Xiong G, Cheng K, Pauly M (2013) Xylan O-acetylation impacts xylem development and enzymatic recalcitrance as indicated by the *Arabidopsis* mutant *tbl29*. Mol Plant **6**: 1373–1375

Yamaguchi M, Goué N, Igarashi H, Ohtani M, Nakano Y, Mortimer JC, Nishikubo N, Kubo M, Katayama Y, Kakegawa K, et al (2010a) VASCULAR-RELATED NAC-DOMAIN6 and VASCULAR-RELATED NAC-DOMAIN7 effectively induce transdifferentiation into xylem vessel elements under control of an induction system. Plant Physiol **153**: 906–914

Yamaguchi M, Kubo M, Fukuda H, Demura T (2008) VASCULAR-RELATED NAC-DOMAIN7 is involved in the differentiation of all types of xylem vessels in *Arabidopsis* roots and shoots. Plant J **55**: 652–664

Yamaguchi M, Mitsuda N, Ohtani M, Ohme-Takagi M, Kato K, Demura T (2011) VASCULAR-RELATED NAC-DOMAIN7 directly regulates the expression of a broad range of genes for xylem vessel formation. Plant J **66**: 579–590

Yamaguchi M, Ohtani M, Mitsuda N, Kubo M, Ohme-Takagi M, Fukuda H, Demura T (2010b) VND-INTERACTING2, a NAC domain transcription factor, negatively regulates xylem vessel formation in *Arabidopsis*. Plant Cell **22**: 1249–1263

Yang J-S, Valente C, Polishchuk RS, Turacchio G, Layre E, Moody DB, Leslie CC, Gelb MH, Brown WJ, Corda D, et al (2011) COPI acts in both vesicular and tubular transport. Nat Cell Biol **13**: 996–1003

York WS, O'Neill MA (2008) Biochemical control of xylan biosynthesis - which end is up? Curr Opin Plant Biol **11**: 258–265

Young AM, Wendel PJ, Esson JM, Plank KM (2018) Motivational decline and recovery in higher education STEM courses. Int J Sci Educ **40**: 1016–1033

Young RE, McFarlane HE, Hahn MG, Western TL, Haughn GW, Samuels AL (2008) Analysis of the Golgi apparatus in *Arabidopsis* seed coat cells during polarized secretion of pectin-rich mucilage. Plant Cell **20**: 1623–1638

Yu AM (2015) Using worked-out examples of written explanation for writing-to-learn in evolutionary biology. University of Western Ontario

Yuan Y, Teng Q, Zhong R, Ye Z-H (2016a) Roles of *Arabidopsis* TBL34 and TBL35 in xylan acetylation and plant growth. Plant Sci **243**: 120–130

Yuan Y, Teng Q, Zhong R, Ye Z-HH (2013) The *Arabidopsis* DUF231 domain-containing protein ESK1 mediates 2-O- and 3-O-acetylation of xylosyl residues in xylan. Plant Cell Physiol **54**: 1186–1199

Yuan Y, Teng Q, Zhong R, Ye Z (2016b) TBL3 and TBL31, two *Arabidopsis* DUF231 domain proteins, are required for 3-O-monoacetylation of xylan. Plant Cell Physiol **57**: 35–45

Zeng W, Jiang N, Nadella R, Killen TL, Nadella V, Faik A (2010) A glucurono(arabino)xylan synthase complex from wheat contains members of the GT43, GT47, and GT75 families and functions cooperatively. Plant Physiol **154**: 78–97

Zeng W, Lampugnani ER, Picard KL, Song L, Wu AA, Farion IM, Zhao J, Ford K, Doblin MS, Bacic A (2016) *Asparagus* IRX9, IRX10, and IRX14A are components of an active xylan backbone synthase complex that forms in the Golgi apparatus. Plant Physiol **171**: 93–109

Zhang B, Zhang L, Li F, Zhang D, Liu X, Wang H, Xu Z, Chu C, Zhou Y (2017) Control of secondary cell wall patterning involves xylan deacetylation by a GDSL esterase. Nat Plants **3**: 1–9

Zhang GF, Driouich A, Staehelin LA (1993) Effect of monensin on plant Golgi: re-examination of the monensin-induced changes in cisternal architecture and functional activities of the Golgi apparatus of sycamore suspension-cultured cells. J Cell Sci **104 (Pt 3**: 819–831

Zhang GF, Staehelin LA (1992) Functional compartmentation of the Golgi apparatus of plant cells. Plant Physiol **99**: 1070–1083

Zhang Y, Nikolovski N, Sorieul M, Vellosillo T, McFarlane HE, Dupree R, Kesten C, Schneider R, Driemeier C, Lathe R, et al (2016) Golgi-localized STELLO proteins regulate the assembly and trafficking of cellulose synthase complexes in *Arabidopsis*. Nat Commun **7**: 1–14

Zhao X, Liu N, Shang N, Zeng W, Ebert B, Rautengarten C, Zeng Q-Y, Li H, Chen X, Beahan C, et al (2018) Three UDP-xylose transporters participate in xylan biosynthesis by conveying cytosolic UDP-xylose into the Golgi lumen in *Arabidopsis*. J Exp Bot **69**: 1125–1134

Zhong R, Cui D, Ye Z-H (2017) Regiospecific acetylation of xylan is mediated by a group of DUF231-containing O-acetyltransferases. Plant Cell Physiol **58**: 2126–2138

Zhong R, Peña MJ, Zhou G-K, Nairn CJ, Wood-Jones A, Richardson E a, Morrison WH, Darvill AG, York WS, Ye Z-H (2005) *Arabidopsis fragile fiber 8*, which encodes a putative glucuronyltransferase, is essential for normal secondary wall synthesis. Plant Cell **17**: 3390–3408

Zhong R, Teng Q, Haghighat M, Yuan Y, Furey ST, Dasher RL, Ye Z-H (2016) Cytosol-

localized UDP-xylose synthases provide the major source of UDP-xylose for the biosynthesis of xylan and xyloglucan. Plant Cell Physiol **58**: 156–174

Appendices

Appendix A BIOL362 - Example Case Study

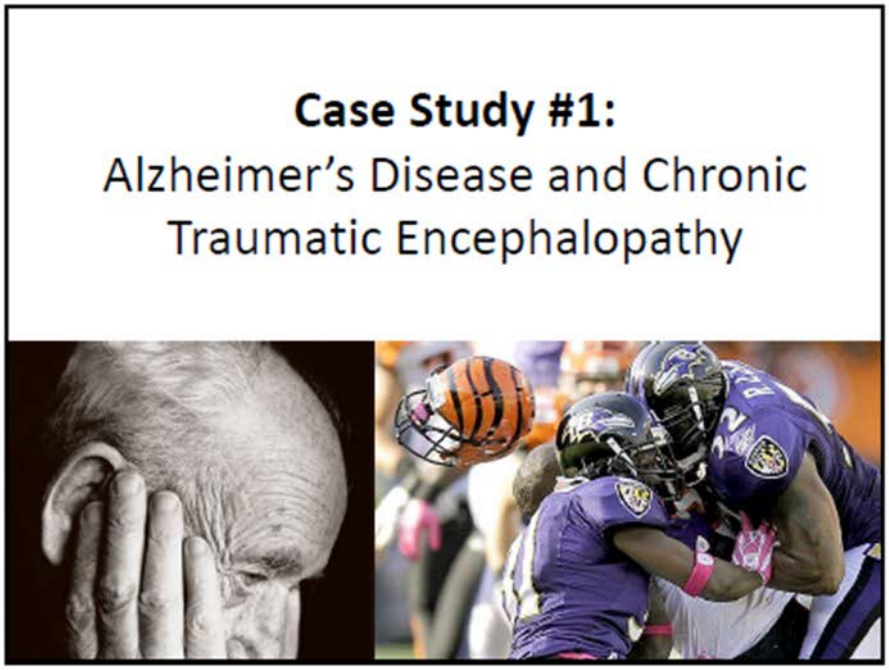

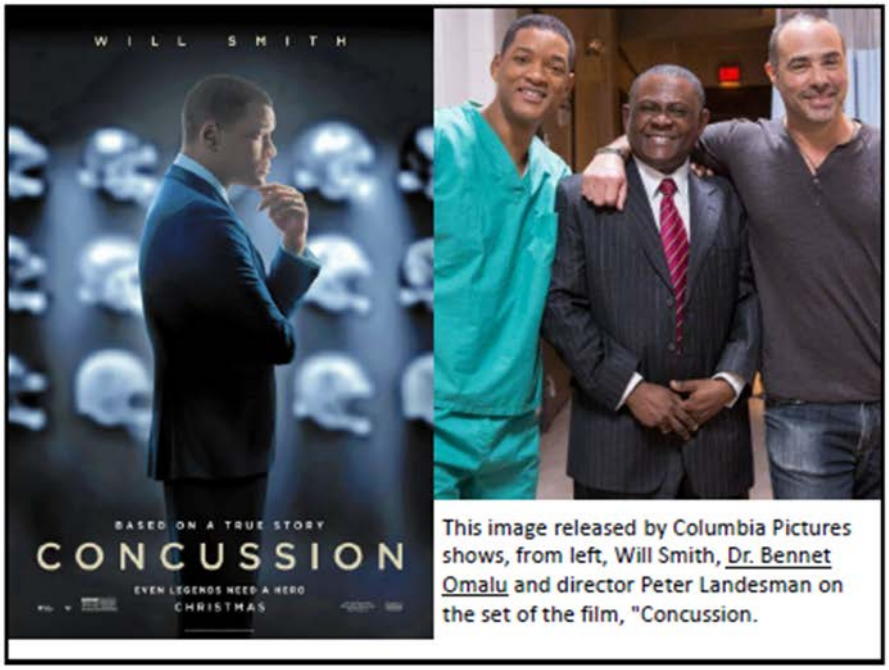

This Case Study will have 2 parts

- **Part 1 – Analysis of the data (~45 minutes)**
  - In this part you should be working to understand the data. It may help to try and write your own hypothesis, before you analyze those of others.
- **Part 2 – Assessment of Previous Student Work**
  - After you have a handle on the data, you will spend the rest of the class analyzing 2 hypotheses & rationales from previous years.
  - You will be attempting to identify strengths & areas of improvement, as well as assigning a grade.

Rules for Case Study #1

1. Work must be done in your groups. One person should be designated the secretary and take notes on your discussion (you may use your computer for this, as long as you are not using the internet).
2. One person should also be elected as facilitator to help make sure that all voices are being heard and that you stay on task.
3. You may only rely on your class notes, class materials, and your collective knowledge. **NO OUTSIDE SOURCES** (I'm looking at you, Wikipedia!). You can also ask questions of the teaching team.
4. At the end you must fill out the End of Task Group Report.

Naming conventions for submission of work

In order to make it easier to find each group's work, please resave the file using the following naming convention:

– GroupName-CaseStudy1.docx (or .doc is fine)

By the end of class today, please submit the file to the Assignment Dropbox in the Case Study #1 folder on Connect.

It MUST be in a Word compatible format or we will not be able to mark it.

Unit 2 Case Study

Alzheimer's Disease (AD) is an incurable disease that most commonly affects the elderly. Chronic Traumatic Encephalopathy (CTE) is a brain disorder that has been shown to affect individuals exposed to repeated head impacts (e.g. boxer, football players).

Both are progressive neurodegenerative disorders where the individual loses brain function over time, resulting in confusion, mood swings, memory loss behavioral changes and debilitating dementia. Eventually, body function can also be lost, leading to death.

Your task is to examine the evidence presented to try and find a connect between it and the neuronal dysfunction of these diseases.

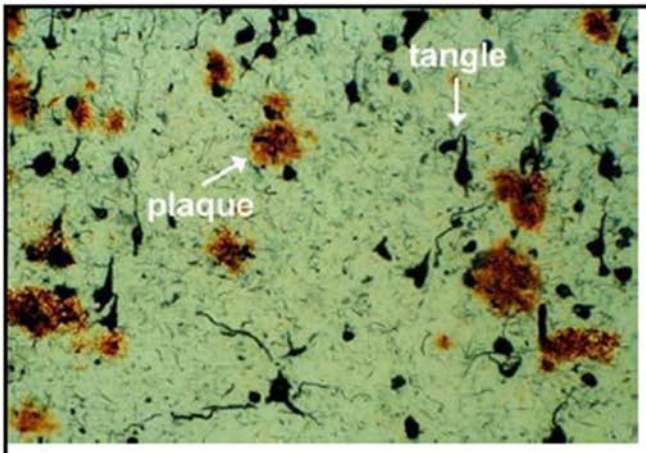

What you know

1. Images of the brain tissue in both diseases show intracellular, proteinaceous 'tangles' in the cytosol, which are composed of the microtubule associated protein, Tau.

Ignore the plaques for today's exercise.

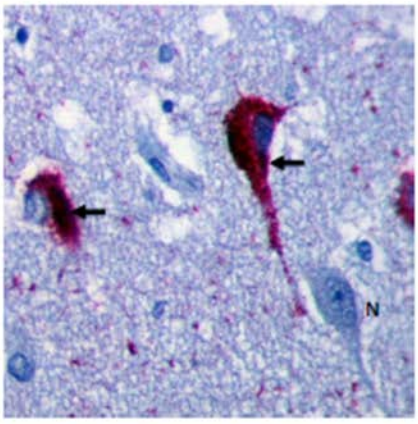

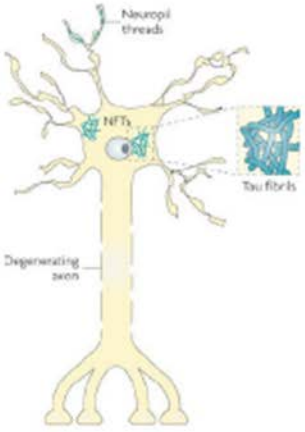

2. Immunohistochemistry for tau protein in the brain of an individual with Alzheimer's shows neurofibrillary tangles (red) visible in some neurons (arrows) but not in others (N).

Cartoon from: Brunden KR, et al. 2009 Nat Rev Drug Discov. Oct;8(10):783-93.

What you know

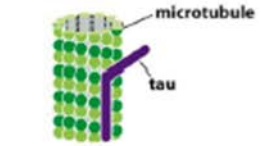

(B)

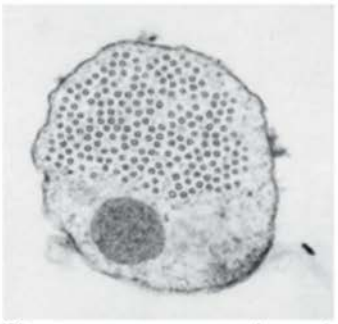

(D)

300 nm

10 μm

3. Figure 16-51 of our textbook tells us that Tau is involved in the formation of the MT network in the axon of neurons

What you know

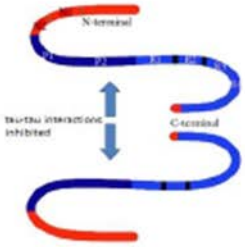

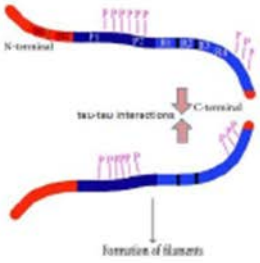

4. Studies have shown that the neuronal tangles of Tau are hyper-phosphorylated and have a different shape, but if they are de-phoshorylated *in vitro*, the protein regains normal shape and function.

Kolarova M, et al. 2012 International Journal of Alzheimer's Disease doi:10.1155/2012/731526

Axons Expressing Wild-type tau (wt)

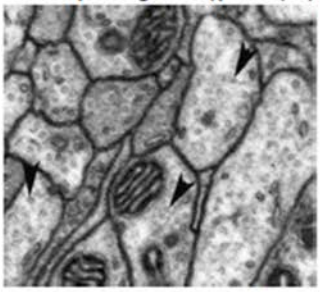

Axons Expressing human phosphorylated tau (htau)

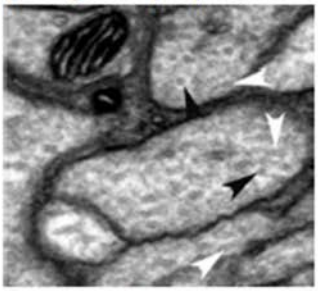

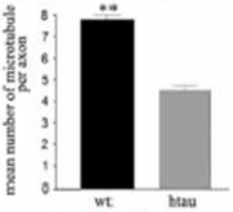

The mean number of correctly aligned microtubles is significantly higher (**) for wt tau-expressing neurons

5. In wild type (wt) tau-expressing neurons the axon profiles show numerous regularly-spaced correctly-aligned microtubules (black arrowheads).

In human phosphorylated tau (htau)-expressing axons the microtubules are dramatically disrupted. There are many fewer correctly-aligned microtubules (black arrowheads) than in the wt control and there is additional evidence of disorganised (wrongly oriented) microtubules (white arrowheads)

Cowan CM, et al. 2010 Acta Neuropathol. Nov;120(5):593-604

Case Study 1 - Central Question:

Given this information, can you explain whether there is a relationship between the microtubule associated protein Tau and the neurodegeneration present in AD and CTE? If so, how does Tau contribute to disease pathology?

Appendix B BIOL362 - Step-By-Step Worksheet

For this Case Study, you are required to come up with a hypothesis that attempts to answer the central question, as well as a short rationale for your hypothesis. To help you with this, we have built the following worksheet for you to use. You may fill out your answers directly in this worksheet and hand it in.

Hypothesis = [Subject] + [claim/interpretation]
Rationale = paragraph (ish) that explains how
the data connects to your hypothesis

Part 1. (10% of total time, 1 pt) Look at the Central Question of your Case Study. Based on the central question:
1A. What do you think the subject of your hypothesis should be?

1B. Based on the Central Question, where should you focus your attention when interpreting the experimental evidence?

Part 2. (50% of total time, 5 pts) Now look at each slide that presents experimental evidence in this case study. For each slide summarize the main conclusion of that experimental evidence, using the same format as your hypothesis (H=[S]+[C]). List each one below.

Part 3. (30% of total time, 3 pts) Look at your summaries of the experimental evidence. Try to find the thread that links them to each other and the Central Question.
3A. Look at Part 1 again to see what the question tells you about the subject of your hypothesis. Do you still agree with your answer there? Explain your answer.

3B. Now its time to write your full hypothesis. Use the subject you decided on in part 3A. Then re-examine Parts 1B and 2 to decide what the rest of your hypothesis should be. Remember that your hypothesis should summarize what the results you described in Part 2 in a way that is related to the Central Question that you described in Part 1A. Your entire hypothesis should be about one sentence long. Write it down here.

Part 4. (10% of total time, 1pt) The summaries that you wrote in Part 2 are your rationale. Copy and paste those points into the area below. Re-examine them to make sure that they are complete and address the various claims of your hypothesis, and connect to the experimental evidence. Make any wording tweaks necessary here and not in Part 2 so that we can see the progression.

Appendix C BIOL362 - Example Answer Worksheet

Instructions

Spend 5 minutes with your group reading and evaluating each hypothesis and rationale.
Some things to think about when marking include:

- Are all pieces of data accounted for?
- Are there logical jumps being made that aren't explained, or don't make sense?
- Is each piece of data correctly identified as being linked by correlation, or causation?
- After you decide on a mark, does it reflect your overall impression of the hypothesis/rationale? If not, think about where this disconnect is happening and readjust.

Example Hypothesis 1

"Phosphorylation of Tau proteins cause defects in microtubule orientation found in the neuronal axons associated with neurodegenerative AD and CTE."

Strengths:

-

Areas for Improvement:

-
-

Are all relevant components incorporated?	(/1)
Are the relationships between components clear and accurate?	(/2)
Is all terminology and language used correctly	(/1)
Hypothesis	**(/4)**

Example Hypothesis 2

"In people with Alzheimer's Disease and Chronic Traumatic Encephalopathy, hyper-phosphorylated tau proteins undergo a shape change, allowing them to interact with each other to form neurofibrillary tangles, and cannot therefore help in the formation of orderly microtubule networks in the axons of some neurons in the brain, impairing neuron function."

Strengths:

-

Areas for Improvement:

-
-

Are all relevant components incorporated?	(/1)
Are the relationships between components clear and accurate?	(/2)
Is all terminology and language used correctly?	(/1)
Hypothesis	**(/4)**

Example Rationale 1

"Under normal circumstances, tau is involved with organizing evenly-spaced bundles of MTs in neuronal axons. Hyperphosphorylation of tau proteins changes the protein's conformation, allowing the proteins to interact with each other and form filaments. The presence of phosphorylated tau proteins results in the presence of poorly-aligned MTs as well as a significant decrease in the number of correctly-aligned MTs than when only wild-type tau is present. Abnormal tangles of tau protein throughout the cell are seen in all AD & CTE brains. Tangles of tau fibrils are definitely present in some, but not all, neurons in AD."

Strengths:

-
-

Areas for Improvements:

-
-
-

Is the data described clearly and completely?	(/2)
Is it made clear how the data supports the hypothesis?	(/2)
Is all terminology and language used correctly?	(/1)
When used, is speculation identified and reasonable?	(/0.5)
Is it well written? (ideas flow naturally, no major typos/grammar problems)	(/0.5)
Rationale	**(/6)**

Example Rationale 2

"The Tau protein forms proteinaceous tangles in both AD and CTE in some neurons. Neurofibrillary tangles in AD are found in neurons that are degenerating neurons. The Tau protein is involved in the formation of parallel arrays that are necessary for the microtubule network in functional axons. Hyper-phosphorylation affects the shape and function of Tau. Phosphorylated Tau affects the correct alignment of microtubules."

Strengths:

-
-

Areas for Improvement:

-
-
-

Is the data described clearly and completely?	(/2)
Is it made clear how the data supports the hypothesis?	(/2)
Is all terminology and language used correctly?	(/1)
When used, is speculation identified and reasonable?	(/0.5)
Is it well written? (ideas flow naturally, no major typos/grammar problems)	(/0.5)
Rationale	**(/6)**

Appendix D BIOL200 - Problem Sets Excerpt

Biology 200 Problem Sets

Table of Contents

Introduction to the Problem Sets **4**

Unit 1: Eukaryotic Cells and Microscopy **7**
Content Review Questions **7**
Practice Problems **9**
Topic 1.1 – Eukaryotic Cells & Organelles 9
Topic 1.2 – Microscopy 11
Unit 2: Biological Membranes **16**
Content Review Questions **16**
Practice Problems **18**
Topic 2.1 – Review of the Features of Biological Membranes 18
Topic 2.2 – The Lipid Bilayer 23
Topic 2.3 – Membrane Proteins 26

Unit 3: Nuclear Structure and Function **30**
Content Review Questions **30**
Topic 3.1 – Nuclear Structure & Protein Import 30
Topic 3.2 – Chromatin and Chromosomes 30
Topic 3.3 – Regulation of Gene Expression 31
Practice Problems **32**
Topic 3.1 – Nuclear Structure & Protein Import 32
Topic 3.2 – Chromatin and Chromosomes 36
Topic 3.3 – Regulation of Gene Expression 39

Unit 4: Endomembranes **44**
Content Review Questions **44**
Practice Problems **47**
Topic 4.1 – Overview of Secretion & Protein Import 47
Topic 4.2 – Vesicle Transport 51
Topic 4.3 – Golgi and Protein Processing 53
Topic 4.4 – Post-Golgi Traffic 56
Topic 4.5 – Endocytosis 60

Unit 5: Mitochondria and Chloroplasts **62**
Content Review Questions **62**
Practice Problems **63**
Topic 5.1 – Introduction & Protein Import 63
Topic 5.2 & 5.3 – Mitochondria and Chloroplasts 67

Unit 6: Cytoskeleton **69**
Content Review Questions **69**
Practice Problems **71**
Topic 6.1 – Introduction & Intermediate Filaments 71
Topic 6.2 – Microtubules 74
Topic 6.3 – Actin Filaments 80

Unit 7: Cell Cycle and Mitosis **84**
Content Review Questions **84**
Practice Problems **85**
Topic 7.1 – Cell Cycle & Checkpoints 85
Topic 7.2 – CDK-Cylin Regulation 90
Topic 7.3 – Mitosis and Cell Division 94

Example Problem Walkthroughs **95**
Introduction to the Problem Walkthroughs **95**
Unit 1: Eukaryotic Cells and Microscopy **96**
Identifying Organelles and Cellular Structures Using Microscopy 96
TUTORIAL: Understanding the Plane of Section in Microscopy Images 98
TUTORIAL: How to Select the Appropriate Type of Microscopy to Answer Different Scientific Questions 98
TUTORIAL: Using Micrographs to Identify the Type of Microscopy and the Organelles Imaged 98
Unit 2: Biological Membranes **99**
TUTORIAL: Essay Outline (Unit 2: Membrane Fluidity) 99
Using Fluorescence Recovery after Photobleaching (FRAP) to Investigate Protein Mobility 99
Relating Protein Secondary Structure to Protein Function 101
TUTORIAL: Determining Protein Topology Using Protease Digestion and SDS-PAGE 103
Determining Protein Topology Using Protease Digestion and SDS-PAGE 103
Unit 3: Nuclear Structure and Function **105**
Identifying the Function of Protein Domains by Fluorescence Microscopy of Protein Fragments 105
TUTORIAL: Using Nuclease Digestion to Study How DNA is Packaged 106
Analyzing Changes in Gene Expression Using Parts of a Transcription Factor 107
Unit 4: Endomembranes **109**
Using Protein Domain Diagrams to Predict Topology and Targeting 109
Using Mutant Analysis to Study How Proteins Move Through the Endomembrane System 111
TUTORIAL: Using Radiolabelling, Differential Centrifugation and Mutant Analysis to Study Golgi Processing 112
Unit 5: Mitochondria and Chloroplasts **113**
TUTORIAL: Essay Outline (Unit 5: Mitochondria and Chloroplasts) 113
Relating Protein Targeting Signals to Protein Function 113
Unit 6: Cytoskeleton **116**
Using Fluorescence Recovery After Photobleaching (FRAP) to Investigate Microtubule Dynamics at Different Stages in the Cell Cycle 116
Investigating the Effect of Tubulin Concentration on Microtubule Dynamics During Mitosis 118
TUTORIAL: Investigating the Effect of Tubulin Concentration on Microtubule Dynamics 119
Unit 7: Cell Cycle and Mitosis **120**
Using Mutant Analysis to Investigate the Effect of Protein Regulation on the Cell Cycle 120
TUTORIAL: Using Temperature Sensitive Mutants and Drug Treatments to Investigate the Cell Cycle . 122
Other Skills **122**
Essay Outline (Unit 7: Cell Cycle) 122
TUTORIAL: Essay Outline (Unit 2: Membrane Fluidity) 125
TUTORIAL: Essay Outline (Unit 5: Mitochondria and Chloroplasts) 125

Index by Key Word **126**

Introduction to the Problem Sets

Welcome to the BIOL200 problem sets! In these pages are contained the keys to your success in BIOL200! This workbook is designed to help guide your studying and to help you practice the skills that will be required for success on the midterm and final exam.

BIOL200 is a 3-credit course, with 3 hours/ week of class time and 1h/ week of tutorial. The most commonly accepted rule of thumb is that for every hour of class time, you should be spending 2 hours outside of class working on the course. That means we're expecting that for every week of class in BIOL200, you should be expecting to spend 6-8 hours outside of class working on the course.

During an average week, 'outside of class' time can be broken up into a few different parts:

1. **The Pre-Readings and Quizzes (~1-2h per week)**
   These quizzes happen on average about once a week, they involved reading material on Connect (based on the pre-reading guides) and then taking a 10-15 question quiz on the material. The goal here is not to learn everything on your own, but rather begin to get some of the basics (i.e. specific jargon, definitions, chemical structures and some of the simpler concepts). If there are things you still don't understand after the pre-reading, that's ok. Simply tell us about it in the last question of the quiz and we'll know to focus on it in class.

2. **Tutorial Preparation (~1h per week)**
   In each week, we will be working through a specific problem from this Problem Set in tutorial, as a way to help you practice your problem-solving skills and prepare for the midterm and final. To prepare for tutorial, we expect you to review the course material for the unit in question, as you will need to know something about cell biology in order to successfully apply your knowledge to the problems. The tutorial problems are identified in the problem set, and you're welcome to take a look at them ahead of time. You will be given time during tutorial to try them on your own and in groups, so it's perfectly ok if you haven't solved the problem (or even attempted it!) before you get to class. But we think you'll get more out of it if you know what's going to be asked of you before you get there.

3. **Personal Study Time (3-5h per week)**
   This is when you work on the course material on your own (or in study groups, including office hours), work on the press release assignment, and practice the problem-solving skills you will need to succeed on the midterm and final exam. If you don't work on this throughout the term, you can assume that the accumulated time is how many hours you're going to need to put in to prepare for the midterm/ final.

This Problem Set is designed to help you structure your personal study time.

What's in the Problem Sets, and how do they help?

The Problem Set starts with a Table of Contents that is clickable in pdf format, so that you can easily find the unit that you want to work on. We've also broken up this problem set into individual units, and posted them on Connect for you, in case you want to work with a smaller document. The complete document can be downloaded in a single file from the Resources Section of Connect.

In each unit, we have 2 different kinds of questions for you, which have an entirely different purpose for your studying:

1. **Content Review Questions**
   - This section is designed to help you review the material. Answers can be found more or less easily in your notes, on Connect, in the textbook or on the Web. While this background content knowledge is needed, and will help you on the exam, these review questions are not considered 'exam-style'.
   - A question's difficulty rating is noted by the 1 (easiest), 2 or 3 (hardest) in brackets beside the question. You should expect to look these up as you go.
   - There are no answer keys to questions in this section. We suggest using these questions as a way to review & discuss the material with your peers, rather than writing out answers for each one. It's ok not to have complete answers for all of these.

2. **Practice Problems**
   - The focus on the exam will be to assess your ability to interpret data, and use it to draw conclusions about cellular function. This is a conceptual task, which requires critical thinking skills in addition to the knowledge of the material. But practice will help you get better at it.
   - Most of these questions come from old exams. Some of them are designed to make you think critically, rather than to practice exam-writing (Some may even show up on future exams…).
   - We will cover many of these questions in class and/or tutorial. We encourage you to practice writing out your answers for these questions, as it will help you improve your clarity in writing for the exam.
   - Note that the problems are roughly divided by topic, but you should expect to use knowledge from other parts of the course as well.

Where to find more questions on a topic?

In addition to the material in each Unit, we've tried to help identify the interconnected nature of these problems by creating an index for you. The questions have several meta tags associated with them, which helps to identify specific similarities (i.e. common technique or course topic). For example → (tags: #TEM)

If you want to find more questions on a topic or technique use the tags, and/ or look the tag/ topic up in the index. This can help you find questions that link content from different units, similar to what you would see on the exam. Unfortunately, this index is not clickable in the pdf, so you'll have to go to those pages manually.

Where to find more help?

If you are having problems with a question, check out the related Problem Walkthroughs at the end of the booklet. They are designed not only to show you what the answer to the question is, but to help you understand why its correct, and to help you better understand what a 'good' answer contains. If you need additional help you can post on the discussion board or come to talk to us in office hours.

What to do if you find an error?

Like all of the documents in this course, they are written by people. Sometimes mistakes happen. If you think you've spotted an error, please don't hesitate to let us know. The most efficient way is to contact the course coordinator directly as she is the curator of the common course material. You may also contact your instructor if you prefer, who will take note of the information and pass it on to the course coordinator if necessary.
We do everything that we can to avoid errors, and we rely on you to help us find the ones that we've missed. Feedback on course material helps it to evolve and improve… Future BIOL200 students appreciate your help!

Unit 1: Eukaryotic Cells and Microscopy
Topic 1.2 – Microscopy

Problem 1.2.1 (Walkthrough Available)
(tags: #TEM, #SEM, #brightfield microscopy, #fluorescence microscopy, #organelle identification, #identify microscopy type, #plants, #animals)

Classify each of the images shown into the tables below, based on the type of microscopy and the organelles that you can SEE. Be aware that each image may fit into more than one category and not all categories may be present. Marks will be deducted for wrong answers.

Image 1:

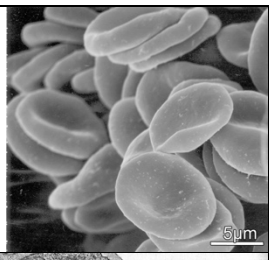

Image 2:

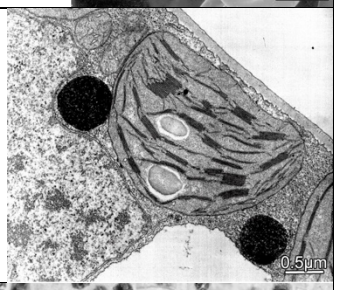

Image 3:

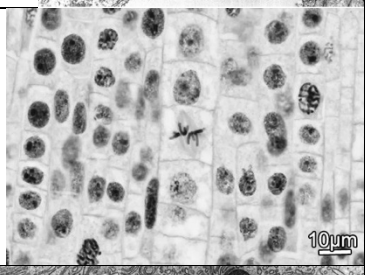

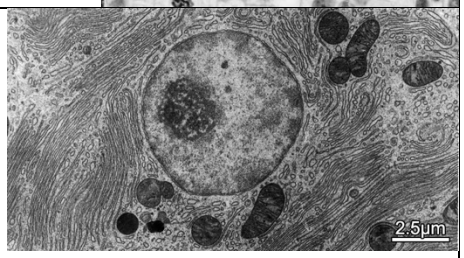

Image 4:

Type of microscopy:	
Brightfield light microscopy	
Fluorescence microscopy	
Transmission electron microscopy	
Scanning electron microscopy	

Organelles:	
Plasma membrane	
Nucleus	
Nucleolus	
Endoplasmic reticulum	
Mitochondria	
Cytosol	
Chloroplast	
Heterochromatin	
Mitotic Chromosome	
Flagella	

Unit 3: Nuclear Structure and Function
Topic 3.1 Nuclear Structure and Protein Import

Problem 3.1.6 (Walkthrough Available)
(tags: #fluorescence microscopy, #NLS, #mutant analysis, #animals)
Wodrich et al. (2006) looked at the location of nuclear localization signals (NLS) within Adenovirus protein pVII. This is one of their experiments:

- Full length and deletion mutants of pVII were fused to GFP (green fluorescent protein) and injected into the cytoplasm of cells.
- Injected cells were viewed using fluorescence microscopy.

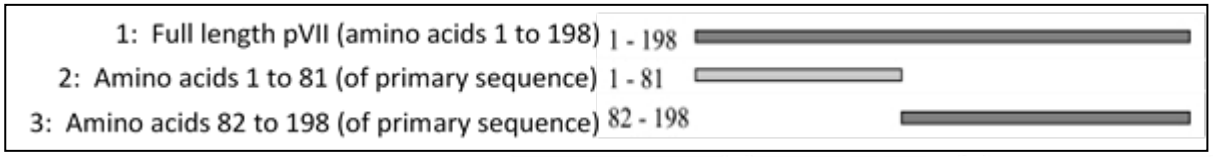

a) Identify the cellular location of the fluorescence in each panel (1, 2 & 3)

b) What can you conclude about the location of the NLS in pVII? Explain.

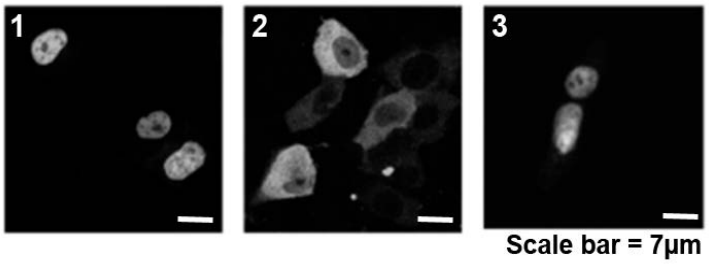

Unit 6: Cytoskeleton
Topic 6.2 – Microtubules

Problem 6.2.1 (Walkthrough Available)
(tags: #microtubules, #FRAP, #cell cycle)
One approach to characterize microtubule assembly and disassembly involves injecting fluorescently-labeled tubulin into cells. The fluorescent tubulin is then incorporated into microtubules, thereby allowing visualization of the microtubules inside living cells. When these cells are used in FRAP (fluorescence-recovery-after photobleaching) experiments, the following results are found for cells that are in interphase and cells that are in metaphase.

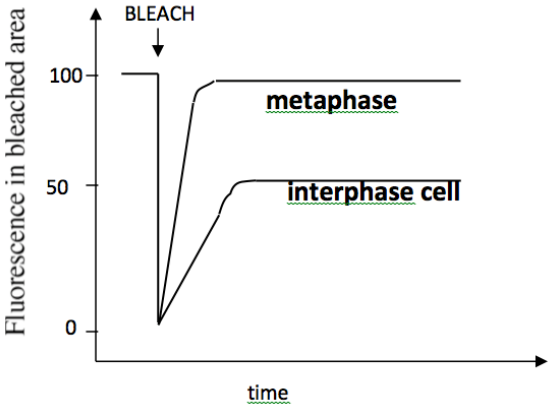

a) When doing FRAP in cells with labeled microtubules, why does the fluorescence intensity in the bleached area recover (i.e. it does not stay at zero)?

b) What can you conclude about the relative stability of the microtubules in metaphase cells as compared to the microtubules in cells in interphase? Interpret these results in terms of the function of microtubules in metaphase.

Appendix E BIOL200 - Problem Walkthroughs Excerpt

Unit 1: Eukaryotic Cells and Microscopy

Identifying Organelles and Cellular Structures Using Microscopy
Problem 1.2.1
(tags: #TEM, #SEM, #brightfield microscopy, #fluorescence microscopy, #organelle identification, #identify microscopy type, #plants, #animals)

Example Answer: Orange Text
Instructor Comments: Blue Text

Classify each of the images shown into the table below, based on the type of microscopy and the organelles that you can SEE. Be aware that each image may fit into more than one category and not all categories may be present. Marks will be deducted for wrong answers.

IMAGE 1

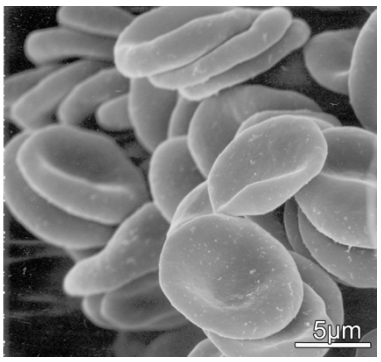

Type of Microscopy: Scanning Electron Microscopy
Explanation: In this image we are seeing the surface of many 3D structures, suggesting SEM.
Organelles: Plasma Membrane
Explanation: Eukaryotic cells usually range from 5-50 µm. The scale bar suggests that these structures are ~15 µm in diameter, so they are much too big to be organelles, and are more likely to be cells. This would mean we are looking at the 3D structure of the outer leaflet of the plasma membrane of these cells.

IMAGE 2

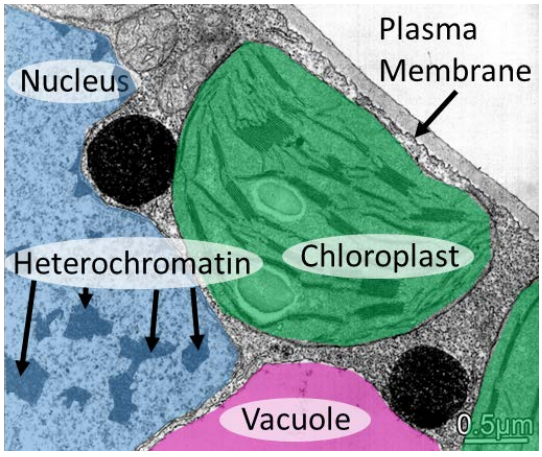

Type of Microscopy: Transmission Electron Microscopy
Explanation: The scale bar tells you the magnification is quite large, and the resolution of the image is also very good. It also looks like you are seeing cross-sectioned material. All this suggests this is TEM.
Organelles:
Chloroplasts (**easiest**: Chloroplasts are around 4µm long. We can also see the characteristic thylakoid membranes stacked in grana inside.)
Cytosol (**easiest**: Surrounding the chloroplast and other organelles)
Nucleus, Heterochromatin (**harder**: On the left side of this image you can see a structure with the double membrane characteristic of the nucleus. Note the difference in texture compared to the cytosol. We can only see part of this structure, but it is of a similar size to the cell nucleus which usually around 10µm in diameter. There are also darker and lighter regions inside, as we would expect for a nucleus containing heterchromatin and euchromatin.)

Plasma Membrane (**hardest**: the light area at the top right is probably the outside of the cell, making the membrane in between the plasma membrane. You might also notice a grey layer outside the plasma membrane, which is the plant cell wall.)
Vacuole (**hardest**: the light areas at the bottom of the image is likely the large plant vacuole)
Other Structures (The two dark circles, and the oval structures above the chloroplast, are hard to identify even for experts. Some of them may be mitochondria, but more information about the samples, and more experiments, may be required to say for sure.)

IMAGE 3
Type of Microscopy: Brightfield Light Microscopy
Explanation: The scale bar indicates a low-magnification image, and the lack of resolution suggests this is brightfield microscopy, rather than TEM.

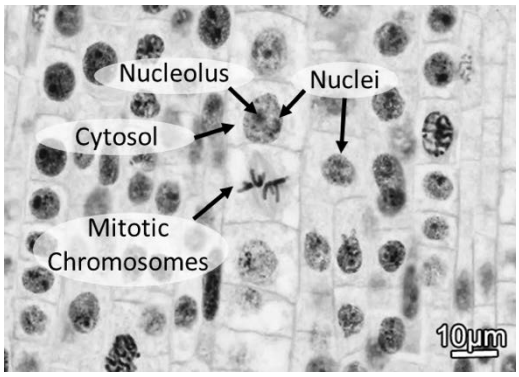

Organelles:
Explanation: The scale bar suggests the repeating structures arranged in columns are quite large (10-15µm across), and therefore probably cells (see explanation for image 1).
Nucleus, Nucleolus (The dark circles inside each cell are around 10µm across, which is the right size for a nucleus. They also contain an even darker spot, which is the nucleolus)
Mitotic Chromosome (Some of the cells are undergoing cell division, as we can see chromosomes at different stages of mitosis. As we would expect, the circular nuclei are not present in these dividing cells.)
Cytosol (There is not enough resolution to see the smaller organelles that would be present in these cells, however you know that the cytosol is filling these cells and surrounding the nucleus.)

IMAGE 4
Type of Microscopy: Transmission Electron Microscopy
Explanation: Similar to image 2, you are looking at an image at very high magnification and very high resolution, and it looks like a cross-section of a cell, suggesting TEM.

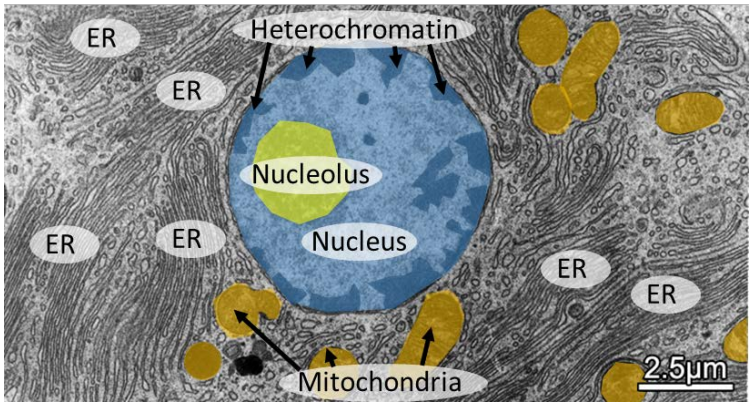

Organelles:
Nucleus, Nucleolus, Heterochromatin (The circular structure in the center is around 10µm in diameter and is surrounded by a double membrane, just as we would expect the nucleus to be. We can also see the darker nucleolus inside the nucleus. There are other patches of dark material, especially around the margins of the nucleus, where we expect heterochromatin to be more abundant.)
Mitochondria (TEM mitochondria tend to be darker than many organelles, like the dark oval structures seen here. These structures are also the right size, as mitochondria are usually 1-2µm

long, and 0.5µm in diameter. We can also see the inner cristae membranes. The variation in shape of these mitochondria is due to their different orientations relative to the plane of section.)
Endoplasmic Reticulum (This cell contains many layers of long, thin threads of membrane with very lightly stained contents. This is typical of ER.)
Cytosol (The cytosol surrounds all of these other organelles.)

Unit 3: Nuclear Structure and Function

Identifying the Function of Protein Domains by Fluorescence Microscopy of Protein Fragments
Problem 3.1.6
(tags: #fluorescence microscopy, #NLS, #mutant analysis, #animals)

Example Answer: Orange Text
Instructor Comments: Blue Text

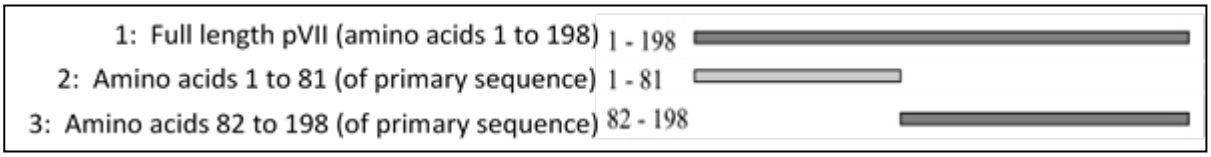

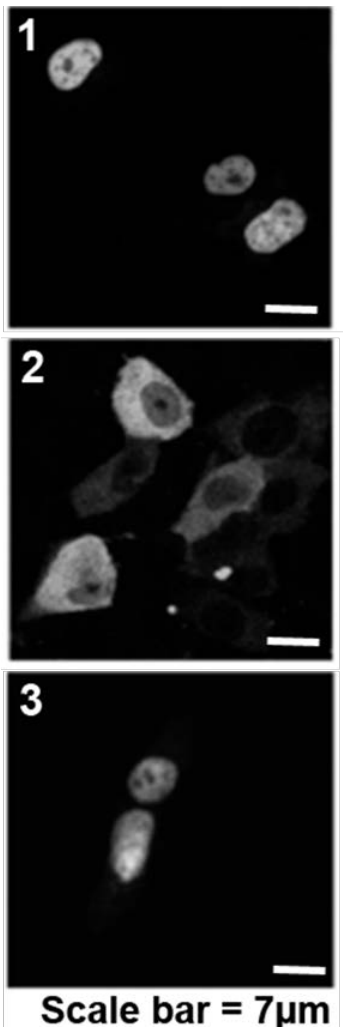

Wodrich et al. (2006) looked at the location of nuclear localization signals (NLS) in the Adenovirus protein pVII. Full length and deletion mutants of pVII were fused to GFP (green fluorescent protein) and injected into the cytoplasm of cells. Injected cells were viewed using fluorescence microscopy.

a) Identify the cellular location of the fluorescence in each panel (1, 2 & 3).

Describe the Results: Demonstrate your correct understanding of the data by describing, in your own words, the results shown in the figure.

Example Answer:

- *Panel 1 (construct 1, full length pVII) detected in the nucleus but not the cytoplasm*
- *Panel 2 (construct 2, pVII aa 1-81) detected in the cytoplasm but not the nucleus*
- *Panel 3 (construct 3, pVII aa 82-198) detected in nucleus but not the cytoplasm*

Explanation: This is a bit challenging because no brightfield image is available for comparison, but we can compare the three panels to make things clearer.
Identifying Nuclear Signal: Panel 1 and Panel 3 appear very similar, with labelling of roughly oval-shaped objects approximately 10 μm across (approximately the size of a nucleus), often with darker spots inside which may be the nucleolus. The 10 μm ovals are still visible in Panel 2, but as an absence of fluorescence. Panel 2 also tells us that the cells are much bigger than the oval structures, as it appears that the rest of the cell (each irregular structure is a cell, characteristic of mammalian cell cultures) is being labelled.

Identifying Cytoplasmic Signal: Cytoplasmic signal is generally characterized by a uniform fluorescence throughout the cell, that is excluded from organelles in the endomembrane system and the nucleus. It is not possible to see the exclusion from the endomembrane system in these images, but exclusion from the nucleus is clear.

b) What can you conclude about the location of the NLS in pVII? Explain.

This question is asking us to make some connections between the results above, and the function of the different part of the pVII protein. Your job in answering questions like this is to make these connections as clear and obvious as possible. In the example below, the 'logical progression' of the answer is clearly laid out.

Example Answer:

- *Conclusion: pVII has an NLS, and it is found somewhere within aa 82-198 of the protein.*
- *Explanation:*
  - *Full-length pVII is detected in the nucleus but not the cytoplasm, indicating that pVII contains a signal for nuclear import somewhere.*
  - *The aa 1-81 protein is found only in the cytoplasm, indicating that there is no signal for nuclear import in this region of pVII.*
  - *The aa 82-198 protein is found only in the nucleus, indicating that this region of pVII contains the signal for nuclear import.*

Unit 6: Cytoskeleton

Using Fluorescence Recovery After Photobleaching (FRAP) to Investigate Microtubule Dynamics at Different Stages in the Cell Cycle
Problem 6.2.1
(tags: #microtubules, #FRAP, #cell cycle)

Example Answer: Orange Text
Instructor Comments: Blue Text

One approach to characterize microtubule assembly and disassembly involves injecting fluorescently-labeled tubulin into cells. The fluorescent tubulin is then incorporated into microtubules, thereby allowing visualization of the microtubules inside living cells. When these cells are used in fluorescence-recovery-after photobleaching experiments (FRAP), the following results are found for cells that are in interphase and cells that are in metaphase.

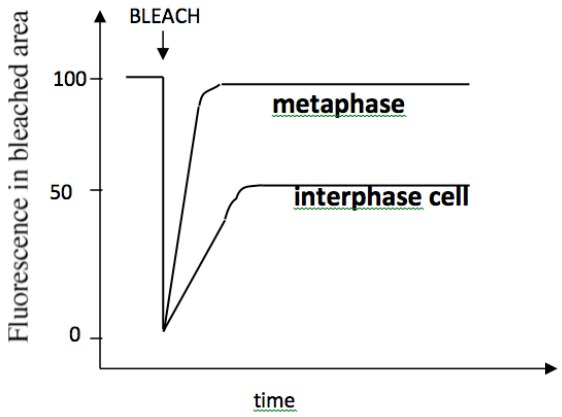

A. When doing FRAP in cells with labeled microtubules, why does the fluorescence intensity in the bleached area recover (i.e. it does not stay at zero)?
A complete answer must connect the principles of FRAP (as displayed in the graph above) to the underlying cell biology of microtubules.

Principles of FRAP: FRAP lets you detect movement of fluorescently-tagged proteins by bleaching the fluorescence and measuring how long it takes for fluorescent proteins to move into the bleached area. If the fluorescence doesn't recover, we can infer that the proteins are not mobile.

Cell Biology of Microtubules: It makes sense that fluorescence intensity is recovered when microtubules are fluorescently-tagged because we know that microtubules are dynamically unstable. The proper functioning of the cytoskeleton requires continual disassembly and assembly. Therefore, there are many opportunities for the tubulin monomers in the bleached area to be exchanged for new, fluorescing tubulin monomers.

Example answer:

> *"Fluorescence intensity recovers because of the dynamic instability of microtubules. While the microtubules with "bleached" tubulin are no longer visible, fluorescently-labeled tubulin from outside the bleached area can move into the bleached area and become incorporated into microtubules, allowing recovery of fluorescence."*

B. What can you conclude about the relative stability of the microtubules in metaphase cells as compared to the microtubules in cells in interphase? Interpret these results in terms of the function of microtubules in metaphase.

This question is asking us to make some connections between the results in the graph above, and the function of microtubules in different stages of the cell cycle. Your job in answering questions like this, is to make these connections as clear, and obvious as possible.

In this case, there are three key points that need to be covered.

1. **Describe the Results**: Demonstrate your correct understanding of the data by describing, in your own words, the results shown in the graph. In this question, you need to compare the fluorescence recovery of microtubules in interphase and metaphase.
2. **Provide a Cell Biology Interpretation**: What do these results suggest about the behavior of microtubules in interphase and metaphase?
3. **Make a Conclusion**: How do these differing behaviors relate to the differing function of microtubules in interphase and metaphase?

Example Answer: *"Fluorescence recovery of microtubules in metaphase is faster than that of microtubules in interphase. This indicates that during metaphase microtubules exhibit a greater degree of dynamic instability (MTs in metaphase cells are turning over faster), and that microtubules in interphase cells are more stable than those in metaphase cells. This reflects the function of metaphase microtubules in capturing chromosomes and maintaining them at the metaphase plate, with increased dynamic instability (and treadmilling)."*

Describe the Results: *"Fluorescence recovery of microtubules in metaphase is faster than that of microtubules in interphase."*
Provide a Cell Biology Interpretation: *"This indicates that during metaphase microtubules exhibit a greater degree of dynamic instability (MTs in metaphase cells are turning over faster), and that microtubules in interphase cells are more stable than those in metaphase cells."*
Make a Conclusion: *"This reflects the function of metaphase microtubules in capturing chromosomes and maintaining them at the metaphase plate, with increased dynamic instability (and treadmilling)."*

Appendix F BIOL200 - Exam Questions

Question 1: Protein Targeting

You have just joined a lab that uses temperature-sensitive yeast mutants to study the lysosomal pathway, and your supervisor wants to test your understanding of the role of different endomembrane proteins involved. You are asked to make predictions about the location of a tagged lysosomal protein accumulating in the different temperature-sensitive mutants indicated below, when they are grown at restrictive temperatures. **Note:** The tagged lysosomal protein you are tracking has no mutation.

In each case, label the diagram with stars (i.e. ★) at the location where you would expect the lysosomal protein to accumulate when the yeast cell is shifted to restrictive temperature (1 mark). Provide a short, one-sentence rationale for your choice (1 mark).

Yeast mutant grown at permissive temperature, with normal location of tagged-lysosomal protein shown.

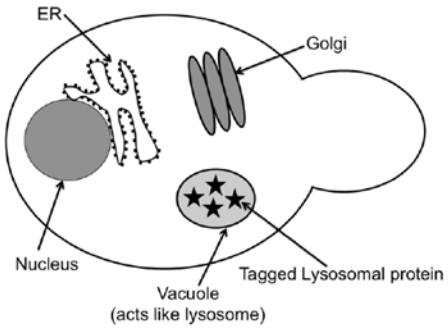

A. Yeast mutant grown at restrictive temperature.
Mutation in Golgi t-SNARE.

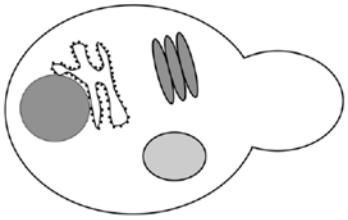

Rationale:

B. Yeast mutant grown at restrictive temperature.
Mutation in the signal-recognition particle (SRP).

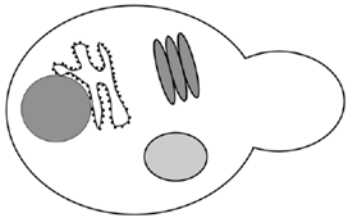

Rationale:

C. Yeast mutant grown at restrictive temperature.
Mutation in COPII coat protein.

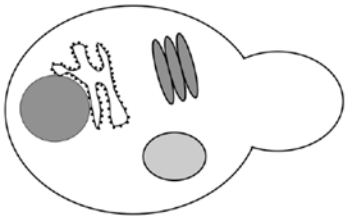

Rationale:

D. Yeast mutant grown at restrictive temperature.
Mutation in M6P Receptor.

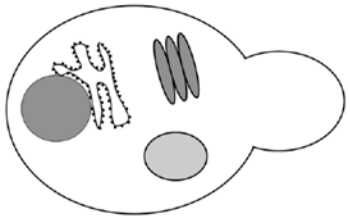

Rationale:

E. Yeast mutant grown at restrictive temperature.
Mutation in lysosomal proton pump, **lysosomal pH=7.0**.

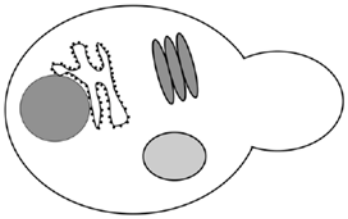

Rationale:

Question 2: Cytoskeleton Dynamics

Nocodazole is used as an anti-cancer drug that binds to α/β tubulin subunits inside cells. Shown below are fluorescence images of cells in the presence or absence of nocodazole, after fluorescence immunolabeling of α-tubulin.

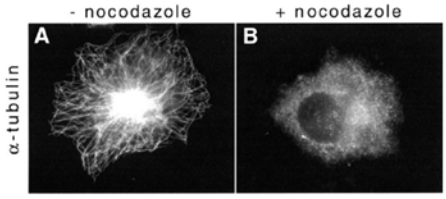

A. Describe the fluorescence pattern seen in Panels A and B. What does this tell us about the effect of nocodazole on microtubules? (3 marks)

	Describe the Fluorescence Pattern	The Effect of Nocodazole
Panel A		
Panel B		

B. Based on your knowledge of microtubule polymerization at the plus end, propose a model for how Nocodazole might be leading to the results shown. (2 mark)

C. Predict what would happen to the cell in Panel B if the nocodazole was washed away and the cell was allowed to recover. (1 mark)

D. Predict the impact of nocodazole treatment on constitutive secretion in these cells? Explain why. (2 marks)

E. Propose a role for nocodazole in the M-phase which makes it useful as an anti-cancer drug. (1 mark)

Question 3: Cell Signalling

The epidermal growth factor receptor (EGFR) is a transmembrane protein localized to the plasma membrane in skin epithelial cells. When EGFR is activated by binding to the extracellular peptide, EGF, it is internalized via vesicles. Ultimately, this internalization will lead to changes in cell growth and division. Researchers studied the relationship between EGFR internalization and cell growth by investigating wild type cells compared to cells with a non-functional mutant form of clathrin.

A. The first experiment examined the amount of EGFR found in early endosomes in the wild type and mutant cells, in the absence (-EGF) or presence (+EGF) of the extracellular peptide. Describe the results shown, and explain what you can conclude based on these data. (3 marks)

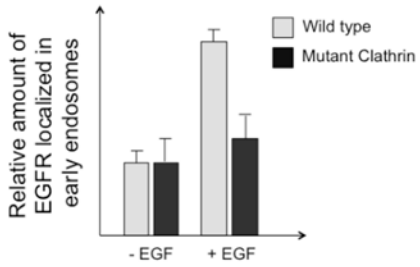

B. In the next experiment, they examined the effect of EGFR internalization on cell cycle proteins, to see whether there were any changes. The SDS-PAGE data below shows the results for Mitotic Cyclin (M-Cyclin), a protein known to promote entry into mitosis, in the absence or presence of EGF. Describe the results, and explain what you can conclude based on the gel shown. (2 marks).

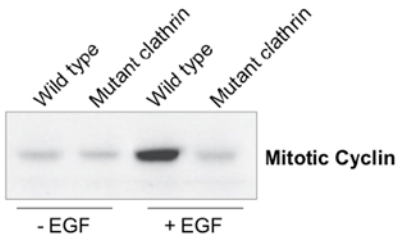

C. The researchers discovered that after the wild-type cells are exposed to EGF, a transcription factor (called ERK1/2) moves into the nucleus. On the other hand, ERK1/2 remained localized in the cytoplasm when the clathrin mutants were exposed to EGF. Considering this and the rest of the data in this question, propose a model describing how EGF-binding to EGFR might affect the cell cycle progression. In your explanation, include the role of EGF and its receptor, clathrin, the transcription factor ERK1/2 and Mitotic Cyclin. (4 marks)

Question 4: Cell Cycle

A temperature sensitive yeast mutant that arrests the cell cycle at the restrictive temperature (37°C) was isolated and named cdc200. To characterize this mutant, normal (wild-type) cells and cdc200 cells exposed to the restrictive temperature were labeled with a fluorescent dye that binds DNA and then the labeled cells were sorted in a flow cytometer. The following FACS profiles were obtained:

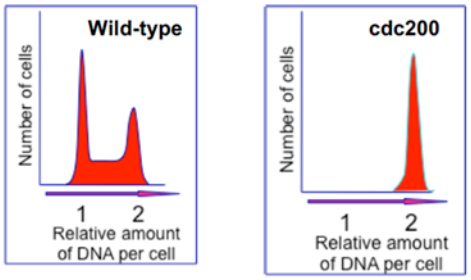

A. Describe the change in DNA amount in wild-type and cdc200 yeast cells. (2 marks)

Wild type	Cdc200

B. What stage(s) of the cell cycle are represented in each case? Explain your reasoning briefly. (2 marks)

Wild type	Cdc200

C. Based on these FACS profiles, in which phase(s) in the cell cycle are the cdc200 cells likely arrested? Briefly explain your answer. (2 marks)

D. To confirm where in the cell cycle the cdc200 cells were blocked, the cells were examined by TEM. The result showed that the cdc200 mutant cells have intact nuclear envelopes and decondensed chromosomes. Based on this evidence, explain in which stage of the cell cycle the mutant is likely arrested. (1 mark)

E. The mutated genes of cdc200 were further characterized and it was found that the gene coding for cdc25 is mutated in these cells. Explain the mechanism how a mutation in cdc25 affects the cell cycle of cdc200 cells. (2 marks)

Question 5: Essay Outline

During normal cellular function, protein activity must be strictly controlled such that cellular processes can be turned 'off' or 'on' quickly and reversibly, without degrading or synthesizing new proteins. Write an essay outline to critically assess the following statement: "Reversible protein activation and deactivation through conformation change are crucial to proper cellular function." Your arguments (and associated supporting evidence) should provide examples from 3 different Units of Biology 200.

Thesis statement: **(1 sentence recommended, 2 sentences MAX)**

-

Score: _____/2

Argument 1 and evidence: **(2 sentences recommended, 3 sentences MAX. 1 sentence per bullet)**

-
-
-

Score: _____/4

Argument 2 and evidence: **(2 sentences recommended, 3 sentences MAX. 1 sentence per bullet)**

-
-
-

Score: _____/4

Argument 3 on next page

Appendix G BIOL200 - Survey Questions

	Biology 200 Survey Qs
Q#	Q (yes/no)
1	While enrolled in Biology 200, did you use the problem set practice questions outside of tutorial/lecture?
Q#	Q (not enough, enough, too many)
2	Regarding the number of practice questions in the problem sets, there were:
Q#	Q (not challenging, challenging enough, too challenging)
3	Regarding the difficulty of the practice questions in the problem sets, the problems were:
Q#	Please indicated how frequently you did the following: (never, rarely, occasionally, frequently, very frequently)
4	Read through the problems
5	Attempted problems on my own
6	Attempted problems with classmates in person
7	Attempted problems with classmates online
8	Went over answers with classmates in person
9	Went over answers with classmates online
10	Posted about the problems on the class discussion board
11	Read things other people had posted about the problems on the discussion board
12	Contacted or met with an instructor about the problems
13	Contacted or met with a TA about the problems outside of tutorial
14	Contacted or met with a peer tutor about the problems
Q#	To what extent do you agree or disagree with the following statements about the MIDTERM exam? (strongly disagree, disagree, neither, agree, strongly agree)
15	Using the problem sets was an important part of my studying for the midterm
16	The questions in the problem sets were similar to those on the midterm exam
17	I wish I had spent more time on the problem sets when studying for the midterm exam
18	I wanted to work more on the problem sets when studying for the midterm, but I didn't have the time
Q#	To what extent do you agree or disagree with the following statements about the FINAL exam? (strongly disagree, disagree, neither, agree, strongly agree)
19	Using the problem sets was an important part of my studying for the final exam
20	The questions in the problem sets were similar to those on the final exam
21	I wish I had spent more time on the problem sets when studying for the final exam

22	I wanted to work more on the problem sets when studying for the final, but I didn't have the time
Q#	To what extent to you agree or disagree with each of the following statements? (strongly disagree, disagree, neither, agree, strongly agree)
23	I was not sure how to use the practice problems to study
24	It was too hard to tell if I was successfully answering the questions
25	I am happy with how much help I received from instructors, TAs, and peer tutors on problem set questions
26	If I wanted more practice for a specific type of question, it was easy to find an example in the problem sets
27	The problem sets helped me understand the connections between different topics and units
28	The wording of questions in the problem sets made it easy to understand what was being asked
29	Using the problem sets helped me improve my problem-solving skills
30	The problem sets are an important part of the course
31	Working on the practice problems was frustrating
32	Working on the practice problems was rewarding
33	Working with the practice problems helped me interpret real experimental results
Q#	Q (yes/no)
34	While enrolled in Biology 200, did you use the 'example answers' for questions not covered in tutorial?
35	While enrolled in Biology 200, did you use the 'example answers' for questions that were covered in tutorial?
Q#	Q (not enough, enough, too many)
36	Regarding the number of example answers for the problem sets, there were:
Q#	Please indicated how frequently you did the following: (never, rarely, occasionally, frequently, very frequently)
37	Read through the example answers for questions covered in tutorial
38	Read through the example answers for questions NOT covered in tutorial
39	Attempted problems with example answers before looking at the answer
40	Used an example answer to help me answer a different problem set question
Q#	To what extent to you agree or disagree with each of the following statements?
41	It was easy to find the example answers on the course website
42	Using the example answers was an important part of my studying for the MIDTERM
43	Using the example answers was an important part of my studying for the FINAL EXAM
44	It was easy to understand why the example answers were correct

45	I could use the example answers to help me attempt other questions in the problem sets
46	Using the example answers helped improve my problem-solving skills
47	The example answers were an important part of the course
48	The example answers helped me figure out what the instructor expected of me
Q#	Q (separate files, combined in one, both)
49	What format do you prefer when accessing the problem sets and example answers?
Q#	Please indicated how frequently you did the following: (never, rarely, occasionally, frequently, very frequently)
50	Used the table of contents
51	Used the question tags
52	Used the index
Q#	To what extent to you agree or disagree with each of the following statements? (strongly disagree, disagree, neither, agree, strongly agree)
53	The table of contents is a valuable resource
54	The question tags are a valuable resource
55	The index is a valuable resource

Appendix H BIOL200 - Survey Codebook

How to Use the Codebook:

Code Format: With the exception of 'Emotion Coding', comments about the problem set questions will be coded separately from comments about the answers. Negative comments are preceded by a minus sign (-), while positive comments are preceded by a plus sign (+). The codes are described according to the following format.

1. **Code**
   Description of the code, including what it should and should not be applied to.
   "Example of text that the code should be applied to"

Code the Whole Comment: When coding a comment, include the whole comment in the code to maintain the context in which the comment was made.

Applying Multiple Codes: If multiple ideas are discussed in a single comment, code that comment with every code that applies. Emotion codes should be applied on top of other codes.

Off-Topic Comments: If the student's comments are off topic (e.g. about the 'answers' when asked about the problem questions) code it based on the content of the comment rather than the question (ie. code it with an 'answers' code). If the student is commenting on something outside the scope of our analysis, please code it with a generic **'Other'** code. Comments about the survey, 'not remembering', or 'N/A" should not be coded.

Combine Codes for Each Year: Code survey responses from each year using the same codes (i.e. do not create separate 2015 and 2016 codes).

Problem Comments: If a student may have misunderstood the question, or made a mistake in their answer that might affect how it should be interpreted or coded, flag it by coding it as **'Possible Problem'**.

A. Emotion

1. **+ Emotion**
   Comments that have an especially positive response. You may feel that they highlight student excitement, pleasure, interest, curiosity. Look for ALL CAPS, exclamation points!, qualifiers like (e.g. very, really) and superlatives (e.g. excellent, great). Do not include comments that students simply 'like' something, as this was prompted in the question.
   "EXAMPLE ANSWERS. It gave me a really good idea for what was expected of an answer to get full marks."
   "They were perfect."
   They would change "Nothing!"
   "All of it :)"
   "These were very helpful, because they targeted more challenging questions"

2. **– Emotion**
   Comments that convey an especially negative response. You may feel that they highlight student frustration, anger, sadness, aggression, disappointment, anxiety, hopelessness, confusion etc. Look for ALL CAPS, exclamation points!, qualifiers like "very, really" and words with strongly negative values (e.g. waste, useless, impossible, awful).
   "POST ANSWERS!!!!!!"
   "I understood the purpose of not having one for each problem but it was frustrating to not know if I was doing the problems like I am expected to."
   "Please bring back answers to all the sets. Especially in such a subjective marking rubric, you are not benefitting the students in any form or way by leading them a stray on what is expected of them"
   "Answers for everything. Although they say its beneficial to discuss, you don't even know if you're discussing the right things. Regardless of whether or not you get the answers, there will still be discussions if you don't understand.

B. Questions: Codes about the problem set questions.

3. **– #Qs - too few**
   The student was unhappy that there were not enough practice questions. This may include comments asking for additional examples of specific kinds of questions.
   "I wish that there were more problems to attempt."
4. **– #Qs - too many**
   The student was unhappy that there were so many practice questions.
   "less of them - the amount was overwhelming"
5. **+ #Qs - just right**
   The student was happy with the number of questions.
   "There were a lot but it allowed you to have a lot of practice material"
6. **– Qs - give different**
   The student asks for different types of questions. Comments asking for fewer, or more questions, should be included in both codes. Include suggestions for improvement.
   "I wish that there were more problems to attempt."

7. **– Difficulty - too easy**
   The student found the questions too easy. Do not include comments about question number.
   "Make them a bit more challenging"
8. **– Difficulty - too hard**
   The student found the questions too hard. Do not include comments about question number.
   "The problem set questions were much more difficult than what was tested on the exams"
9. **+ Difficulty - just right**
   The student thought the questions had a good difficulty level. This may include enjoying the variety in difficulty levels. Do not include comments about question number.
   "questions were challenging but made me think about how to solve the question"

10. **+ Benefit - exam prep**
    The student liked that the questions could be used to study for exams. They may mention using them to study, or just state that they liked that the questions were "exam-style".
    "Used them to study for exams"/ "Exam-style Questions"

11. **– Quality - wording**

Comments about disliking the wording of questions.

"Some of the wording was confusing and some of the problems had a lot of intro background (hard to focus)"

12. **– Quality - Q format**

Students did not like the format of the problem sets, or suggest a different format. This includes comments that the problems should be more similar to exam questions, or about specific features like the question tags or how the problem sets as a whole are organized.

" I did not think the test your understanding sections were helpful." /
"Add more questions with a range of difficulties"

13. **+ Quality - Q variety**

The student liked the variety of questions available. Variety could be in difficulty level, topic covered, format of the question, etc.

" Variety in difficulty level" / "Variety in type of questions"

14. **+ Quality - real data**

The student liked that the questions used 'real data'. This includes comments about 'real world' applicability.

"Questions are related to real world" / "I liked the questions that had interpretation of lab data"

15. **+ Generic**

Respondent expresses a generic positive statement about the problem set questions. Only code if the comment does not fit into one of the other codes.

"Good" / "Liked them" / "It's overall fine"/ Would change "Nothing"/ Liked "Everything"

16. **+ Other**

Any other specific positive comments about the questions not covered elsewhere.

"Most of the real "learning" of the course I did while doing the problem sets."
"I thought the practice problems are a great way of getting away from all the memorizing that goes on in University."

17. **– Other**

Any other specific negative comments about the questions not covered elsewhere.

"Provide more incentive to do the practice problems without answers." / "Work on them in class"

C. Answers: Codes about the problem set answers.

18. **– #Ans - give more**

The student says they would like ‘more’ answers, but do not specifically ask for ‘all’ of the answers.

“There were a lot of practice problems for the number of answered ones, I get that it's practice but it got tedious because I couldn't find out how well or poorly I was doing.”

19. **– #Ans - give all**

The student specifically asks for ‘all’ of the answers. This includes asking for a ‘key’.

“It would have been extremely helpful to have an answer key to the problem sets” / “I would have liked to have all the answers to the practice problems”

20. **+ #Ans - just right**

The student is happy with the number of answers given.

Student likes “The amount of them.”

21. **– Ans - give different**

The student asks for answers to different types of questions. Comments asking for additional/all answers should be included in both codes. Include suggestions for improvement.

“I would definitely ask for the sample questions to be the more complex ones so we can get a better grasp of style of answering needed.”

22. **– Ans - change implementation**

The student suggests a change in how the answers are used in the course. Do not include comments on the content of the answers (see ‘– Quality - content’) or which questions have answers (see ‘- Ans - give different’). Comments also asking for additional/all answers should be included in both codes.

“Post answer key in point form after a week” / “A review session to go over answers collectively as a group or in tutorial would have been appreciated.”

23. **+ Quality - content**

The student is happy with the content and the level of detail in the answers. This includes comments that the answers were clear, and that it broke down the answer.

“The explanations were easy to follow” / “I liked the systematic, step-by-step approach of the example answers.”

24. **– Quality - content**

The student did not like the content of the answers. Include comments about the type of information or level of detail in the answers. Include suggestions.

“Give examples of answers that aren't quite right and why they don't warrant full score” / “Provide a marking scheme to see why the example answers are good” / “more explanation on process/thinking” / “I usually found the answers too short, or too long”

25. **+ Benefits - expectations**

The student found that the answers informed them of their instructor's expectations for answering questions. They may not mention the instructors explicitly, but may refer to marking or studying for exams.

"Examples of the kind of answers expected on tests" / "The format of each response was useful to show how the instructor wanted you to answer the questions"

26. **+ Benefits - assess your work**

The student found that the answers helped them assess their work. Comments about not being able to assess their work without answers should be coded here as well. Do not code comments about marking or exams here (see '+ Benefits - Expectations').

"Can't assess work without answers"/ "Allowed me to see how I was doing" / "Help students know they were in the right track."

27. **+ Benefits - learning**

The student found that the answers helped them learn the skills required to answer the questions. Do not code comments about exam preparation (see '+ Benefits - expectations') or assessing their work (see '+ Benefits - assess your work') here.

"I liked that they walked you through the exact thinking you need to find the full answer."/ "Example answers were similar to academic writing and scientific paper writing. This helps me to visualize the level of writing that I should aim for as I continue my learning in the faculty of science."

28. **+ Generic**

Respondent expresses a generic positive statement about the question answers.

"Good", "Liked them", "It's overall fine", Would change "Nothing", Liked "Everything"

29. **+ Other**

Any other specific positive comments about the questions answers not covered elsewhere.

"The thought that went in to constructing them" / "I liked how they gave instant feedback rather than having to post them online and wait for someone to give me feedback."

30. **– Other**

Any other negative comments about the question answers not covered elsewhere. This includes suggestions for improvement.

"Reorder Qs" / "They were not obvious to find"

Appendix I BIOL200 - Interview Protocol

Interview Protocol

Effect of Example Answers on Problem Solving by Undergraduate Cell Biology Students

Sep 15, 2016 (v1)

Interviewer: Miranda Meents

Interview Date/Time: _____ Participant Name: _____

1. Introductory Script

- "My name is Miranda Meents, and I'm a PhD student here at UBC. My research is focused on cell biology, and biology education, which is what this interview is about."
- "In this project, I am studying how learning changes when students are given example answers to questions they encounter in the course."
- "In Biology 200, these example answers have been included in the problem sets as the problem 'walkthroughs'."
- "We're really interested in hearing your perspective on these changes, because you have experienced different versions of the course, and have a valuable perspective."
- "While comments you make may be shared with others, I will be the only person who knows if a comment was made by you. You will not be identified to any of the instructors, your fellow peer mentors, or if the results of this research are shared with others."
- "Before we start, I'd like you to read and sign the consent form, so we can make sure you're ok with proceeding with the interview."

[consent form signed? Yes / No]

- "I'd like to record our conversation, so I can have an accurate record to refer back to. I will be the only one who will listen to it. Is it alright with you if I record?"

[consent to record? Yes / No]

3. Concluding Script

- "I think we need to wrap up our conversation now. Before we go I want to give you a copy of the consent form. This has my contact information on it, so if you have any questions or concerns, please feel free to get in touch with me."
- "Is it alright if I e-mail you if I have any follow-up questions, or need to clarify something?"

[consent to follow-up e-mails? Yes / No]

- "Thank you very much for taking the time to speak with me today."

2. Interview Questions

Note: Questions are in Red/Black, Prompts are in Blue

1. "Why don't we start, and you can tell me a little about yourself."
   - i. "What program and year are you in?"
   - ii. "When did you take BIOL200? What did you think about the course?"
   - iii. "Why did you want to be a peer mentor for Biology 200?"
     - Feelings about BIOL200
     - Feelings about cell biology
2. "Tell me about your experiences with the practice problems when you were a student in Biology 200."
   - Studying, tutorial, lecture
   - For midterm and/or final
3. "Tell me what it was like when you encountered a practice problem you were unsure about, and how you dealt with that."
   - How often did that happen?
   - How did that make you feel?
   - What strategies did you use?
4. "This year a few changes were made to the problem sets, and I wanted to ask you how you feel about these differences."
   - i. "To start with, how do you think the problem walkthroughs have changed the experience of working with the problem sets?"
   - ii. "How has your interaction with the problem sets changed, now that there's a table of contents and an index?"
   - iii. "How do you feel about including the keyword 'tags' for the practice problems?"
     - Are the students this year using the problems more/less?
     - Are they asking more questions, or different questions?
     - Are they applying what they learn to new problems?